The Geometrical Interaction of the Stylus and the Measured Surface in 3D Roughness Measurements

Helmy A.M. Dowidar

A thesis submitted in partial fulfillment of the requirements for the degree of Doctor of Philosophy in Engineering

University of Warwick
School of Engineering

December 2003

Contents

List of Figures

List of Tables

Acknowledgment

I would like to take this opportunity to express my sincere thanks to my supervisor, Prof. D.G Chetwynd, for his support and encouragement during the period of the research and his suggestions and comments on this piece of work, and also for his help in correcting this thesis.

Many thanks go to the people in the Centre for Nanotechnology and Micro-engineering, specially Dave Robinson and Steve Wallace, for their general help to progress my experimental work.

Declaration

This thesis is presented in accordance with the regulations for the degree of Doctor of Philosophy at the University of Warwick. The thesis has been composed and written by myself based on the research undertaken by myself. This research has not been submitted in any previous application for a higher degree. All sources of information used are specifically acknowledged at the relevant points in the text.

Helmy A.M. Dowidar

Summary

The target of this work is to study the effect of the stylus tip geometry on the surface roughness measurements by the stylus methods. A computer simulation of the measuring process in 3D using arbitrary tip shapes has been undertaken. A novel feature of this simulation is that it determines and reports the contact distribution of the contact points on the stylus when scanning each surface. Following analysis of fully simulated data to establish the fidelity of the simulation process, it was applied to data set from real surfaces. First these were examined using ideal (sometimes truncated) pyramid, conical and spherical tips. Then tip shapes determined from the measurement of real styli were used. Relatively large tips (of the order of 10 μm) were used in order to ease the need for measurement resolution. The simulation results were evaluated against real measurements of the surfaces. A bespoke measuring system was developed for this, adding X-Y scanning and a means of interchanging styli while maintaining micrometer lateral positioning between measurements. The shape of each stylus tip has been determined using a technique based on the replication by indentation into a soft substrate (typically lead).

The roughness values of the real surfaces when scanned (theoretically) by the real tips have been compared to the roughness values of the same surfaces when measured by the measuring system with different tips. This comparison has shown a good compliance of both the theoretical and the practical results. This provides a degree of confidence for interpreting details of the simulation as having practical relevance.

Both computer simulation and real measurements confirm the trends that would be expected from earlier studies. For example, amplitude parameters tend to drop in value as stylus size increases. The distribution of stylus contacts in simulation suggests that it is rarely to be found near the nominal centre of the tip. It is also clearly demonstrated that real worn tips do not necessary act as if blunt, contacts concentration in small regions when local features dominate. These results have significant implementations for the uncertainty in topographic measurements.

1. Introduction

The industrial and economic drives towards more efficient use of energy and material resources, towards higher technology and towards improved control of machining processes are all placing new levels of demand on high-precision dimensional measurements.

Interest in measuring surface roughness has been increasing during the last decade for several reasons. It is known that the surface structure plays a vital role in the lifetime and the function of almost every machined surface. Lubrication, efficiency, probability of crack formation and corrosion stability are some examples of the influence of roughness of the produced surfaces on their performance. Besides, the production cost of a mechanical part is closely related to the specified roughness. The surface roughness is therefore an extremely important parameter in design and production, which must consequently be measured in a correct manner relevant to the required accuracy.

The stylus technique is one of the most commonly used techniques for measuring surface roughness. Its main advantage is that it is easy to use, moderately tolerant of minor contaminations and also it is able to give a profile along a well defined direction. The vertical displacement of a stylus is converted into an electrical signal that could be analyzed by computers to determine a large number of parameters that have been proposed over the years for the assessment of surface roughness features. Further background on these general issues can be found in [1-5]. This being the case, no general review of the topic is offered in this thesis.

In consequence there is currently a considerable international effort invested in refining the fundamental metrology and Standards associated with the measurement of surfaces on the micrometer to sub-micrometer scale.

The geometry of contact between the real surface and the stylus is complex and one direction for this project is to provide experimental data for verifying ideas so far considered only in simulations. There has been some work on the ideal interaction of a stylus and surface in two dimensions, with the aim of predicting the true surface structure. However, real measurements do not involve perfect tips, conditions or surfaces, so the real question is how a stylus tip interacts with a surface.

The longer term purpose of the current proposal is to provide evidence of how stylus size and shape affect the surface roughness measurement. The primary motivation is to use it as a step in the process of developing an understanding of, and then models for, stylus-surface interactions that is of increasing important to National Standards in roughness measurements. For example, comparing data from stylus and optical instruments requires models of their interaction with surfaces. [Trends in Nanometre Metrology, Workshop discussion at Warwick University, 2003, unpublished].

1.1 Measuring Surface roughness

In recent years surface texture has been recognized as being significant in many fields. In particular the surface roughness is an important factor in determining the satisfactory performance of the workpiece, for example resistance

to wear. The roughness of surfaces has many applications in the industry as well as the daily life. The earliest ways of measuring the surfaces were using the thumb-nail and the eye. Both of these are highly effective but completely subjective. Demand for quantitative results led to the development of two parallel branches of instrumentation: one following the tactile example of the nail (stylus methods), the other mimicking the eye (optical methods). The two methods actually evolved to measure different things. The optical methods looked for lateral structure, namely spacing and detail in the plane of the surface, whereas the stylus method examined heights in the plane perpendicular to the surface. Optical methods were developed to help the metallurgist or biologist whereas the stylus method was for engineers' use [6]. The stylus instrument is the most widely used technique for measuring surface topography. One of its great advantage is the fact that the stylus profiling results are easily quantifiable in a number of ways [6].

The earliest types of the surface measuring instruments by stylus methods were mainly designed to measure a profile along the surface in two dimensions producing a graph representing the surface profile. With the increasing progress in advanced technology and personal computers, the capability of these instruments has increased over the years to measure the surface roughness quantitatively sometimes fully in three dimensions. Most modern stylus instruments use digital data recording methods. These have revolutionized surface metrology because a digital instrument with a computer can produce almost any analysis of the surface geometry that is requested [7]. Work has been done on upgrading the traditional surface measuring instruments by the aid of personal computers to measure and analyze surface roughness [8]. Other work has been done to study the different

variables affecting the quality and reliability of these systems like the conditions of digitalizing data from the measuring instruments [9] and the effect of the environments noise on the roughness measuring systems [10].

Surface roughness measuring instruments have been used for many years and their applications have been widespread. However, new demands are being made such as increased speed of measurement and also the capability of measuring more complex surfaces [11].

Anther direction for the research on the surface roughness measurements was toward measuring an area of the surface rather than a line (profile) i.e. measuring surface roughness in 3D. One of the earliest attempts was by Sayles & Thomas [12]. Tsukada and Sasajima, [13] developed a broadly similar measuring system for the evaluation of the three-dimensional characteristics of machined surface roughness. Their measuring system consisted of a conventional profilometer of the stylus type and a precision table moving perpendicular to the tracing direction of the stylus. Surface asperity heights were sampled as digital data at the nodes of the matrix on the surface to be measured. Measurements were made automatically by a controller. Asperities of many machined and worn surfaces were measured using the system, and three-dimensional representations and contour maps were given. They showed that their measuring device was sufficiently accurate to be of use in investigating the three-dimensional characteristics of asperities.

George, et al [14] described a highly accurate system that has been developed for providing three-dimensional assessments of engineering surfaces. It was based on a stylus profile-tracing instrument and incorporates an automatically-

controlled parallel-profile digitizing stage. The authors developed a software package to facilitate the processing, manipulation and visualization of the numerical descriptors obtained for the surfaces.

Jeng [15] developed a 3-D surface topography measurement system for the surface characterization of an area. This system consisted of a personal computer, a microdisplacement stage and a surface profilometer. The microdisplacement system moves the samples laterally for successive traces and ensures the parallelism of each surface profile. The personal computer coordinates the stage movement and surface profile measurements, provides large data storage, and allows rapid data manipulation. This system provides an easy, effective way to characterize a surface, together with versatile displays to observe and record surface topography. While having important differences in detail, all these systems (and others) are conceptually quite similar. A number of commercial instruments now offer this technology.

1.2 Stylus- Surface interaction

The stylus instrument is the most widely used surface profiling techniques. However, the recorded profile from the stylus instrument is not exactly a "true" profile of the measured surface. The surface profile information is subject to distortion as it passes through the instrument from the stylus tip to the recorder. Some of this is intentional. For example, profile filters separate the roughness of the measured surface from the waviness and form errors [15]. Other distortion is unavoidable due to practical considerations such as the finite size of the stylus [1].

Work has been done in several places to discuss the interaction of the stylus and the measured surface roughness and also to discuss different variables affecting the measuring accuracy. These variables are such as, the traversing speed, force/friction on the stylus and stylus radius (shape) [16].

The idea of investigating stylus distortion of surfaces by simulation or modeling grew from the same ideas that underline the E-system of surface evaluation [17], [18]. In 1970, Radhakrishnan [19] studied theoretically the effect of the tracing stylus radius on the measured roughness values in two dimensional surface profiles. He observed that while certain roughness parameters were considerably affected by the stylus radius, others were not so much affected. This variation also depended on the production process (the surface roughness). Only when a high accuracy is needed for measuring finely finished surfaces, a small radius of the stylus is needed. For ordinary measurements on comparatively rougher surfaces a stylus radius of between 10 and 25 μm was claimed to be satisfactory.

McCool [20] studied theoretically the effect of the stylus tip radius on surface roughness measurements. It was shown that the values of the mean square height, slope and curvature deduced from stylus profile traces are distorted by the nonlinear filtering effect of the finite stylus tip and by the failure, at high enough tracing speeds of the stylus to maintain contact with the profile being traced. The author developed a simulation model for assessing the magnitude of this distortion as well as the effect of record length and sampling frequency with tracing profiles that are realizations of a random process having a specified spectrum.

Church and Takacs [21] found that smooth surfaces are likely to be reported as rough because of the tip-size effects, while rough surfaces are smoothed.

Odonnell [22] studied the effect of stylus width in the profilometry of a randomly rough surface. An approximate solution for the path of a flat-tipped stylus on an arbitrary surface was expressed as a nonlinear function of the local surface height and its first two derivatives. This solution was then averaged to find the first two moments of the measured profile when the surface and its derivatives are jointly Gaussian varieties. The measured surface variance was found to decrease with increasing stylus size in a manner consistent with computer simulations.

Liu et al [23] studied the friction forces of a diamond stylus and a surface at different loads. Surfaces of lapped specimens of mild steel, copper, brass, aluminum and polished silicon were traversed by a stylus-based profilometer that was modified to allow continuous variation of the tracking force. System testing, by loading up to 6 mN and then relaxing, resulted in permanent deformation of the metal specimens from 80 nm for steel up to 340 nm for aluminum. Horizontal drag forces were also measured by fixing the specimens to a linear spring with its displacement axis parallel to the traverse axis of the stylus. Drag forces during traverse cause submicrometre deflections of the spring platform which were measured by an inductive transducer. The friction coefficients varied little with the load and showed a slight tendency to decrease with increasing traverse speed. Variations of the drag force about a mean value were observed to be dependent upon the surface finish.

Zahwi and Mekawi [24] studied experimentally the scratching effect of the stylus on the measured surface of the standard calibration specimens. The investigation

was done by scanning the same position of a Sinusoidal specimen many times and monitoring the values of calibration constant of the measuring system. It was found that the mean values of the calibration constants continually decrease.

1.3 The simulation of Surface Roughness Measuring Process:

To study the effect of stylus radius on the measured roughness parameters, there has been some work on simulating the roughness measurement of a surface by the stylus method using the computer. Nearly all the published attempts are in two dimensions.

Kartz et al [25] investigated the dependence of surface topography and statistical surface parameters on tip radius and data digitization by using a numerical simulation model. In contrast to existing models, the simulation algorithm presented determines the surface profile convoluted with the probe profile for any selection of surface and probe. For a sinusoidal and a fractal-like surface the distortion of the real profile by the probe geometry and the data digitalization was investigated and statistical surface parameters like root-mean-square roughness and correlation length were calculated. The statistical surface data achieved from the simulation procedure were compared with experimental data measured by a mechanical profile using different tips. This work was in two dimensions and not representing the three dimensional effect even along a single profile.

Wu [26] investigated the tracing of a random profile by a mechanical profiler with a spherical tipped stylus by the computer simulation. It was shown that the

measuring error strongly depends on the ratio of the radius of stylus tip to the root mean square roughness. In year 2000, the author made a similar study but in three dimensions [27]. A similar work was done by Mendeleyev [28] to study the effect of the stylus tip size on the measuring error of the root mean square value of a surface.

Yang [29] presented the 3D assessment of the surface roughness and its implementation with the software package MATLAB. The basic concepts and methods of the 3D assessment were discussed. The author used The MATLAB software to deal with the practical data, plotting the surface of the part, computing some parameters of 2D and 3D surface roughness and proved the superiority of the 3D assessment over the 2D assessment.

The body of published work concentrates almost on surface amplitude measurement and totally on the effect on the surface. The detailed behavior of the stylus itself has been regarded as unimportant.

1.4 Methods for measuring the stylus tip radius

In stylus measurements of surface texture the measured results for roughness depend on the stylus radius. Therefore, it is important to determine the stylus radius. Since stylus tips are not perfectly spherical, the local radius of curvature varies significantly over the surface, which makes the determination of effective radius difficult [30].

Vorburger [30], tried to measure the effective radius of the tip by generating a profile across the tip and then using algorithms to derive an effective radius. The idea used for measuring the tip radius was using a sharp edge (typically razor

blade). The technique is based on measuring a profile across the razor blade by the stylus. The measured profile will represent the effective shape of the stylus tip, assuming that the radius of the stylus tip is large compared with the radius of the blade. The author compared the razor blade technique with other techniques using optical microscopy and scanning electron microscopy. The author concluded that the presented method for measuring the tip was accurate. Because this method is based on measuring the effective radius of the stylus and not the actual radius, it could be misleading if the centre of the tip is damaged or having a dent.

Elewa and Koura in [31], discussed the importance of checking the stylus radius in the measurement of surface roughness. As all national and international standards on the assessment of surface roughness are based on the profile of a surface traced by a suitable stylus, the accuracy of this measurement and its numerical evaluation for determining the surface parameters depend on the fidelity of the representation of the trace to the cross-sectional profile of the part. However, for a perfect reproduction of the traced surface, the stylus tip radius should be as small as possible. Different styli or worn styli present different results. The difference lies in the determination of the trajectory drawn through the surface profile, to which the surface roughness height is referred.

Form the previous review, it has been shown that the published work on the stylus surface interaction has neglected several highly relevant areas. Measuring the tip radius has been done in two dimensions while the real tip could be worn or damaged and resulting in misleading results. Even if the tip is not damaged, the razor blade method gives the outer form of the tip regardless of any irregularities in its profile. Most of the computer simulation work has been done in two dimensions

and based mainly on using spherical tips. There is no published work investigating the contact area of the tip when scanning a rough surface. Also, there is a lack of information about the real effect of the stylus size on the measured roughness of a surface in three dimensions. The work done in this thesis is an attempt to cover some of these areas to reveal more secrets of the geometrical interaction of the stylus and the surface.

1.5 Thesis layout

The organization of this thesis is explained by the following brief notes on the contents of each chapter.

Chapter 1 gives a historical perspective of the small volume of work done on the area of this thesis including the interaction of the stylus and measured surface roughness. It covers different areas relevant to the interaction such as: force, friction and stylus tip radius and measuring the surface roughness of a surface by the stylus method in three dimensions. It reviews some published work on the computer simulation of the measuring process by a spherical stylus tip and on measuring the tip radius by the razor blade technique.

Chapter 2 investigates the computer simulation of the three dimensional surface roughness measuring process by the stylus method. The simulation is based on scanning a small area of a surface using different styli tips. The simulation has been applied first to artificial surfaces and tips which have been created by the computer. The same area of each surface has been scanned by different tips including spherical, pyramid and conical shapes in either perfect or

worn conditions. The simulation has then been applied to real surfaces representing different machining processes like: lapping, milling and grinding. The roughness parameters of each surface, when scanned with each tip has been calculated and compared and also the contact distributions on each tip when scanning each surface has been presented.

Chapter 3 presents the measuring setup which has been developed to study the interaction of the stylus and the surface practically in three dimensions. The main idea of the setup is to be able to measure the same area of a surface with different tips. This allows a proper comparison of the effect of the stylus geometry on the measured roughness of the surface. This chapter includes the details of developing a two dimensional traditional profilometer to measure roughness in three dimensions by using an X-Y stage. The design of a mount for exchanging the stylus is given. A specific relocation technique for the specimens to allow scanning the same are of the surface is evaluated. A novel technique for measuring the tip shape based on the replica method is presented.

Chapter 4 presents and evaluates all the results of the practical measurements. It shows the outputs when scanning different specimens with different tips in three dimensions. Three different tips have been used to scan twelve different specimens representing different machining processes: grinding, lapping, milling and turning. The real shapes and dimensions of the three tips used are given. The graphical outputs of the surfaces are presented as well as roughness parameters of each surface when scanned with each tip.

Chapter 5 includes the detailed discussion of the theoretical results of the simulation in the context of the practical results. It also includes the main conclusions of the work done in the thesis and some recommendations for work to be carried out in the future.

2. Computer Simulation

2.1 Introduction

Surface micro-topography is measured most commonly by either a fine stylus contact or by one of several optical probing methods. Debate continues on their relative merits and disadvantages, but it is clear that both will be used for a long while to come. There is, therefore, a need for good ways of comparing the output of these methods. There is also a need for better guidelines or Standards on applying styli to the fine or delicate surface structures that are increasingly demanded by applications across mechanical, electronic, optical and bio-medical engineering.

As part of continuing work towards such ends, this project is mainly to study the geometrical interaction of styli with engineering surfaces. The project involves computer simulation and direct experimental phases in order to investigate the extent to which the forms might be used to practical real behaviour. A simulation process represented in this chapter is used to gain data on the filtering effects of the stylus and on the distribution of contact points. The aim is to inform choices of stylus geometry (e.g. tip radius and cone angles) for the benefits of instrument design and uses and especially, for the information of standards organizations. Longer term, the simulation may help the development of instrument diagnostics for stylus wear and damage.

Figure 2.1 shows a schematic of a stylus with radius *R* making a contact with a rough surface. The ideal contact of the stylus with the surface should be at point *b*, the lowest point of the stylus. Instruments record the topography using the assumption that contact is always at point *b*. In reality, this doesn't always happen as the stylus could be touching the surface at a different point like point *a*, and sometimes touching the surface at more than one point like *a, c*. The likelihood of this happening will depend on the stylus geometry and the roughness of the measured surface.

Figure 2.2 shows the effect of the stylus tip size on the measured profile of a surface. When measuring the real profile with a spherical tip, the measuring system will report the locus of a certain point of the tip normally the centre point. However, if the profile is scanned with tip1, the locus of the centre point of the tip will represent the measured profile (locus 1) by tip1. The measured profile will be different from the real profile as the valleys tend to be sharpened while the peaks tend to be flattened. Rescanning the same real profile with a bigger stylus tip (tip2) produces another profile (locus 2) which is more different from the real profile. As shown in the figure locus 2 is more different from locus 1 produced by tip1. This is logically as the smaller tip will be able to go deeper in the valleys more than the bigger tip.

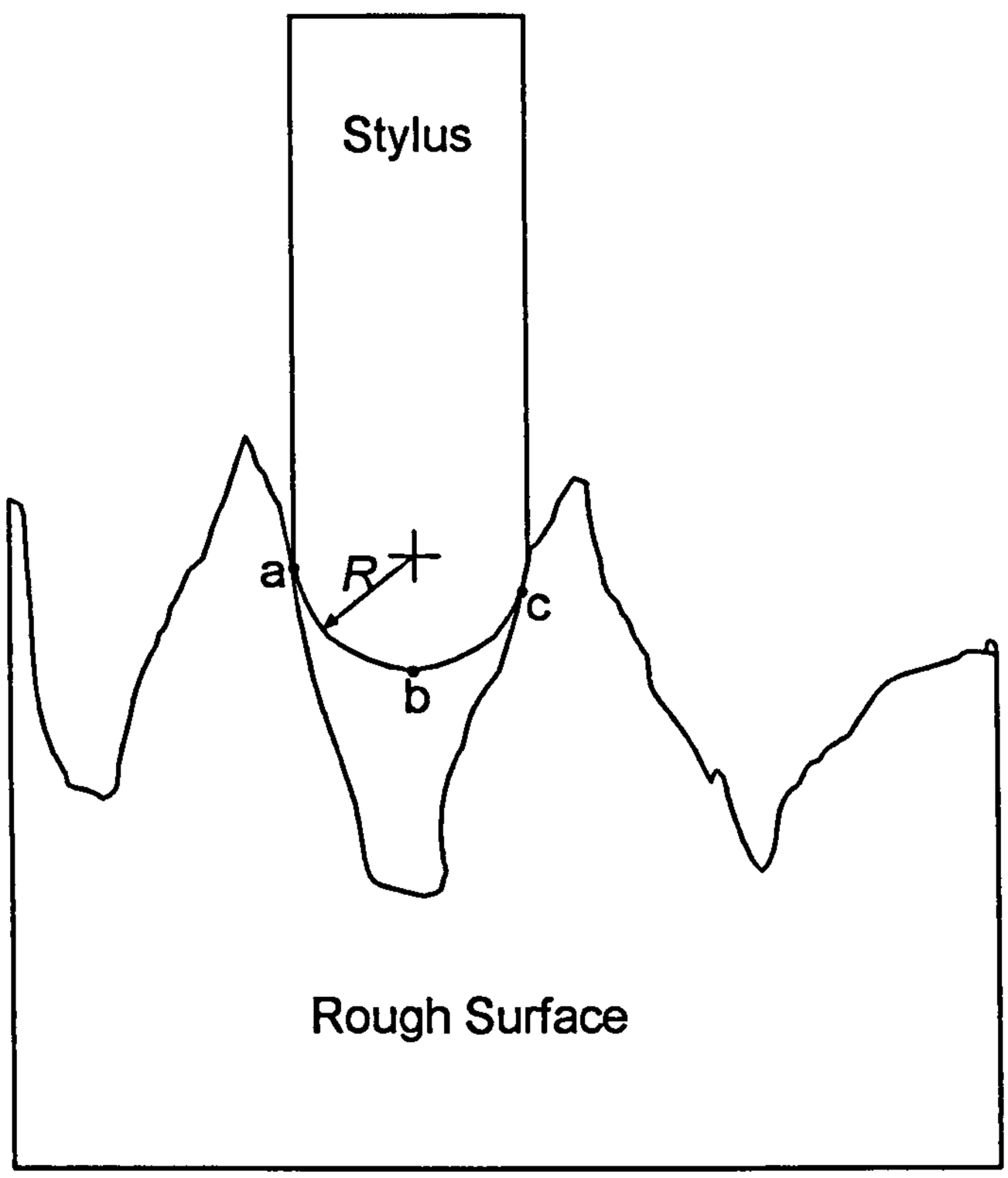

Figure 2.1: A schematic of the contact of the stylus with a rough surface.

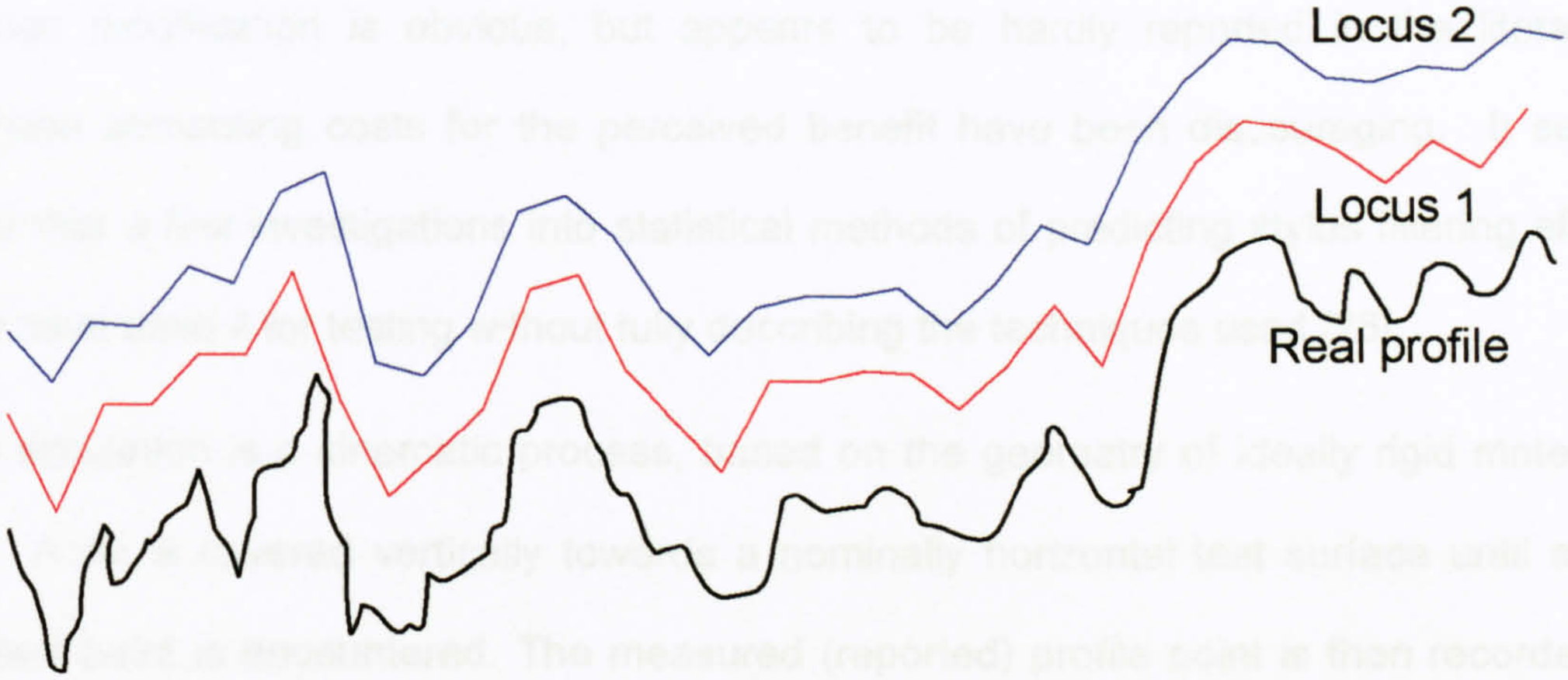

Figure 2.2: The effect of stylus tip radius on the measured profile

2.2 Simulation Process

The basic concept of the simulation method has been widely used. It is a simple extension of that used for many years to show how a circular (disc) 'stylus' filters (smoothes) a roughness profile [32]. The extension from these 2-D methods to 3-D (real) surface modification is obvious, but appears to be hardly reported in the literature. Perhaps computing costs for the perceived benefit have been discouraging. It seems likely that a few investigations into statistical methods of predicting stylus filtering effects may have used it for testing without fully describing the techniques used [26].

The simulation is a kinematic process, based on the geometry of ideally rigid materials, etc. A tip is lowered vertically towards a nominally horizontal test surface until a first contact point is encountered. The measured (reported) profile point is then recorded as the height of a reference point on the stylus (e.g. centre of spherical tip or lowest point) positioned at the lateral location of the centre of the tip. We assume that real styli are adequately constrained by their guiding mechanisms to be modelled as single degree of freedom systems. The slightly arcuate motion of many real profilometers is neglected. This is acceptable on spherical tips and, although less rigorous, for other shapes over small deflections. Effects such as contact friction are also ignored. Conventional instruments might typically have a range of ±50 μm and use a 50 mm stylus arm, so the maximum change of angle is only around 1 m Radian. Some modern, long range profilers cause more concern but angular deviation still only a few hundredth of a radian.

Figure 2.3 shows the principle of the simulation process of measuring a surface with a stylus. The height reported by the stylus at any point P of the surface will not always represent the height of point P unless the contact occurs exactly on the top of point P with the centre of the stylus tip (point 5). The contact could happen at any point of the surface within the size of the stylus tip. To find out the actual height of the stylus at any point P of the surface, the height of each point of the stylus is added to the height of each opposite

point of the surface. The maximum value of the determined heights will represent the actual height of the stylus when measuring point P. It will also give which point of the stylus that makes an actual contact with the surface. The stylus is then moved to the next point of the surface and its actual height is determined as well as the points of the stylus which make contacts with the surface. This process is repeated on all surface points.

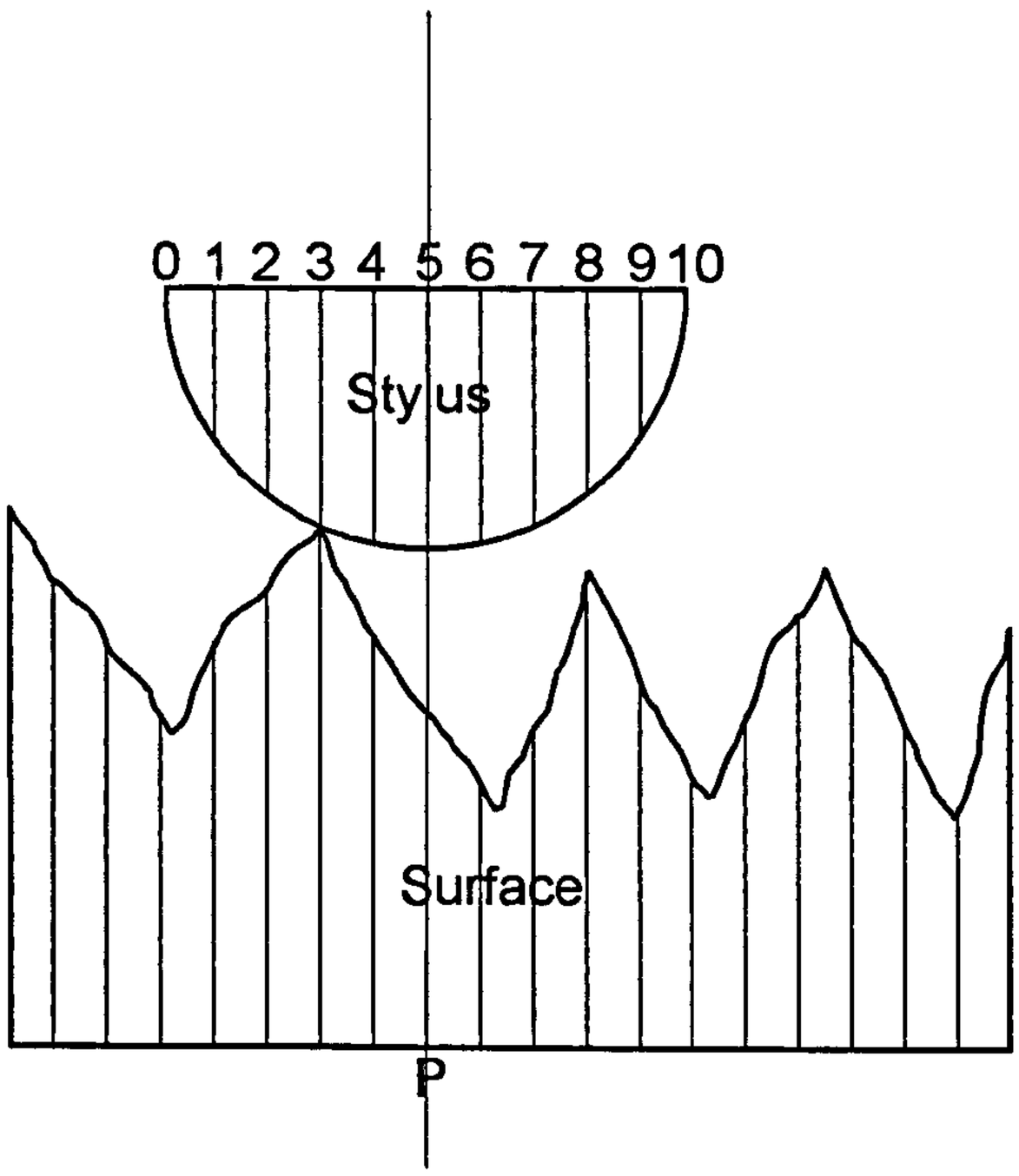

Figure 2.3: The principle of the simulation process of measuring a surface with a stylus

Figure 2.4 shows the algorithm used in the simulation process. The surface and the stylus are represented by two sampling grids in arrays Z(N,M) and S(2R,2R) respectively, where N is the number of traces of the surface, M is the number of points in each trace and R is the tip radius. Two new arrays L(N,M) and C(2R,2R) are created. The array L(N,M) has the same size as the surface array Z(N,M) and is used to report the locus of the stylus on each point of the surface. The other array C(2R,2R) has the same size as

the stylus array S(2R,2R) and is used for counting the number of times that each point of the stylus has made a contact with the surface.

The central point of the stylus array S is set, in turn, above each point of the surface array Z(i,j). The actual height of the stylus is determined on each point of the surface Z(i,j) and is stored into the array L(i,j). Stylus points making contacts with the surface are determined. The counter C(a,b) of each point making a contact with the surface will be increased by one while other points' counters will remain the same.

The output of the simulation process will be the array L(N,M) representing the locus of the centre of the stylus S(2R,2R) when scanning the surface Z(N,M) and the array C(2R,2R) representing the number of times that each point of the stylus has contacted the surface.

The locus array will be compared to the actual surface array, either graphically or quantitatively to show the effect of the stylus geometry on the roughness parameters of the scanned surface. The contact array will show which part of the stylus is most often making contact with the surface and that helps in defining the appropriate stylus shapes for scanning such surfaces.

The algorithm is implemented in MATLAB for ease of array handling, etc., at the expense of relatively poor computational speed. Appendix A shows the Matlab program used for the simulation process. A simulation of scanning a 20 μm tip radius over an area of 300 μm by 300 μm takes about two hours to run on a Pentium II personal computer with 400 MHz speed and 64 MB ram. The operating system of the PC is Win98.

In this study, the simulation is achieved by theoretically scanning a small area of a surface with a stylus in 3D by the computer. The surface could be any set of data representing a real or an arbitrary surface. The stylus could also be any set of data representing a real or an arbitrary stylus shape. Both data sets of the surface and the stylus are dealt with as arrays.

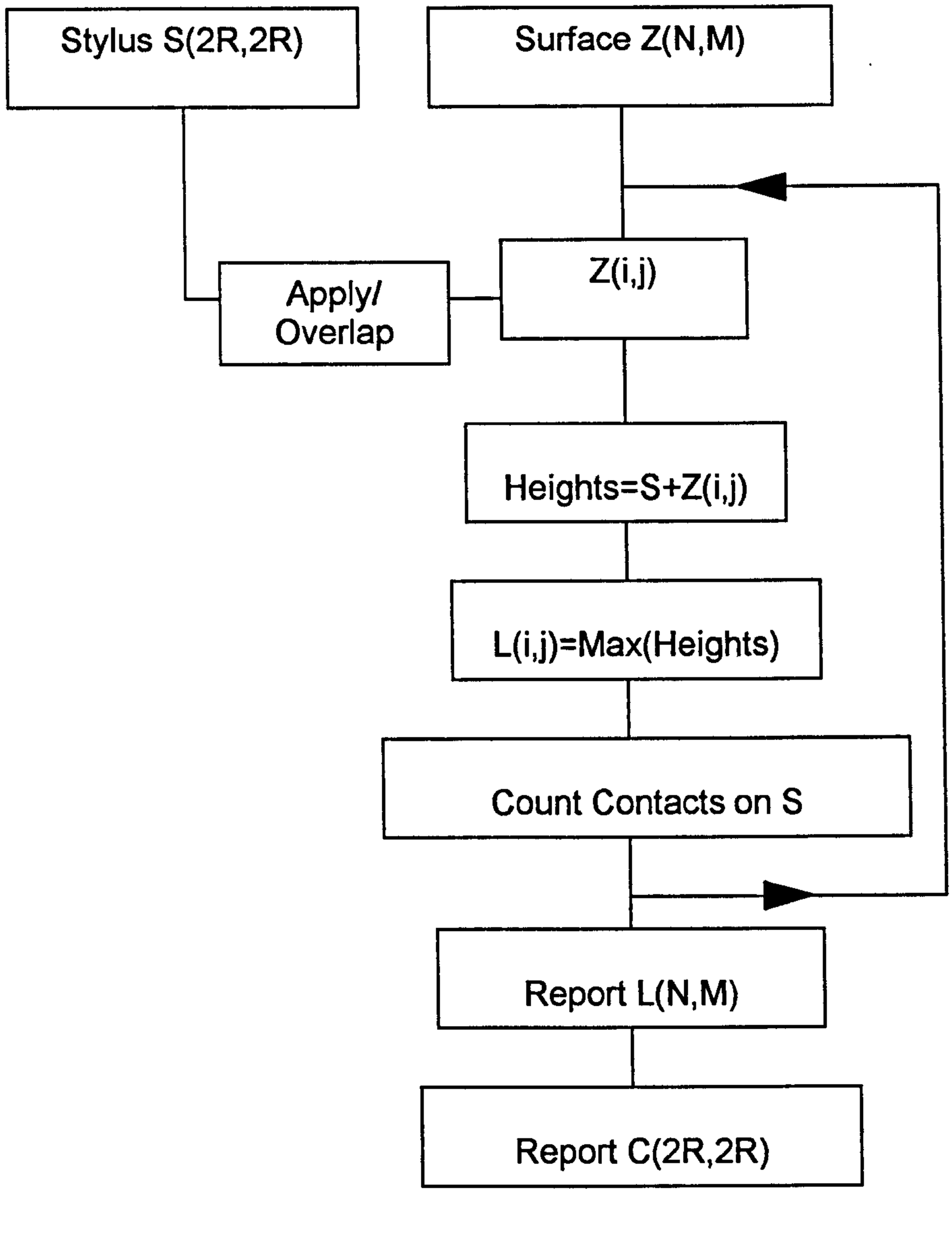

Figure 2.4: The algorithm of the simulation process.

2.3 Simulation on non-real surfaces

Initial testing of the simulation process was by scanning surfaces created by the computer with styli created also by the computer to simulate the real scanning process. Scanning over a computer created surface structures such as sinusoidal prismatic gratings demonstrated the expected patterns of distortion, mainly in the valleys. It helped to verify that the software correctly handled cases where, contingently, more than one contact point arises simultaneously. Test surfaces of laterally uncorrelated random data were generated by the internal MATLAB function. Scanning these generates accretions of copies of the stylus tip profile and tests the collection of contact statistics since the extreme points dominate the contact conditions.

Three ideal (computer generated) stylus tips with different shapes have been used: conical, pyramid and spherical tips. The heights of all tips are 5 μm and 10 μm. The tip angles of the conical and pyramid shapes are 90°. The tip radius of the spherical shape is 5 μm and 10 μm. Each tip has been used in three forms: the perfect shape, and with truncation at 1 μm and 2 μm truncation below the original tip, representing an ideal wear process. Figure 2.5 shows both 20 μm perfect tips and "worn" tips (truncated) and figure 2.6 shows both 10 μm perfect tips and "worn" tips (truncated).

Three different surfaces have been used in the simulation to represent real surfaces with both regular and random surface roughness features. The surfaces are Sinusoidal, random and random normalised shapes and are shown in figure 2.7. The wavelength of the sine wave surface has been set to 60μm to be close to the real pattern of a surface produced by traditional machining process (Turning or Scraping). All the surfaces generated by the computer have the same maximum peak to valley heights of 20 μm which should be enough for the 10μm to fully penetrate the surface.

Each surface has been scanned with all different styli tips and the locus of each tip has been reported as well as the contact distribution on the tip when scanning each surface. To quantify the results, roughness parameters have been calculated for all outputs as well as the original surfaces. A commercial software package which is designed for processing roughness measurements has been used to calculate the roughness parameters (SPIP). Appendix B shows the definitions and the calculations of the Roughness parameters implemented by this software.

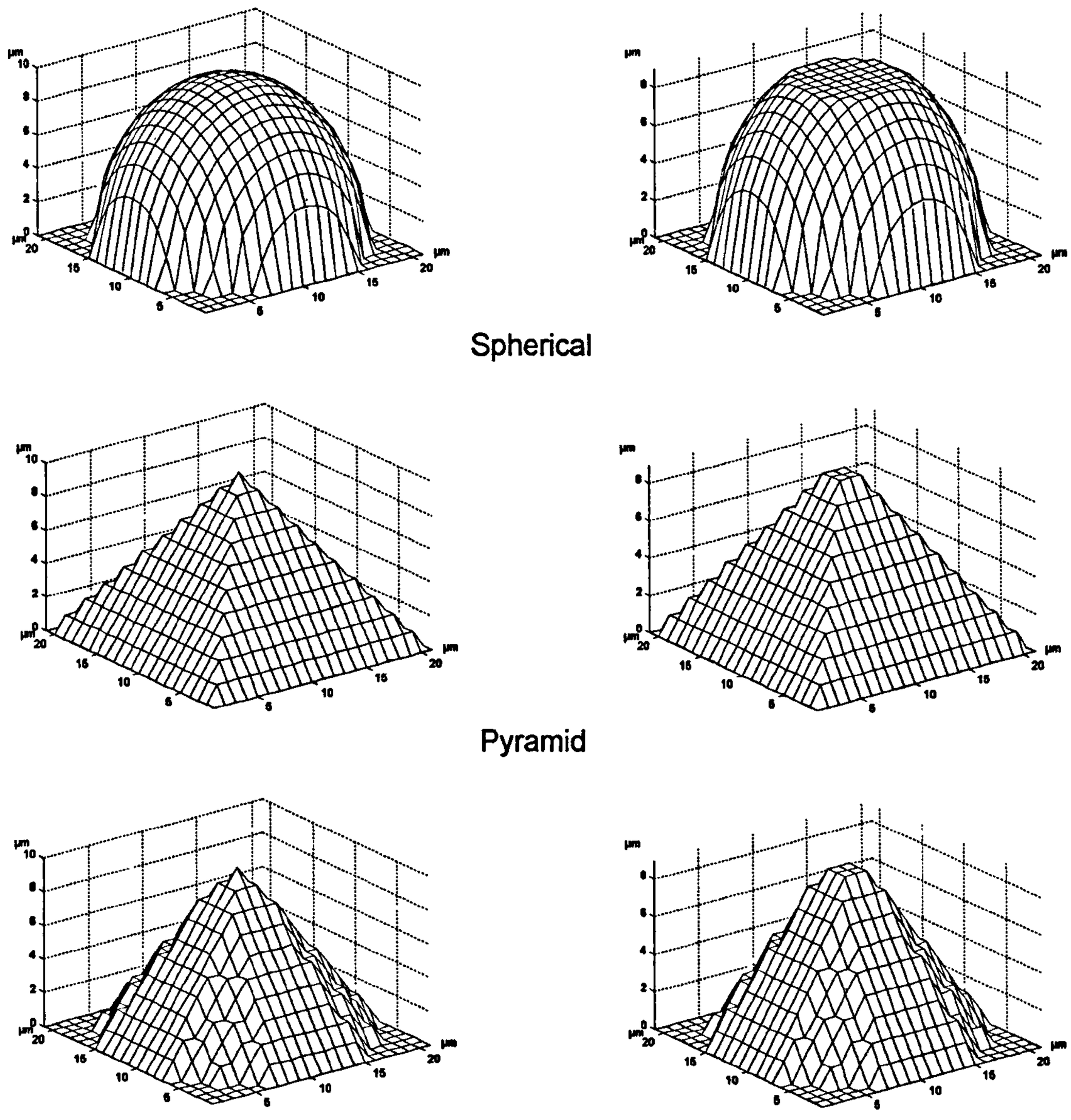

Figure 2.5: Perfect and truncated 10 μm styli tip shapes

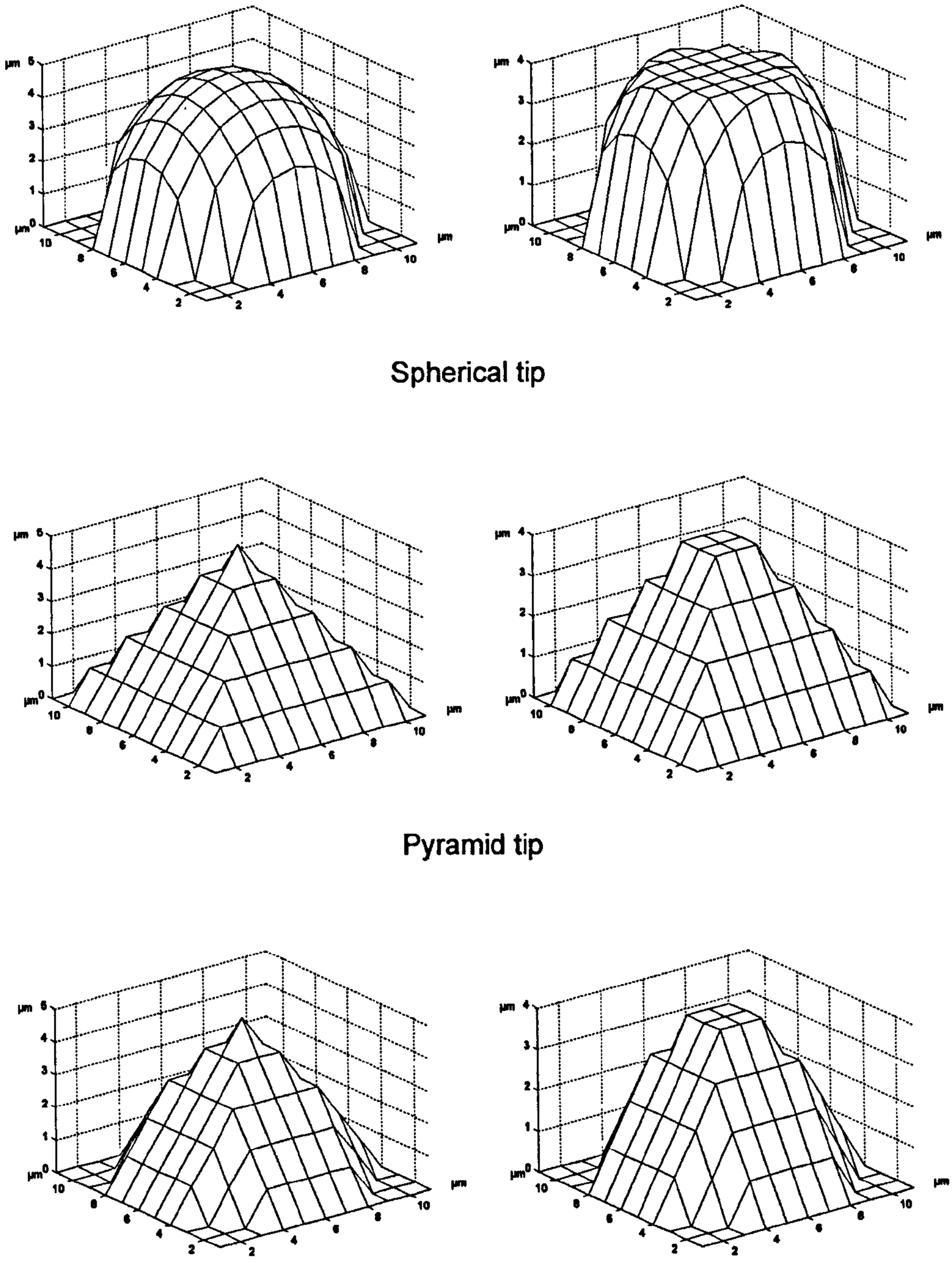

Figure 2.6: Perfect and truncated 5 µm styli tip shapes

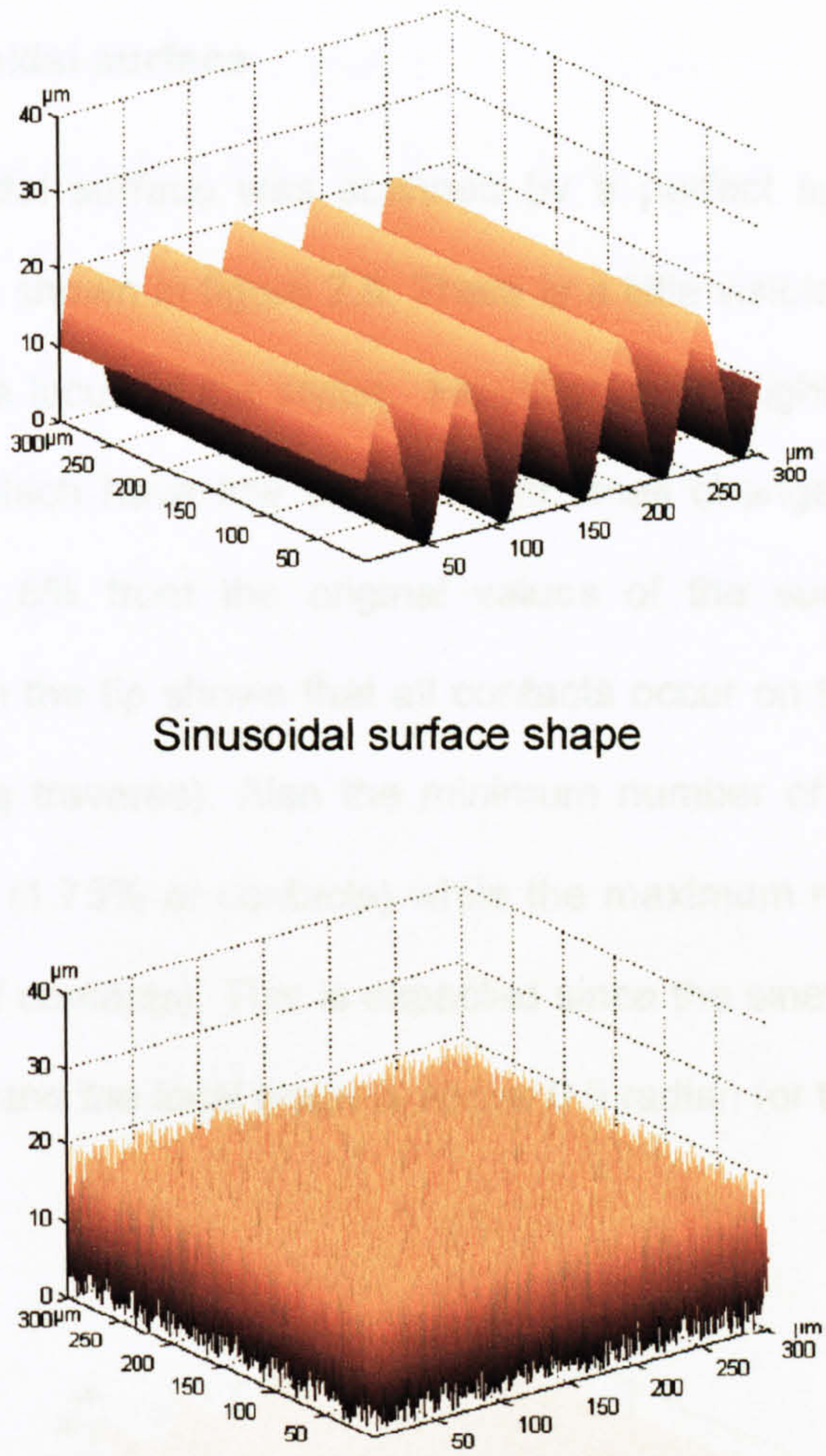

Sinusoidal surface shape

Random surface shape

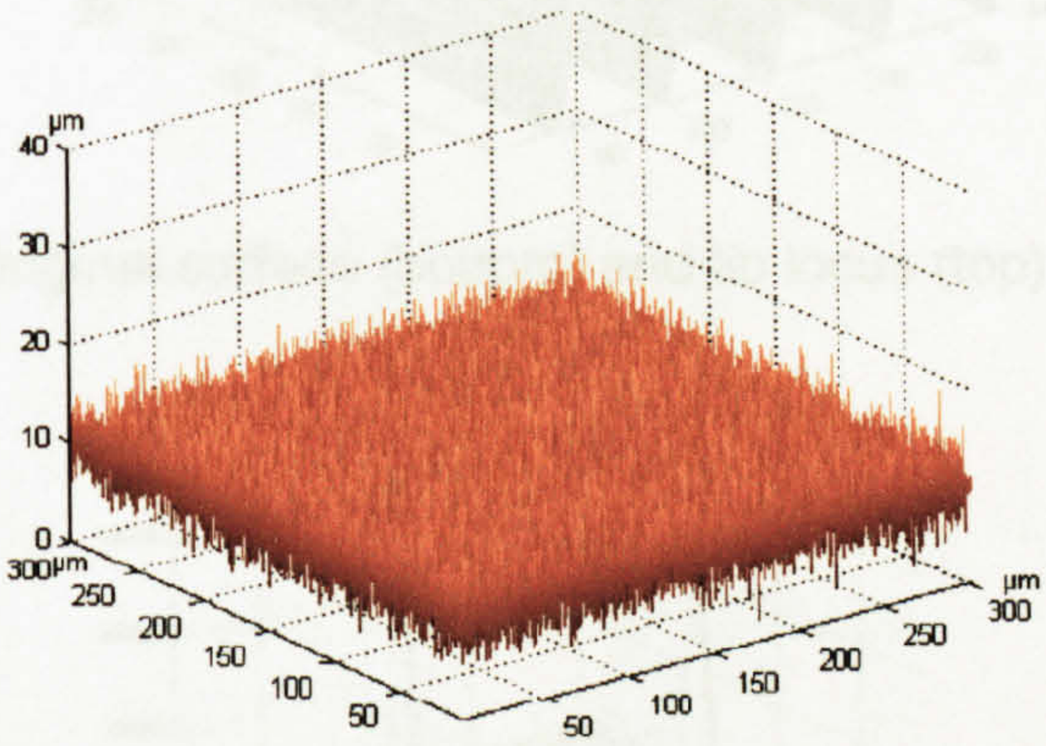

Random Gaussian surface shape

Figure 2.7: Computer generated surfaces shapes

2.3.1 Scanning sinusoidal surface

The simulated sinosoidal surface was scanned by a perfect spherical tip with 10 μm radious, the results are shown in figure 2.8. There is a little visible difference between the original surface and the locus of the stylus. However, even highly averaging parameters such as Sa and Sq which have low sensitivity to small changes of shape, have been reduced by 10% and 8% from the original values of the surface, respectively. The contacts distribution on the tip shows that all contacts occur on the central line of the tip crossing the lay (along traverse). Also the minimum number of contacts occurs on the central point of the tip (1.75% of contacts) while the maximum number is on the two far ends of the tip (21% of contacts). This is expected since the sinewave wavelength is only a few times the height and the local slope is above 0.5 radian for the majority of the cycle.

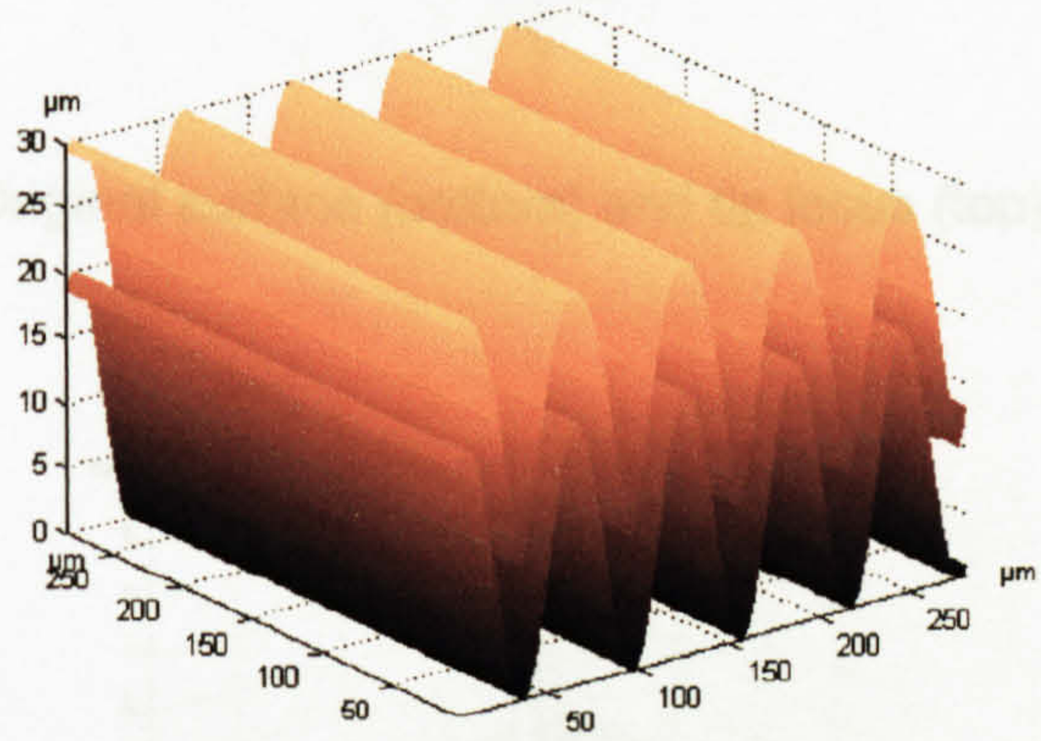

Original surface (bottom) and tip locus (top)

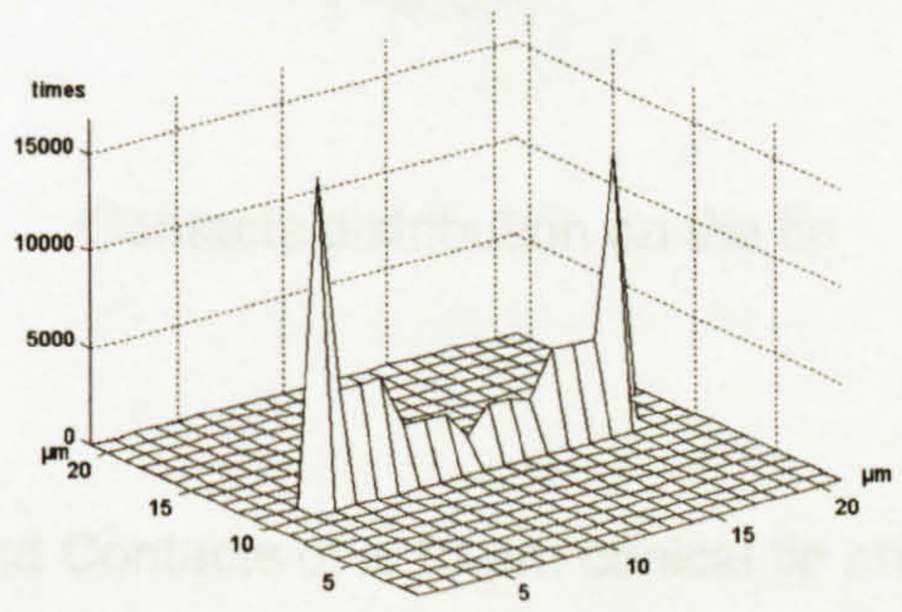

Contacts distribution on the tip

Figure 2.8: Locus and Contacts of a 10μm spherical tip on a sinusoidal surface

The same sinosoidal surface was scanned by a 10 μm perfect conical tip perfect conical tip and the results are shown in figure 2.9. There is also a little visible difference between the original surface and the locus of the stylus. The roughness parameters Sa and Sq are nearly the same as the original values of the surface. The contacts distribution on the tip shows that most contacts (32.5%) occur at the central point of the tip.

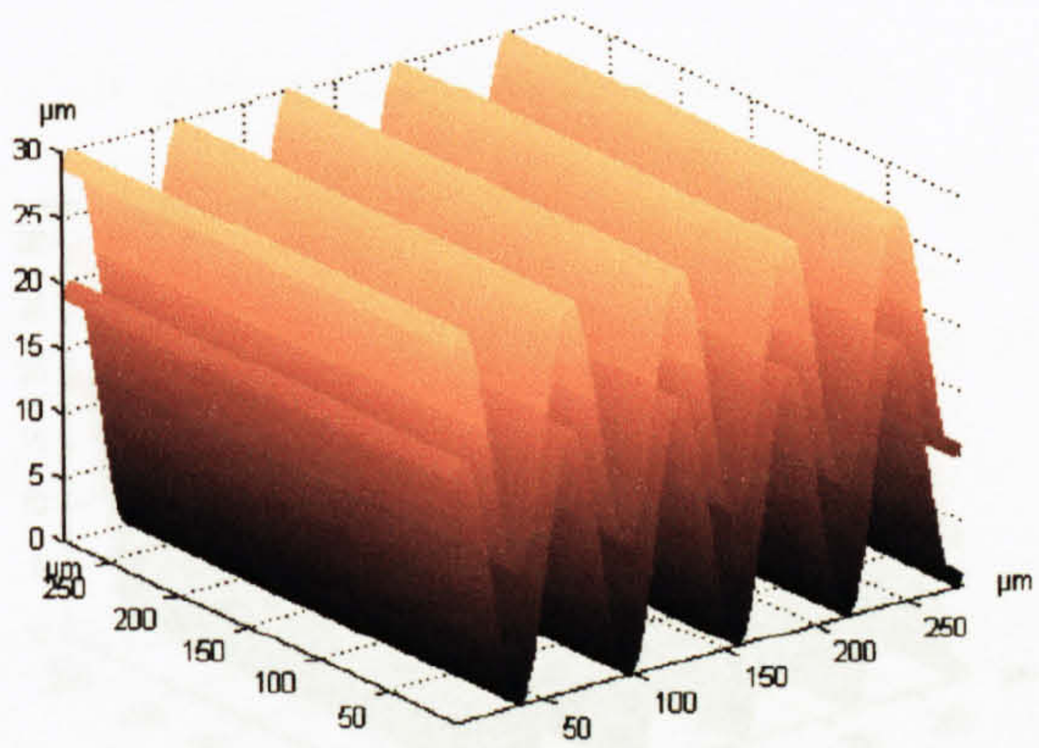

Original surface (bottom) and tip locus (top)

Contacts distribution on the tip

Figure 2.9: Locus and Contacts of a 10 μm conical tip on a sinusoidal surface

Then a 10 μm perfect conical tip was used to scan the sinosoidal surface and the results are shown in figure 2.10. There is also a little visible difference between the original surface and the locus of the stylus. The roughness parameters Sa and Sq are nearly the same as the original values of the surface. The contacts distribution on the tip shows that most contacts (22.5%) occur on the central point of the tip. It is noticed that the distribution of the few contacts at the tip of the conical and pyramid tips reflect the shapes of their respective flank surfaces.

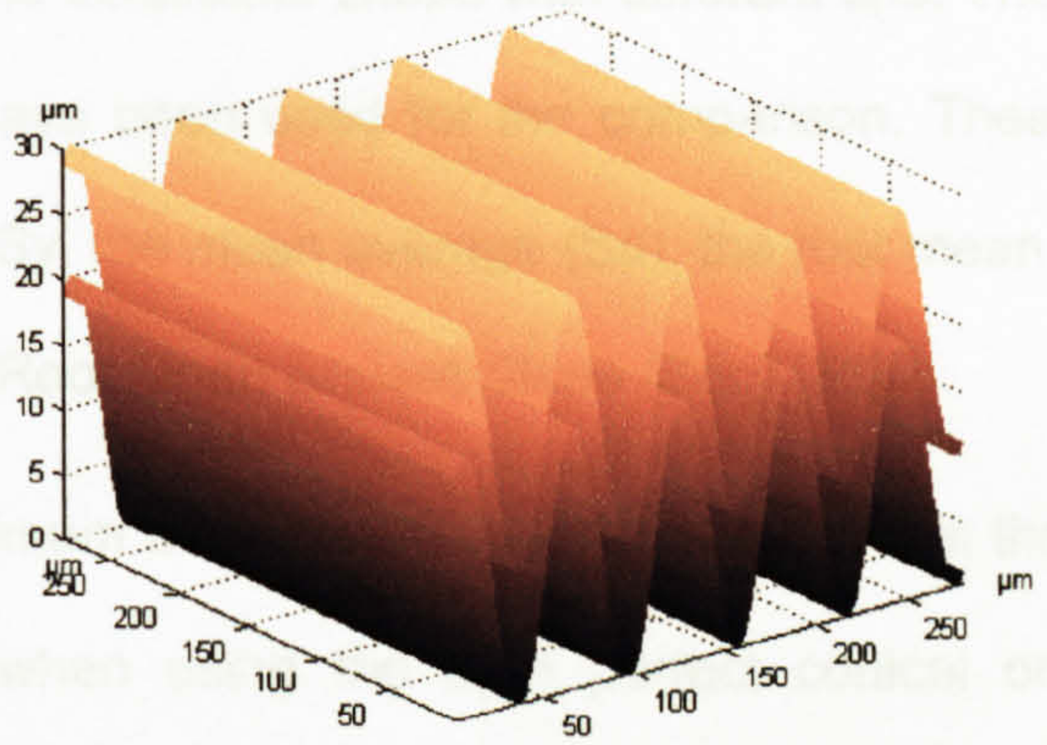

Original surface (bottom) and tip locus (top)

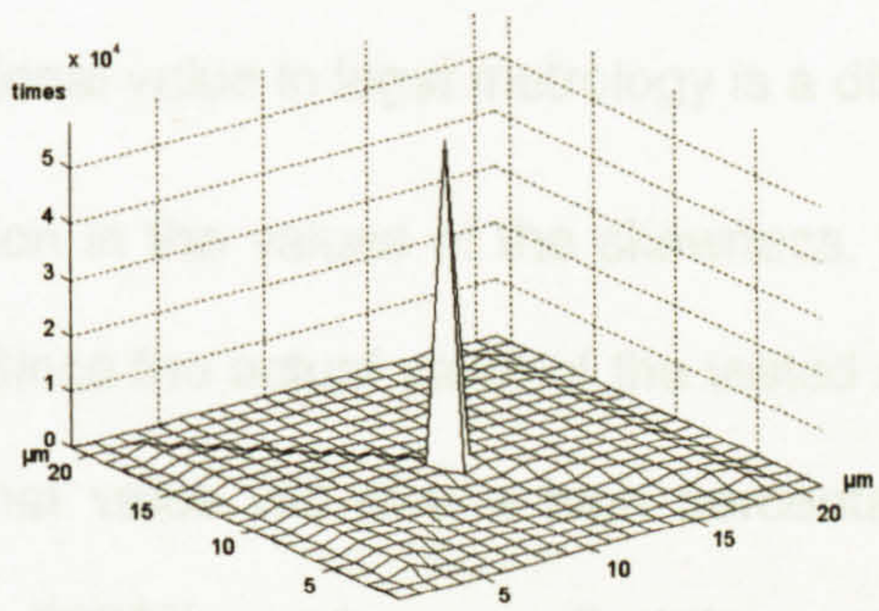

Contacts distribution on the tip

Figure 2.10: Locus and Contacts of a 10 μm pyramid tip on a sinusoidal surface

The contacts distributions on two different 10 μm tips when truncated by 1 and 2 μm below the original tips are shown in figure 2.11. It is clear that the contacts distribution on each tip differs significantly according to the tip shape. While the conical and the pyramid tips are showing very close results.

Scanning the sinusoidal surface with same tips as before, but with different dimensions (5μm) has shown nearly the same locus and contact distributions shapes as the 10μm tips. Table 2.1 shows the percentage error of the roughness parameters of different outputs when scanning the sinusoidal shape with different tips. The most commonly used roughness parameters have been used for the comparison. These parameters are: the maximum peak to valley Sy, the mean average (Sa), the root mean square value (Sq), the Skewness (Ssk) and the Root Mean Square Slope (Sdq) [33].

It is noticed that the minimum deviation of the parameters from their actual values of the surface always occurs when using the 5μm perfect conical or pyramid shape. The maximum deviation occurs when using the truncated 10 μm spherical tip. The worst case deviation in Sq is less than 14% from the actual value which will somtimes be important but in many applications such variations could have limitid functional significance. The position with meeting conditional value in legal metrology is a different issue.

There is an extreme deviation in the values of the skewness. Most real surfaces have a skewness in the range ±2. Since the actual value of the tested sinusoidal surface is -0.01, any small deviation from that value will give a high percentage error. The worst case deviation in the skewness is 8398% which means that the measured skewness is 0.8298 while the actual one is -0.01.

The 10 μm spherical tip with 2 μm truncation has the worst effect on the roughness parameters. It has reduced Sa nearly by 16%, Sq by 14% and Sy by 10% from their actual values. It has reduced the root mean square slope by only 1.81% from the actual value.

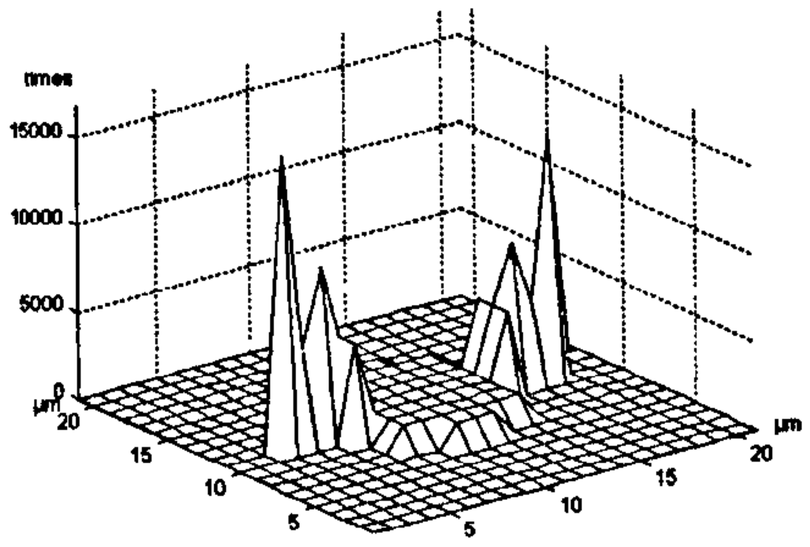

1 μm truncation

Spherical tip

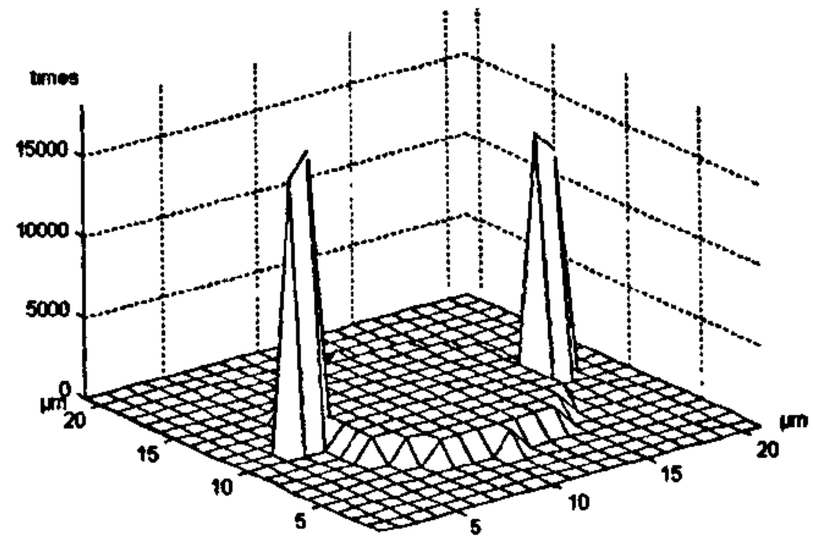

2 μm truncation

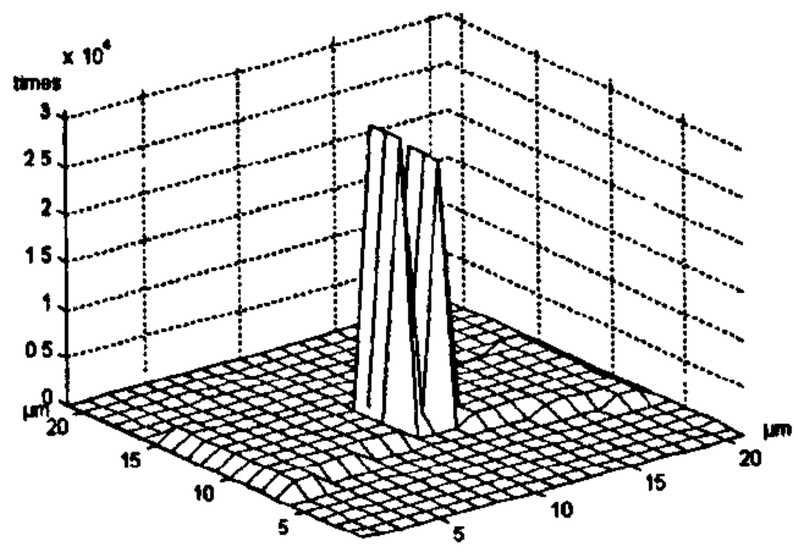

1 μm truncation

Conical tip

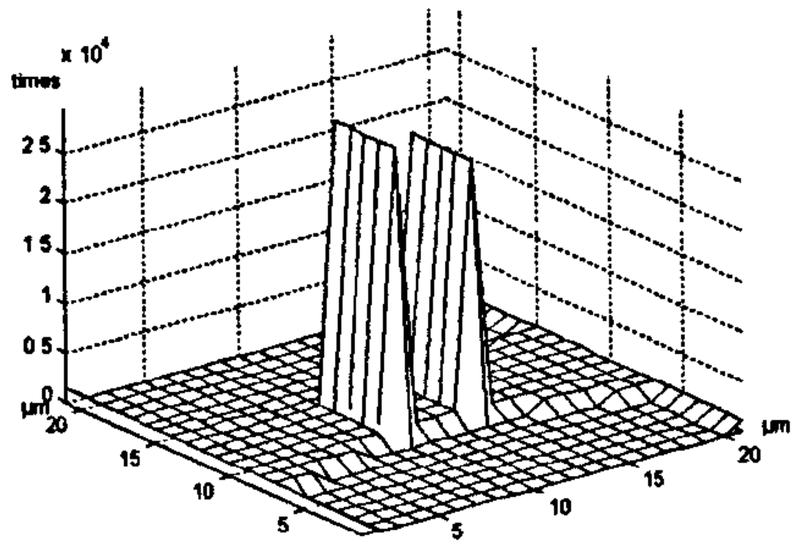

2 μm truncation

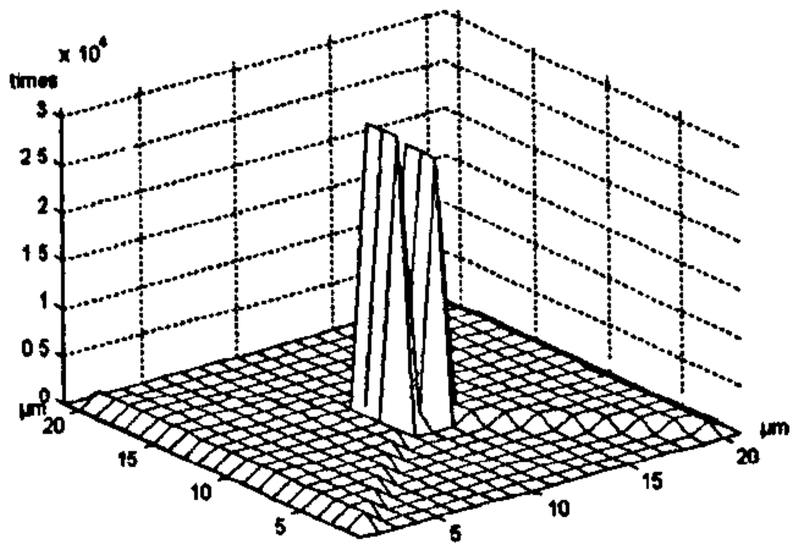

1 μm truncation

Pyramid tip

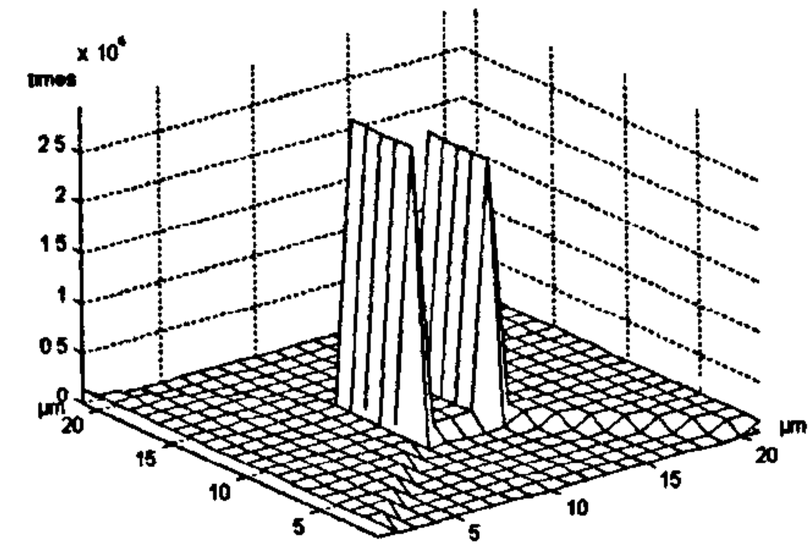

2 μm truncation

Figure 2.11: Contacts distributions of 10 μm truncated tips on a sinusoidal surface

		Parameter (μm)	Sa	Sq	Sy	Ssk	Sdq
			6.47	7.17	20.00	-0.01	0.73
Tip	Size	Shape	% error				
Conical	5 μm	Perfect	-0.26	-0.09	0.00	131.60	-0.03
		1 μm Truncated	-0.65	-0.53	-0.27	1498.14	-0.04
		2 μm Truncated	-2.00	-1.77	-1.09	2850.79	-0.05
	10 μm	Perfect	-0.34	-0.13	0.00	149.40	-0.08
		1 μm Truncated	-0.77	-0.60	-0.27	1527.58	-0.09
		2 μm Truncated	-2.19	-1.89	-1.09	2898.01	-0.12
Spherical	5 μm	Perfect	-2.39	-1.83	0.00	3344.14	0.05
		1 μm Truncated	-4.07	-3.70	-2.45	4156.75	-0.17
		2 μm Truncated	-6.82	-6.34	-4.32	5473.15	-0.46
	10 μm	Perfect	-9.62	-7.66	-0.15	6546.66	0.55
		1 μm Truncated	-11.89	-10.12	-5.00	7323.38	-0.50
		2 μm Truncated	-15.32	-13.84	-9.55	8398.17	-1.81
Pyramid	5 μm	Perfect	-0.26	-0.09	0.00	131.60	-0.03
		1 μm Truncated	-0.65	-0.53	-0.27	1498.14	-0.04
		2 μm Truncated	-2.00	-1.77	-1.09	2850.79	-0.05
	10 μm	Perfect	-0.34	-0.13	0.00	149.40	-0.08
		1 μm Truncated	-0.77	-0.60	-0.27	1527.58	-0.09
		2 μm Truncated	-2.19	-1.89	-1.09	2898.01	-0.12

% error=100*(Measured Value - Actual Value)/ actual Value

Table 2.1: % error of roughness parameters of different tips on the Sinusoidal surface

2.3.2 Scanning random surface

The output of scanning the random surface with the 10 μm radius perfect spherical tip is shown in figure 2.12. As expected on this data, which has much higher bandwidth than the effective stylus filter, the locus of the stylus is almost flat. Sa and Sq have been reduced by 94% and 93.5% from the original values of the surface, respectively. The reason of using such surface is to fully sample the tip with the high bandwidth surface. The contact distributions, models the tip shape providing further verification for the process and software implementation. The maximum number of contacts occurs at the central point of the tip (3.6% of contacts).

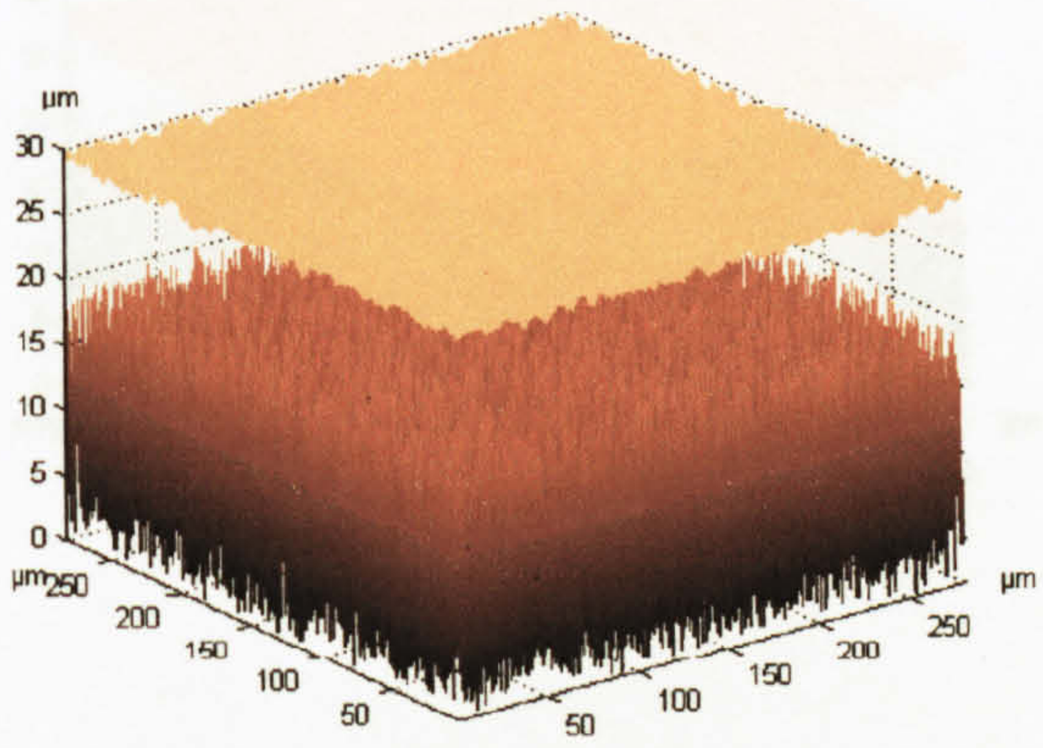

Original surface (bottom) and tip locus (top)

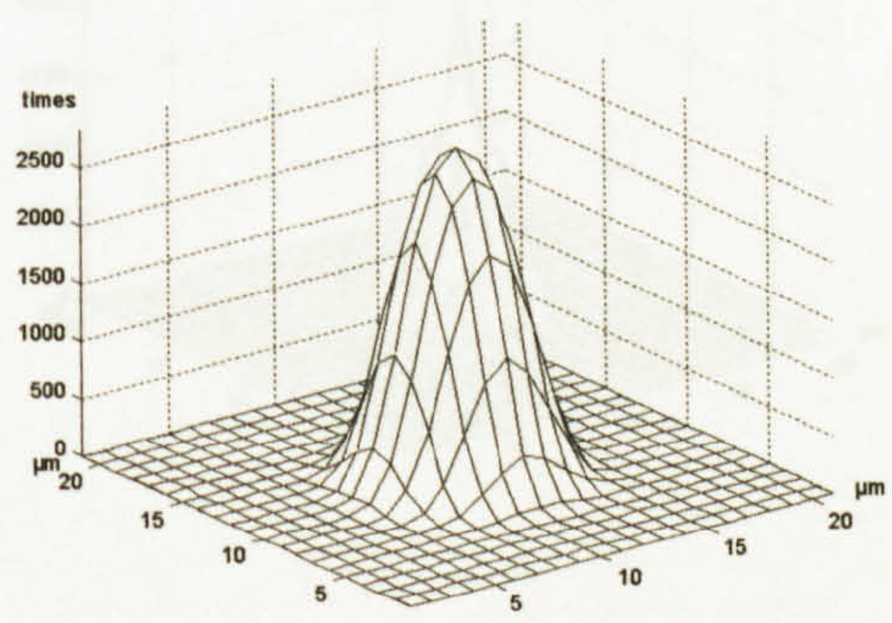

Contacts distribution on the tip

Figure 2.12: Locus and Contacts of a 10 μm spherical tip on a random surface

The output of scanning the random surface with a 10 μm perfect conical tip is shown in figure 2.13. There is also a large visible difference between the original surface and the locus of the stylus. There is a visible difference from that generated by the spherical tip. The roughness parameters Sa and Sq have been reduced by 87% and 85.5% from the original values of the surface, respectively. The contacts distribution on the tip shows that all contacts occur around the central point of the tip within an 8μm square area of the tip and looking like the tip shape. The maximum number of contacts occurs at the central point of the tip (11.4% of contacts).

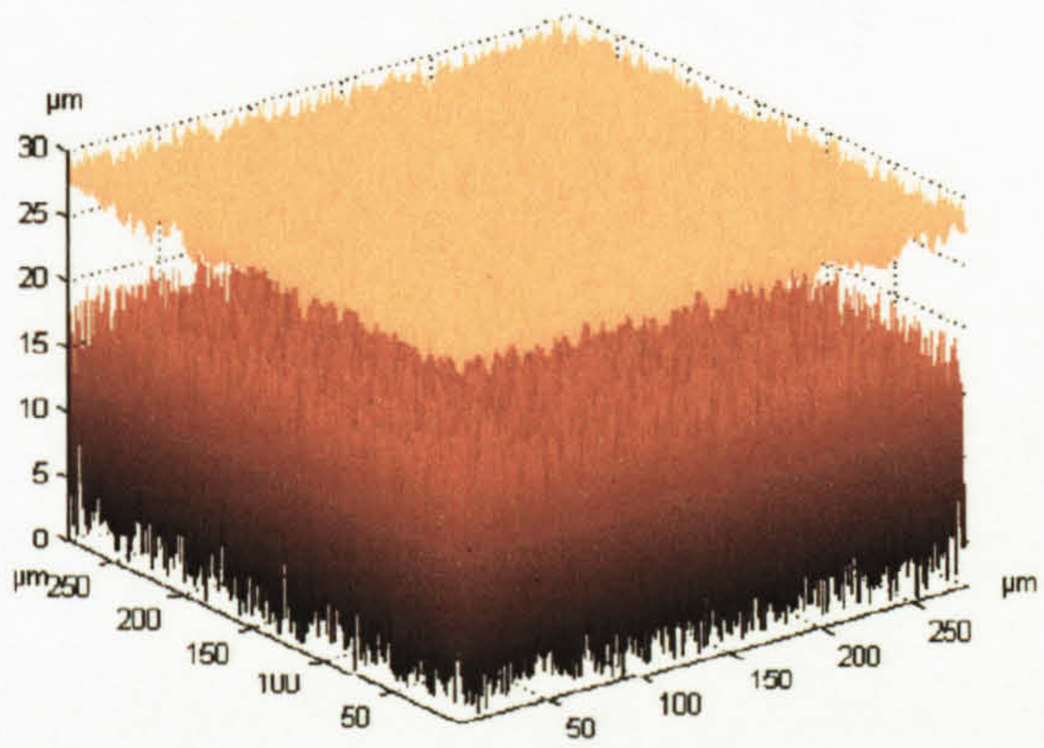

Original surface (bottom) and tip locus (top)

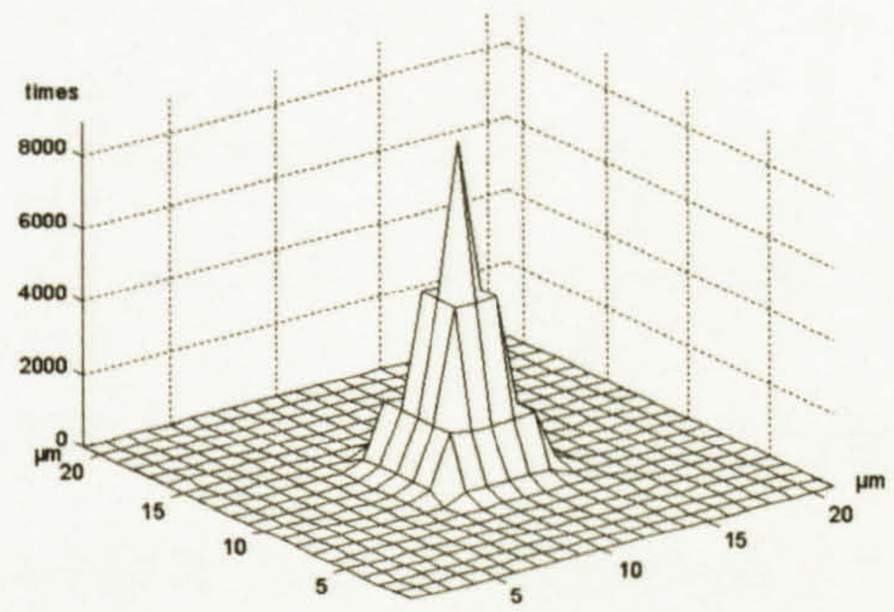

Contacts distribution on the tip

Figure 2.13: Locus and Contacts of a 10 μm conical tip on a random surface

The output of scanning the random surface with a 10 μm perfect pyramid tip is shown in figure 2.14. There is also a large visible difference between the original surface and the locus of the stylus. The surface is visibly similar to that from the conical tip. The roughness parameters Sa and Sq have been reduced by 87% and 86% from the original values of the surface, respectively. The contacts distribution on the tip shows that all contacts occur around the central point of the tip within an 8μm square area of the tip and looking like the tip shape. The maximum number of contacts occurs at the central point of the tip (11.4% of contacts).

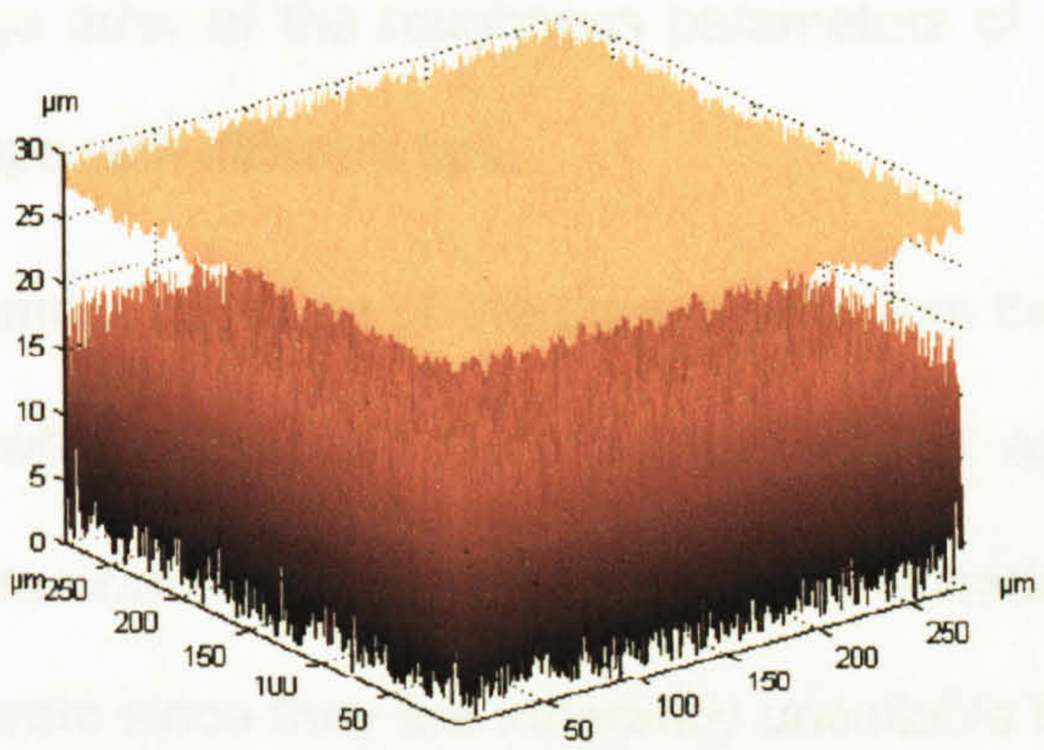

Original surface (bottom) and tip locus (top)

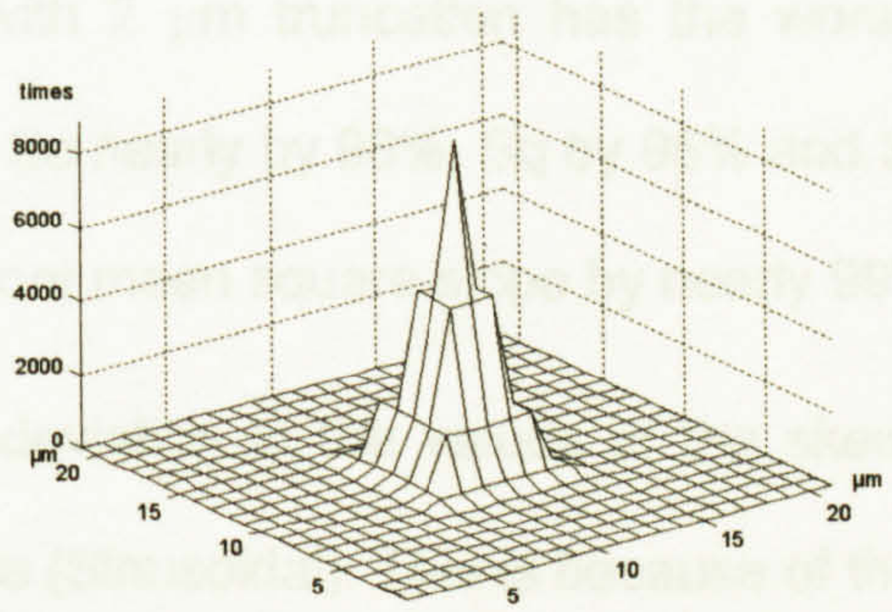

Contacts distribution on the tip

Figure 2.14: Locus and Contacts of a 10 μm pyramid tip on a random surface

The contacts distributions of the 1 and 2 μm truncated tips when scanning the random surface are shown in figure 2.15. The conical and the pyramid tips show nearly identical results. Generally, the large majority of the contacts sample uniformly the platform area of the truncated shape, with few flank contacts. This could be expected for such high bandwidth original surface.

Scanning the random surface with same tips as before, but with different sizes (5μm) resulted in nearly the same locus and contact distributions shapes as the 10μm tips. Table 2.2 shows the percentage error of the roughness parameters of different outputs when scanning the random shape with different tips.

It is noticed that the minimum deviation of the parameters from their actual values of the surface always occurs when using the 5μm perfect conical or pyramid shape. The maximum deviation occurs when using the truncated 10 μm spherical tip. However, all the tips provide very large errors since they are inherently unsuitable for such a surface. The difference between the result from the ideal conical or pyramid tips and from spherical and truncated ones is significant.

The 10 μm spherical tip with 2 μm truncation has the worst effect on the roughness parameters. It has reduced Sa nearly by 98%, Sq by 98% and Sy by 93% from their actual values. It has reduced the root mean square slope by nearly 99% from the actual value.

There is also an extreme deviation in the values of the skewness even more than the values with previous surface (Sinusoidal). This is because of the actual value of the tested surface which is typically -0.003. The worst case deviation in the skewness is 53293% which means that the measured skewness is 1.63 while the actual one is -0.003.

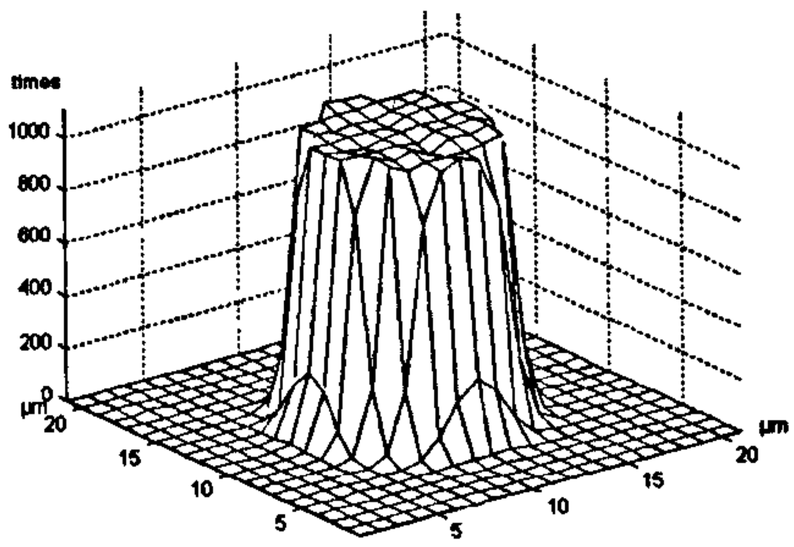

1 µm truncation

Spherical tip

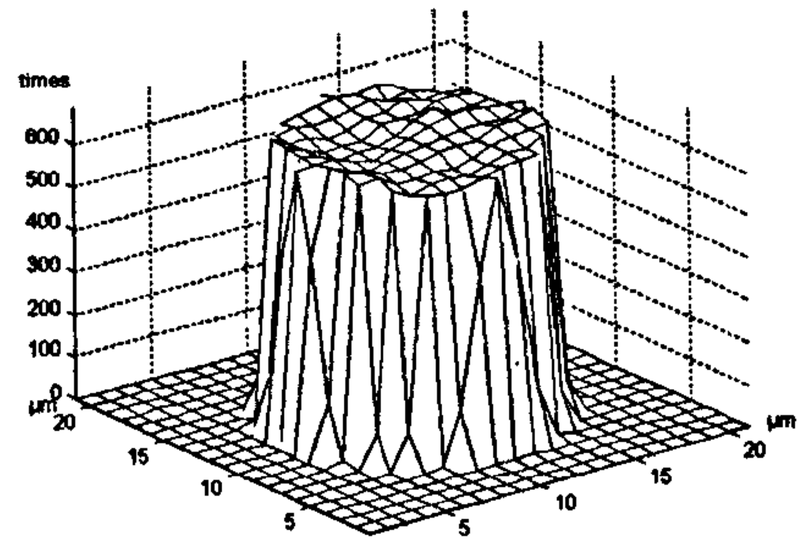

2 µm truncation

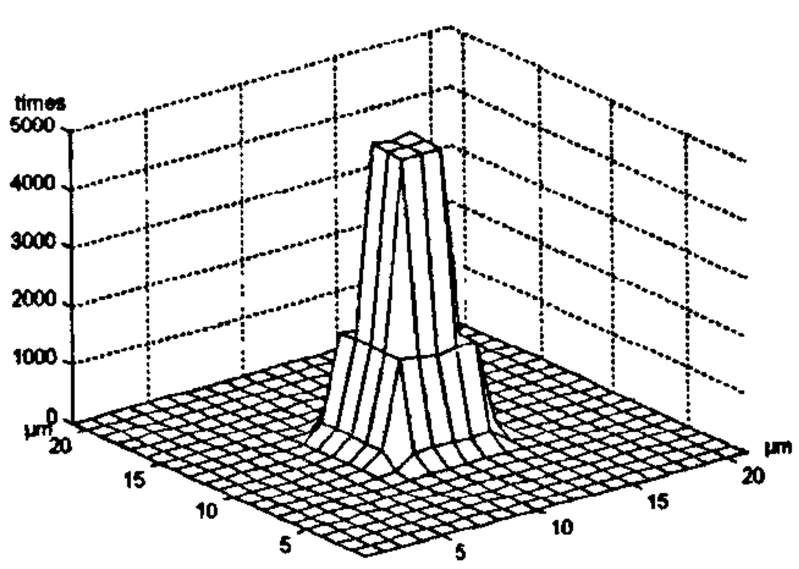

1 µm truncation

Conical tip

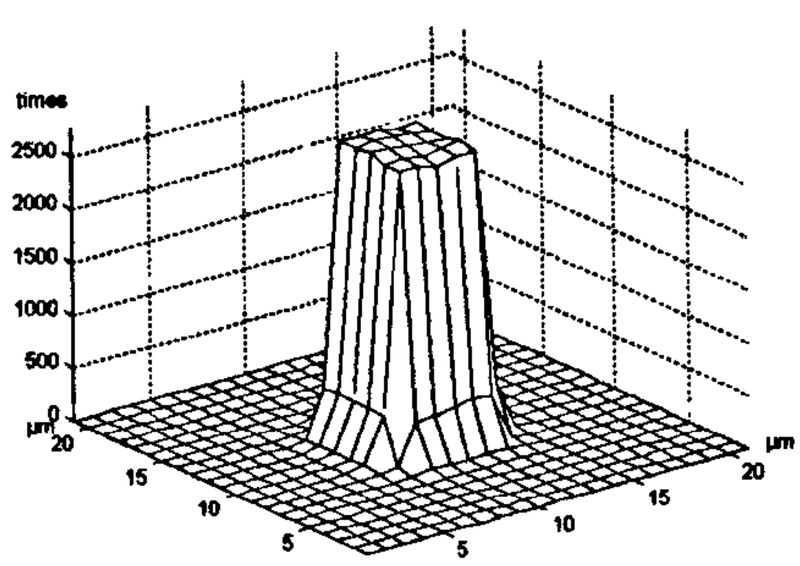

2 µm truncation

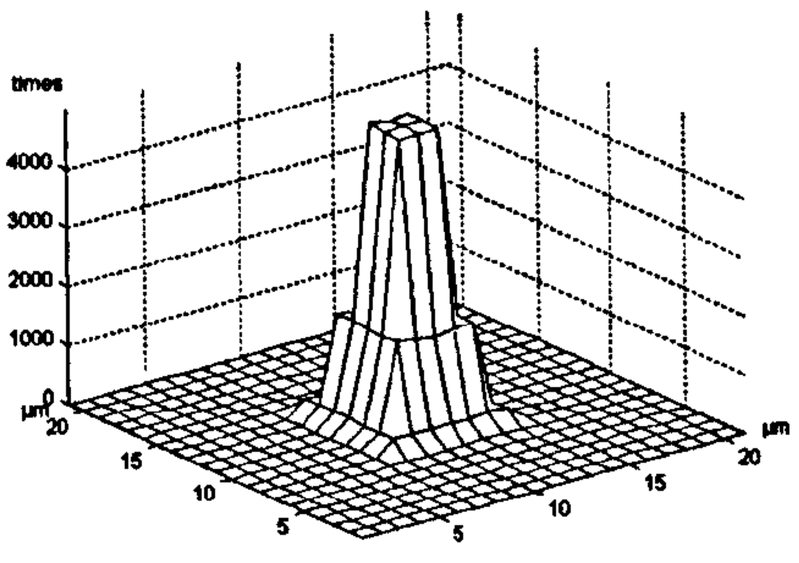

1 µm truncation

Pyramid tip

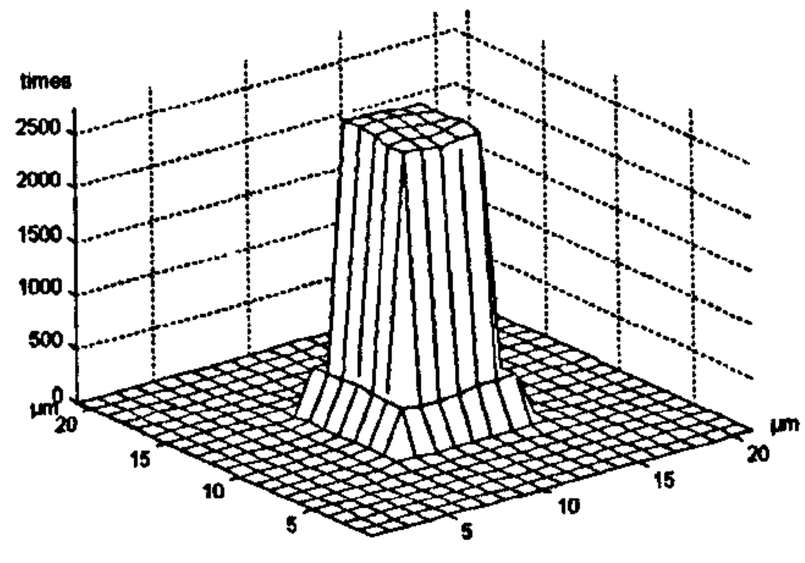

2 µm truncation

Figure 2.15: Contacts distributions of 10 µm truncated tips on a random surface

		Parameter (μm)	Sa	Sq	Sy	Ssk	Sdq
			5.01	5.78	20.00	0.00	11.52
Tip	Size	Shape	% error				
Conical	5 μm	Perfect	-86.95	-85.76	-72.03	3607.60	-92.30
		1 μm Truncated	-87.97	-87.05	-77.03	13566.07	-93.67
		2 μm Truncated	-90.99	-90.47	-82.03	31785.37	-95.57
	10 μm	Perfect	-86.95	-85.76	-72.03	3610.76	-92.30
		1 μm Truncated	-87.97	-87.05	-77.03	13570.11	-93.67
		2 μm Truncated	-90.99	-90.47	-82.03	31813.01	-95.57
Spherical	5 μm	Perfect	-91.03	-90.29	-77.21	24061.62	-96.22
		1 μm Truncated	-93.40	-92.66	-81.44	43131.99	-96.85
		2 μm Truncated	-95.27	-94.55	-82.70	54267.66	-97.60
	10 μm	Perfect	-94.01	-93.51	-86.72	22188.02	-97.89
		1 μm Truncated	-96.41	-95.99	-91.17	45311.99	-98.53
		2 μm Truncated	-97.73	-97.41	-93.30	53293.05	-99.02
Pyramid	5 μm	Perfect	-87.04	-85.93	-72.70	1941.17	-92.35
		1 μm Truncated	-88.08	-87.23	-77.70	11798.31	-93.73
		2 μm Truncated	-91.19	-90.76	-82.70	29440.40	-95.68
	10 μm	Perfect	-87.04	-85.93	-72.70	1941.17	-92.35
		1 μm Truncated	-88.08	-87.23	-77.70	11798.31	-93.73
		2 μm Truncated	-91.19	-90.76	-82.70	29440.40	-95.68

% error=100*(Measured Value - Actual Value)/ actual Value

Table 2.2: % error of roughness parameters of different tips on the random surface

2.3.3 Scanning random Gaussian surface

The output of scanning the random Gaussian surface with the 10 μm radius perfect spherical tip is shown in figure 2.16. There is a large visible difference between the original surface and the locus of the stylus. Because the distribution contains fewer points at extreme heights, the output appears as small replicas of the tip. The roughness parameters Sa and Sq have been reduced by 59% and 59% from the original values of the surface, respectively. The contacts distribution on the tip shows that all contacts occur around the central point of the tip within a 7μm radius circle and looking like a bell shape. The maximum number of contacts is occurring at the central point of the tip (2% of contacts).

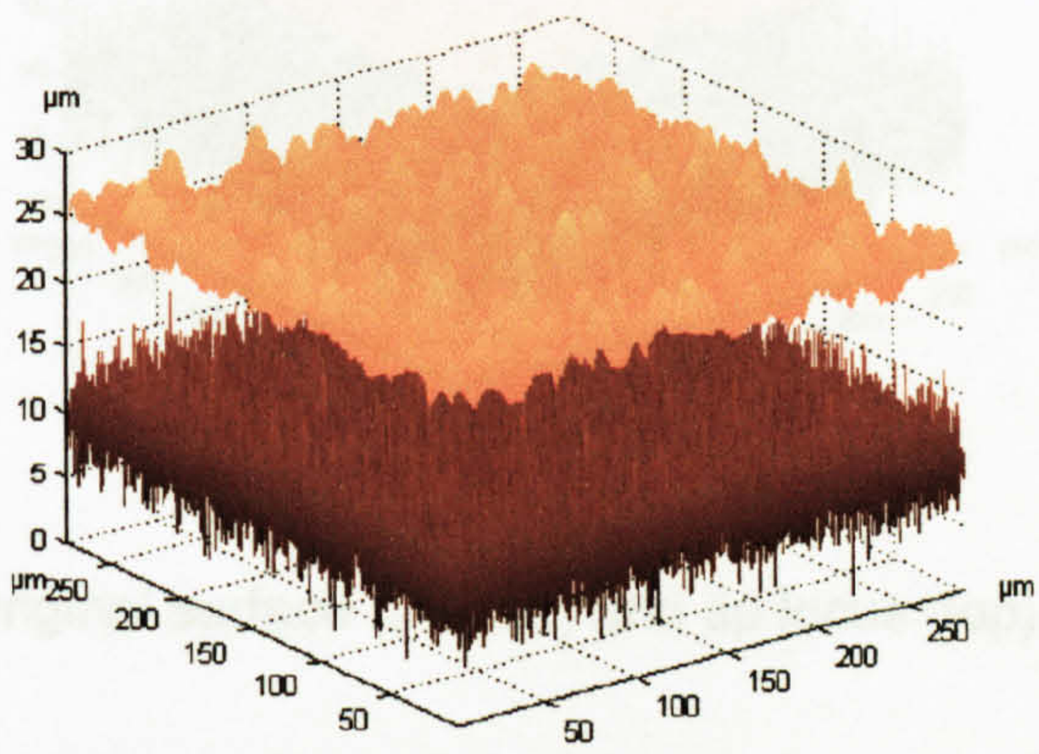

Original surface (bottom) and tip locus (top)

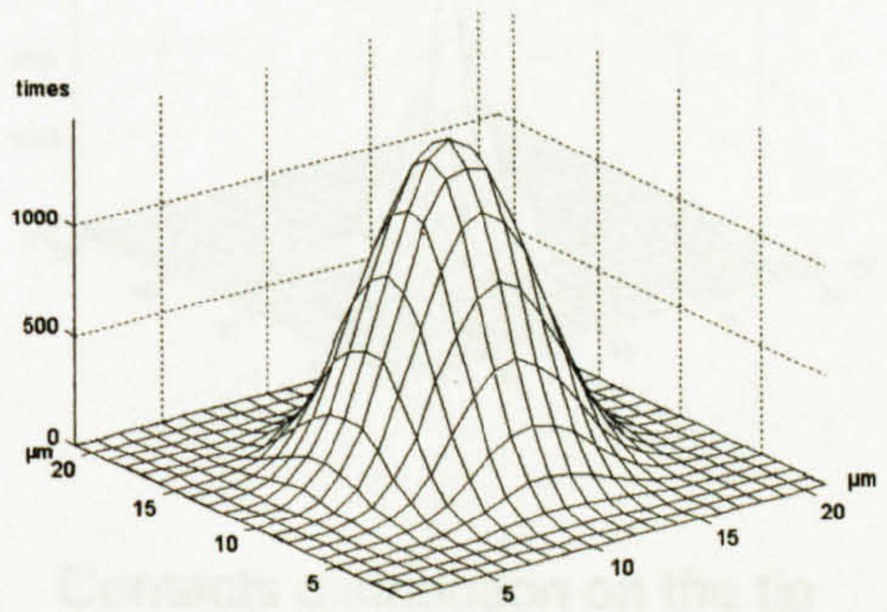

Contacts distribution on the tip

Figure 2.16: Locus and Contacts of a 10 μm spherical tip on a random Gaussian surface

The output of scanning the random Gaussian surface with a 10 μm perfect conical tip is shown in figure 2.17. There is also a large visible difference between the original surface and the locus of the stylus. The roughness parameters Sa and Sq have been reduced by 53% and 52.5% from the original values of the surface, respectively. The contacts distribution on the tip shows that all contacts occur around the central point of the tip within an 8 μm square area of the tip and looking like the tip shape. The maximum number of contacts occurs at the central point of the tip (10.5% of contacts).

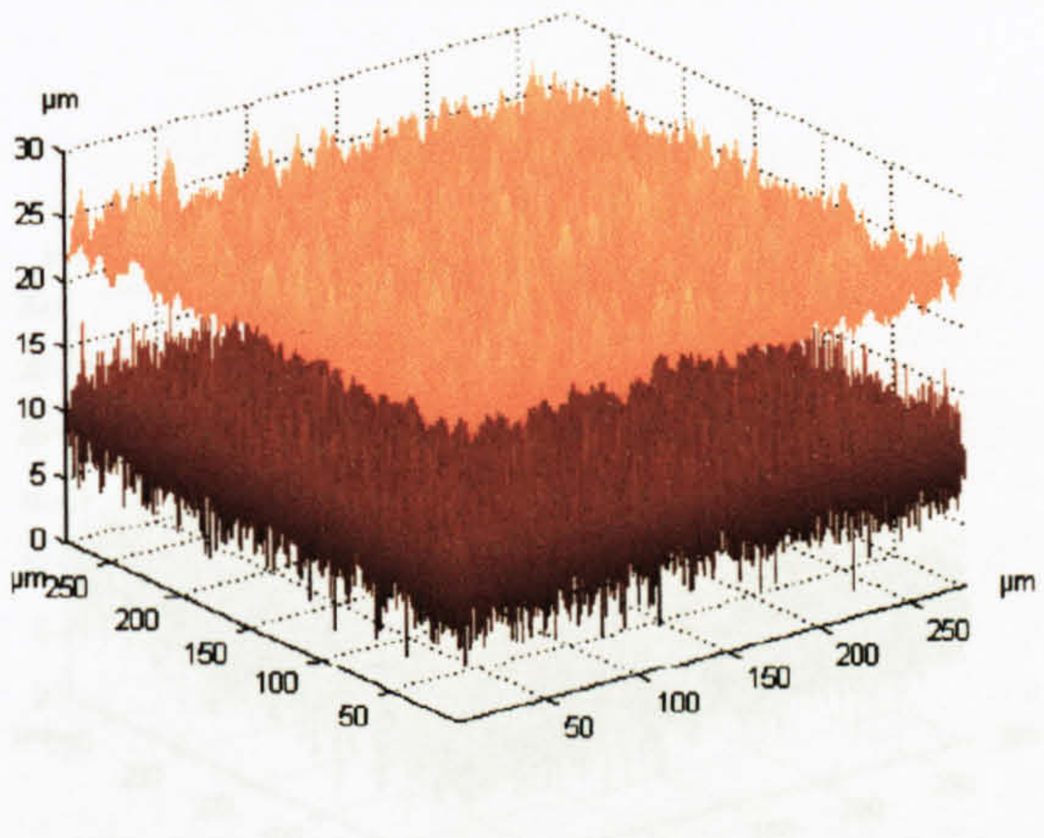

Original surface (bottom) and tip locus (top)

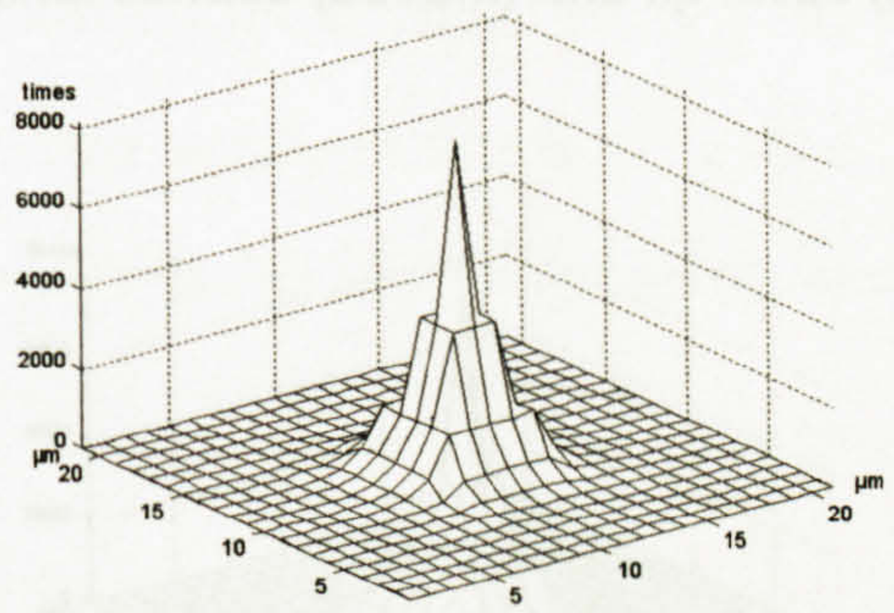

Contacts distribution on the tip

Figure 2.17: Locus and Contacts of a 10 μm conical tip on a random Gaussian surface

The output of scanning the random Gaussian surface with a 10 μm perfect pyramid tip is shown in figure 2.18. There is also a large visible difference between the original surface and the locus of the stylus. The roughness parameters Sa and Sq have been reduced by 53.5% and 53% from the original values of the surface, respectively. The contacts distribution on the tip shows that all contacts occur around the central point of the tip within an 8μm square area of the tip and looking like the tip shape. The maximum number of contacts occurs at the central point of the tip (10% of contacts).

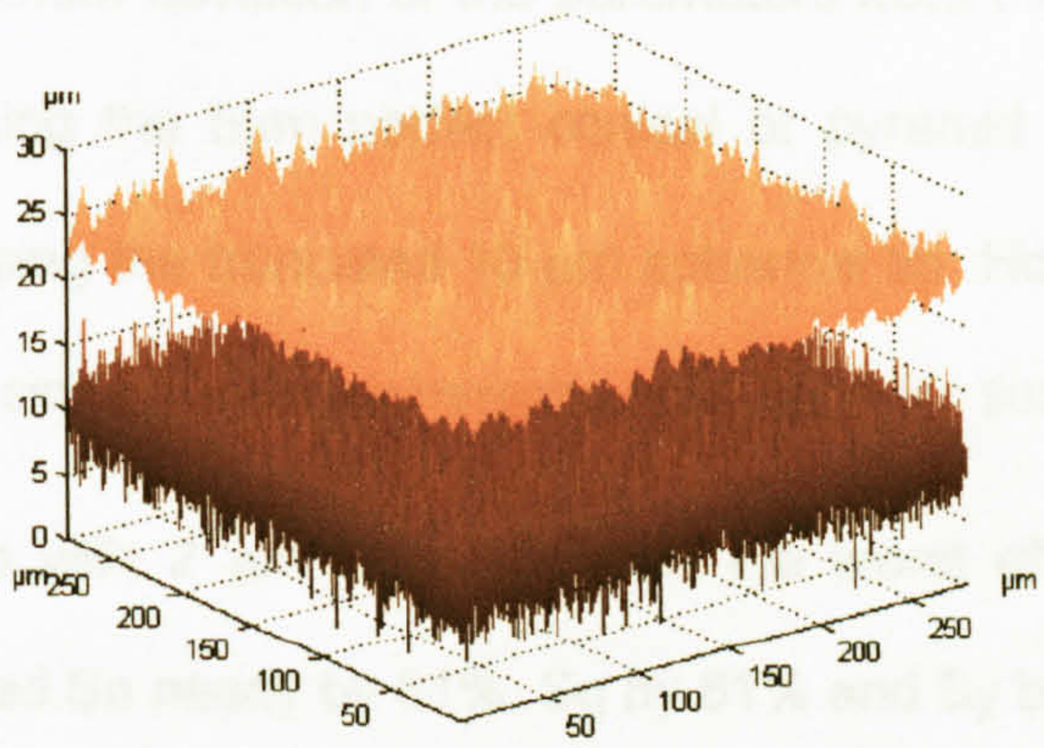

Original surface (bottom) and tip locus (top)

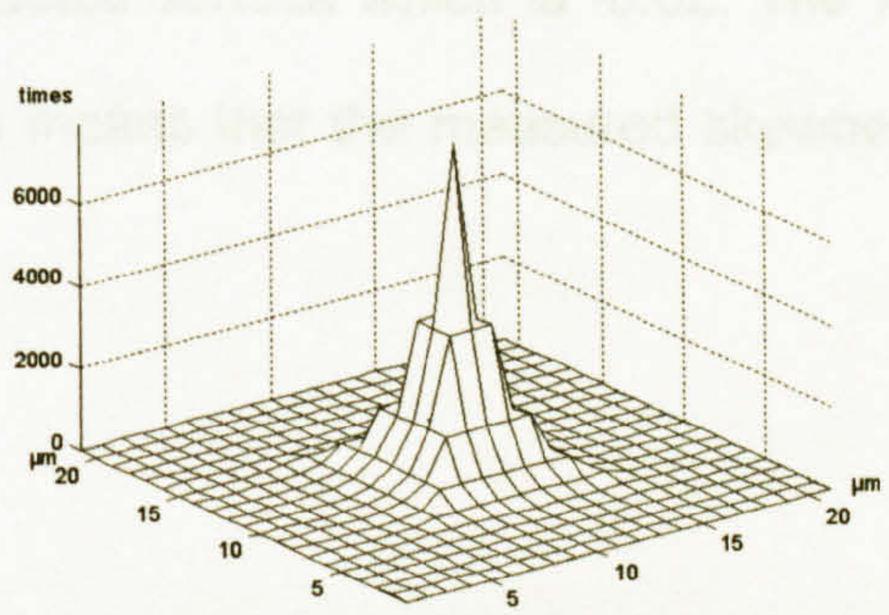

Contacts distribution on the tip

Figure 2.18: Locus and Contacts of a 10 μm pyramid tip on a random Gaussian surface

The contacts distributions of the 1 and 2 μm truncated tips when scanning the random Gaussian surface are shown in figure 2.19. The relative spassity of the extreme events compared to the previous surface mean that while there is still a dominant uniform sampling of the truncation platforms, there is rather more contact on flanks.

Scanning the random Gaussian surface with same tips as before, but with different dimensions (5μm) has shown nearly the same locus and contact distributions shapes as the 10 μm tips. Table 2.3 shows the percentage error of the roughness parameters of different outputs when scanning the random Gaussian surface with different tips.

It is noticed that the minimum deviation of the parameters from their actual values of the surface occurs when using the 5μm perfect conical or pyramid shape. The maximum deviation occurs when using the truncated 10 μm spherical tip. However, all the tips also provide very large errors since they are inherently unsuitable for such a surface.

The 10 μm spherical tip with 2 μm truncation has the worst effect on the roughness parameters. It has reduced Sa nearly by 61%, Sq by 61% and Sy by 68% from their actual values. It has reduced the root mean square slope by nearly 91.5% from the actual value.

There is also an extreme deviation in the values of the skewness. Again, this is because of the actual value of the tested surface which is -0.02. The worst case deviation in the skewness is -2999% which means that the measured skewness is 0.56 while the actual one is -0.02.

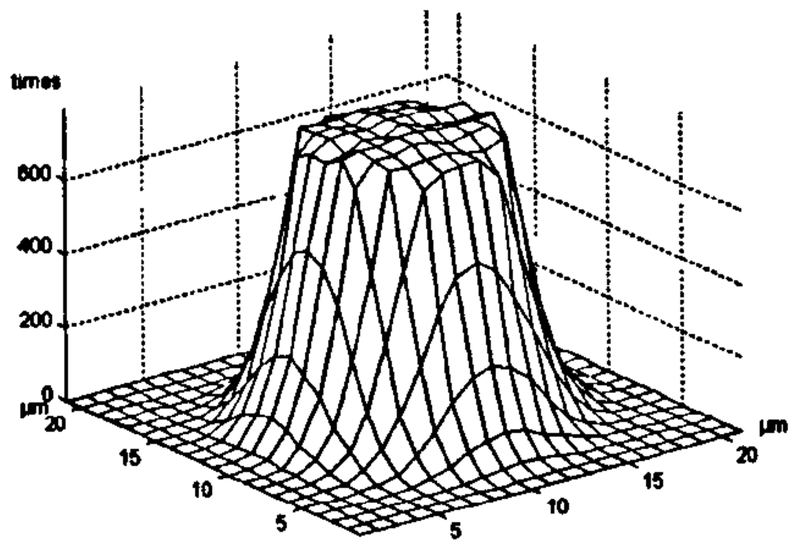

1 µm truncation

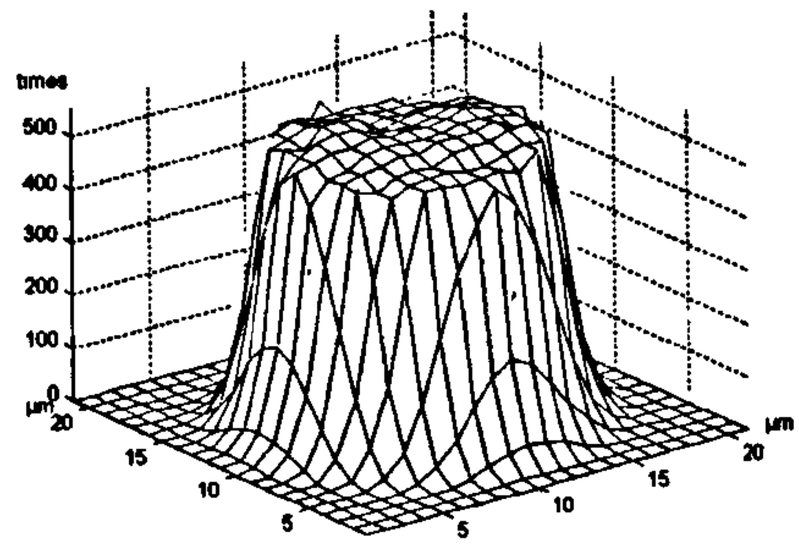

2 µm truncation

Spherical tip

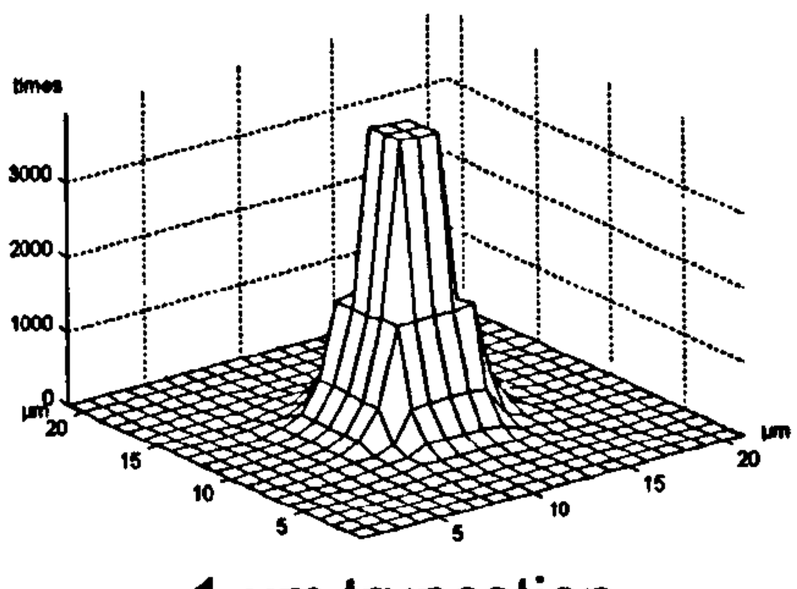

1 µm truncation

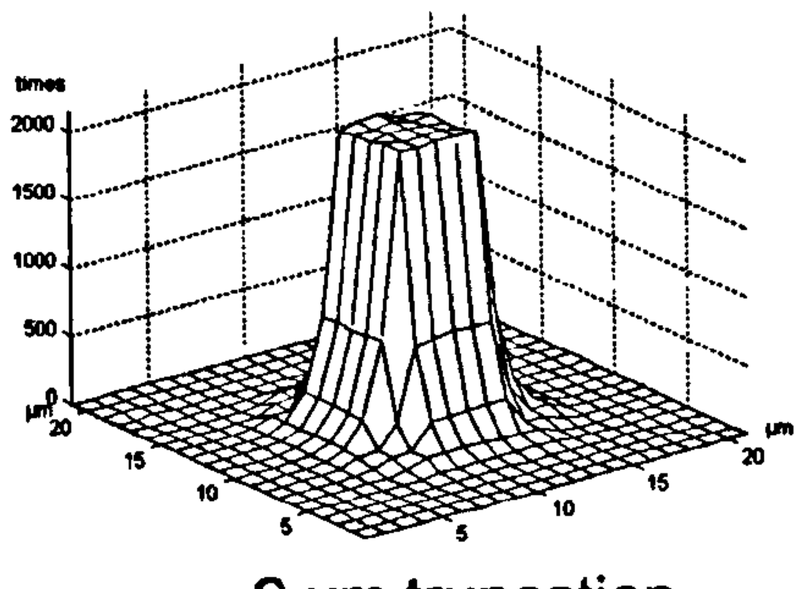

2 µm truncation

Conical tip

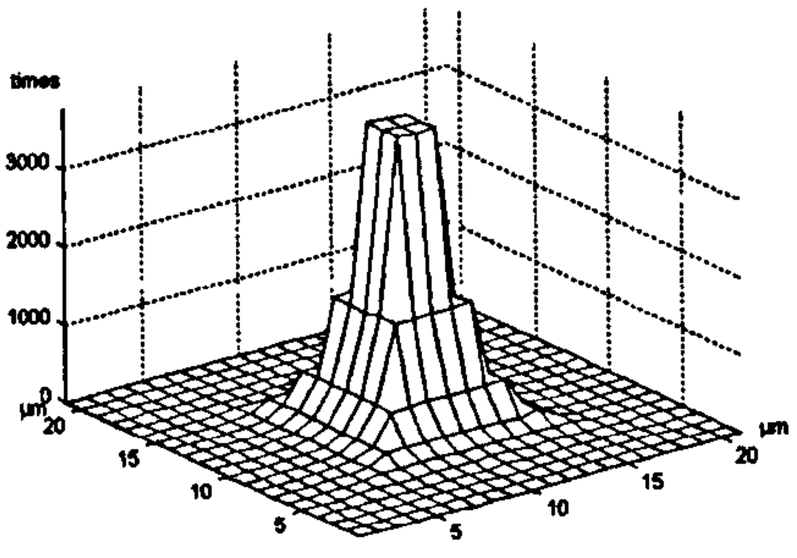

1 µm truncation

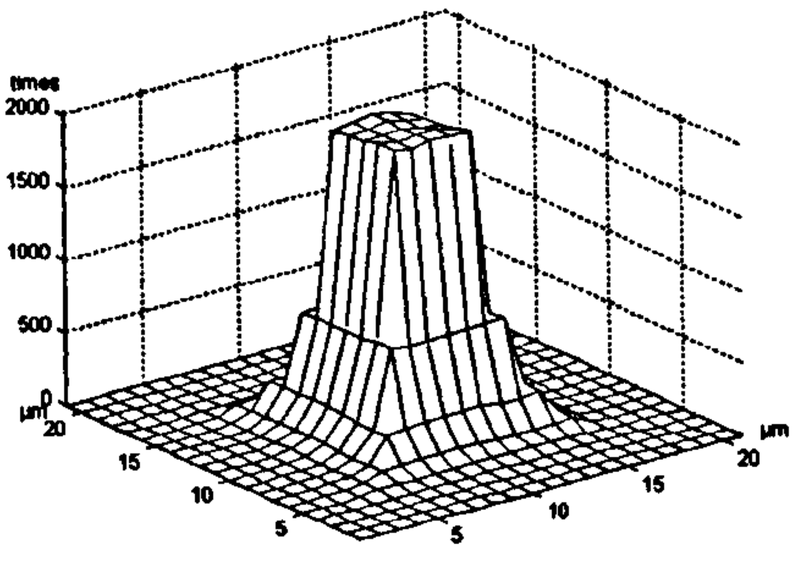

2 µm truncation

Pyramid tip

Figure 2.19: Contacts distributions of 10 μm truncated tips on a random Gaussian surface

		Parameter (μm)	Sa	Sq	Sy	Ssk	Sdq
			1.90	2.38	19.62	-0.02	4.75
Tip	Size	Shape	% error				
Conical	5 μm	Perfect	-53.03	-52.49	-49.49	-2966.63	-80.71
		1 μm Truncated	-53.82	-53.33	-54.59	-2915.98	-83.00
		2 μm Truncated	-55.83	-55.25	-58.24	-2857.79	-85.35
	10 μm	Perfect	-52.99	-52.47	-50.06	-2981.39	-80.75
		1 μm Truncated	-53.79	-53.31	-54.74	-2933.19	-83.06
		2 μm Truncated	-55.86	-55.27	-58.73	-2891.51	-85.51
Spherical	5 μm	Perfect	-55.05	-54.53	-53.94	-2792.72	-86.03
		1 μm Truncated	-56.14	-55.64	-59.03	-2788.56	-85.67
		2 μm Truncated	-57.22	-56.79	-61.14	-2844.86	-84.89
	10 μm	Perfect	-59.36	-58.98	-62.32	-2989.19	-91.38
		1 μm Truncated	-60.39	-60.08	-65.62	-2953.04	-91.54
		2 μm Truncated	-61.25	-61.01	-67.96	-2842.87	-91.52
Pyramid	5 μm	Perfect	-53.46	-52.94	-49.49	-2998.92	-81.04
		1 μm Truncated	-54.24	-53.77	-54.59	-2940.63	-83.33
		2 μm Truncated	-56.28	-55.71	-58.24	-2872.35	-85.76
	10 μm	Perfect	-53.58	-53.07	-51.26	-3043.77	-81.15
		1 μm Truncated	-54.38	-53.91	-54.74	-2987.89	-83.46
		2 μm Truncated	-56.51	-55.93	-59.35	-2932.48	-86.00

% error=100*(Measured Value - Actual Value)/ actual Value

Table 2.3: % error of roughness parameters of different tips on the random Gaussian surface

The previous results are based on surfaces which have been mathematically generated by the computer. The height of these surfaces has been set to 20 μm and also the tip radii used have been set to 10 and 5 μm to show the severe effect of the tip shape on the measured roughness of the surface.

It has been obvious that the tip shape has a significant effect on the measured roughness parameters and also the roughness parameters are closely representative of the actual 'real' value of the surface when using either the conical or the pyramid tip. The contacts distribution on each tip when scanning a random surface is closely representative of the tip shape. There is a tendency of the bigger tip size to decrease the value of roughness parameters, Sa, Sq, Sy and Sdq. The pyramid and conical tips give nearly the same roughness parameters and nearly the same contact distribution with all tested surfaces.

It is also clear that the truncated tips give bigger % error compared with the perfect tips. Applying this to the real surface roughness measurements means that when the tips are used too much and getting worn, they will give more error in the values of the roughness parameters.

The next stage of this work is to use real surfaces instead of the theoretical ones but with the same tips generated by the computer.

2.4 Simulation on real surfaces

The previous simulation has shown that the technique is working properly and giving significant results. The next stage is to apply the technique to data representing real surfaces. The surface roughness of the real samples have been measured by an optical method and the data representing these surfaces have been scanned theoretically in 3D by the computer using the same tip shapes (conical, spherical and pyramid) and same sizes as before.

Three different samples have been measured by the WYKO NT2000 scanning white light interferometer. The samples are made of mild steel and machined by grinding, lapping and milling processes. Data collected by Wyko were checked for no missing data losses interpolation by Wyko software. The value of the roughness parameters of the samples are shown in table 2.4.

Figures 2.19, 2.20, 2.21 Show the shape of the ground, lapped and milled samples respectively.

Parameter (μm)	Sa	Sq	Sy	Ssk	Sdq
Ground Surafce	0.39	0.50	3.73	-0.53	0.22
Milled Surface	0.78	0.95	5.65	-0.28	0.33
Lapped Surface	1.70	2.13	14.03	-0.07	0.76

Table 2.4: Roughness parameters of real surfaces

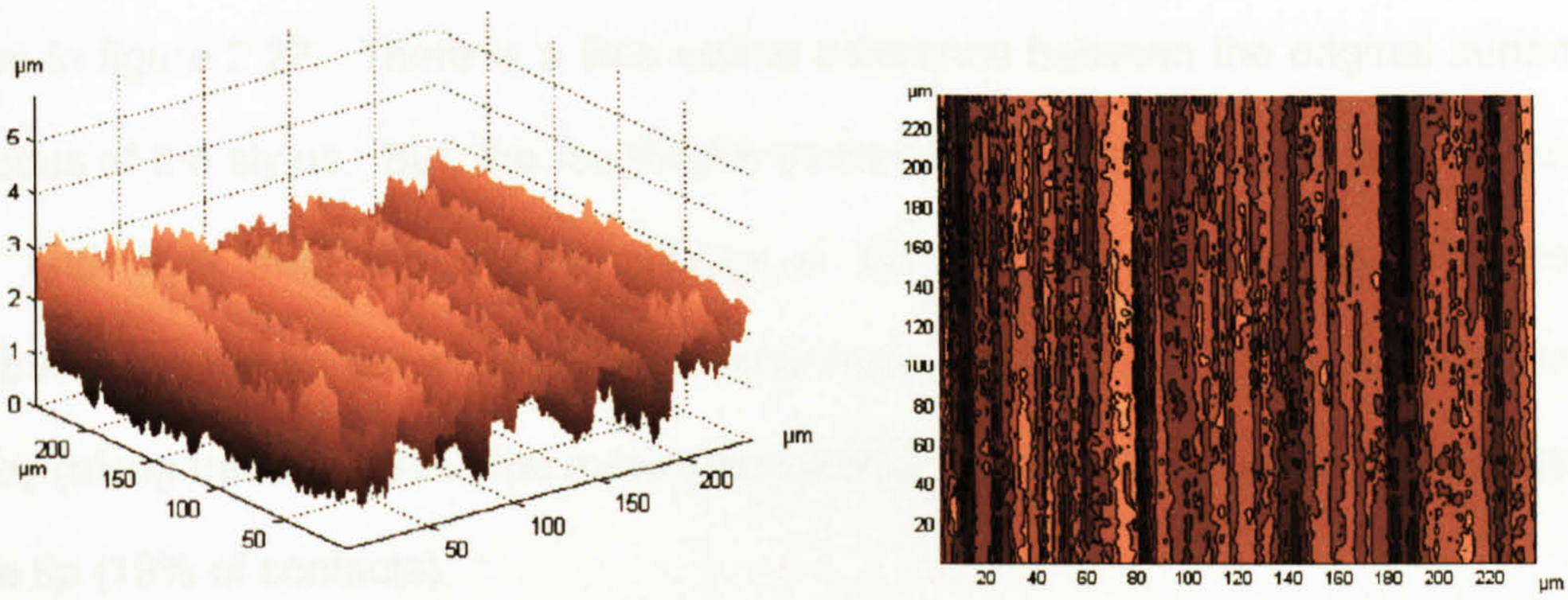

Figure 2.20: Ground surface

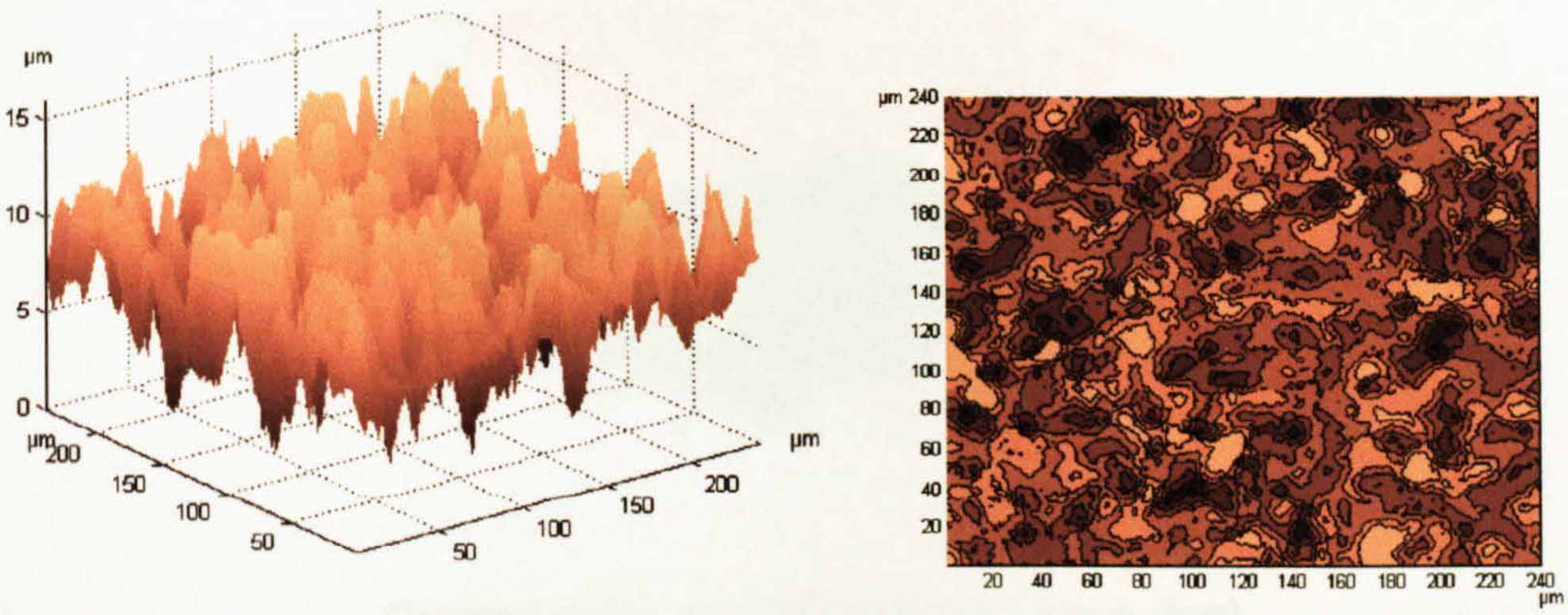

Figure 2.21: Lapped surface

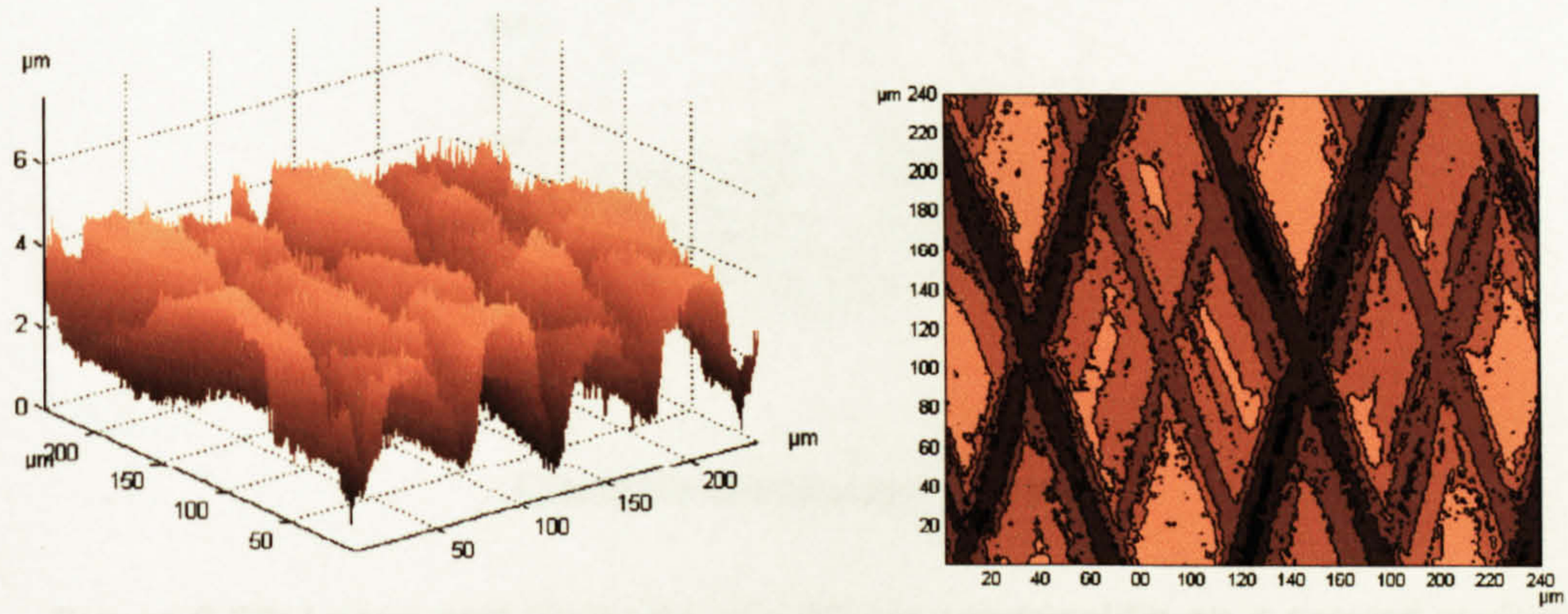

Figure 2.22: Milled surface

2.4.1 Scanning Ground surface

The output of scanning the ground surface with the 10 μm radius perfect spherical tip is shown in figure 2.23. There is a little visible difference between the original surface and the locus of the stylus. But, the roughness parameters Sa and Sq have been reduced by 17% and 16% from the original values of the surface, respectively. The contacts distribution on the tip shows that all contacts occur on the central line of the tip crossing the lay (along traverse). Also the maximum number of contacts occurs on the central point of the tip (19% of contacts).

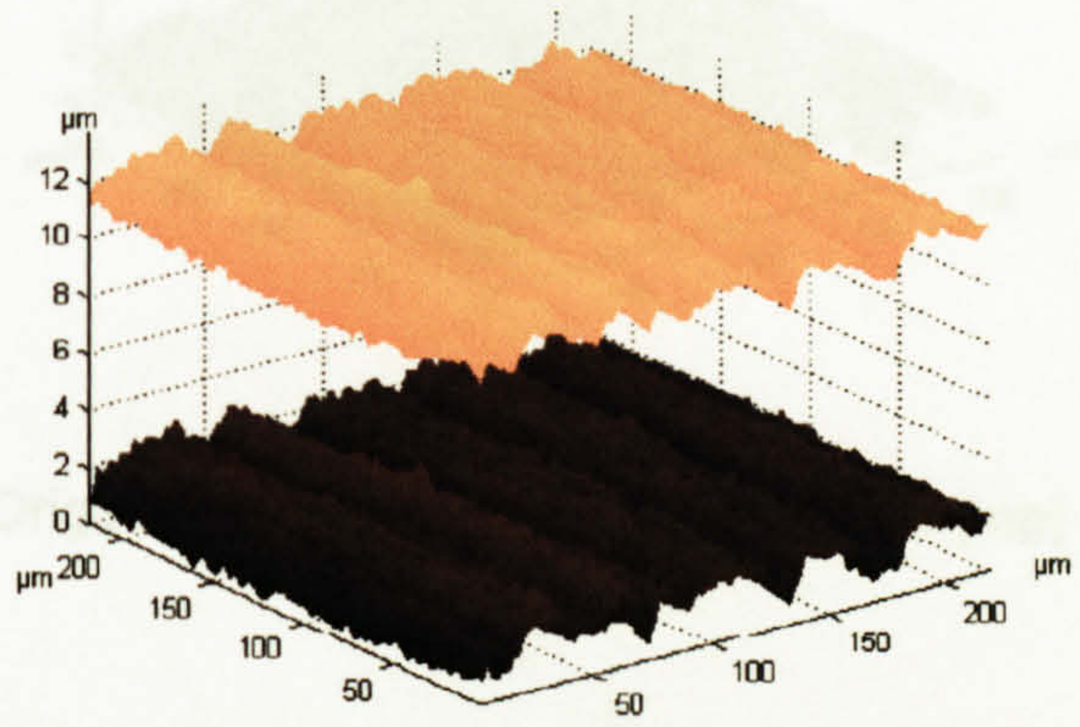

Original surface (bottom) and tip locus (top)

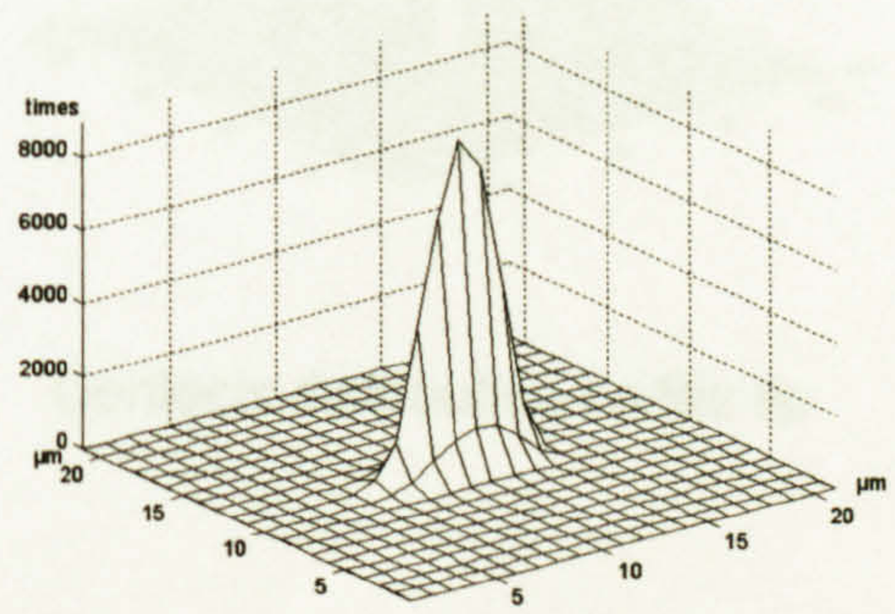

Contacts distribution on the tip

Figure 2.23: Locus and Contacts of a 10 μm spherical tip on a ground surface

The output of scanning the ground surface with a 10 μm perfect conical tip is shown in figure 2.24. There is also a little visible difference between the original surface and the locus of the stylus. The roughness parameters Sa and Sq are nearly the same as the original values of the surface. The contacts distribution on the tip shows that all contacts occur on the central point of the tip.

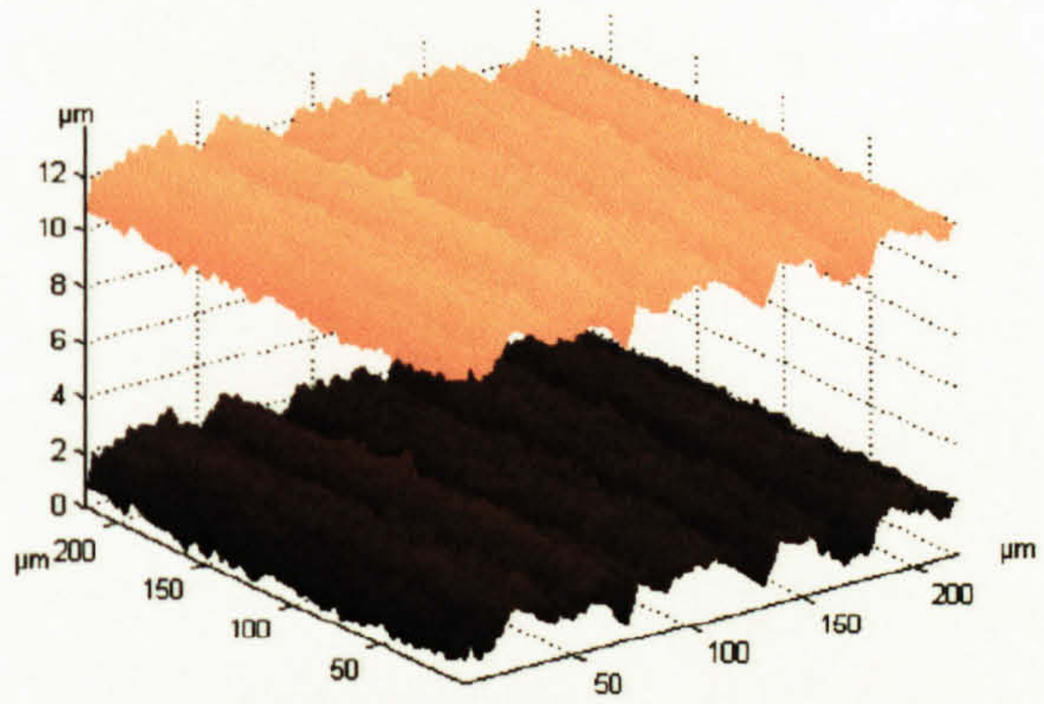

Original surface (bottom) and tip locus (top)

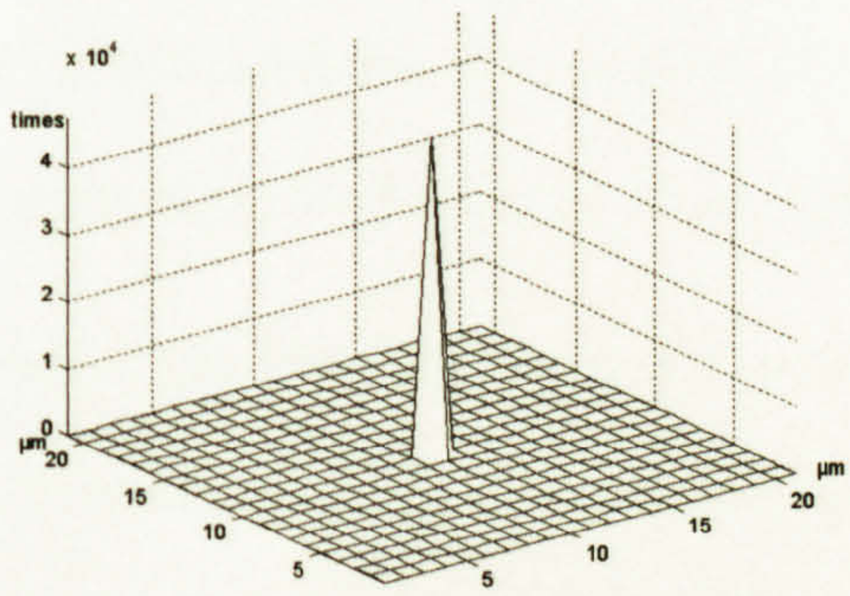

Contacts distribution on the tip

Figure 2.24: Locus and Contacts of a 10 μm conical tip on a ground surface

The output of scanning the ground surface with a 10 μm perfect pyramid tip is shown in figure 2.25. There is also a little visible difference between the original surface and the locus of the stylus. The roughness parameters Sa and Sq are nearly the same as the original values of the surface. The contacts distribution on the tip shows also that all contacts occur on the central point of the tip.

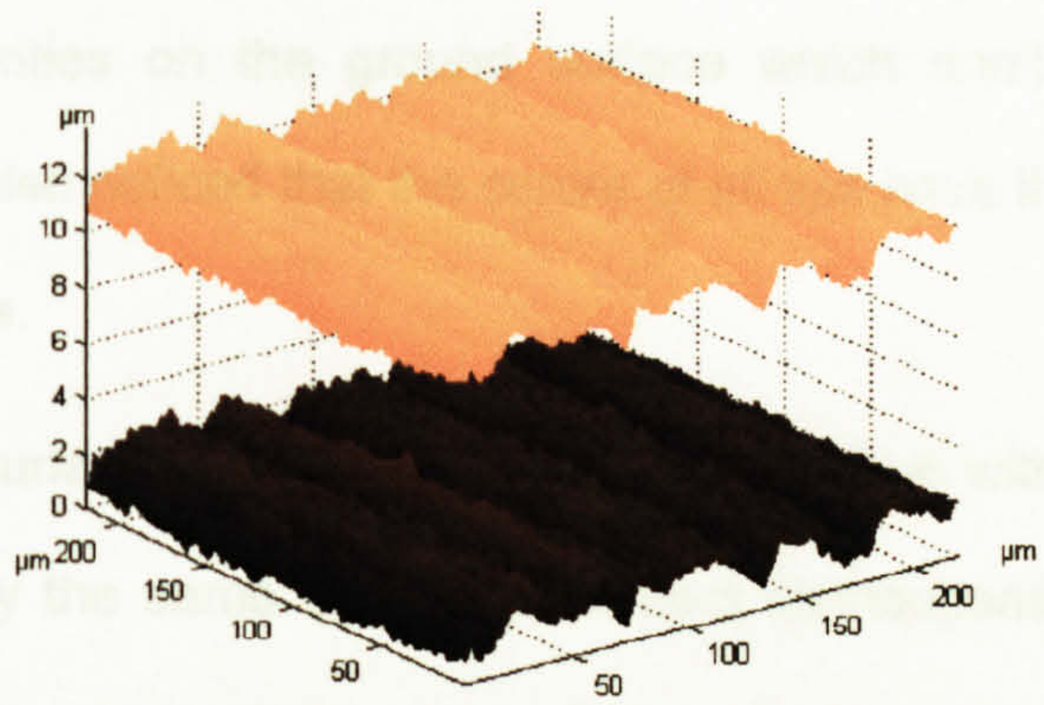

Original surface (bottom) and tip locus (top)

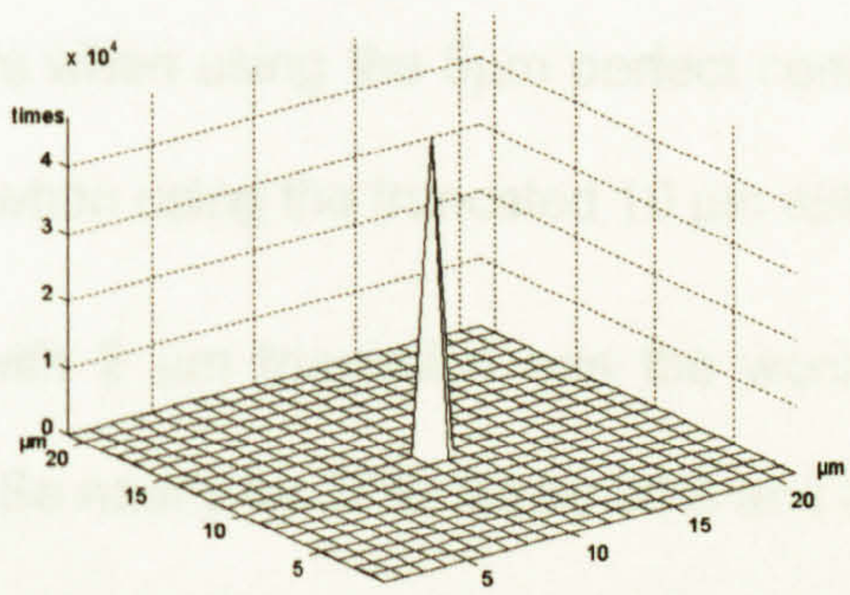

Contacts distribution on the tip

Figure 2.25: Locus and Contacts of a 10 μm pyramid tip on a ground surface

The contacts distributions of the 1 and 2 μm truncated tips when scanning the ground surface are shown in figure 2.26. It is clear that the ground surface gives very similar shapes of the contacts distribution on the spherical tips to the ones of the Sinusoidal surface as most contacts occur along the central line of the spherical tip but with more contacts spread around the edges of the tip end. The conical and the pyramid tips show slightly different distributions as most contacts occur on the corners of the tip. This is due to the existing irregularities on the ground surface which don't exist on the perfect sinusoidal shape. It is also noticed that the centre of all tips have the minimum number of contacts with the surface.

Scanning the ground surface with same tips as before, but with different dimensions (5μm) has shown nearly the same locus and contact distributions shapes as the 10μm tips.Table 2.5 shows the percentage error of the roughness parameters of different outputs when scanning the ground shape with different tips.

It is noticed that the minimum deviation of the parameters (almost zero) from their actual values of the surface occurs when using the 5μm perfect conical or pyramid shape. The maximum deviation occurs when using the truncated 10 μm spherical tip.

The 10 μm spherical tip with 2 μm truncation has the worst effect on the roughness parameters. It has reduced Sa nearly by 37%, Sq by 36% and Sy by 33% from their actual values. It has reduced the root mean square slope by nearly 53.5% from the actual value. The skewness has been reduced by 97% from the actual value of the surface.

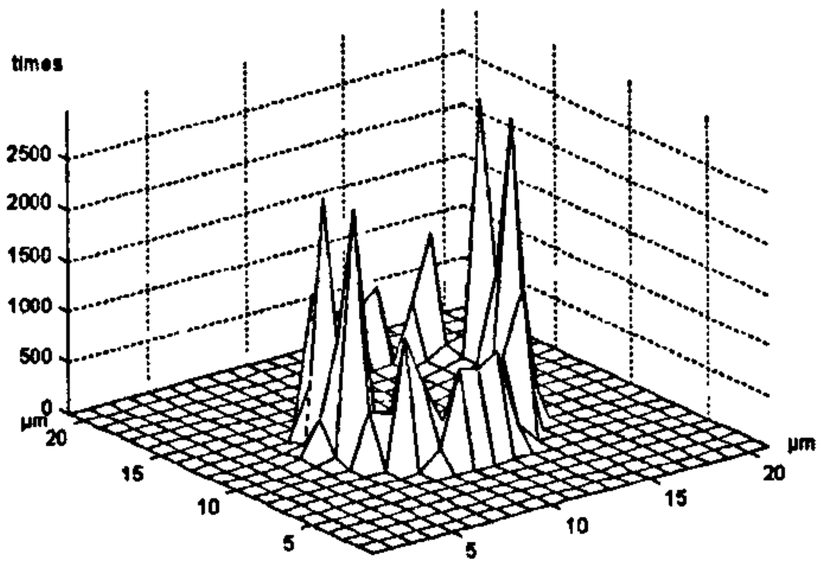

1 μm truncation

Spherical tip

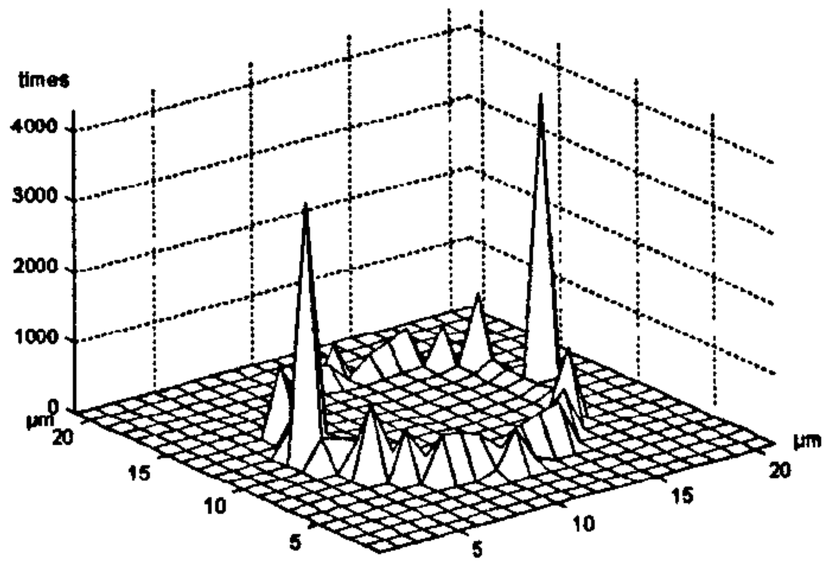

2 μm truncation

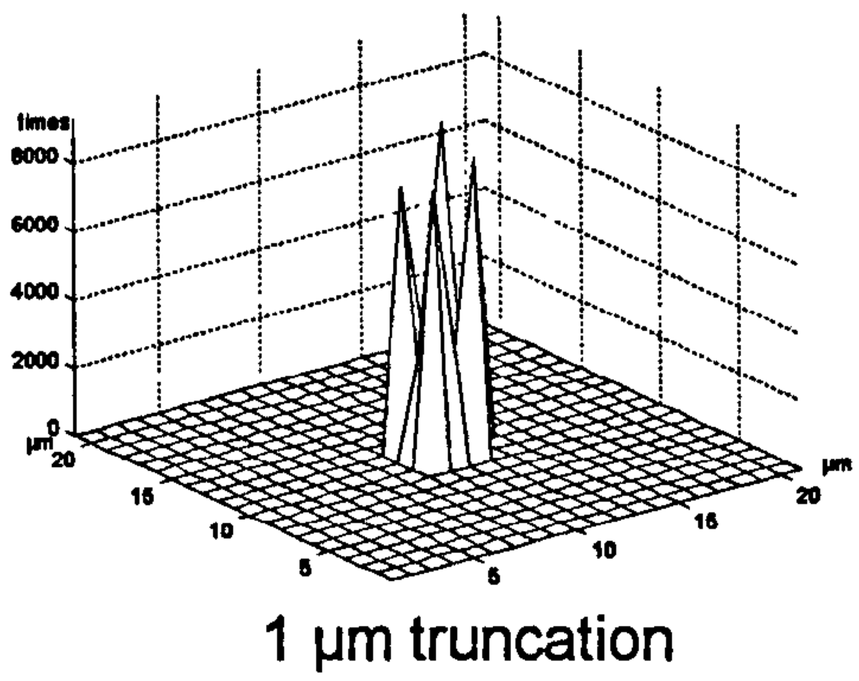

1 μm truncation

Conical tip

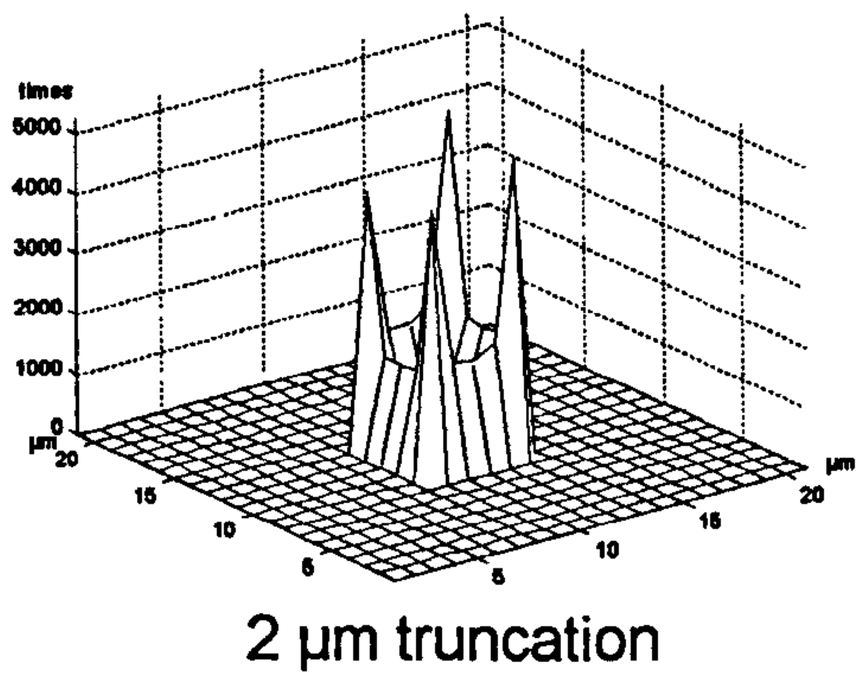

2 μm truncation

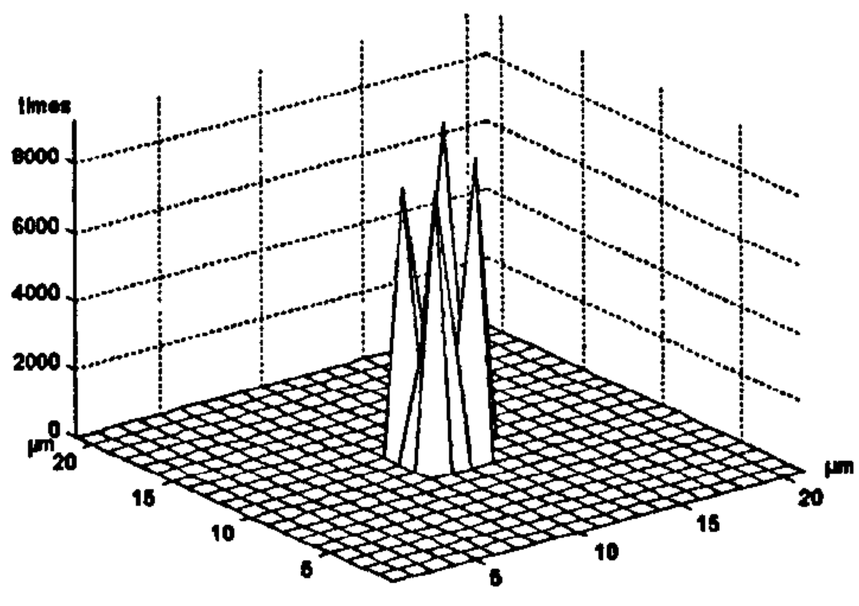

1 μm truncation

Pyramid tip

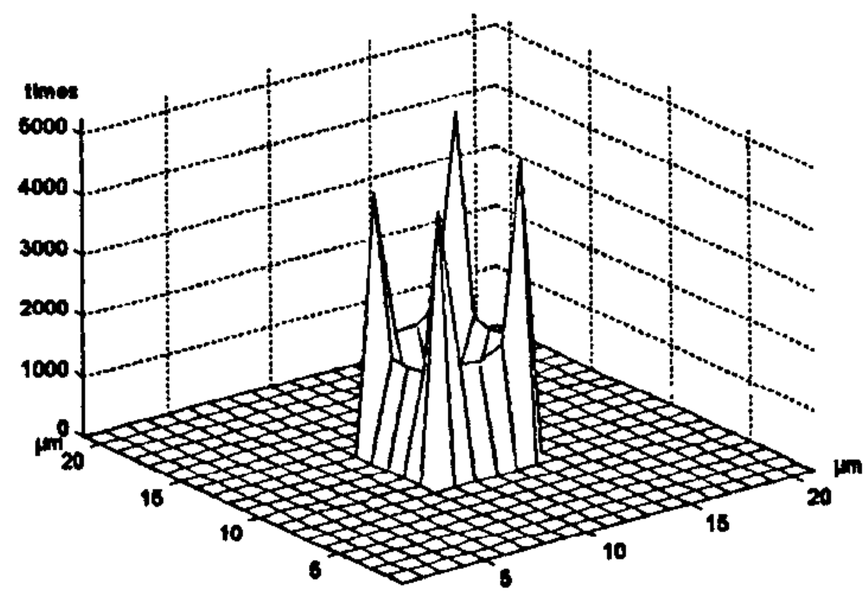

2 μm truncation

Figure 2.26: Contacts distributions of 10 μm truncated tips on a ground surface

		Parameter (μm)	Sa	Sq	Sy	Ssk	Sdq
			0.39	0.50	3.73	-0.53	0.22
Tip	Size	Shape	% error				
Conical	5 μm	Perfect	-0.01	-0.01	0.00	0.00	-0.02
		1 μm Truncated	-10.12	-9.05	-9.03	-2.28	-14.43
		2 μm Truncated	-19.21	-17.59	-16.68	-13.99	-31.72
	10 μm	Perfect	-0.01	-0.01	0.00	0.00	-0.02
		1 μm Truncated	-10.12	-9.05	-9.03	-2.28	-14.43
		2 μm Truncated	-19.21	-17.59	-16.68	-13.99	-31.72
Spherical	5 μm	Perfect	-9.96	-9.11	-5.07	-4.55	-19.14
		1 μm Truncated	-24.18	-22.46	-18.42	-19.56	-40.85
		2 μm Truncated	-28.78	-27.05	-23.39	-32.00	-49.08
	10 μm	Perfect	-16.87	-15.61	-9.98	-16.22	-34.87
		1 μm Truncated	-29.67	-28.02	-24.13	-40.50	-50.93
		2 μm Truncated	-36.91	-35.68	-32.85	-96.65	-53.31
Pyramid	5 μm	Perfect	-0.01	-0.01	0.00	0.00	-0.02
		1 μm Truncated	-10.12	-9.05	-9.03	-2.28	-14.43
		2 μm Truncated	-19.21	-17.59	-16.68	-13.98	-31.74
	10 μm	Perfect	-0.01	-0.01	0.00	0.00	-0.02
		1 μm Truncated	-10.12	-9.05	-9.03	-2.28	-14.43
		2 μm Truncated	-19.21	-17.59	-16.68	-13.98	-31.74

% error=100*(Measured Value - Actual Value)/ actual Value

Table 2.5: % error of roughness parameters of different tips on the ground surface

2.4.2 Scanning milled surface

The output of scanning the milled surface with the 10 μm radius perfect spherical tip, is shown in figure 2.27. There is a little much visible difference between the original surface and the locus of the stylus. But, the roughness parameters Sa and Sq have been reduced by 14% and 12.5% from the original values of the surface, respectively. The contacts distribution on the tip shows that all contacts mainly occur on the central line of the tip crossing the lay (along traverse) such the ground surface but with more contacts spread on both sides Also the maximum number of contacts occur on the central point of the tip (15% of contacts).

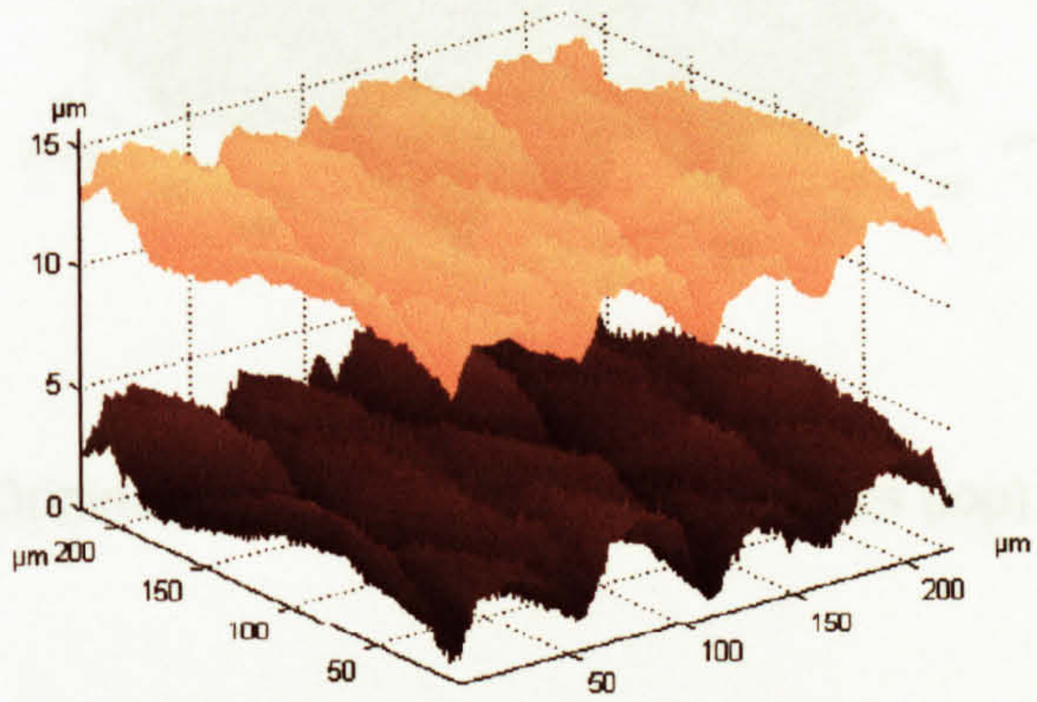

Original surface (bottom) and tip locus (top)

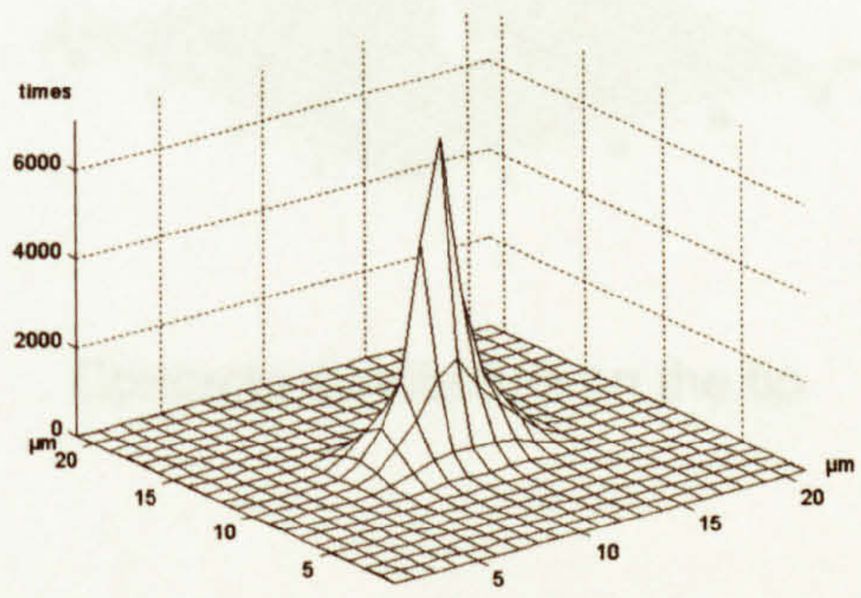

Contacts distribution on the tip

Figure 2.27: Locus and Contacts of a 10 μm spherical tip on a milled surface

The output of scanning the milled surface with a 10 μm perfect conical tip is shown in figure 2.28. There is also a little visible difference between the original surface and the locus of the stylus. The roughness parameters Sa and Sq are nearly the same as the original values of the surface. The contacts distribution on the tip shows that all contacts occur on the central point of the tip. This is due to the small height of the surface and also the tip is very sharp compared to the surface.

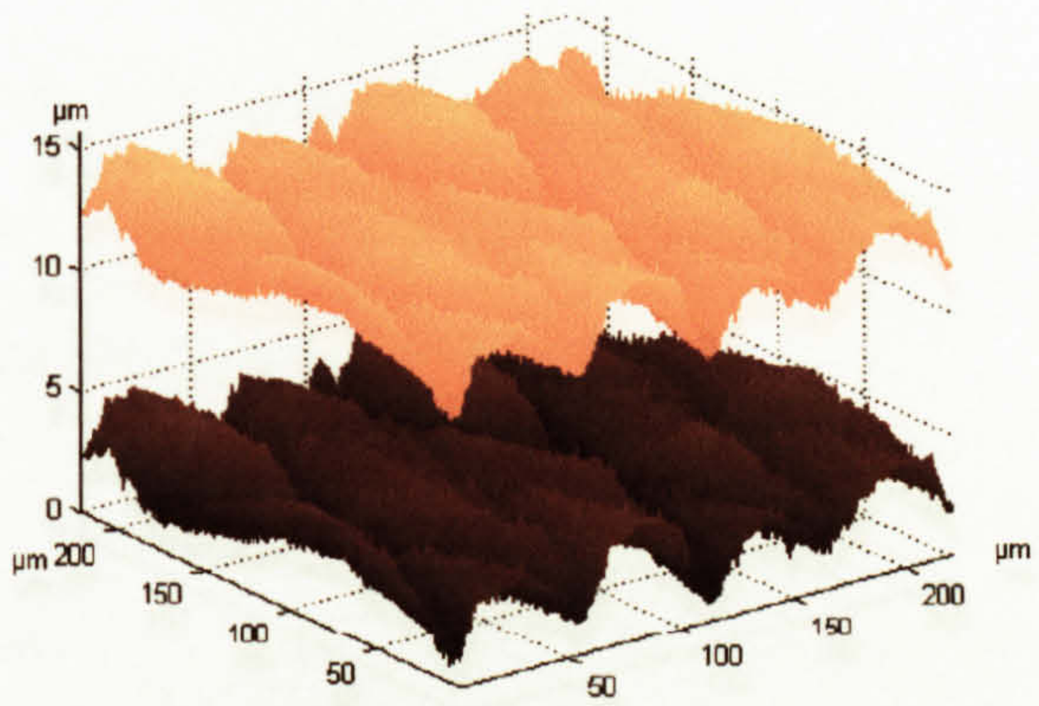

Original surface (bottom) and tip locus (top)

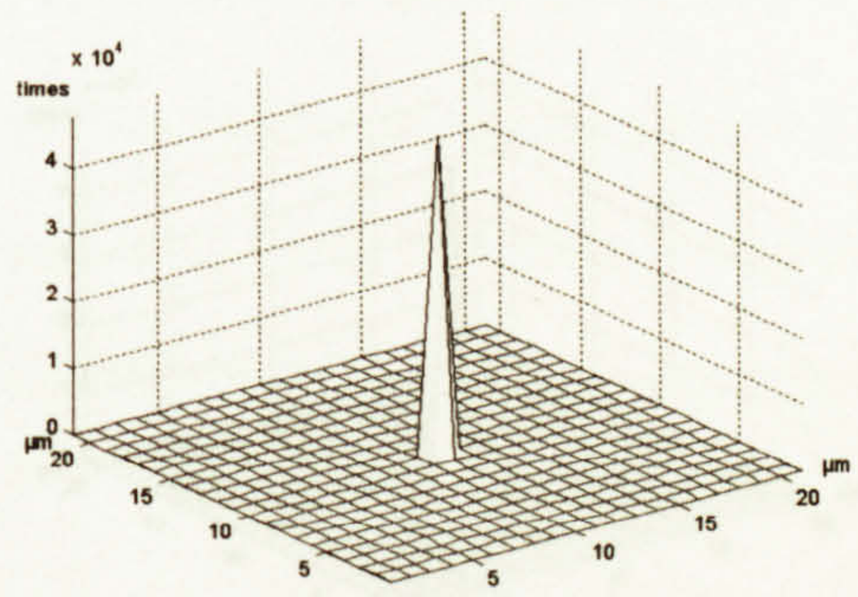

Contacts distribution on the tip

Figure 2.28: Locus and Contacts of a 10 μm conical tip on a milled surface

The output of scanning the milled surface with a 10 μm perfect pyramid tip is shown in figure 2.29. There is also a little visible difference between the original surface and the locus of the stylus. The roughness parameters Sa and Sq are nearly the same as the original values of the surface. The contacts distribution on the tip shows also that all contacts occur on the central point of the tip.

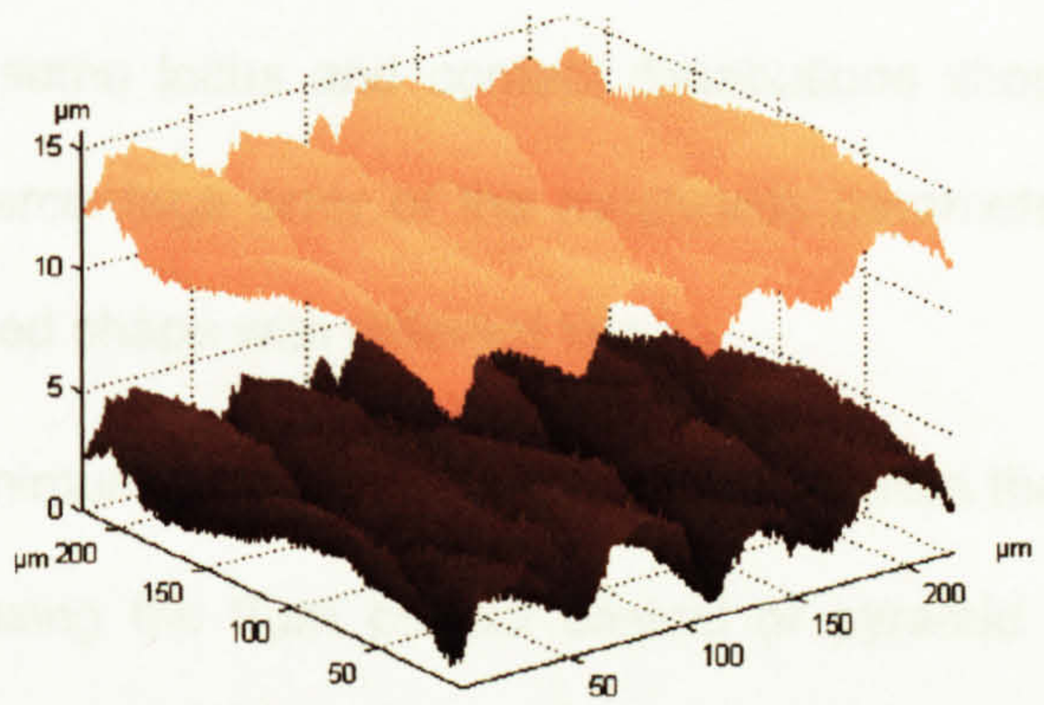

Original surface (bottom) and tip locus (top)

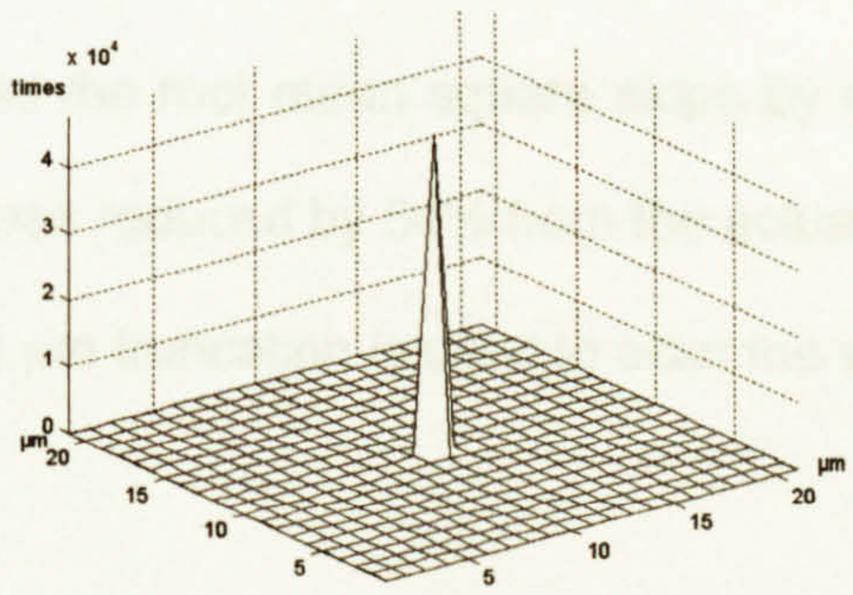

Contacts distribution on the tip

Figure 2.29: Locus and Contacts of a 10 μm pyramid tip on a milled surface

The contacts distributions of the 1 and 2 μm truncated tips when scanning the milled surface are shown in figure 2.30. The milled surface gives very similar shapes of the contacts distribution on all tips to the ones of the ground surface but with more contacts spread around the edges of the tip end. The reason for this is the cross lay of the milled surface where the surface contacts the tip at its sides more than in the case of the ground surface.

Scanning the milled surface with same tips as before, but with different dimensions (5μm) has shown nearly the same locus and contact distributions shapes as the 10μm tips. Table 2.6 shows the percentage error of the roughness parameters of different outputs when scanning the lapped shape with different tips.

It is noticed that the minimum deviation of the parameters from their actual values of the surface occurs when using the 5μm perfect conical or pyramid shape. The maximum deviation occurs when using the truncated 10 μm spherical tip.

The 10 μm spherical tip with 2 μm truncation has the worst effect on the roughness parameters. It has reduced Sa nearly by 33%, Sq by 31.5% and Sy by 30% from their actual values. It has reduced the root mean square slope by nearly 46% from the actual value. The skewness has been reduced by 64% from the actual value of the surface when the 5 μm spherical tip with 1 μm truncation is used to scan the surface.

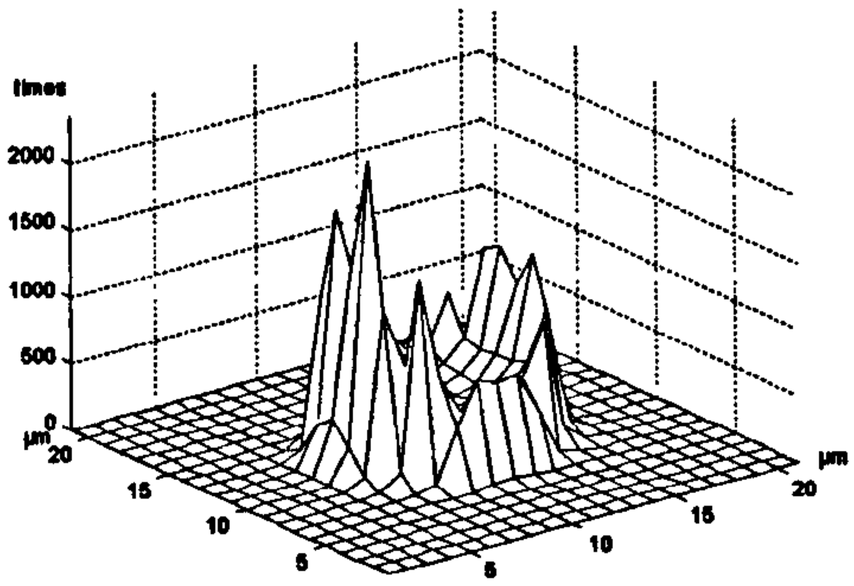

1 µm truncation

Spherical tip

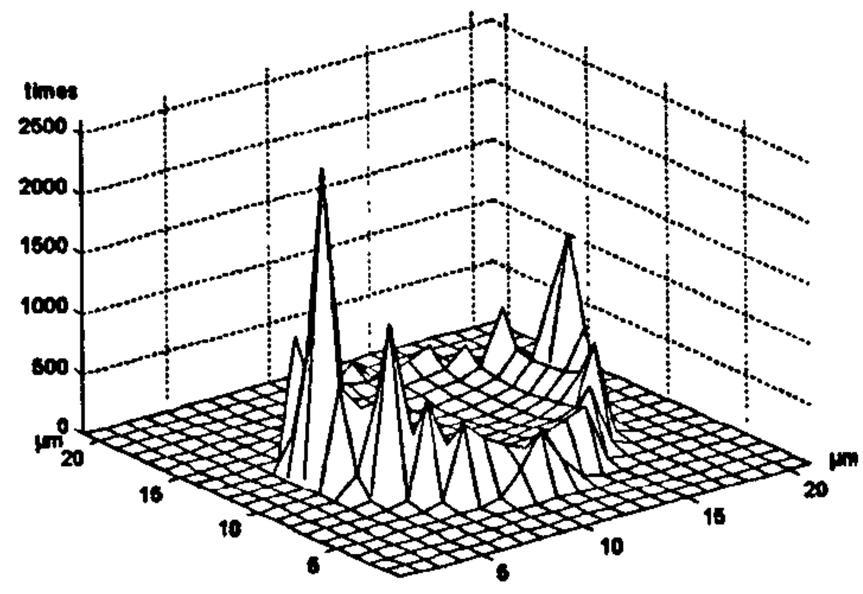

2 µm truncation

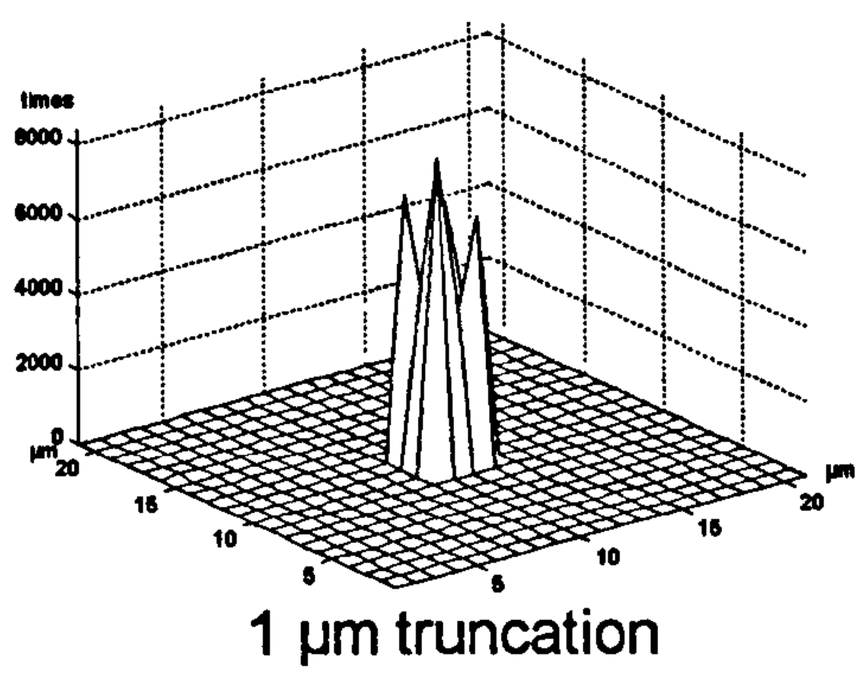

1 µm truncation

Conical tip

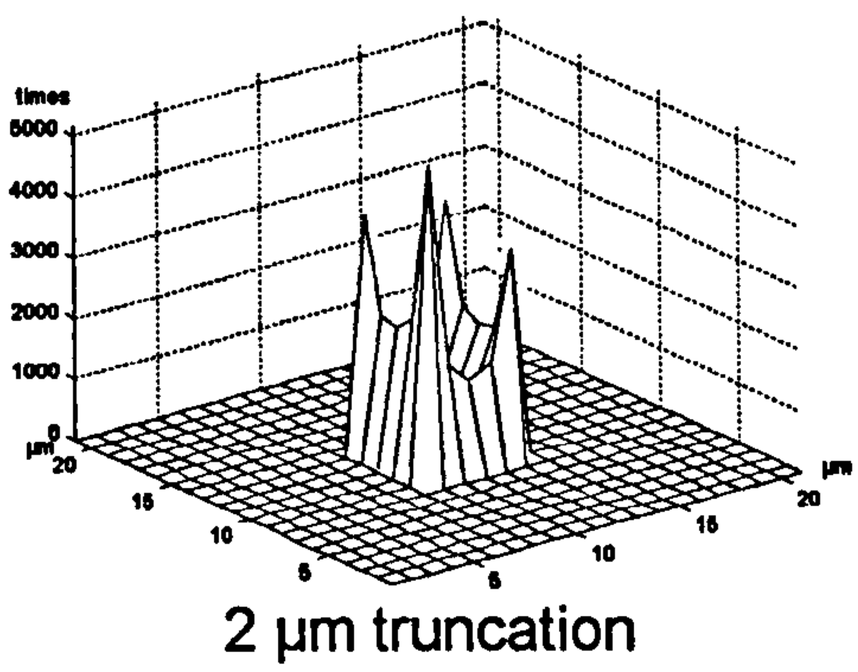

2 µm truncation

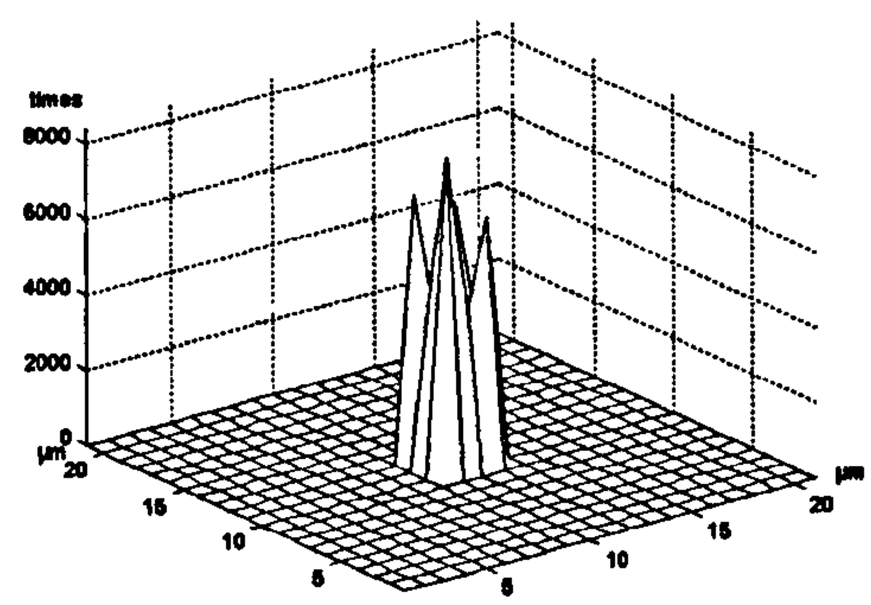

1 µm truncation

Pyramid tp

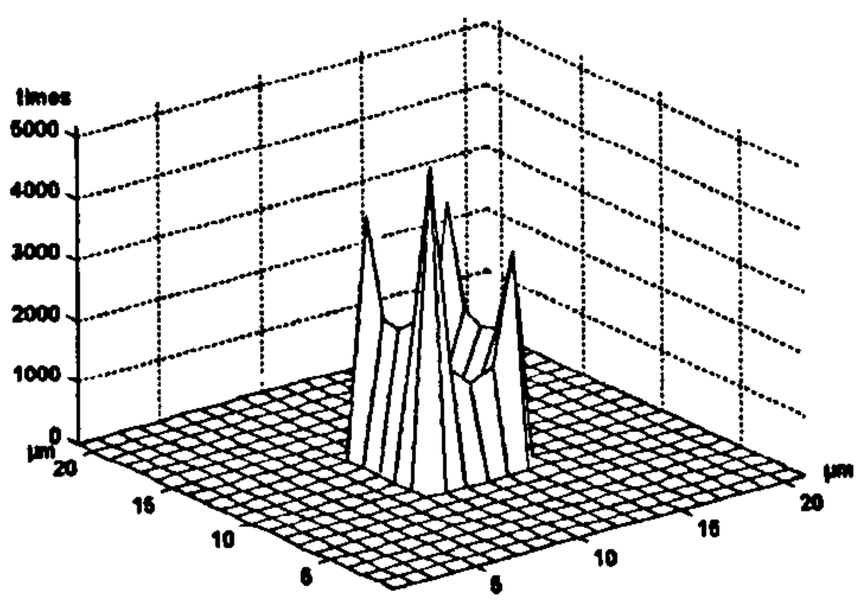

2 µm truncation

Figure 2.30: Contacts distributions of 10 µm truncated tips on a milled surface

		Parameter (μm)	Sa	Sq	Sy	Ssk	Sdq
			0.78	0.95	5.65	-0.28	0.33
Tip	Size	Shape	% error				
Conical	5 μm	Perfect	-0.19	-0.15	-3.07	0.37	-1.68
		1 μm Truncated	-6.93	-6.35	-14.86	37.28	-18.62
		2 μm Truncated	-13.33	-12.35	-18.20	60.85	-24.58
	10 μm	Perfect	-0.19	-0.15	-3.07	0.37	-1.68
		1 μm Truncated	-6.93	-6.35	-14.86	37.28	-18.62
		2 μm Truncated	-13.33	-12.35	-18.20	60.85	-24.58
Spherical	5 μm	Perfect	-7.77	-6.91	-13.07	41.68	-28.64
		1 μm Truncated	-16.49	-15.21	-18.20	68.01	-29.34
		2 μm Truncated	-21.86	-20.18	-22.61	71.31	-33.21
	10 μm	Perfect	-13.75	-12.54	-15.30	58.07	-38.61
		1 μm Truncated	-25.39	-23.56	-25.40	64.19	-41.13
		2 μm Truncated	-33.27	-31.46	-29.69	33.20	-46.03
Pyramid	5 μm	Perfect	-0.19	-0.15	-3.07	0.37	-1.68
		1 μm Truncated	-6.93	-6.35	-14.86	37.28	-18.62
		2 μm Truncated	-13.35	-12.37	-18.20	60.77	-24.67
	10 μm	Perfect	-0.19	-0.15	-3.07	0.37	-1.68
		1 μm Truncated	-6.93	-6.35	-14.86	37.28	-18.62
		2 μm Truncated	-13.35	-12.37	-18.20	60.77	-24.67

% error=100*(Measured Value - Actual Value)/ actual Value

Table 2.6: % error of roughness parameters of different tips on the milled surface

2.4.3 Scanning lapped surface

The output of scanning the lapped surface with the 10 μm radius perfect spherical tip is shown in figure 2.31. There is a little visible difference between the original surface and the locus of the stylus. But, the roughness parameters Sa and Sq have been reduced by 16.5% and 17.5% from the original values of the surface, respectively. The contacts distribution on the tip shows that all contacts occur around the central point of the tip within a 6μm radius circle and looking like a bell shape. The maximum number of contacts occurs at the central point of the tip (2% of contacts).

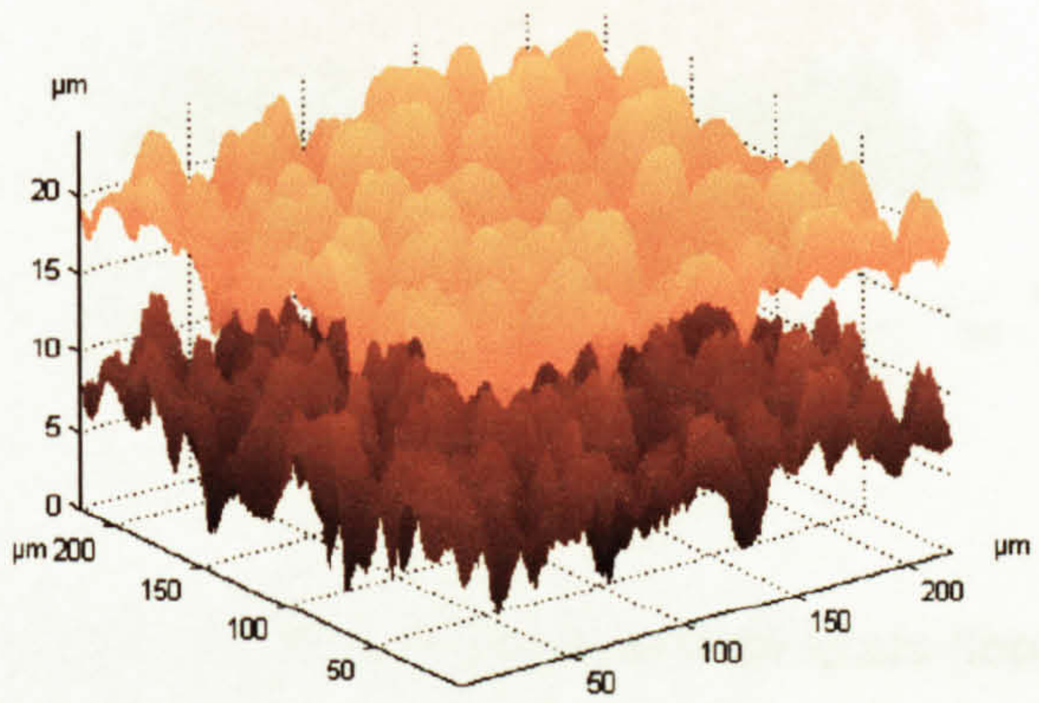

Original surface (bottom) and tip locus (top)

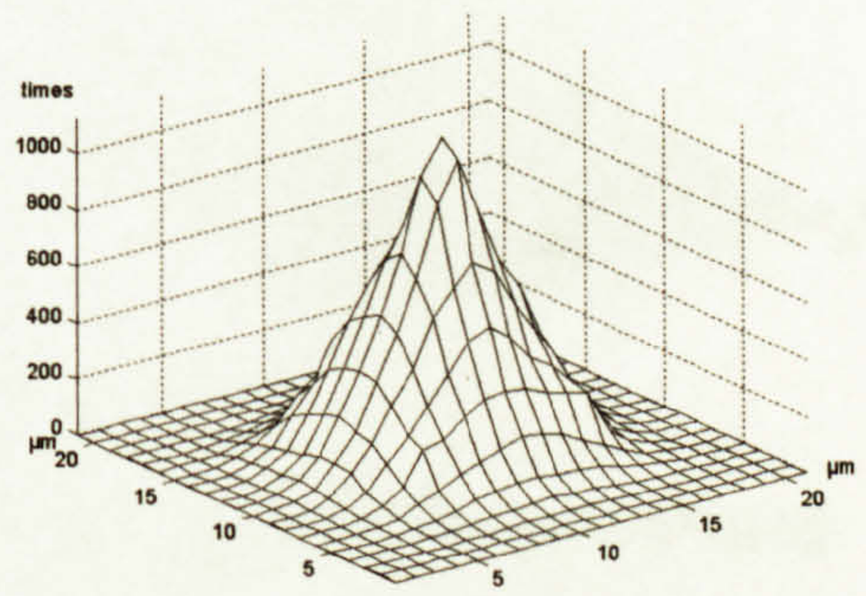

Contacts distribution on the tip

Figure 2.31: Locus and Contacts of a 10 μm spherical tip on a lapped surface

The output of scanning the lapped surface with a 10 μm perfect conical tip is shown in figure 2.32. There is also a little visible difference between the original surface and the locus of the stylus. The roughness parameters Sa and Sq have been reduced by 4.1% and 4.4% from the original values of the surface, respectively. The contacts distribution on the tip shows that all contacts occur on the central point of the tip.

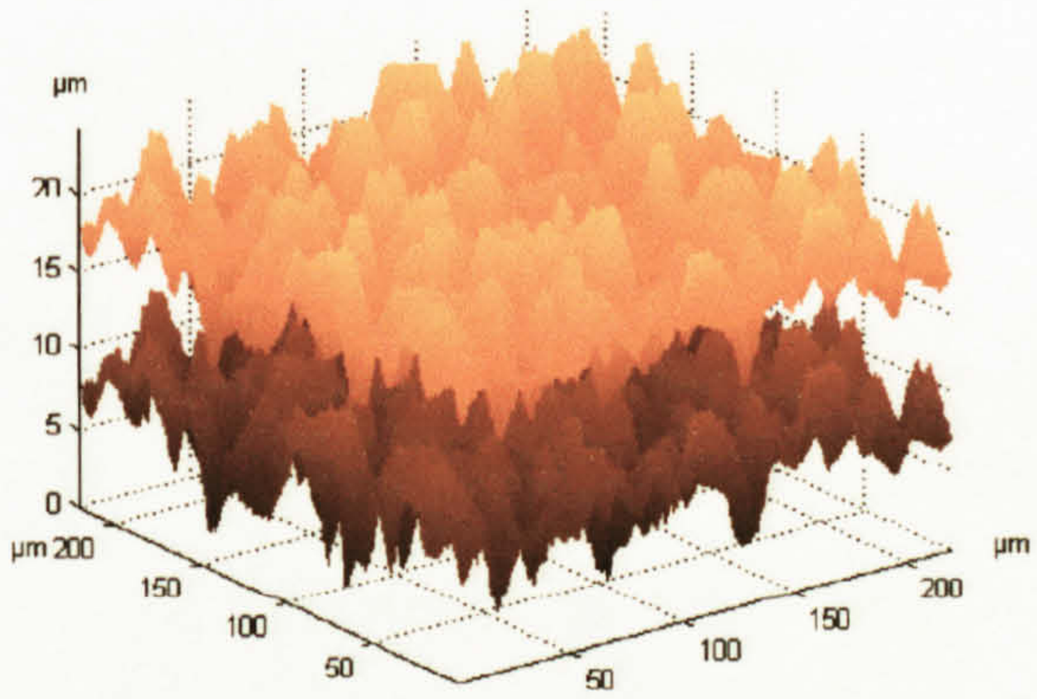

Original surface (bottom) and tip locus (top)

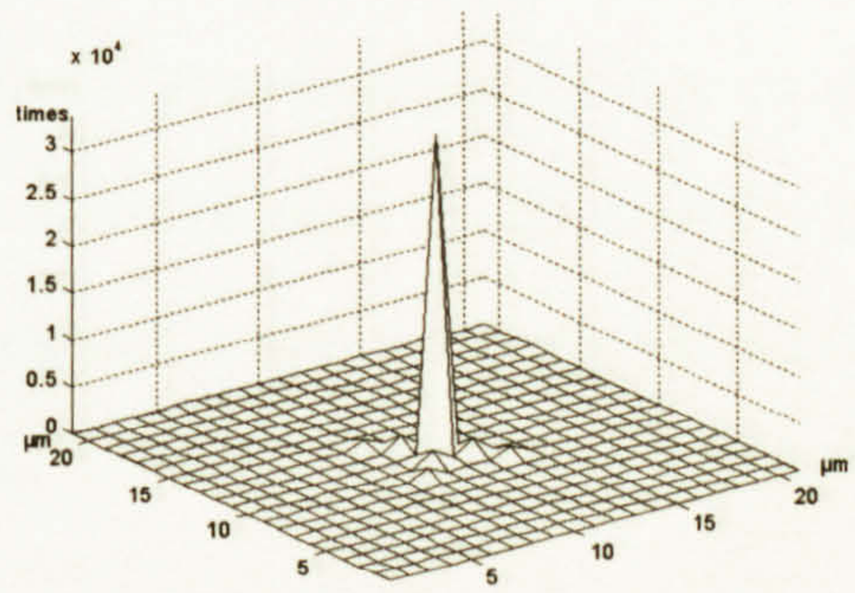

Contacts distribution on the tip

Figure 2.32: Locus and Contacts of a 10 μm conical tip on a lapped surface

The output of scanning the lapped surface with a 10 μm perfect pyramid tip is shown in figure 2.33. There is also a little visible difference between the original surface and the locus of the stylus. The roughness parameters Sa and Sq have been reduced by 5.7% and 6% less than the original values of the surface, respectively. The contacts distribution on the tip shows also that all contacts occur on the central point of the tip.

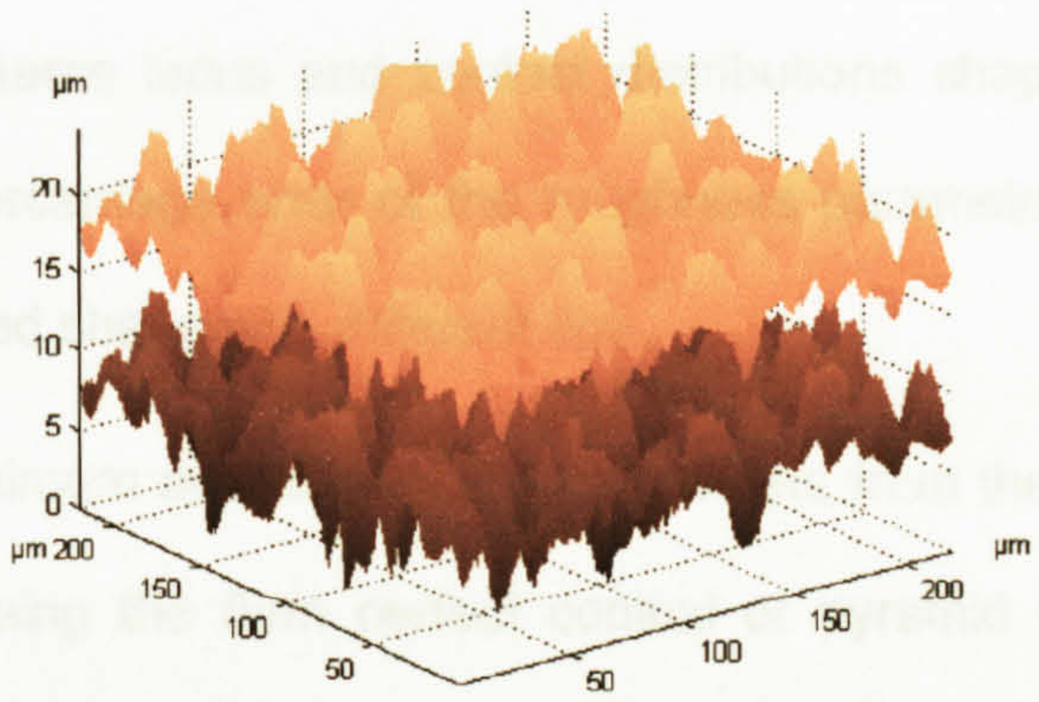

Original surface (bottom) and tip locus (top)

Contacts distribution on the tip

Figure 2.33: Locus and Contacts of a 10 μm pyramid tip on a lapped surface

The contacts distributions of the 1 and 2 μm truncated tips when scanning the lapped surface are shown in figure 2.34. As the lapped surface has random features not like the ground or milled surface, the contacts distributions on the truncated spherical tips are distributed uniformly around the edges of the tip ends producing crown shapes. Most contacts occur on the corners of the truncated pyramid and conical tips but with few contacts along the diagonals of the tips.

Scanning the lapped surface with same tips as before, but with different dimensions (5μm) has shown nearly the same locus and contact distributions shapes as the 10μm tips. Table 2.7 shows the percentage error of the roughness parameters of different outputs when scanning the lapped shape with different tips.

It is noticed that the minimum deviation of the parameters from their actual values of the surface occurs when using the 5μm perfect conical or pyramid shape. The maximum deviation occurs when using the truncated 10 μm spherical tip.

The 10 μm spherical tip with 2 μm truncation has the worst effect on the roughness parameters. It has reduced Sa nearly by 25.5%, Sq by 28% and Sy by 37% from their actual values. It has reduced the root mean square slope by nearly 45.5% from the actual value. The skewness has been reduced by 260% from the actual value. This high percentage error in the skewness is due to the low value of the actual skewness of the surface as explained before.

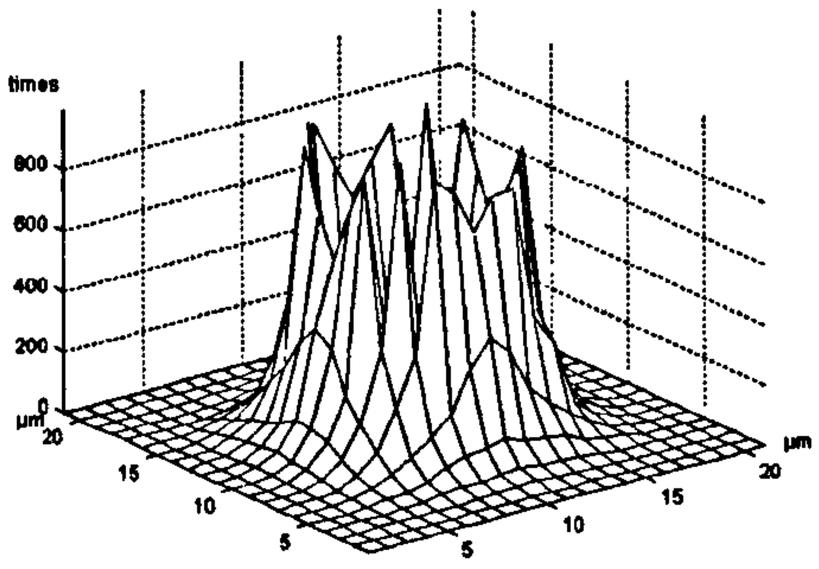

1 μm truncation

Spherical tip

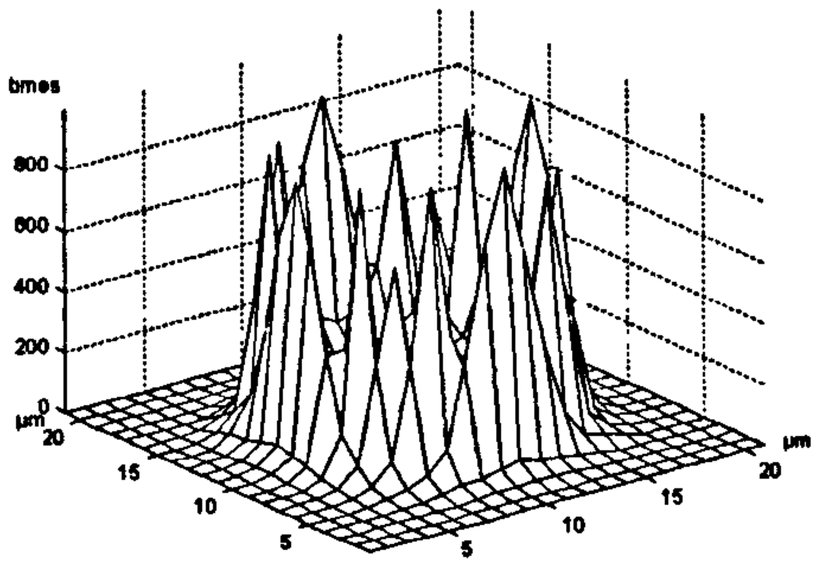

2 μm truncation

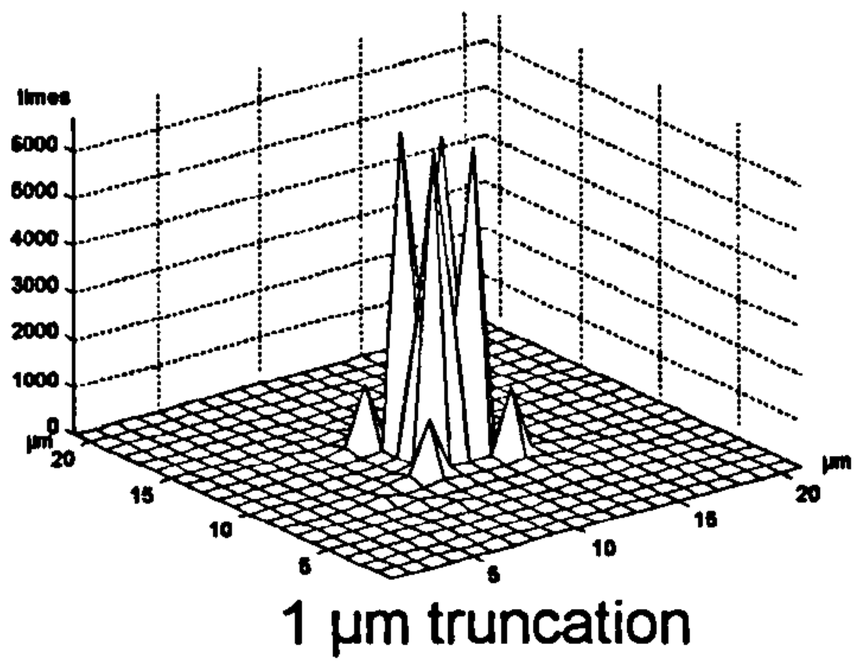

1 μm truncation

Conical tip

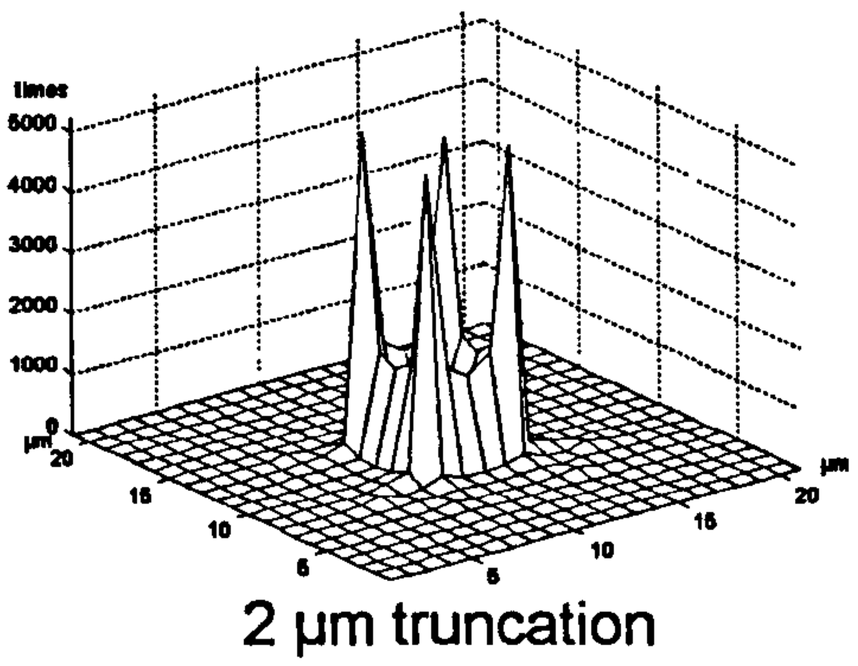

2 μm truncation

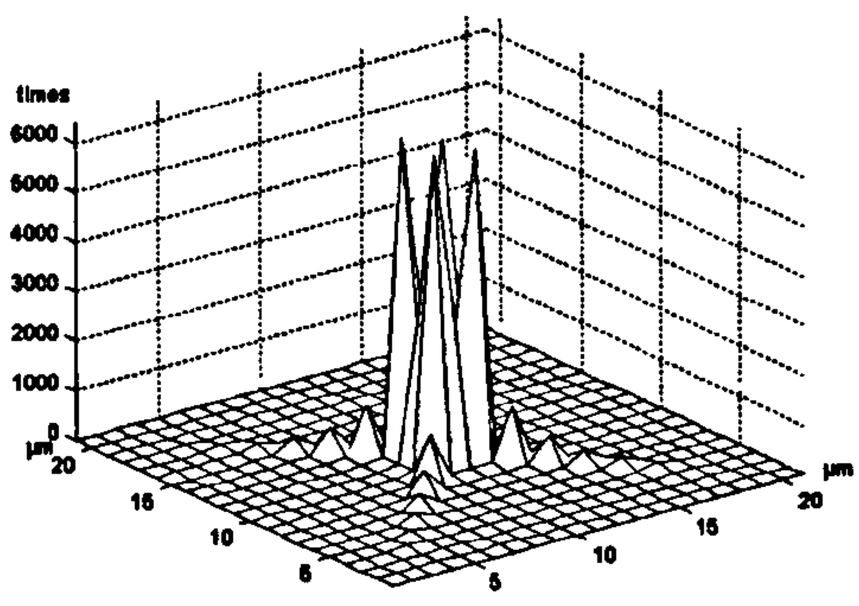

1 μm truncation

Pyramid tip

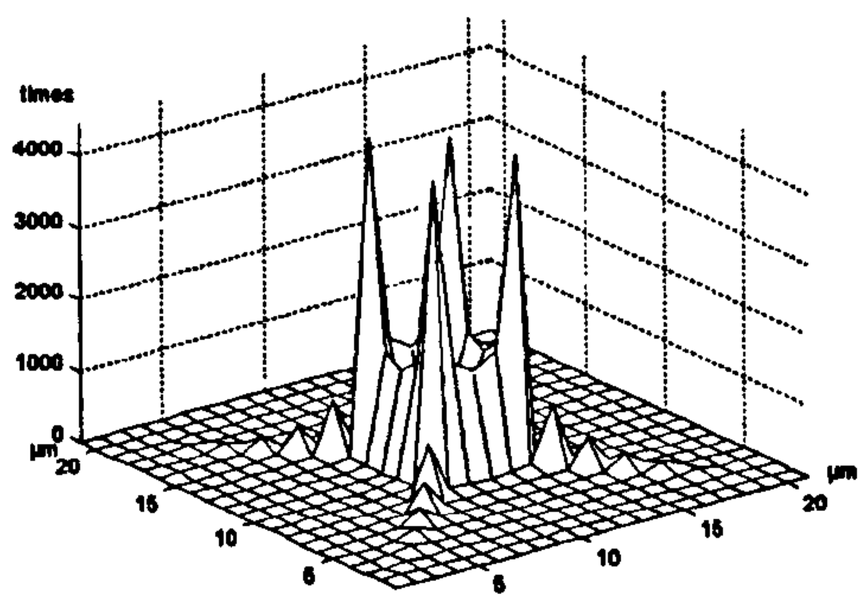

2 μm truncation

Figure 2.34: Contacts distributions of 10 μm truncated tips on a lapped surface

		Parameter (μm)	Sa	Sq	Sy	Ssk	Sdq
			1.70	2.13	14.03	-0.07	0.76
Tip	Size	Shape	% error				
Conical	5 μm	Perfect	-4.73	-4.90	-7.19	-39.31	-15.34
		1 μm Truncated	-7.45	-7.88	-14.32	27.50	-22.87
		2 μm Truncated	-11.57	-12.28	-21.45	101.00	-27.45
	10 μm	Perfect	-4.13	-4.42	-10.74	-34.46	-15.67
		1 μm Truncated	-6.74	-7.33	-17.35	30.94	-23.22
		2 μm Truncated	-10.82	-11.65	-22.62	100.15	-27.82
Spherical	5 μm	Perfect	-7.71	-8.41	-11.45	83.22	-27.21
		1 μm Truncated	-11.74	-12.66	-18.58	162.08	-28.63
		2 μm Truncated	-15.68	-16.74	-24.57	195.78	-31.25
	10 μm	Perfect	-16.49	-17.67	-23.99	101.98	-41.51
		1 μm Truncated	-20.69	-22.25	-30.20	199.07	-42.92
		2 μm Truncated	-25.59	-27.83	-37.25	258.38	-45.48
Pyramid	5 μm	Perfect	-5.20	-5.37	-7.19	-34.38	-16.20
		1 μm Truncated	-7.87	-8.37	-14.32	35.03	-23.93
		2 μm Truncated	-11.96	-12.76	-21.45	112.25	-28.99
	10 μm	Perfect	-5.67	-6.01	-13.03	-71.34	-17.35
		1 μm Truncated	-8.49	-9.16	-18.58	-7.44	-25.43
		2 μm Truncated	-12.77	-13.74	-23.41	61.68	-30.93

% error=100*(Measured Value - Actual Value)/ actual Value

Table 2.7: % error of roughness parameters of different tips on the lapped surface

3. The new 3D mapping system with exchangeable stylus

3.1 Introduction

A system has been developed during the course of this thesis for measuring repeatably surface roughness using different styli within different measuring environments. The system is capable of measuring the roughness of a surface in either two dimensions (2D) or three dimensions (3D). The system can be used to measure the surface roughness by two techniques: I) Start-Stop technique, II) Dynamic technique [34]. In the start-stop technique, a reading is taken on the first point of the surface then the stylus is moved one step to the next point followed by a brief delay while it settles before taking the reading then moving to the next point and so on until the end of the traverse. In the dynamic technique, the stylus is moved over the surface continuously while the readings are taken at pre-determined time intervals between each two consecutive points.

Traditional stylus measuring instruments are based on moving the stylus over the surface in one direction giving the surface roughness in 2D. Experimental 3D Mapping by mounting the sample on a cross-slide while using the traverse system of a 2D profilometer has been undertaken since 1970s [35]. Most commercial instruments makers, now offer a variant of this product based on this idea or on a special rig traverse system. The developed system is based on moving the specimen in the horizontal plane underneath the stylus while the stylus is held stationary during the measurement. By this way, it has become possible to scan an area of the surface giving the surface roughness in 3D using all sensor technology of a 2D measuring instrument.

While the concept of the new system by its means novel, its implementation incorporates several features needed for the close control of the planned experimental program. The

overall approach has been chosen principally to facilitate these needs, but also with a view of providing a metrology system of more general use.

3.2 Measuring Surfaces by Stylus Method

The stylus technique is one of the most commonly used techniques for measuring surface roughness. Its main advantage is that it is easy to use and also it is able to give a profile along a well-defined direction. Traverse speeds and measurement times are slow compared to optical methods [36] but contact metrology is less vulnerable to a range of typical surface contamination. There are many discussions of the relative merits of techniques in the literature. Figure 3.1 shows a layout measuring the surface roughness by the stylus method.

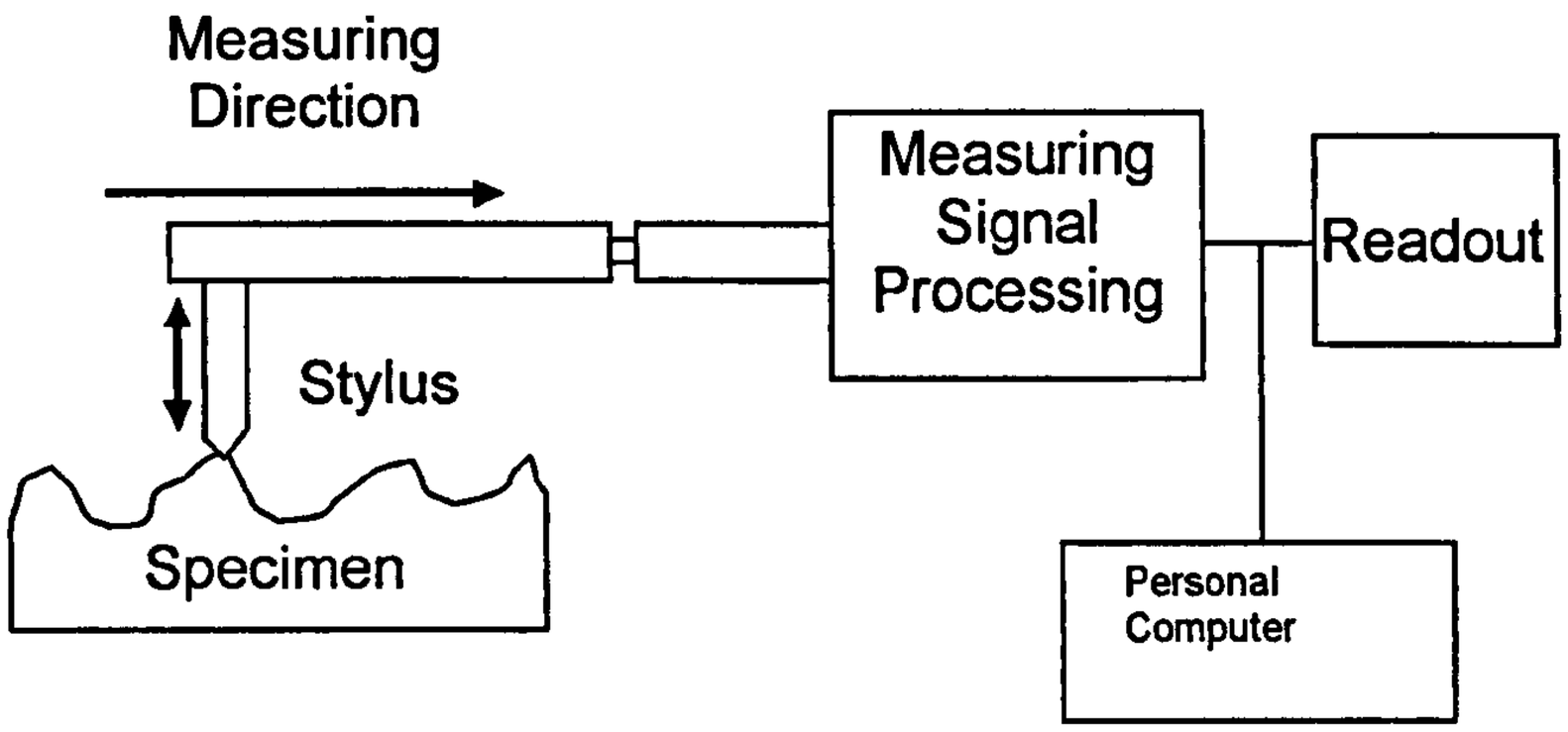

Figure 3.1: Measuring surface roughness by stylus method.

The stylus method is based on moving a very fine stylus along the specimen surface to be measured. The stylus tips are normally made of Diamond with pyramid or conical shape and may have tip radius of 2±0.5, 5±1, or 10±1 μm. The tip angle is normally 60° in the conical shape and is 90° in the pyramid truncated shape [37].

As the stylus moves along the surface it will move vertically following the asperities of the surface. The vertical displacement of the stylus is converted into an electrical signal, which is fed to the signal processing unit to be magnified, filtered or plotted. The signal could be also fed to a Personal Computer to be analyzed to determine a large number of parameters that have been proposed over the years for the assessing the surface roughness features.

Real tips are perfect when new and sharp features may reveal surface details that nominal surface could not. Even diamond wears quite quickly under profilometry so most tips flattened and reveal less than expected, although sometime they chip and leave sharp features.

3.3 Measuring Surface in 3D

The 3D measurement of the surface in this work is based on scanning a small area of the surface using the sensor system of a 2D stylus measuring instrument. The scanned area is divided into a regular rectangles array of points in the X-Y plane at which measurements of stylus heights are taken. This grid is aligned to the X and Y motion axes of the measuring system. The measurement process always proceeds by moving in the positive X-axis, keeping y constant, for a complete line of the grid. The X-axis is then moved back and the Y-axis is shifted one grid position ready for the next line to be measured.

The X- direction (sometimes called the measurement direction) always acts as the 'fast' axis and its motion corresponds to that seen by the stylus if the traverse unit of the 2D profilometer had been used. This orientation is important because the stylus is not of uniform stiffness in all directions. It is also important if asymmetrical styli are used. The distance between each two consecutive points is arbitrary but 1 μm sampling interval has been used in all measurements. The following two techniques could be used for scanning a small area of the surface.

3.3.1 Start-Stop Technique

In this method, the stylus is kept stationary and the specimen is shifted under it by a certain step in the X and Y directions then taking the roughness height readings in the Z direction at each point. Readings are only taken when the stylus stops at the specified points. The first reading is taken on point (1,1) and the last reading is taken when the stylus is at point (n, m) as shown in Figure 3.2.a.

3.3.2 Dynamic Technique

In this method, the stylus traverses the first trace in the measuring direction. During this trace all data representing the readings of roughness heights of the profile in two dimensions Z&X are taken. After completing the first trace, the stylus is moved forward to the start point of the traverse, then, the specimen is shifted with a certain step in Y direction across the traverse. Then a second trace is traversed and so on until the specified area of the surface is scanned as shown in Figure 3.2.b.

Table 3.1 shows a comparison between the two techniques. For the advantages of the start-stop technique, it has been used in this research for all measurements.

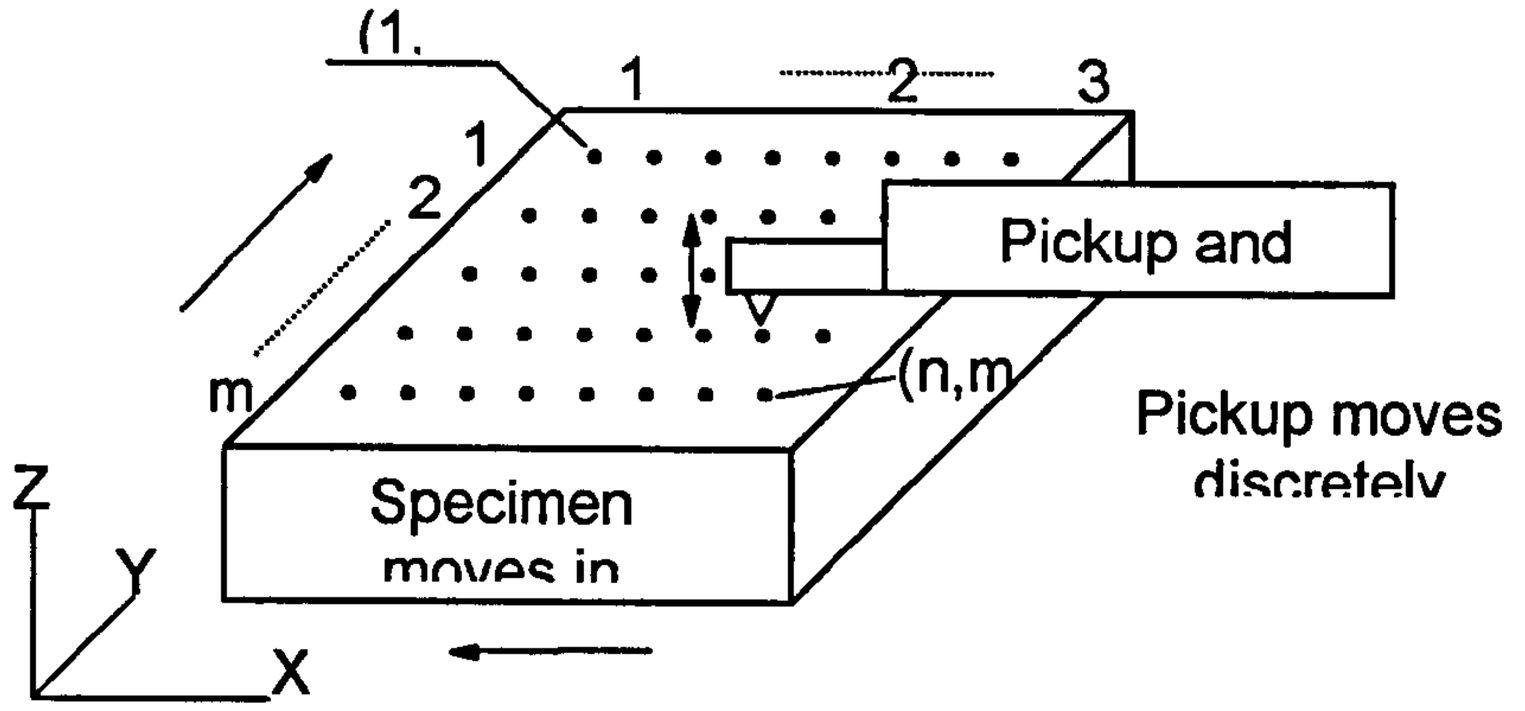

(a)

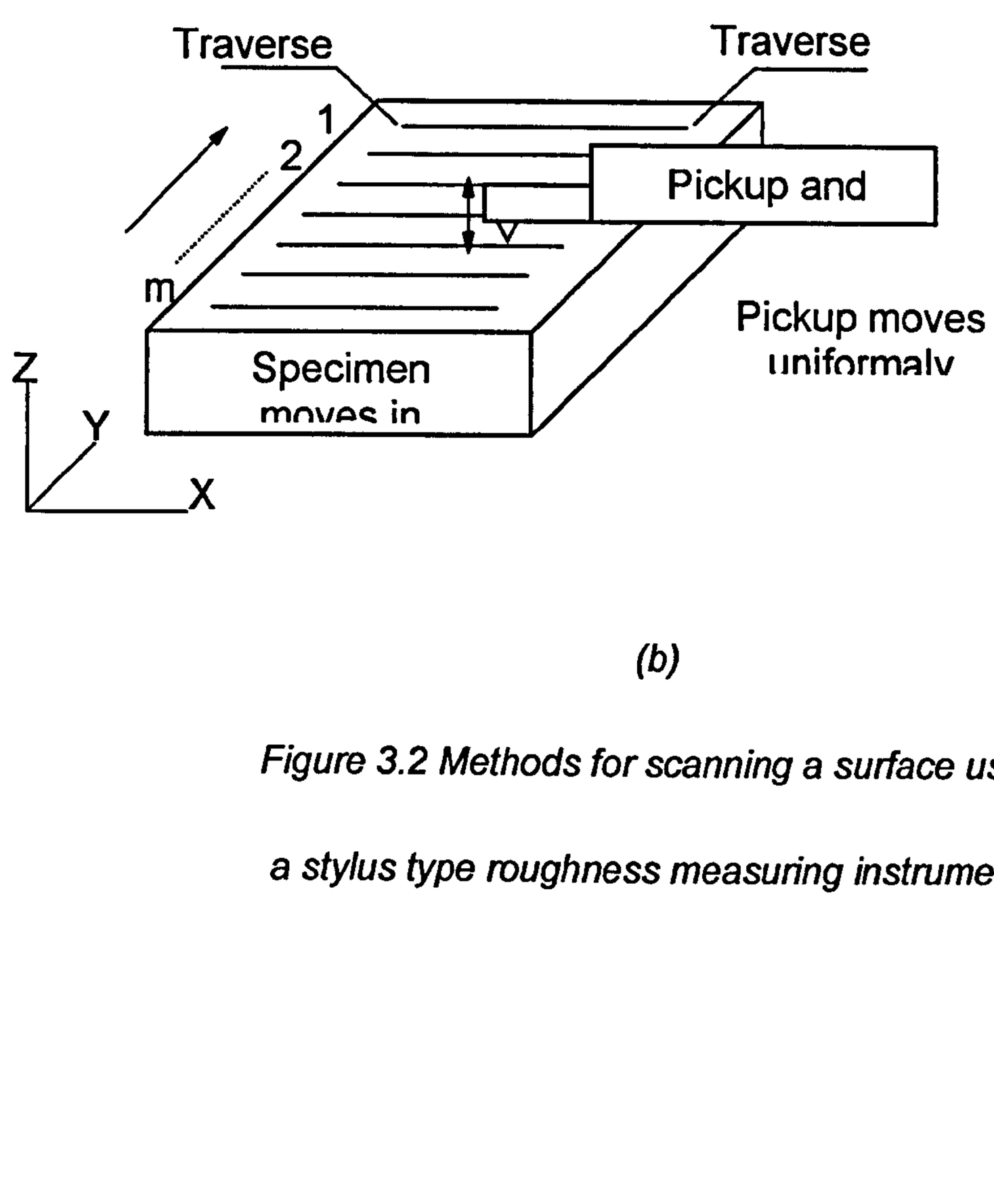

(b)

Figure 3.2 Methods for scanning a surface using a stylus type roughness measuring instruments.

Dynamic Technique	Static Technique
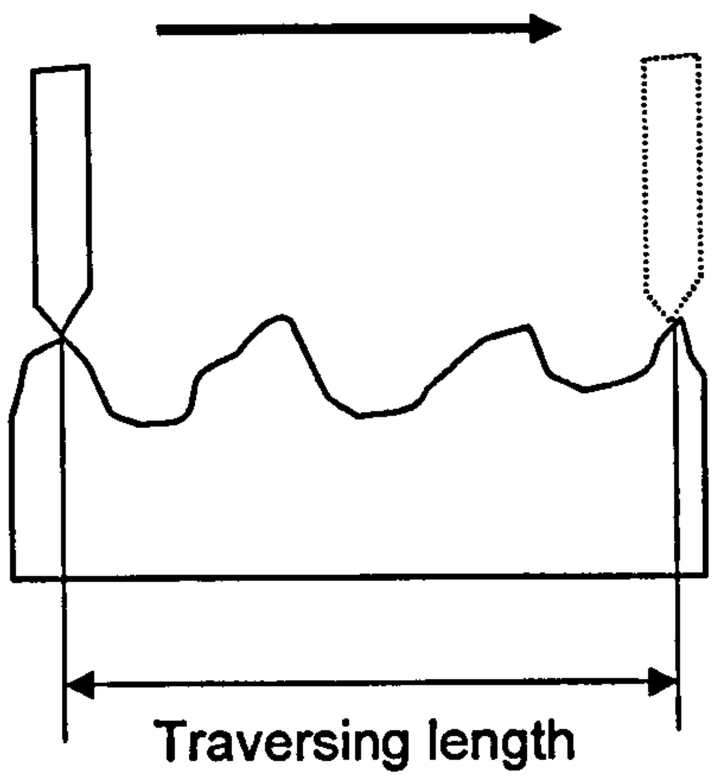	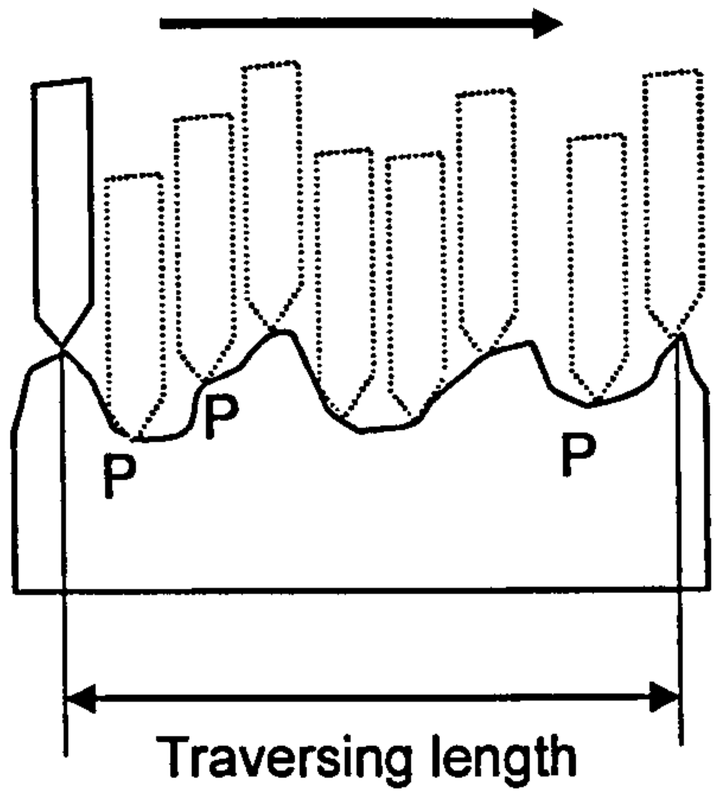
Disadvantages: Dependent on the PC speed. Reasonable repeatability. Limited traversing length. The actual measured distance is less than the traverse length. Surface damage.	Advantages: Independent of the PC speed. High repeatability. Longer traversing length. The actual measured distance is the same as the traverse length. Less surface damage.

Table 3.1: A comparison between the two techniques for measuring surface roughness

3.4 The Measuring System

Figure 3.3 shows the developed measuring system. Its main sub-systems are; traditional surface roughness measuring instrument (stylus type), a Personal Computer and a computer controlled X-Y stage. The measuring instrument used in this study is the Talysurf 5, made by Taylor-Hobson. The specimen to be tested is mounted on the X-Y stage and the pickup is lowered manually until the stylus makes contact with the measured surface. A kinematic mount has been used to relocate each specimen in the same position on the X-Y stage. The mount is also critical to insure measurement of the same area of any specimen when the stylus is changed. An attachment has been developed to allow the interchanging of styli as well as using the original stylus of the Talysurf. This attachment incorporates a system to control the force applied on the surface by the stylus including compensation of the additional weight caused by the extra stylus mount. The geometry of every stylus used in this work has been measured (see chapter 4), since a principal objective is to study its effect on the actual roughness values with different specimens.

3.4.1 Measuring Instrument

The measuring instrument used in the developed system is a Talysurf 5. This particular design arose in the 1970s but its concepts are considerably older. It is a classic example of a general-purpose 2D stylus profilometer. The stylus is presented on a cantilevered arm, sacrifing some rigidity for a clear and large workspace. The vertical range is usefully 100μm with a resolution potentially to around 1nm, but usually limited by the vibration noise-floor. The stylus and sensor are coupled directly to a horizontal traverse unit attached to a single vertical column. The traverse unit contains a Delrin and cylindrical steel datum slideway to provide up to 120mm movement with full traverse straightness of 0.5 μm.

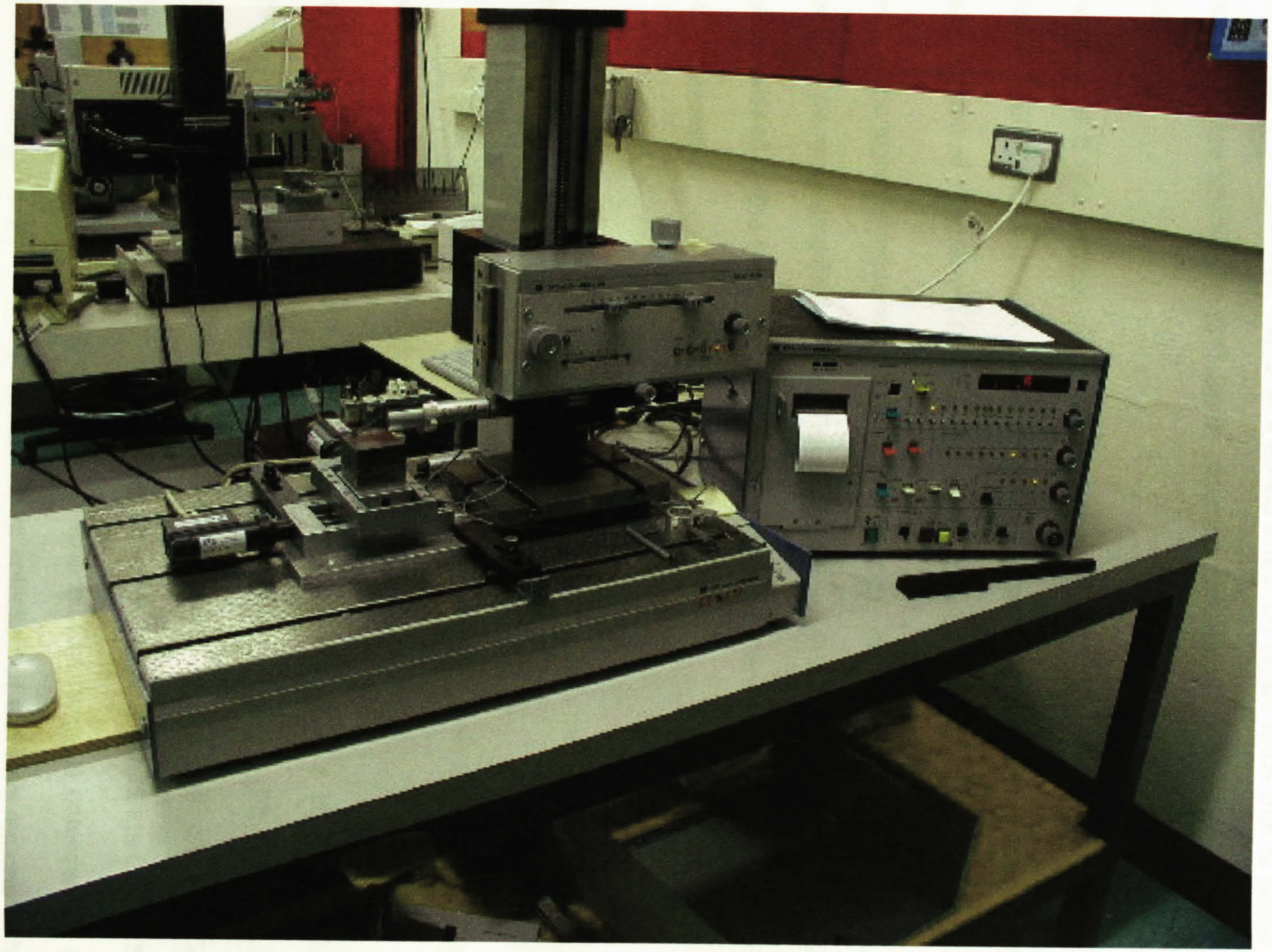

Figure 3.3: The measuring system.

The standard stylus of the Talysurf has the form of four-sided 90° diamond pyramid with a slightly rounded tip about 2.5 µm wide. It bears on the surface with a force of about 0.7 mN (about 70 mg) force. The stylus moves in a slight arc on a 50mm arm pivoted on a knife-edge and ligaments. There is a spring effect on stylus force that is below 35 mN. The values are specified in [37]. Some older instruments have this nominal force set at 1 mN.

The Talysuf 5 has vertical magnifications of 100, 200, 500, 1000, 2000, 5000, 10000, 20000, 50000 and 100000X and scans the surface at 0.05 mm/s giving a horizontal magnification of 100x times. Other lower magnifications use proportional faster speeds.

The electric signal representing the real profile of the measured surface is processed by precision gauging amplifiers of the Talysurf and then intercepted before being sampled and processed by the internal computer. This signal is then fed to the Personal Computer to be analysed.

3.4.2 X-Y Stage

To scan a small area of a surface using a 2D measuring instrument it was necessary to use an X-Y stage to move the specimen in X and Y directions.

The stage used in this study is constructed by stacking at right angles two identical commercial motorized linear stages model M-150.11 by PI (Physik Instrumente, Germany). This is computerized using drives supported by PI and offering down to 0.008 µm resolution. It could be driven at any specified speed in the range 0 to 1.68 mm/s. It has a range of 50 mm in both X and Y directions. This range is considerably greater than that needed experimentally, which allows selection of traverse regions with better straightness than its nominal specifications. Fig 3.4 shows a photograph of the X-Y stage.

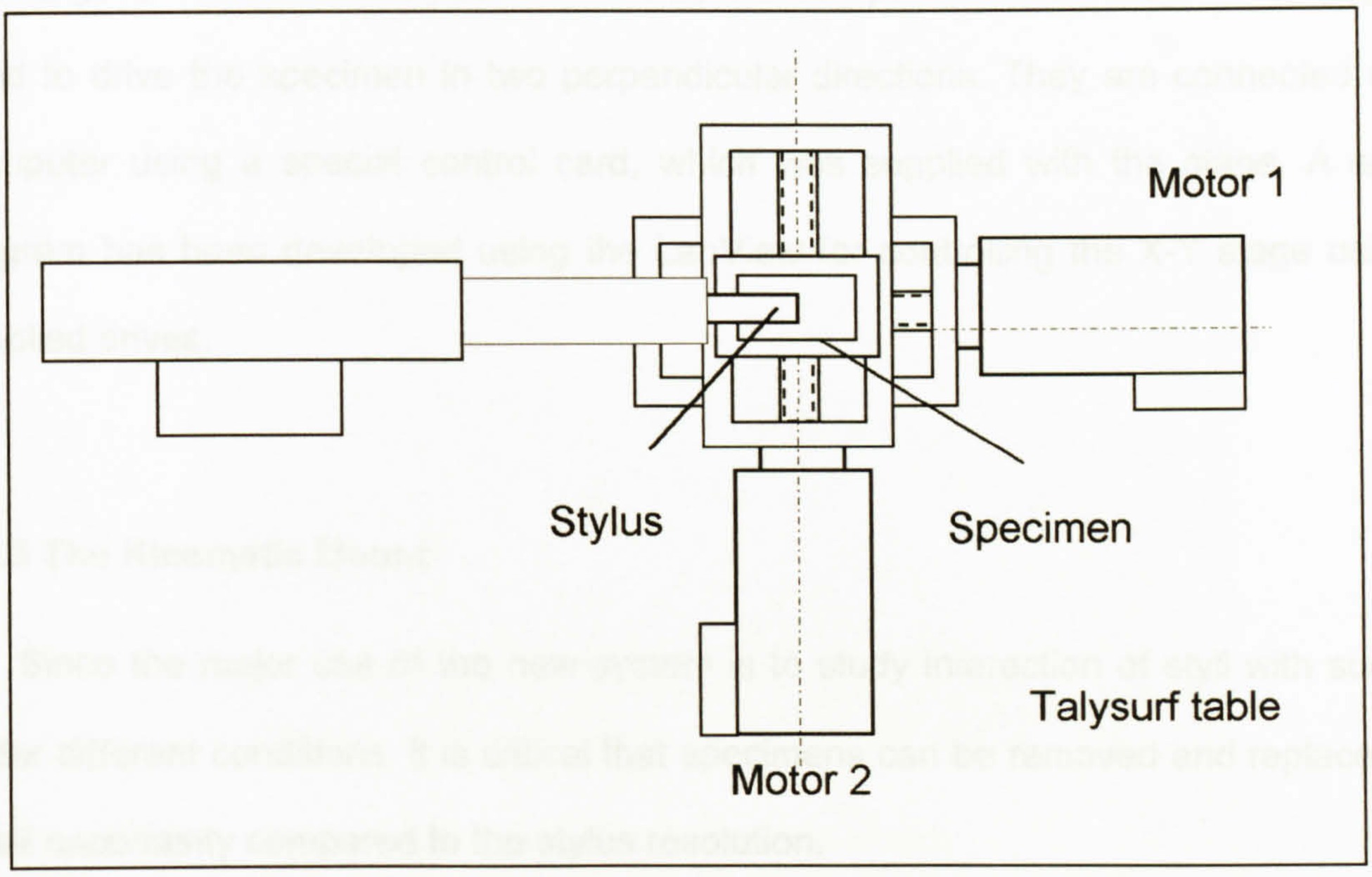

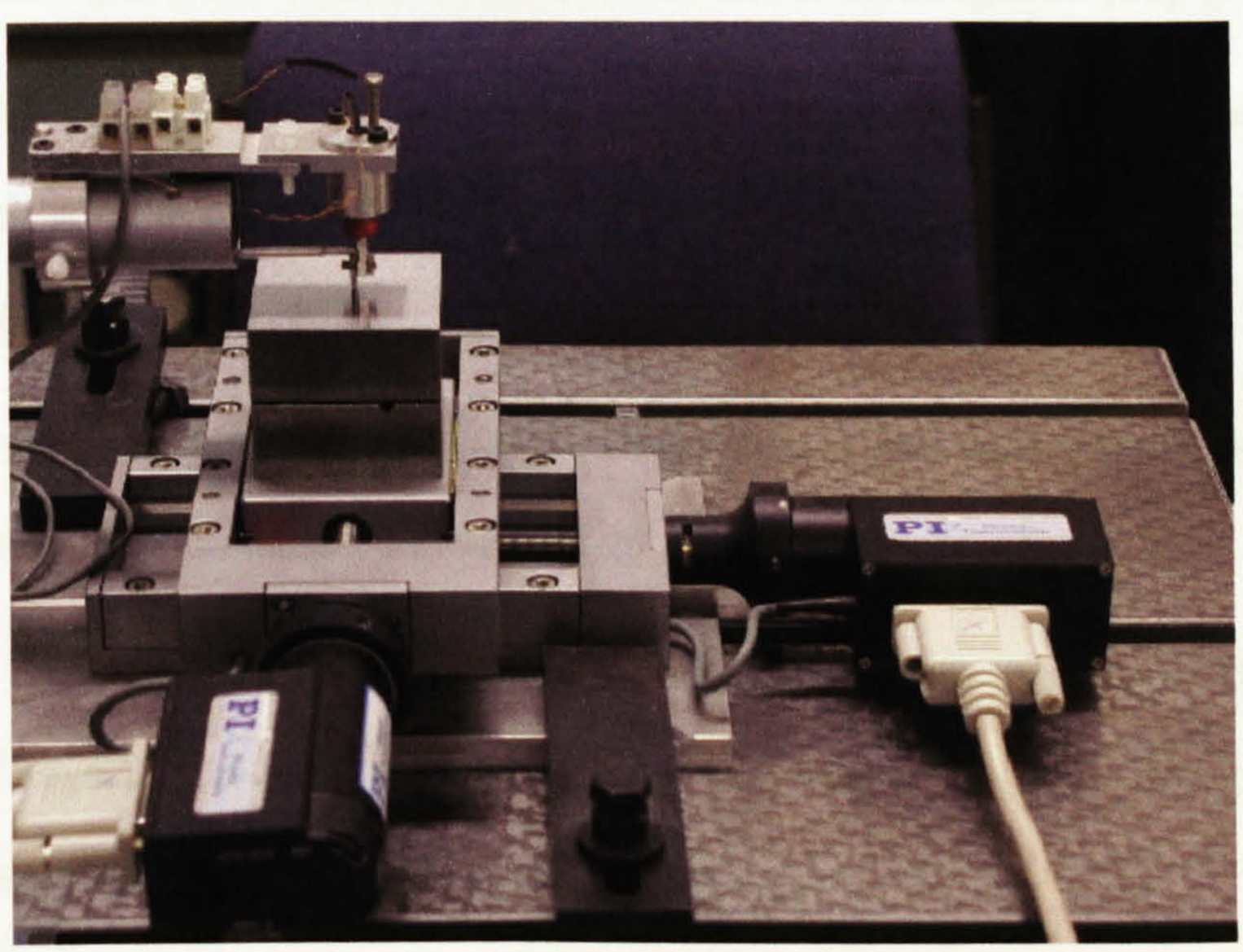

Figure 3.4: X-Y stage on the Talysurf base

The stage is fixed on the Talysurf base using two clamps. The two motors of the stage are used to drive the specimen in two perpendicular directions. They are connected to the Computer using a special control card, which was supplied with the stage. A special program has been developed using the LabView for controlling the X-Y stage using PI supplied drives.

3.4.3 The Kinematic Mount

Since the major use of the new system is to study interaction of styli with surfaces under different conditions, it is critical that specimens can be removed and replaced to a small uncertainty compared to the stylus resolution.

There has been some work on relocating the specimens for surface roughness measurement for comparing purposes. They were mainly based on using computer software to identify the same area of the surface under investigation [38], [39].

Since all specimens in this work are specially prepared and have approximately the same size, relocation can be 'built in'. This allows simple exploitation of classic designs of Kelvin Clamp kinematic locations [40].

For simplicity, a 3 balls and groove version has been used with 4mm diameter of balls glued into conical holes drilled into the bottom surface of the samples.

A steel plate carrying the groove pattern is screwed firmly to the stage. The archetypal design would have 3 equi-spaced radial grooves but, theoretically, any non-parallel set will locate uniquely. Figure 3.5 shows the kinematic mount.

Hence, for ease of manufacture, two perpendicular grooves were used.

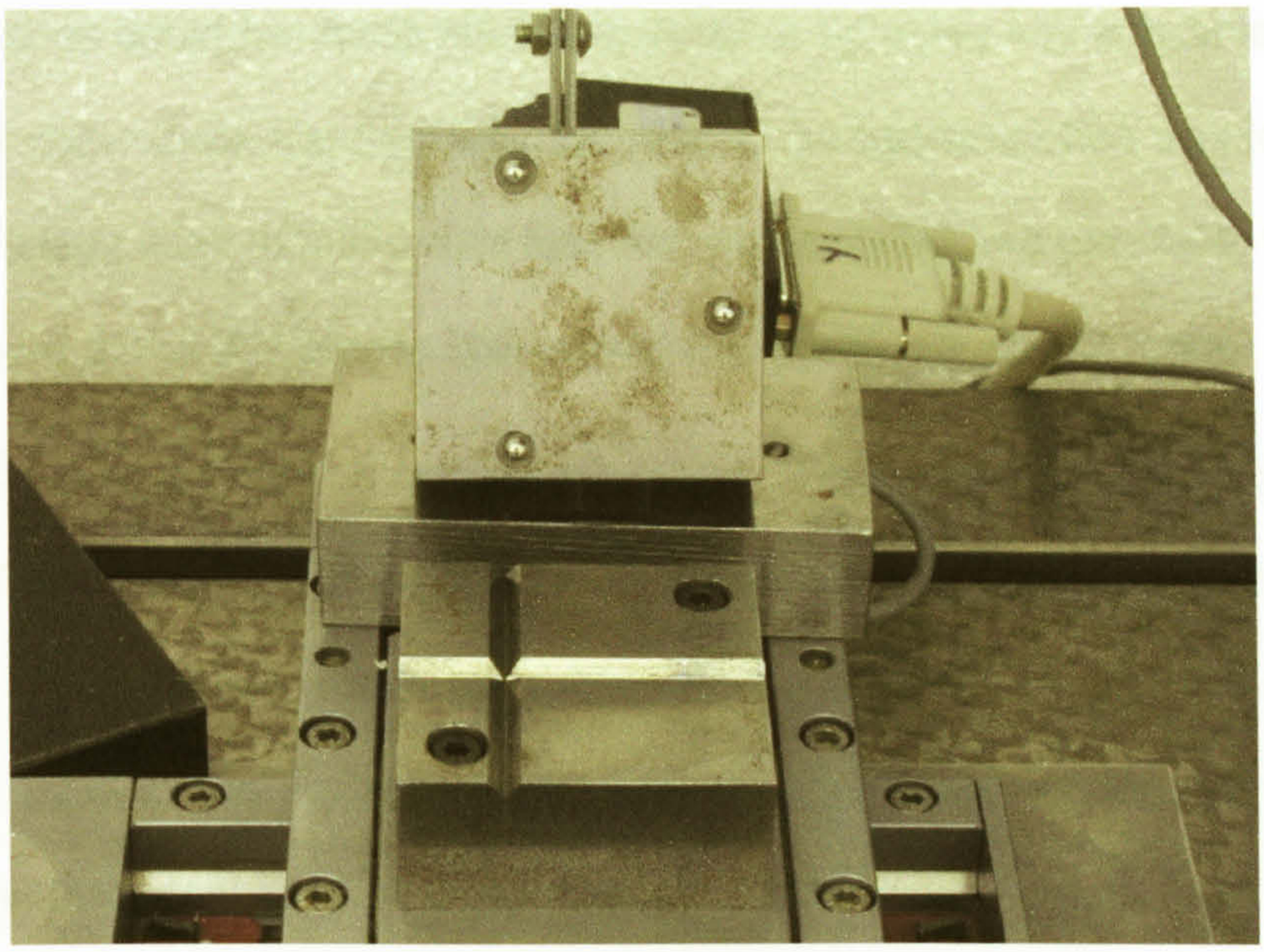

Figure 3.5: Kinematic Mount

3.4.4 Assuring repeat scanning of the same surface area

A conventional Kelvin Clamp kinematic location is found to be good enough for specimen relocation but does not address different styli. A simple idea for the latter is to use a permanent mark on the measured surface, which could be used as a datum for all measurements on the specimen. A single indentation could suffice as a datum for locating the stylus, relying on the kinematic clamp to define the specimen orientation. However, it could be very time consuming to find a small feature. A better alternative is to use two very fine orthogonal lines (or scratches) on the measurement surface, which could provide all the position and orientation information needed. The two lines need to be narrow and having well defined features so that positional analysis is possible to micrometer level of precision. Since scanning and analyzing the lines is also a slow operation, it is better to maintain a kinematic location, as well, using the lines only to define the stylus datum position.

The two scratches could be made either manually or by using any convenient machining process. After many trials, the best way for making the two scratches was found to be by using the X-Y stage itself to make sure that the two scratches are parallel to the directions of the movement of the X-Y stage. This makes it much easier to find them.

A scalpel blade is held firmly on a magnetic stand. The scalpel is lowered gently to touch the surface of the specimen. The specimen is then moved a suitable distance sequentially in the X and Y directions to make the two scratches. With a little practice and care with pressing the blade to the surface grooves with a clearly defined central valley can be created over in mild steel.

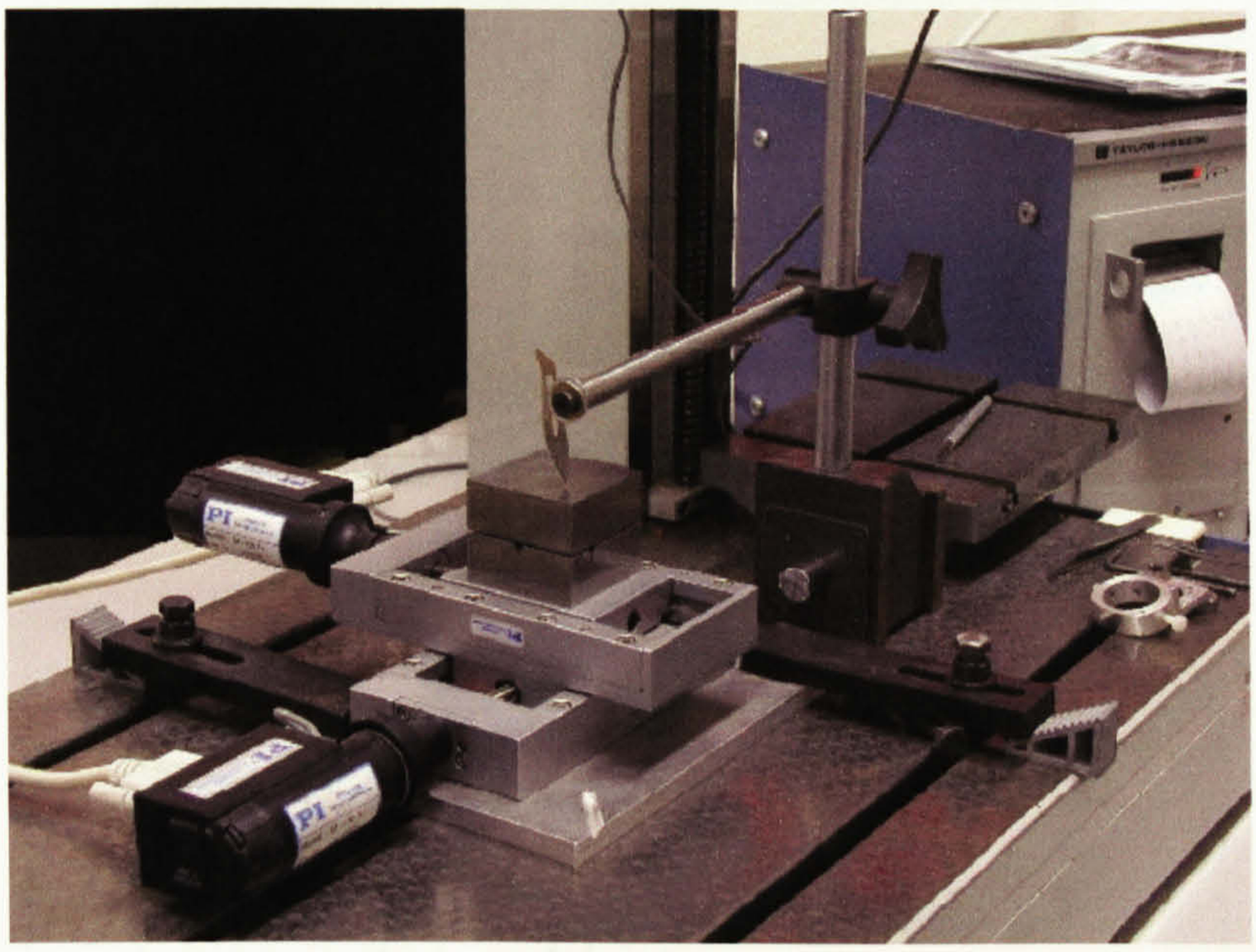

Figure 3.6: Making the reference scratches

Figure 3.6 shows how the scratches are made using the X-Y stage. Making the two scratches and subsequently finding them with the stylus is quite easy on a smooth surface. It is much harder to make well-defined grooves on rough surfaces because the force at the blade tip varies more. It is also more difficult to find and analyze grooves on

rougher surfaces. Since there is a kinematic relocation, this problem can be overcome by using a special reference specimen. The reference specimen is of the same form of the other specimens, made of steel with its top surface smooth to the level of grinding finish. The two reference scratches have been made on the specimen using the previous mentioned method. Figure 3.7 shows the reference specimen with the two scratches. Figure 3.8 shows a real profile across the scratch.

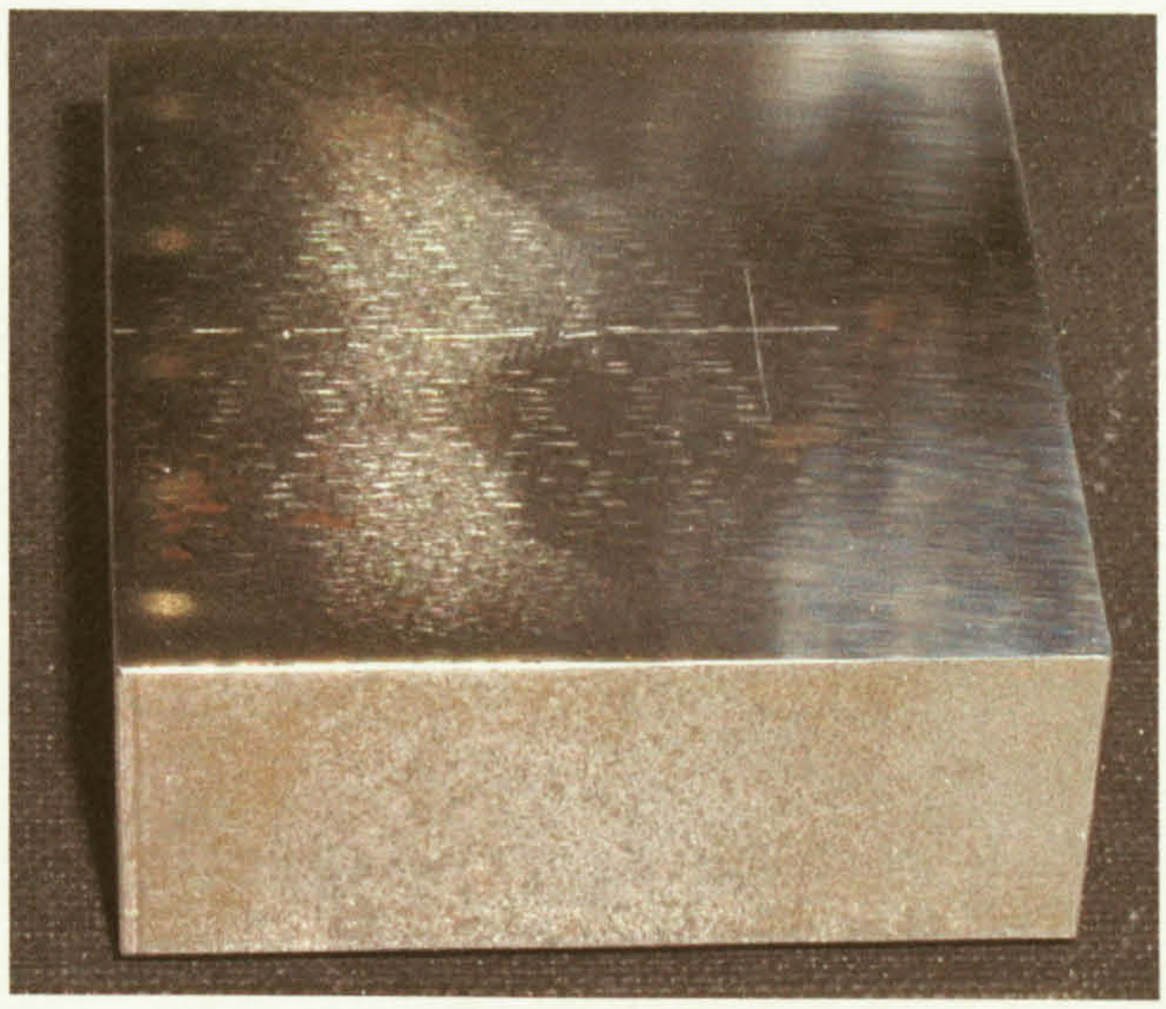

Figure 3.7: The reference specimen

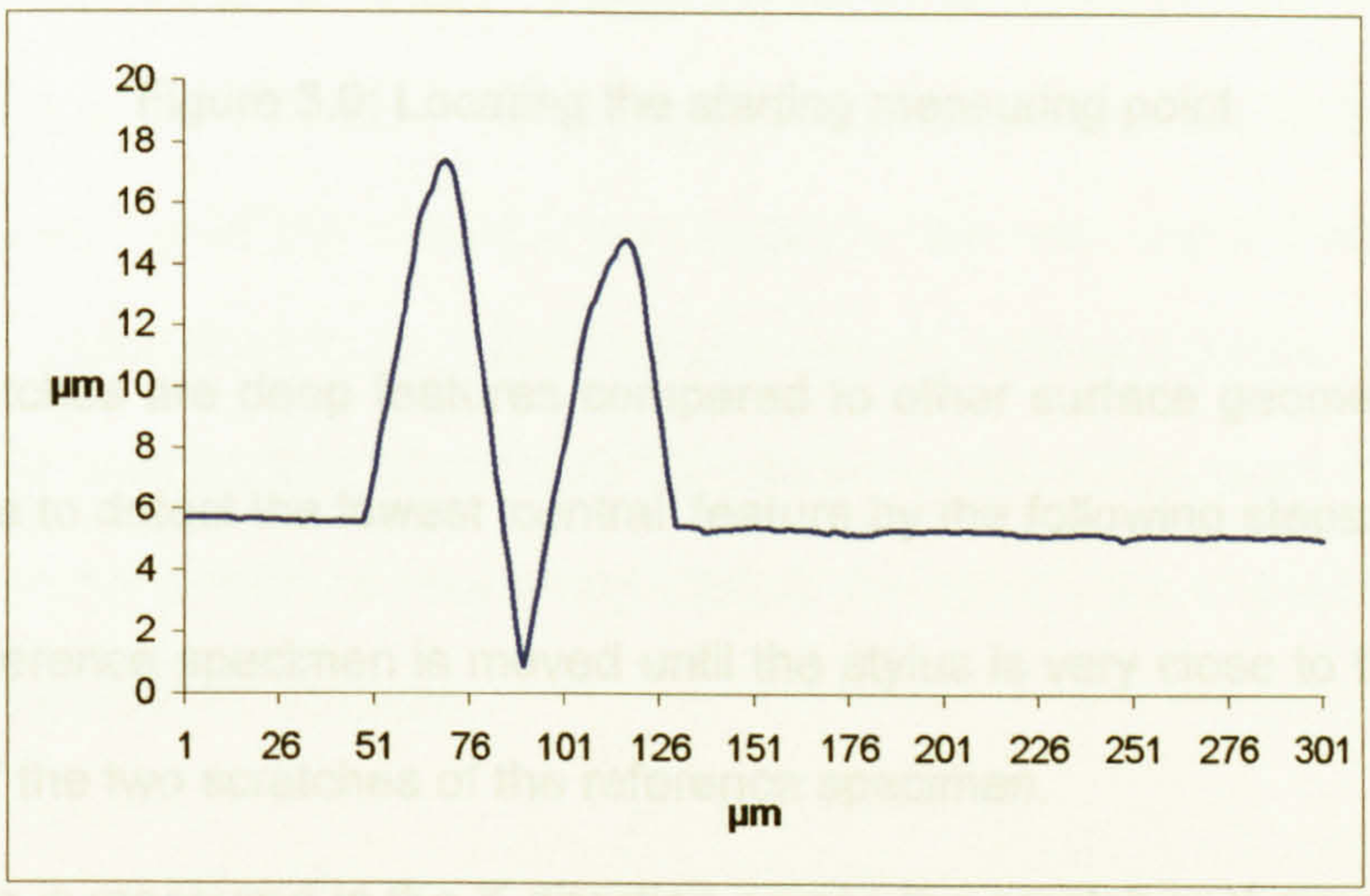

Figure 3.8: A real profile across the scratch

Once the scratch features are identified, the actual coordinates (a, b) of the stylus start position relative to the scratches have been determined. As seen in figure 3.9. Then the stage is moved so that the stylus is located 100 µm from each scratch at position p. This position locates the stylus relative to the fixed part of the kinematic mount.

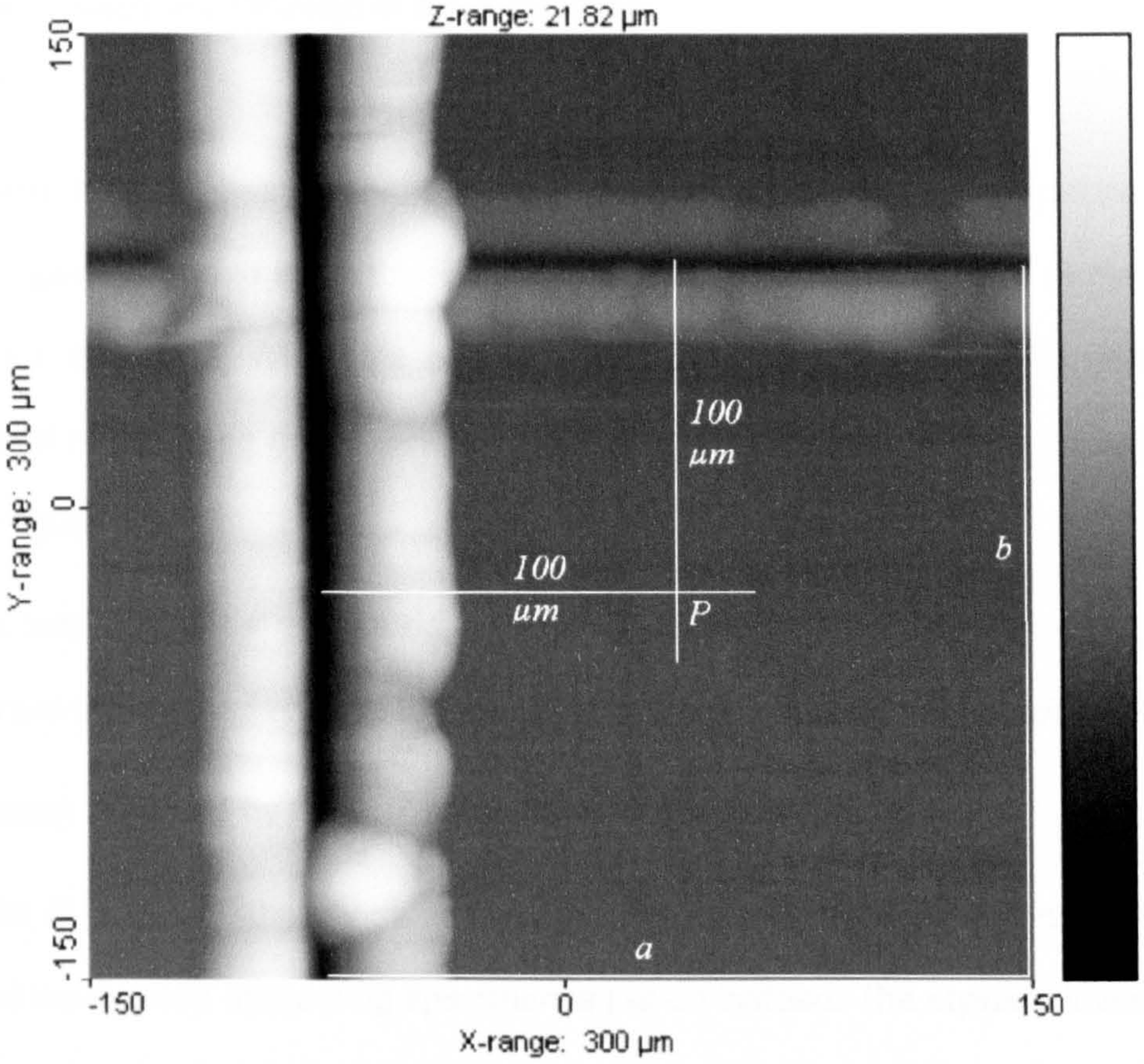

Figure 3.9: Locating the starting measuring point

Since the scratches are deep features compared to other surface geometry (around 10 µm), it is simple to detect the lowest 'central' feature by the following steps:

- The reference specimen is moved until the stylus is very close to the intersection point of the two scratches of the reference specimen.
- A profile is measured in the X direction across the scratch in Y direction.

- The index of the lowest point of the profile is determined relative to the starting point of the profile.
- The specimen is moved so that the distance between the starting point of the profile and the lowest point is 100 µm.
- Same steps are followed in the Y direction.

Before each set of measurements, with a different stylus, the two scratches on the reference specimen have to be found using the stylus by measuring two single traces in the X and Y directions. When the two scratches are found, the distances between the starting point of the trace and the lowest point of each scratch are found. This method is shown in Figure 3.9.

Once the two scratches are found, the coordinates (*a, b*) of the stylus in X and Y directions are determined relative to the two scratches on the reference specimen.

The specimen is moved by the X-Y stage to point *P* where *a*=*b*=100 µm.

Once point *P* is found, the stylus is lifted up, the reference specimen is taken off the mount and the desired measuring specimen is put on instead. The stylus is lowered again until it touches the specimen. When setting the stylus to make the first contact with the reference specimen or with the measured specimen, it is important to finely adjust the stylus height until it is at the center of its range. In this way, point *P* will be the initial location of the stylus for all 3D measurements on all different specimens despite its arcuate motion. For every specimen that it is replaced on the stage, point *P* is used for the start of each measurement, so measuring closely the same area of each specimen with different styli has become possible.

3.4.5 Interchangeable Stylus Attachment

A special rig has been designed and made to allow the use of different styli tips as well as the original Talysurf styli without modifying the Talysurf stylus arm.

The basic concept of the rig is to clamp onto the stylus arm, a fitting that holds a tip on the same line with the original stylus to assure that the magnification is closely the same in terms of the stylus lever. It is important to minimise the weight but it must add some extra so it also incorporates a force actuator to compensate and additionally to give controlled variable contact force. The force actuator is based on, and has used some components from an earlier design [41]. Figure 3.10 shows a photograph of the whole attachment and Figure 3.11 shows a schematic extended view of the construction.

The stylus tip mount is mainly made of Aluminum to minimize its weight. Figure 3.12 shows the stylus mount, which is made of two parts. The lower part fits around the Talysurf stylus and the upper part clamps it into place.

The stylus arm of the Talysurf consists of an Aluminum tube with a short piece of Aluminum rod, carrying the stylus tip attachment almost at its end. The lower part of the new stylus mount has a blind cylindrical hole into which the stylus rod fits loosely and an open section which bridges around the sides and end of the main stylus arm. The upper clamping piece is essentially a small rectangular piece that slides into the open section of the lower one. Both parts have a through hole by which they can be held together by a 1 mm steel pin. A small piece of soft rubber is placed between the block and the stylus arm and is significantly compressed when the holes align, to provide a gentle clamping force. This force ensures that the Talysurf stylus engages definitely with the end of the blind hole to define the metrological path to the end of the stylus mount, where the required tip is glued on.

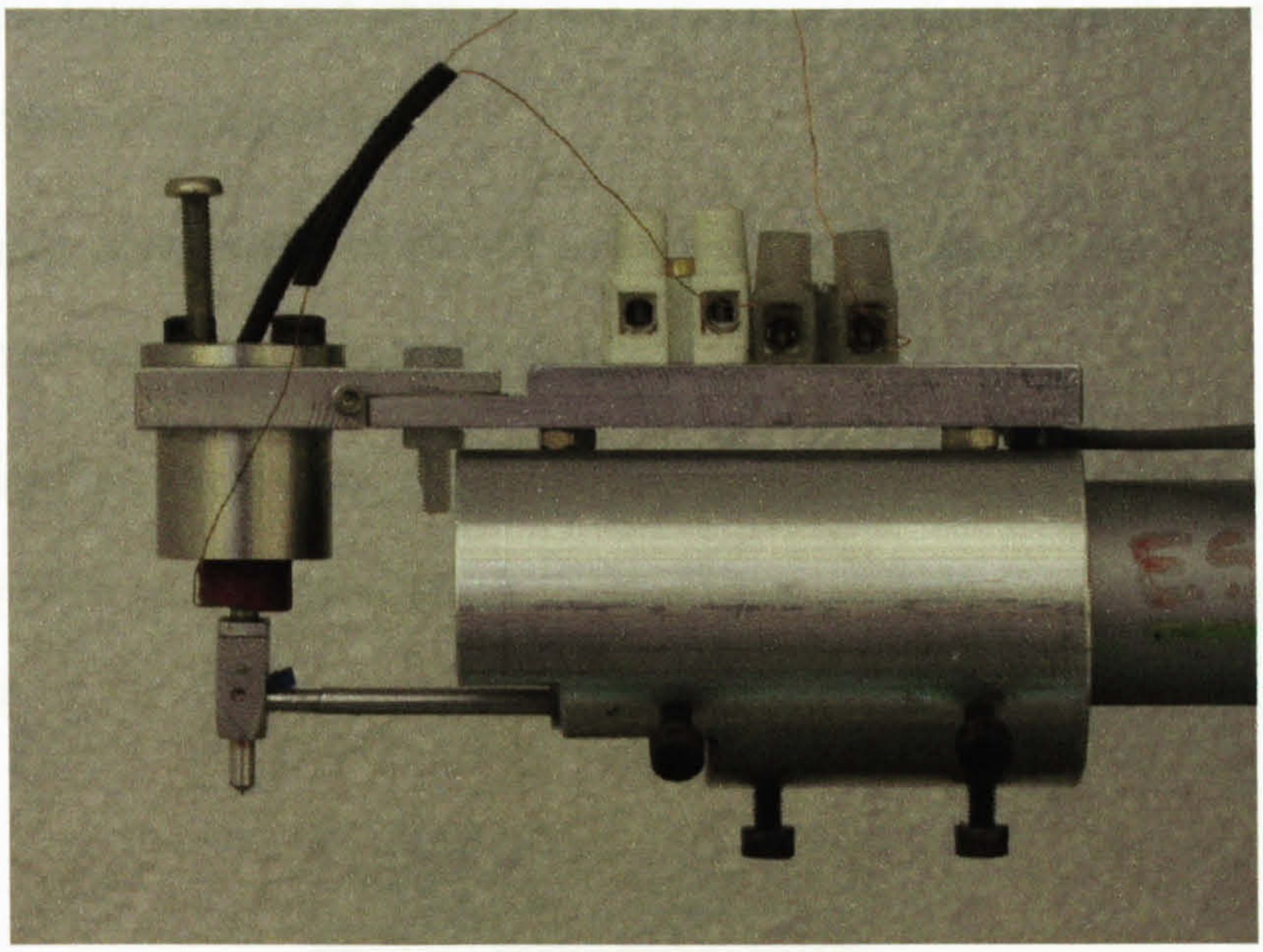

Figure 3.10 The Stylus Exchanging Rig.

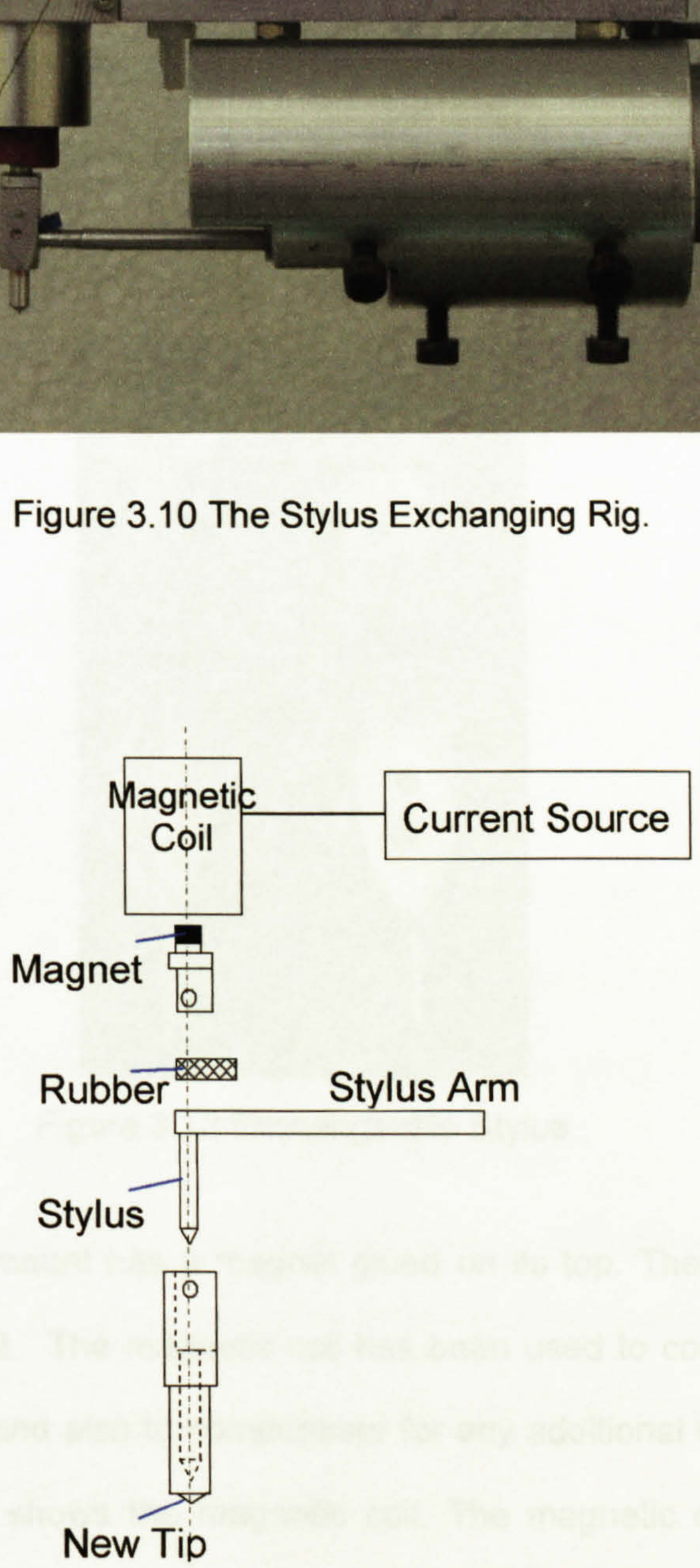

Figure 3.11 Layout of the stylus rig

The practical realization of the upper part makes it T-shaped, partly to act as a mechanical stop against the lower part and partly to make it easier to attach directly to its top surface, the magnet of the force actuator.

The coil, magnet, stylus rod and tip all lie nominally on the same axis. The whole mount, including magnet was made of about 135 mg.

A variant design has the end removed from the tip mount so that the stylus rod and tip of a Talysurf long-read pickup go through. This allows variable fore action with a normal Talysurf stylus.

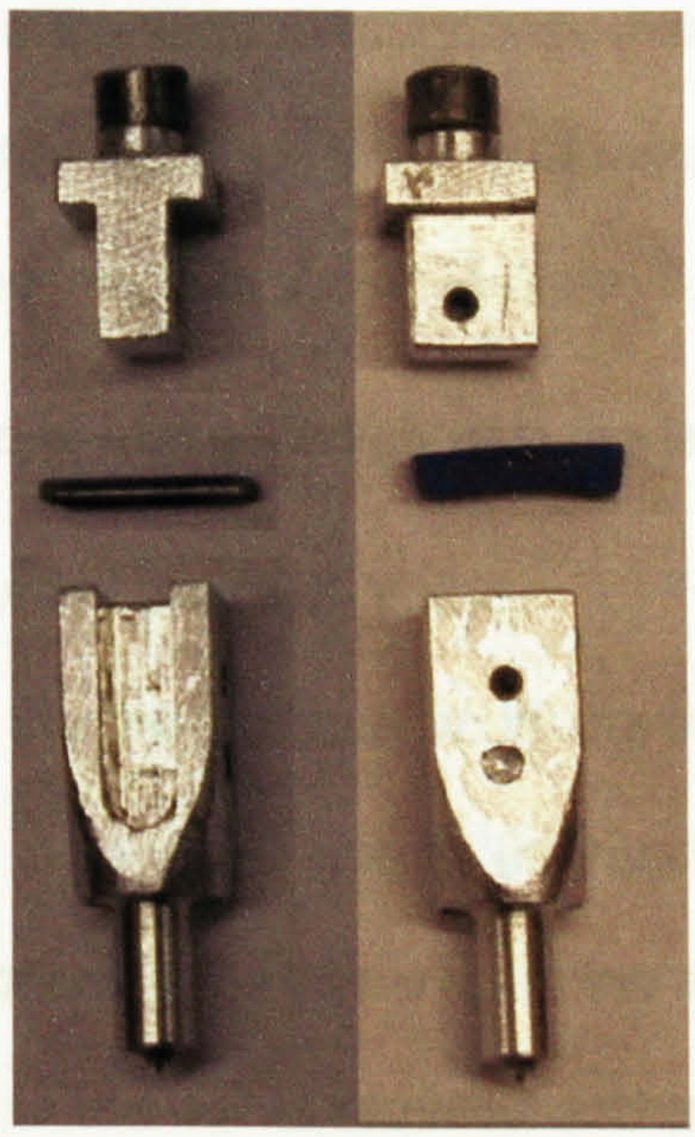

Figure 3.12 Exchangeable Stylus

The upper part of the mount has a magnet glued on its top. The magnet moves freely inside the magnetic coil. The magnetic coil has been used to control the contact force applying on the stylus and also to compensate for any additional weights caused by the stylus rig. Figure 3.13 shows the magnetic coil. The magnetic coil is connected to a variable current source. The amount of the current applying to the coil will define the contact force on the stylus. The current needed to lift the stylus mount (0 force on the

stylus) was found to be around 100 mA. The whole rig is mounted on the Talysurf pick-up arm and held by clamping screws on both sides to prevent any movements of the rig.

3.5 Real Shape of the Tip

As the main target of this project is to study the effect of the stylus geometry on the roughness measurements, it was necessarily to determine the real shape of the styli used.

A simple but highly effective idea has been used to determine the actual shape of all tips used in this study. It is based on the replica method. The replica method is a technique that has been used before in the surface roughness measurements [42], [43]. The stylus is deliberately pushed a certain distance into a soft material to make an indentation. The schematic diagram of this technique is shown in figure 3.14.

The following steps are used to make the indent in the lead substrate:

- The substrate is mounted on the X-Y stage.
- Current is applied to the magnetic coil to lift the stylus up to the 0 µm reading.
- The Talysurf head is lowered gently (manually) until the stylus touches the specimen and then pushing the stylus up to the desired dent height (4 to 5 µm).
- The current applied to the coil is reduced and reversed if necessary to push the stylus down until the reading is brought back to 0 µm.
- The current applied to the magnet is reversed to get the stylus off the dent.

By this way, the indent has been made on the specimen to a predefined depth.

A substrate made of lead has been used to create the stylus indent. The substrate has been polished. Figure 3.15 shows the lead substrate.

The lead substrate has three balls fixed to its bottom face to locate it at the same position on the x-y stage in the same manner as standard specimens.

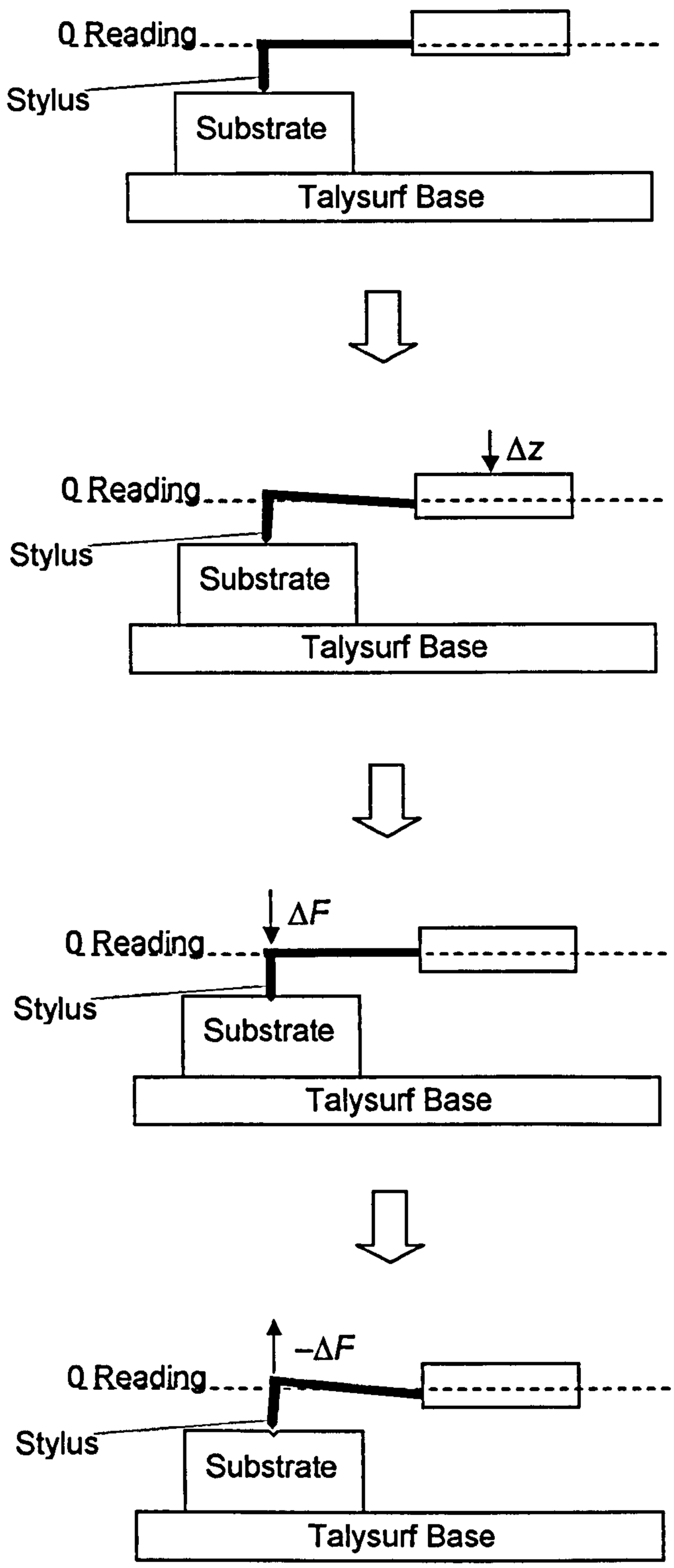

Figure 3.14: Schematic diagram of the stylus indentation technique

Once the indent is made, it could be measured by any advanced roughness measuring instrument with adequate lateral resolution. The Atomic Force Microscope has been used to measure the indents representing different styli as its tip size is very small compared to the tips used in this research.

Figure 3.16 shows a real shape of the dent created by a stylus using the mentioned method. Figure 3.17 shows a real shape the stylus.

The other advantage of this method is that the tip is measured in the same orientations as the measuring process.

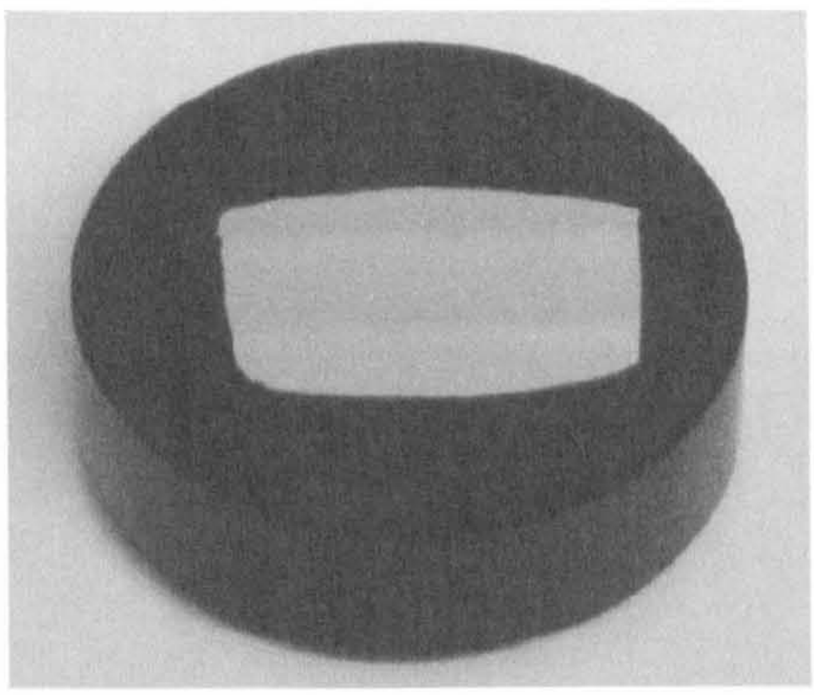

Figure 3.15: The lead substrate

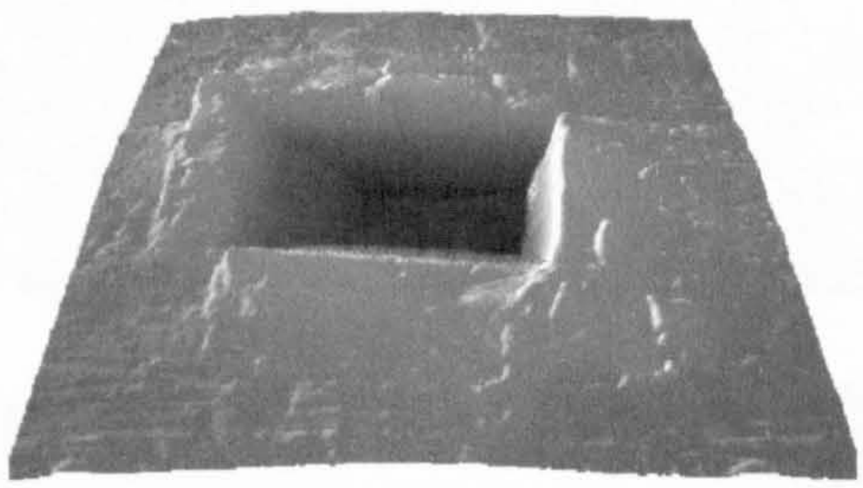

Figure 3.16: Stylus indent

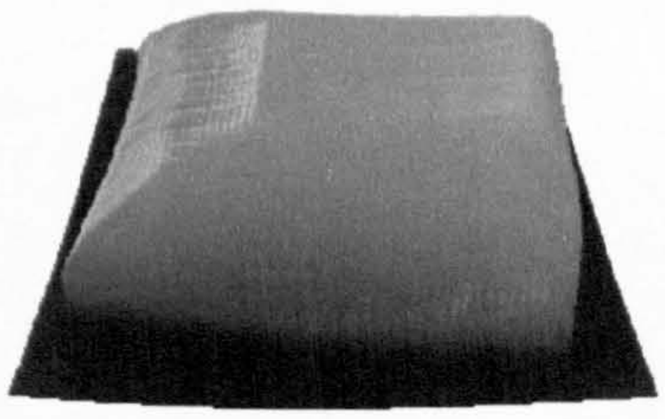

Figure 3.17: Stylus shape

3.6 Specimens

Twelve specimens have been prepared for the purpose of verification of the system. These specimens were machined in mild steel by different processes to give different patterns of surface roughness texture. The machining processes used are turning, milling, lapping and grinding (three specimens of each).

All specimens have cylindrical shapes with 60 mm diameter and 25 mm height. Each specimen has three 4 mm steel balls glued to its bottom face. The balls are equi-spaced on around a 45 mm diameter circle, with position set by spot drilling conical holes of 4 mm. The three balls are used for relocating the specimen on the x-y stage. Figure 3.18 shows a specimen used in this study. Figure 3.19 shows all the specimens used in this study, the roughness of which are measured and are shown later in the relevant chapter.

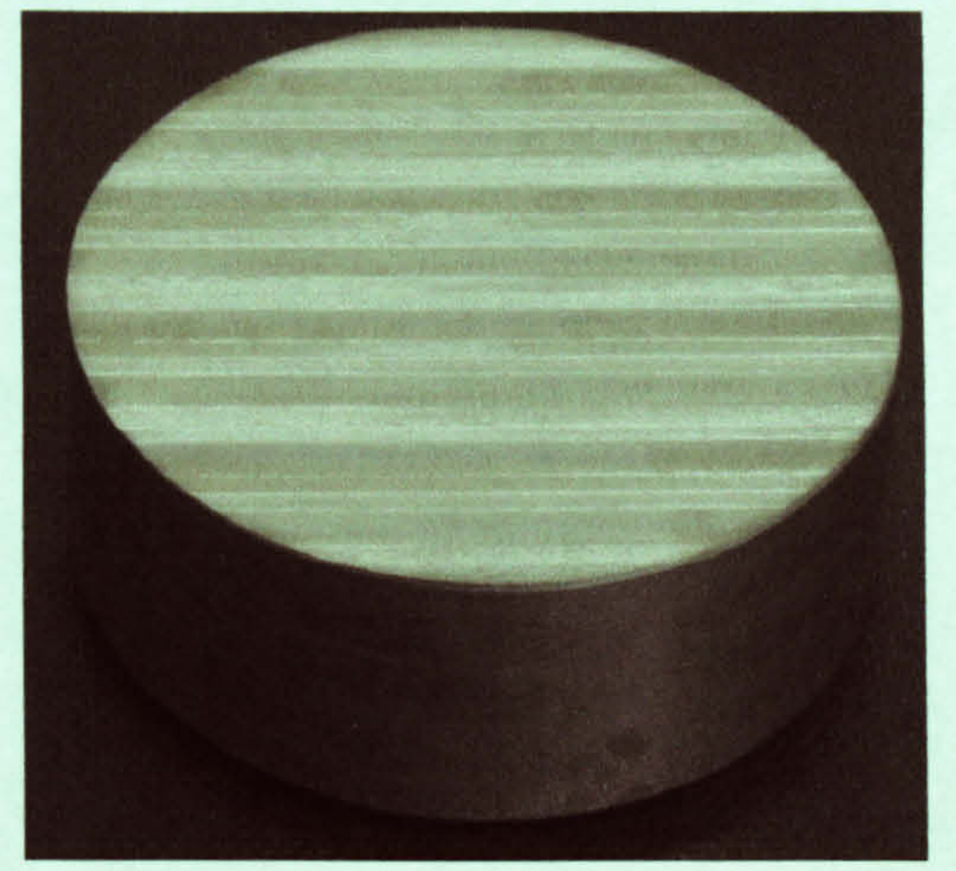

Figure 3.18: A specimen Shape

Figure 3.19: All the specimens used in the study.

3.7 Software

The measurement process is controlled by a specially written routine using LABVIEW®. This program mainly controls the movement of the two motors of the X-Y stage in the measuring process and captures the data from the measuring system. The data is stored in ASCII format on the local hard disk drive at the end of the scan. Since speed is limited by the test rig, not the computations, low specification PC (Pentium II, 400 MHz with 64MB of RAM) has been used. It takes around 5 hours to scan 300x300 μm area of a surface with 1 μm resolution. Data analysis is done off line on a faster machine.

The simulation process is done by a specially written routine using MATLAB®. This program creates the different tips and surfaces shapes and simulates the scanning process of a surface. It also reports the contact distributions on the tips as well as the locus of the center of the tip when scanning a surface. The simulation program take around 20 minutes to scan 300x300 μm area of a surface with 10 μm radius, spherical tip at 1 μm resolution.

Analyzing the data of the surfaces is done using a commercial software package SPIP®. This software is designed for the roughness analysis in two and three dimensions. It gives more than 20 parameters by which a surface structure can be characterized.

4. 3D Roughness Measurement with the System

4.1 Introduction

It has been clear from chapter 2 on the 3D simulation that there can be a significant effect of the stylus geometry on the roughness measurement of engineering surfaces. The results shown in the previous chapter were based on theoretical scans of surfaces. These results show no more than intuitively obvious. The important question is whether the effect is important to measurements of typical finish process. The measuring system developed in chapter 3 is used to show practically the effect of the stylus geometry on the roughness measurements in the real life. It will confirm the extent to which the simulation may be used to deduce the behavior of real systems. It is necessarily to verify the system and the method before using it.

4.2 Calibration of vertical magnification of the system

The vertical calibration of the system is done by measuring a standard step with a known height by the system and determining the equivalent voltage value representing this step height [44]. A step with 10.03 μm height has been used to obtain the calibration constant value K for different vertical magnifications selected from the measuring instrument up to 10,000. Five traces were taken for each magnification. The value of the average K for each vertical magnification is shown in table 4.1. The value of K for higher vertical magnifications has been determined by interpolation. The 10,000 vertical magnification has been used for all measurements in this study. The values of other magnifications show the consistency of process, subject to reasonable 'range-switching' errors.

Vertical magnification	K value µm/volt
1000	27.10
2000	13.52
5000	5.22
10000	2.70
20000	1.32
50000	0.65

Table 4.1: Calibration constant K at different magnifications

4.2.1 Verification of the measuring system

The traditional 2D stylus profilometers use the dynamic technique for measuring the surface roughness where the stylus is moving continuously over the surface of the specimen. Modifying such a system to measure surface roughness in 3D is not very easy. This is due to the need of controls to control the start of the trace and its end and also to move the stylus backward after finishing the traverse to start a new one. Also triggering is needed to set the start of capturing data on each trace. That is beside, using an X-Y stage to allow measuring parallel traces.

The alternative is to use a fully computerized and precise X-Y stage to move the specimen in the horizontal plane under the stylus while the stylus is not moving. In this case the stylus is just used as a sensor in the vertical direction. This will allow the scanning an area of the surface in 3D with nearly the same size as the range of the stage.

4.2.2 Verification in 2D

This verification is done by comparing a profile measured by moving the stylus over the specimen (i.e. using the Talysurf 5 traversing unit) with the same profile measured by moving the specimen underneath the stylus. Figure 4.1 shows the two outputs of measuring the surface roughness of a specimen using these two methods. It can clearly be seen that both produce closely the same profile. It is not expected to get exactly the same profile even using the same technique twice.

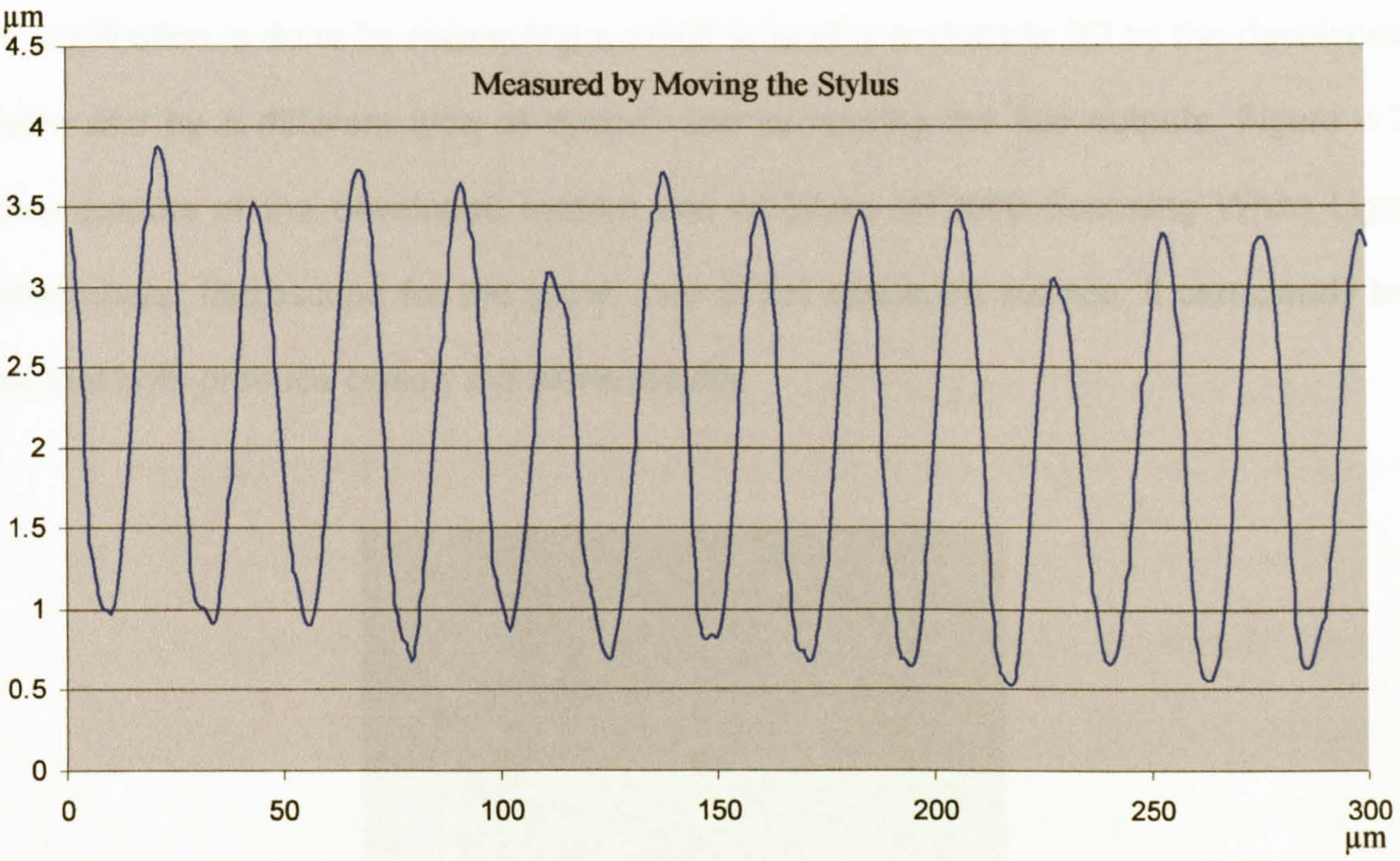

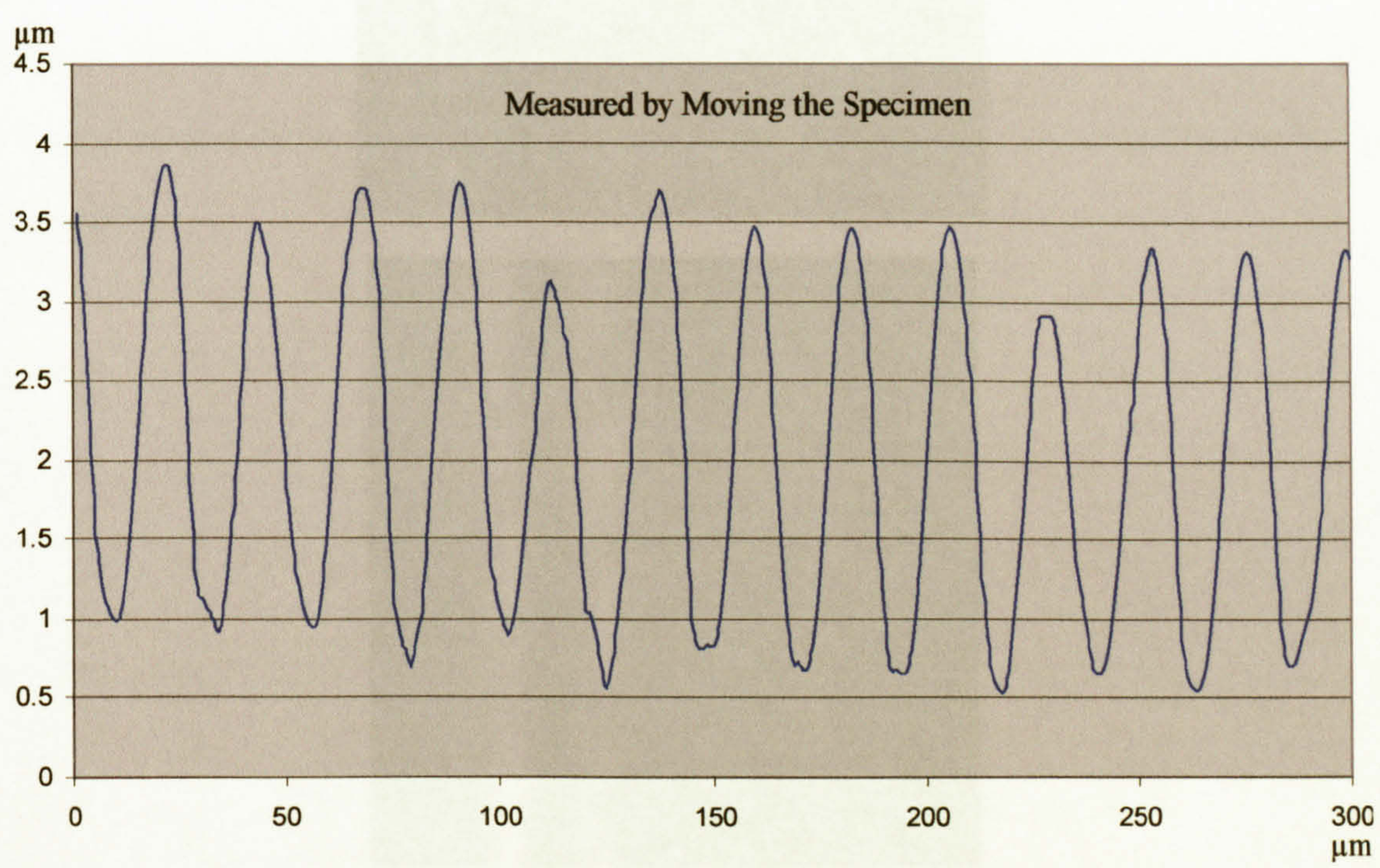

Figure 4.1: Same profile measured in 2D with two measuring techniques

4.2.3 Verification in 3D

This verification is done by measuring a small area of a surface in 3D by the developed system and by a different type of system and comparing the two outputs. Figure 4.2 shows outputs of the developed system and of Wyko NT2000 Scanning White Light Interferometer Microscope for the same area of the specimen surface. It can clearly be seen that both produce closely the same results.

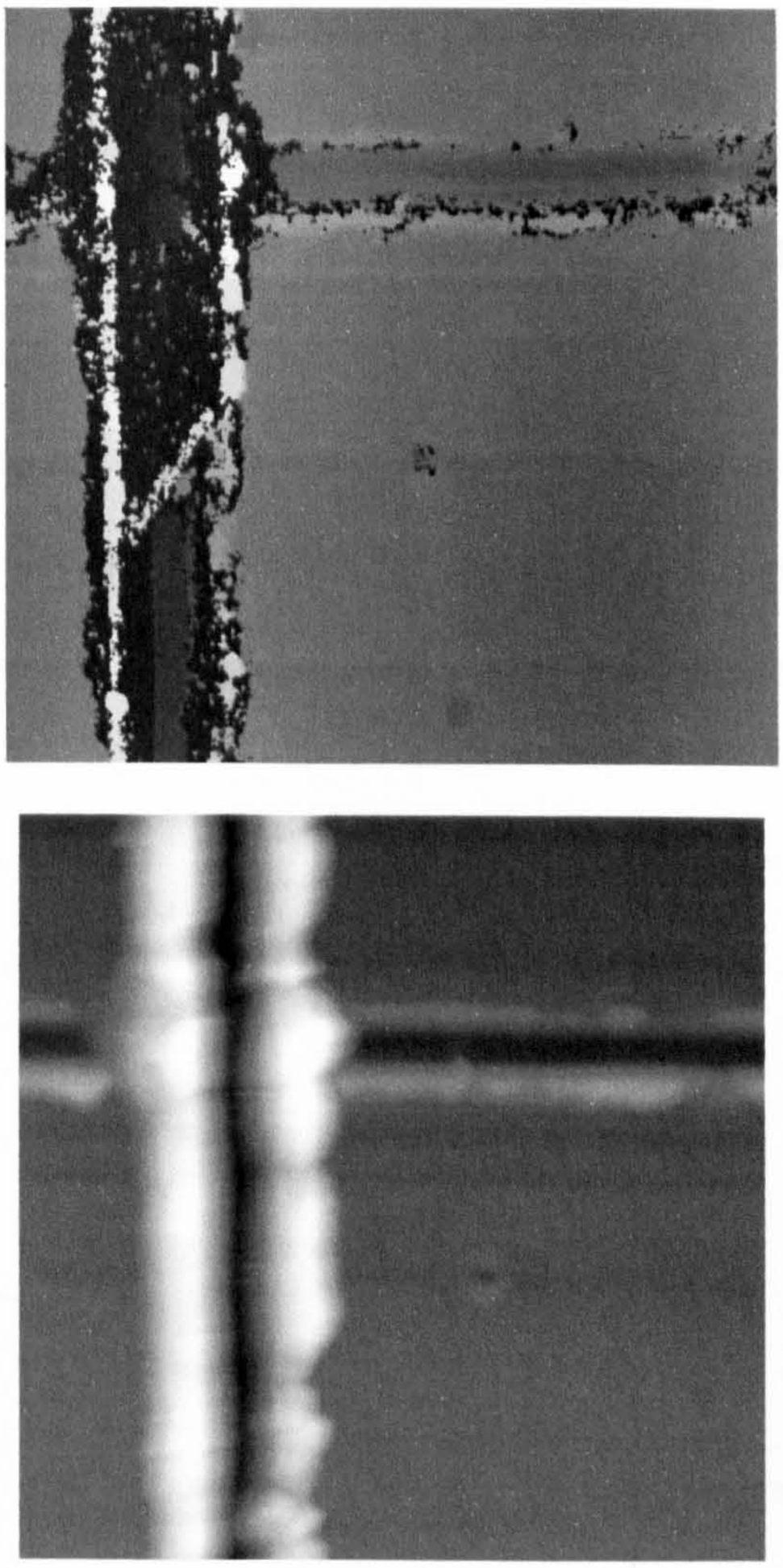

Figure 4.2: Same area measured by two different systems.

4.2.4 Verification of the relocation technique

This verification is done by measuring a profile across a scratch made on the flat surface of the reference specimen by the method described in chapter 3. A sampling interval of 1μm is used in measuring the profile and the index of the lowest point of the profile is determined. It is 90 in the profile shown in Figure 4.3. Then, stylus is lifted up and reference specimen is taken off the mount and relocated again. The stylus is lowered again for measuring a new profile on the same position of the surface. The index of the lowest point of the new profile is determined and compared with the previous one. By repeating these steps for 20 times it has been found that the maximum relocation error is ± 1μm which is as good as the sampling interval used. These steps have been repeated in the other direction across the other scratch and have shown the same level of relocation uncertainty. Backlash has been found in the table drives in both X and Y directions but has been largely eliminated by using springs along each drive axis. The 3D results shown later in this chapter, are further proof that the relocation technique is very reliable.

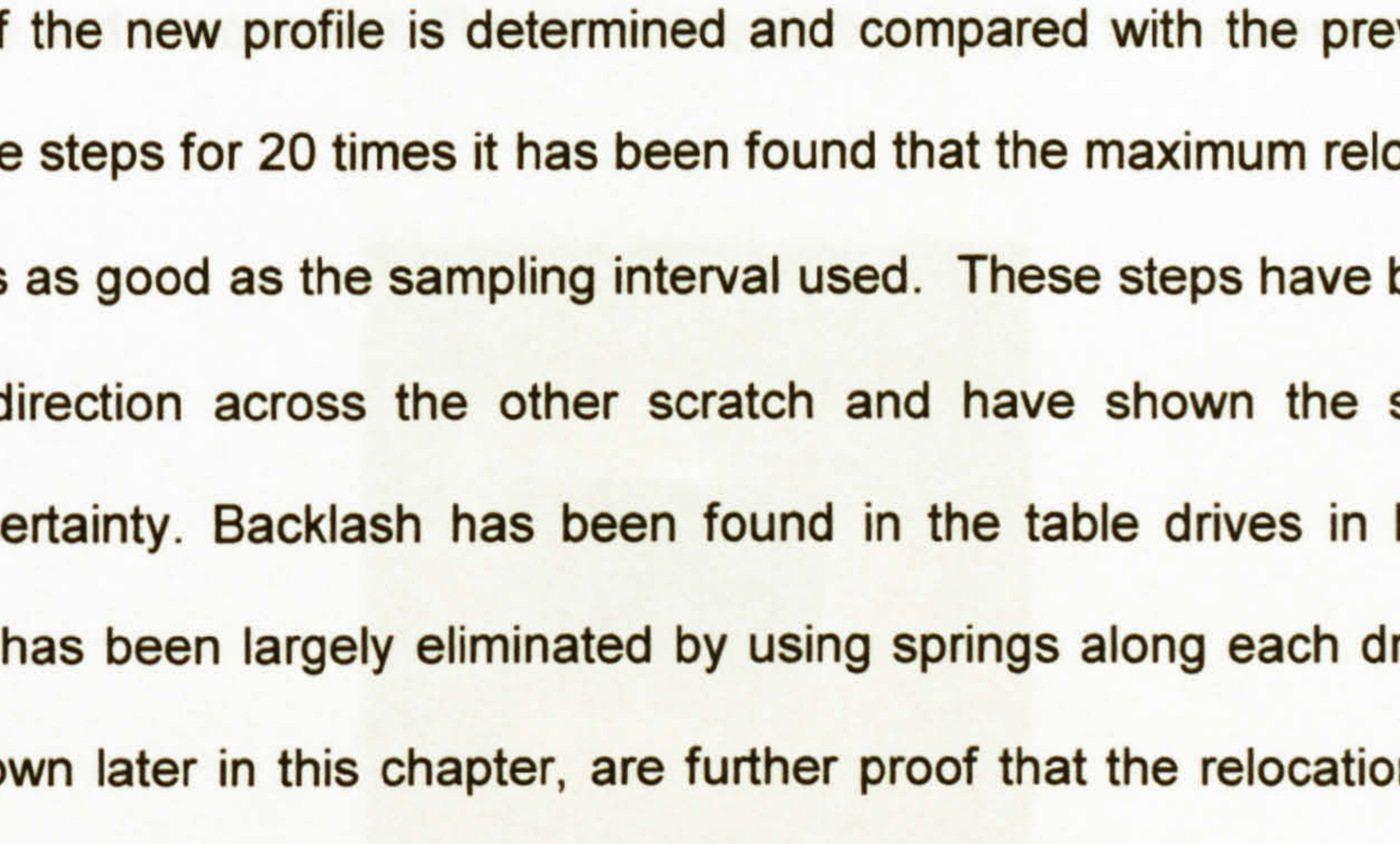

Figure 4.3: A profile measured across the scratch on the reference specimen

4.3 Measuring styli tips

Three different styli tips have been measured by the method described in the previous chapter. Two styli are originally supplied with the Talysurf and the third one is made locally of a record player stylus tip using the exchangeable mount described in chapter 3. The two original tips of the Talysurf will be named tip1 and tip2 while the other one will be named tip3. Tips 1, 2 are pyramids but tip3 is nominally spherical.

Figure 4.4 shows the indentation and real shape of tip1. It has a pyramid shape with 13x20 μm base and a worn end. The tip side is nearly parallel to the traversing direction.

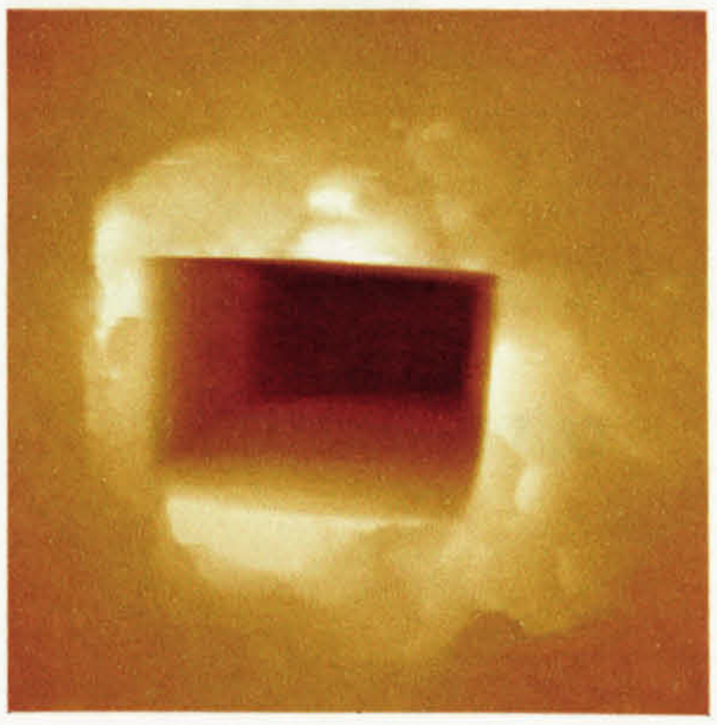

Indentation of Tip1

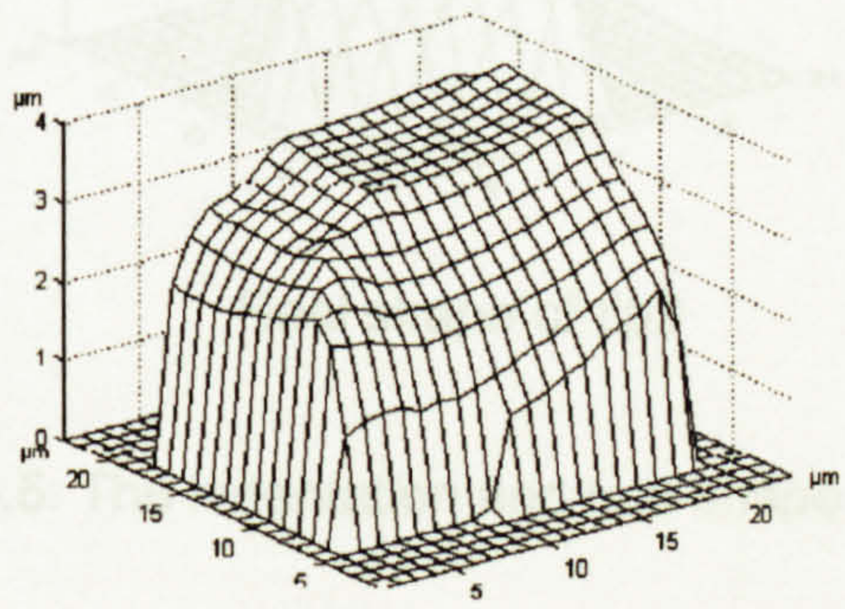

Real shape of tip1

Figure 4.4: The indentation and real shape of tip1.

Figure 4.5 shows the indentation and real shape of tip2. It has a pyramid shape with 14x16 μm base and a worn end similar to tip1 but it is sharper. The diagonal of tip2 is nearly parallel to the traversing direction.

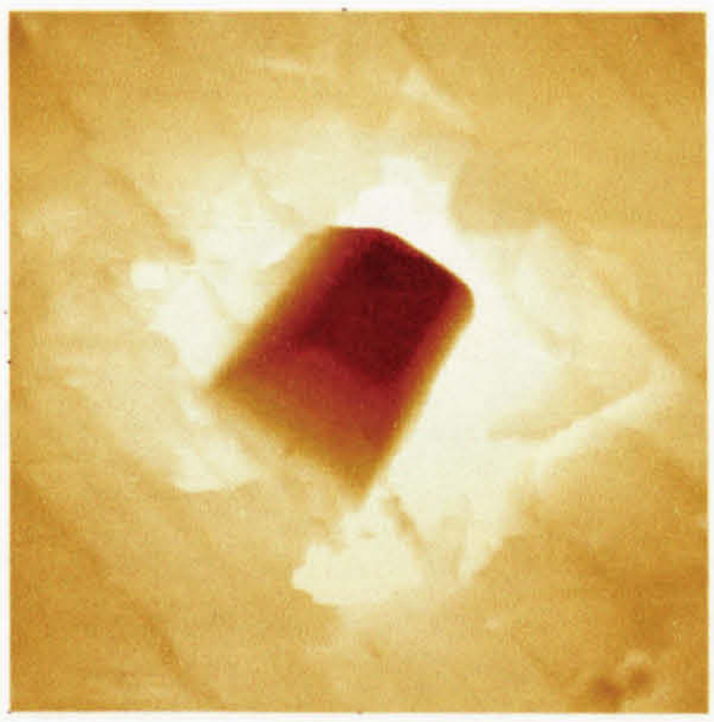

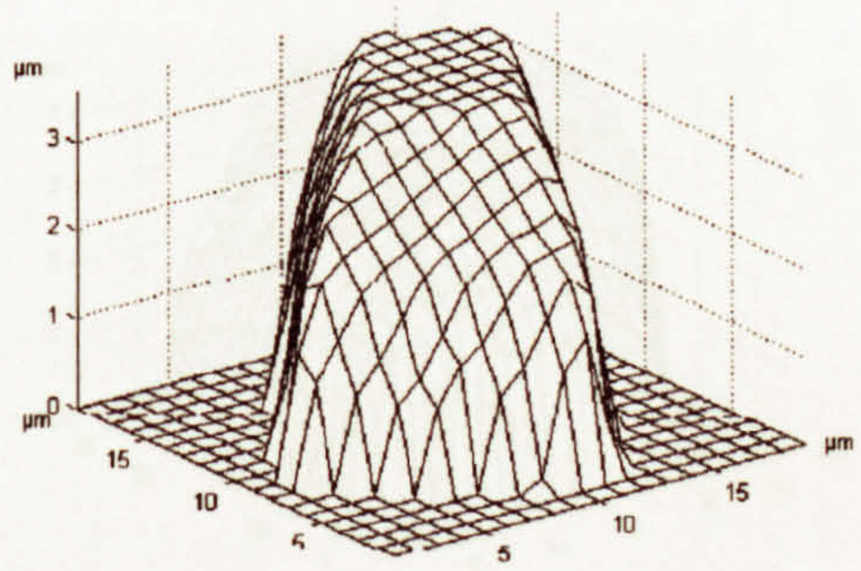

Figure 4.5: The indentation and real shape of tip2.

Figure 4.6 shows the indentation and real shape of tip3. It has a spherical shape with nearly 20 μm base diameter and nearly flat end. The tip end has dent in the middle.

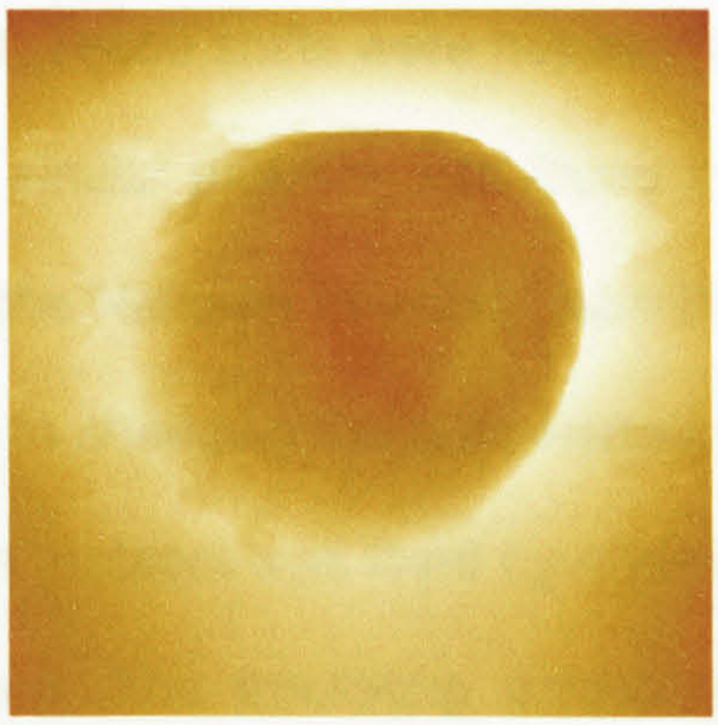

Indentation of Tip3

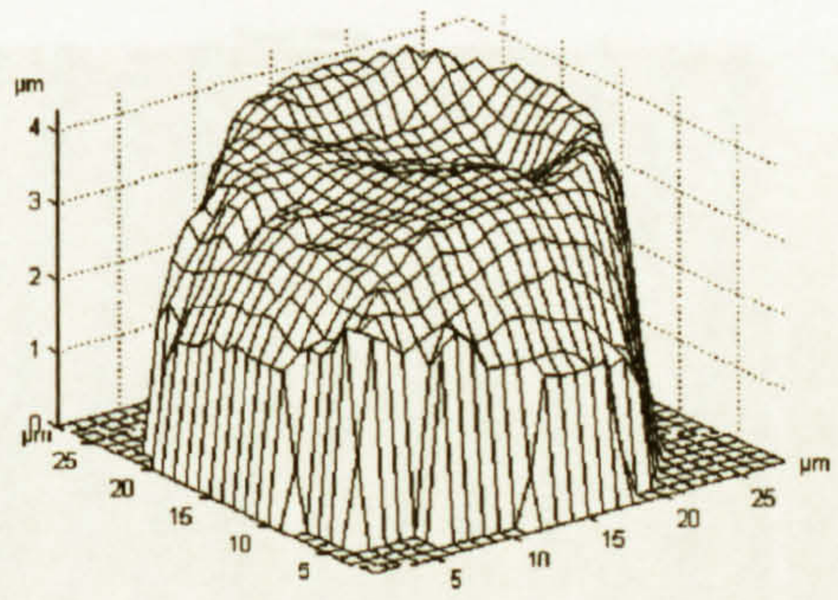

Real shape of tip3

Figure 4.6: The indentation and real shape of tip3.

4.4 3D measurements

The first 3D measurement done by the developed system was on a turned specimen. It contained 300x300 data points and took nearly 5 hours to complete. Figure 4.7 shows the output of scanning a small area of a turned surface. It is clear that the start and end points of all traces ares on the same line in X and Y directions. This confirms that the system is doing the measurement in 3D properly. However, some shifts in the surface profile are shown in the figure. These shifts were happening on nearly all measurements but with different intervals. A similar problem was found in another research which was carried out (not published) at the National Physical Laboratory in London (1997) and was referred to a thermal drift due to changing the temperature around the measuring system during the day. However, this problem was fixed by making a small insulating enclosure around the measuring system. The insulating enclosure was made of 3 cm thick expanded poly-styrene sheets taped together to give 800 x 500 x 600 mm box that fits over the whole instrument and rests on the desk.

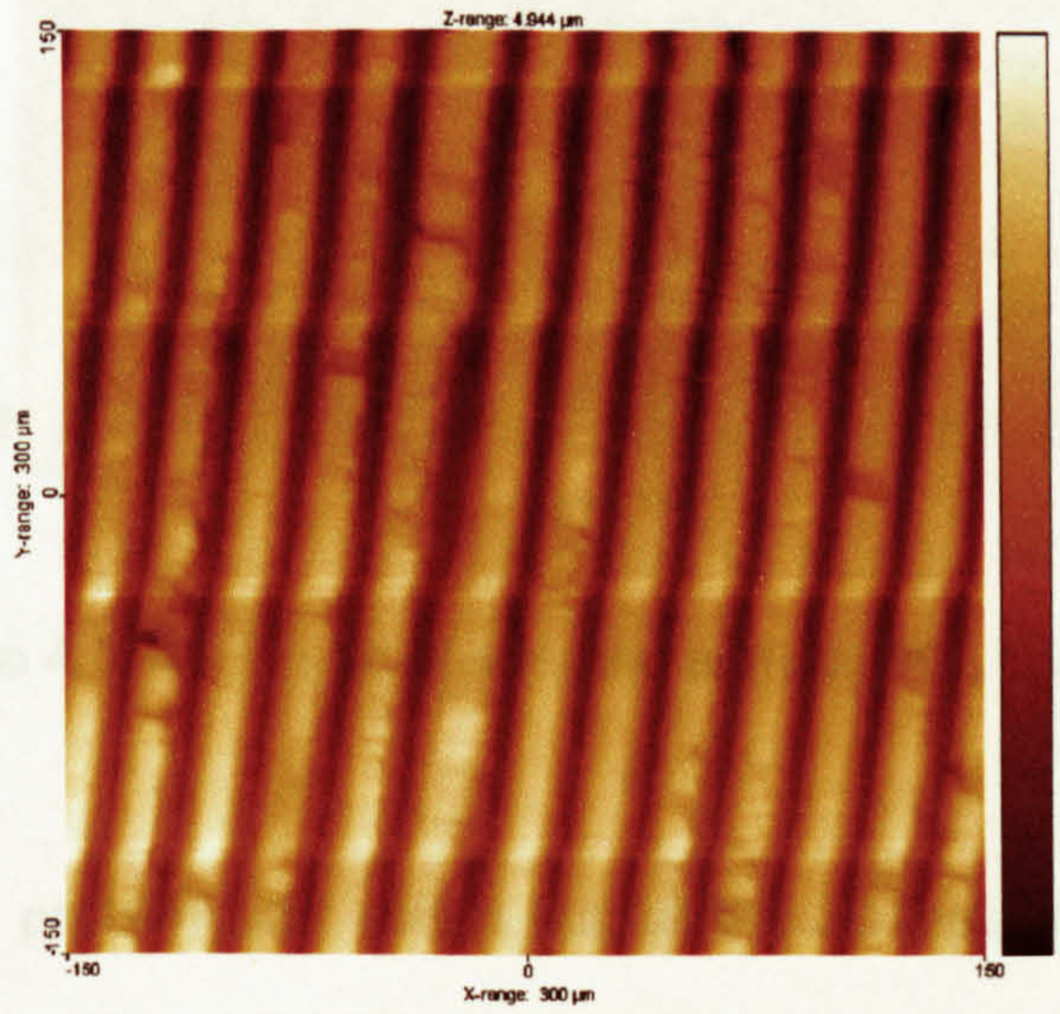

Figure 4.7: 3D image of a turned surface with thermal drift effect

Figure 4.8 shows the image of the turned surface after eliminating the thermal effect. There are no more thermal shifts in the profile but another sort of non-uniformity can be seen in the image. It is happening nearly around the middle vertical line of the surface. It was seen to same extent with all surfaces measured. The main reason of this error was found to be the backlash of the X-Y stage in both axes. Two light force springs have been fitted along each axis to get rid of the backlash effect by introducing a continuous force bias against the drives. The spring force was most successfully by stretched rubber bands, which have more internal damping than metallic springs.

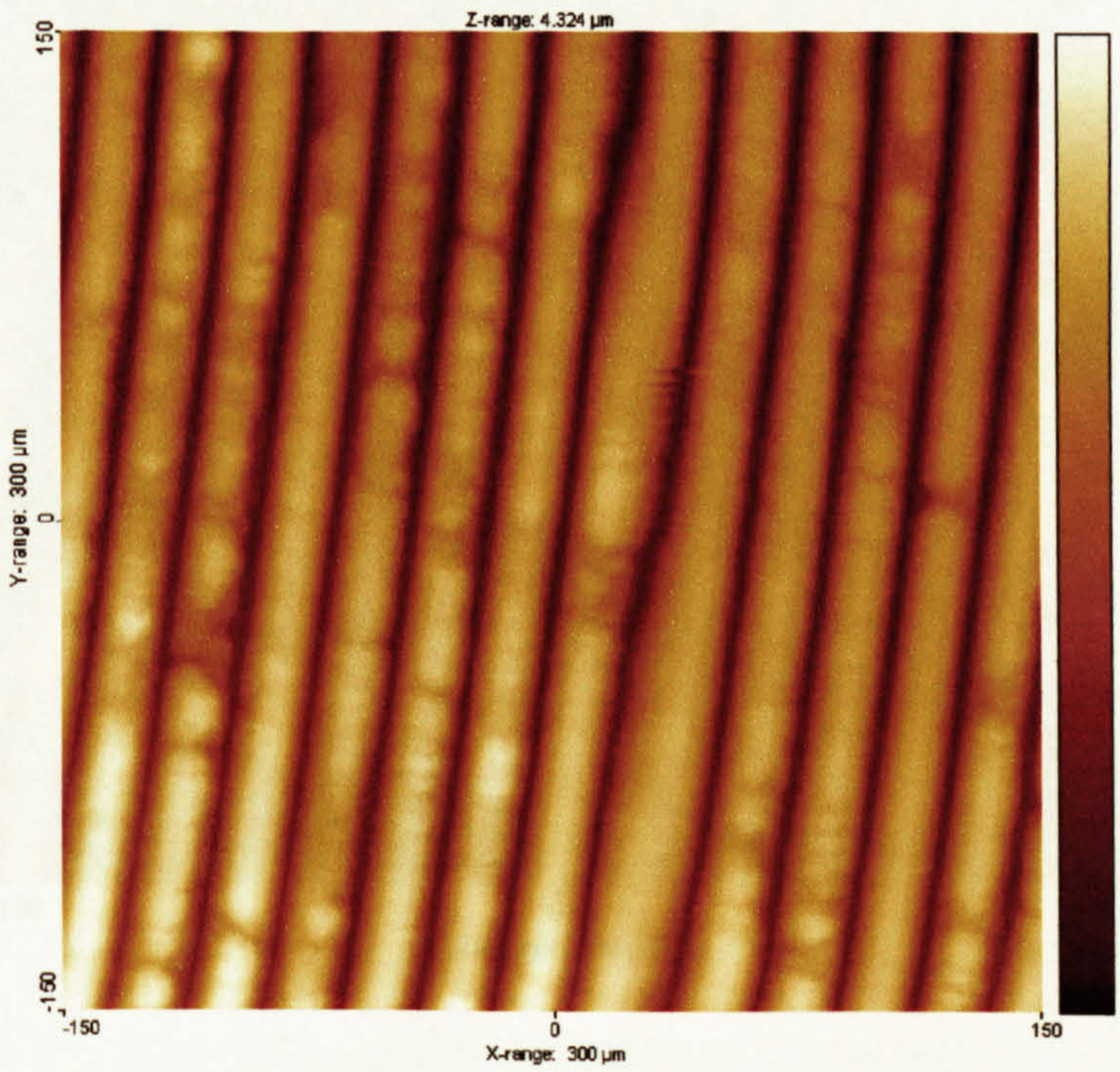

Figure 4.8: 3D image of a turned surface with backlash effect

Once the backlash problem was sorted out, all the 3D measurements by the developed system highly consistent results. Figure 4.9 shows an image of a turned surface without the backlash or thermal drift errors.

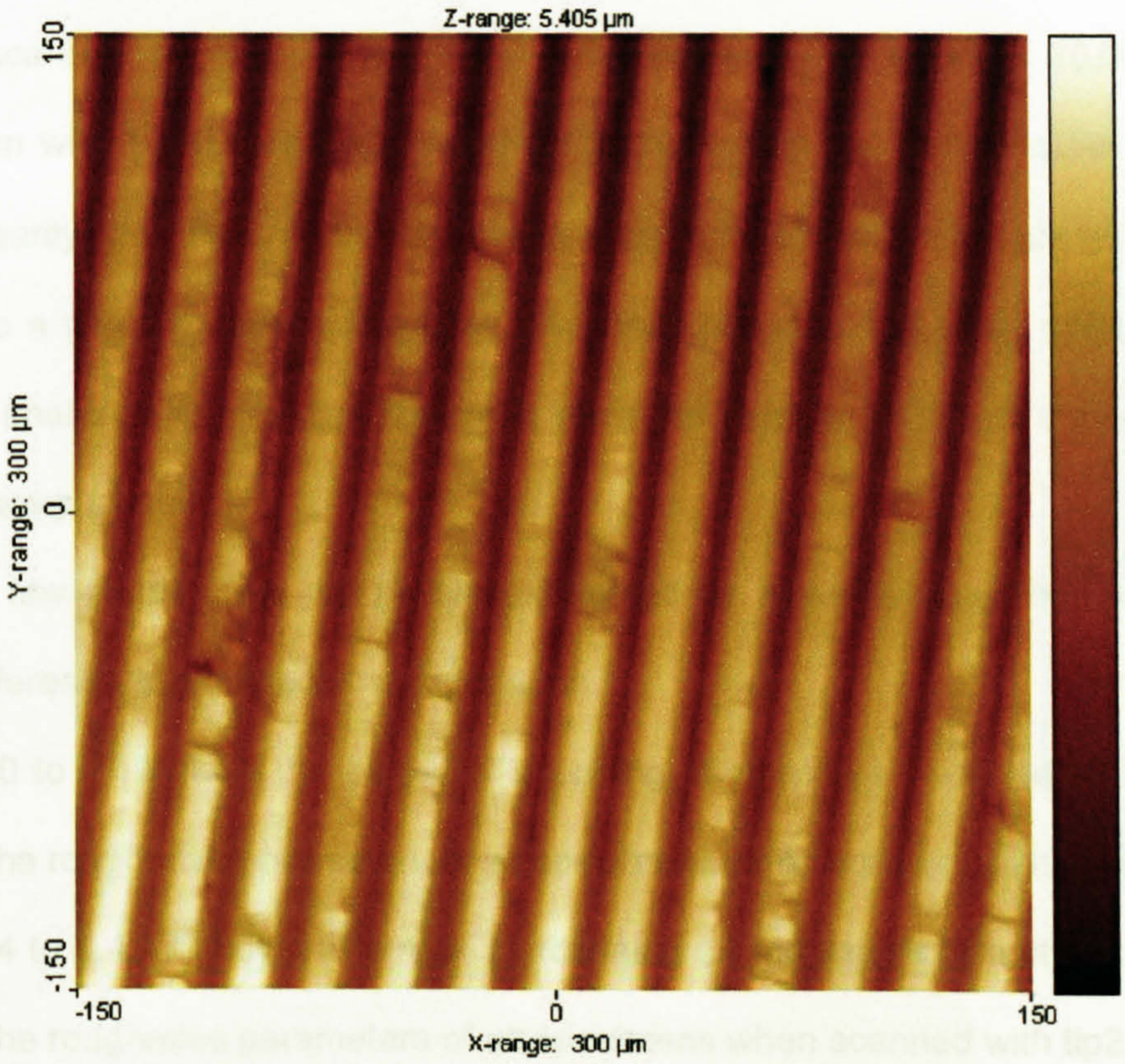

Figure 4.9: 3D image of a turned surface without thermal drift or backlash effects

4.5 Measuring real surfaces with real tips

Twelve specimens have been used to investigate the different aspects of the developed system. The specimens are machined by Grinding, Lapping, Milling and Turning (3 different specimens of each). The same area of each specimen has been scanned in 3D by different styli, by re-alignment procedures described in chapter 3. Repositioning is relative to the stylus centre line to a precision of ±1μm. An area of 300μm x 300μm size has been scanned on all specimens. All measurements are done at 10,000 vertical magnification with 1 μm sampling intervals. Restricting the Talysurf amplifier to ±1 Volt for best linearity, the measurements have a range of nominally ±2.5 μm with a useful resolution to a few nm, limited mostly by environmental vibration. The output data are stored and analyzed and roughness parameters are determined for all surfaces by the SPIP software package.

In the next few pages, data will be first presented for reference and then will later be grouped differently to aid specific comparisons.

Figures 4.10 to 4.13 show the output of scanning all specimens with stylus tip1. Table 4.2 shows the roughness parameters of all specimens when scanned with tip1.

Figures 4.14 to 4.4.17 show the output of scanning all specimens with stylus tip2. Table 4.3 shows the roughness parameters of all specimens when scanned with tip2.

Figures 4.18 to 4.21 show the output of scanning all specimens with stylus tip3. Table 4.4 shows the roughness parameters of all specimens when scanned with tip3.

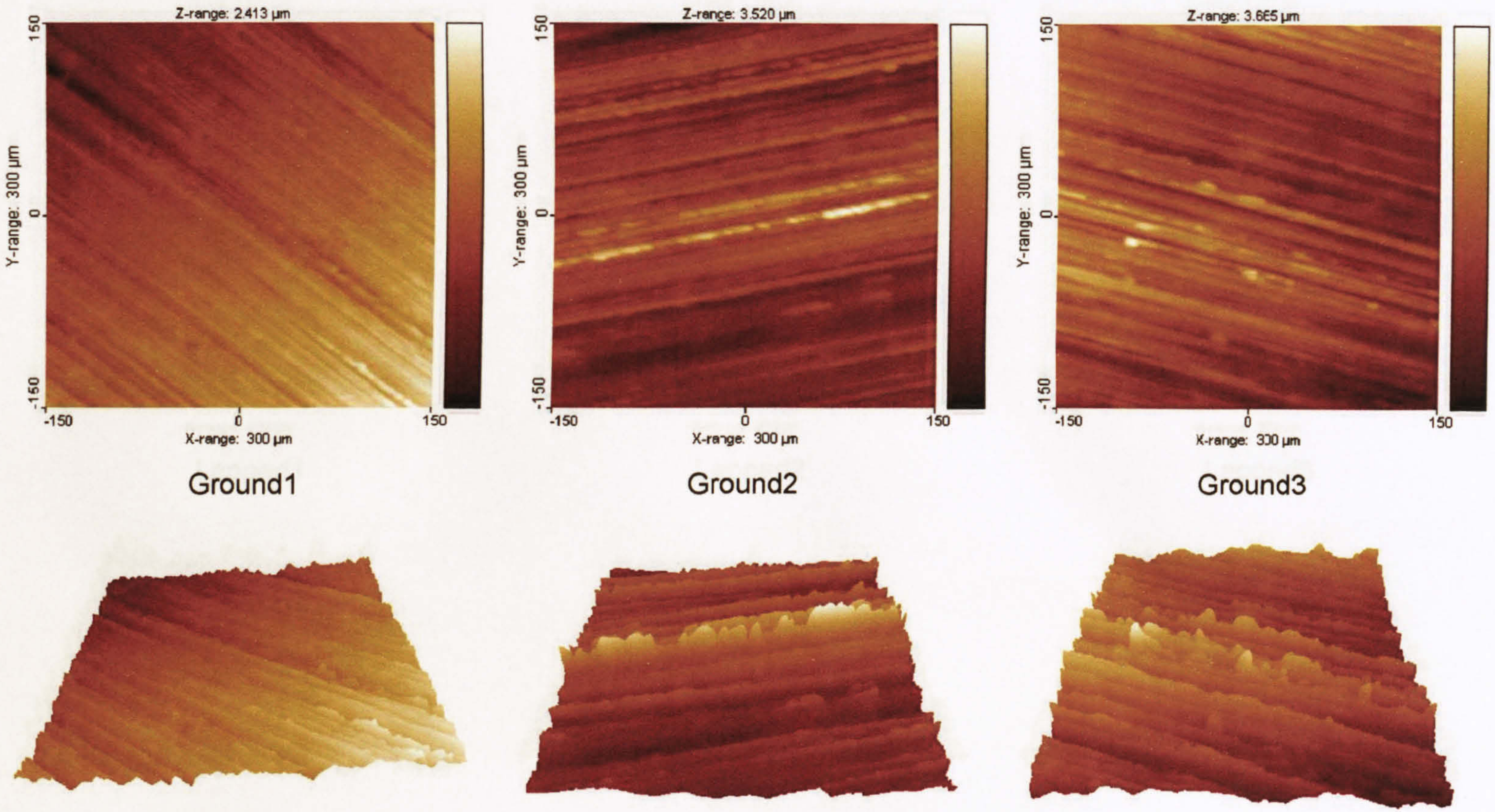

Figure 4.10: Ground specimens measured by tip1

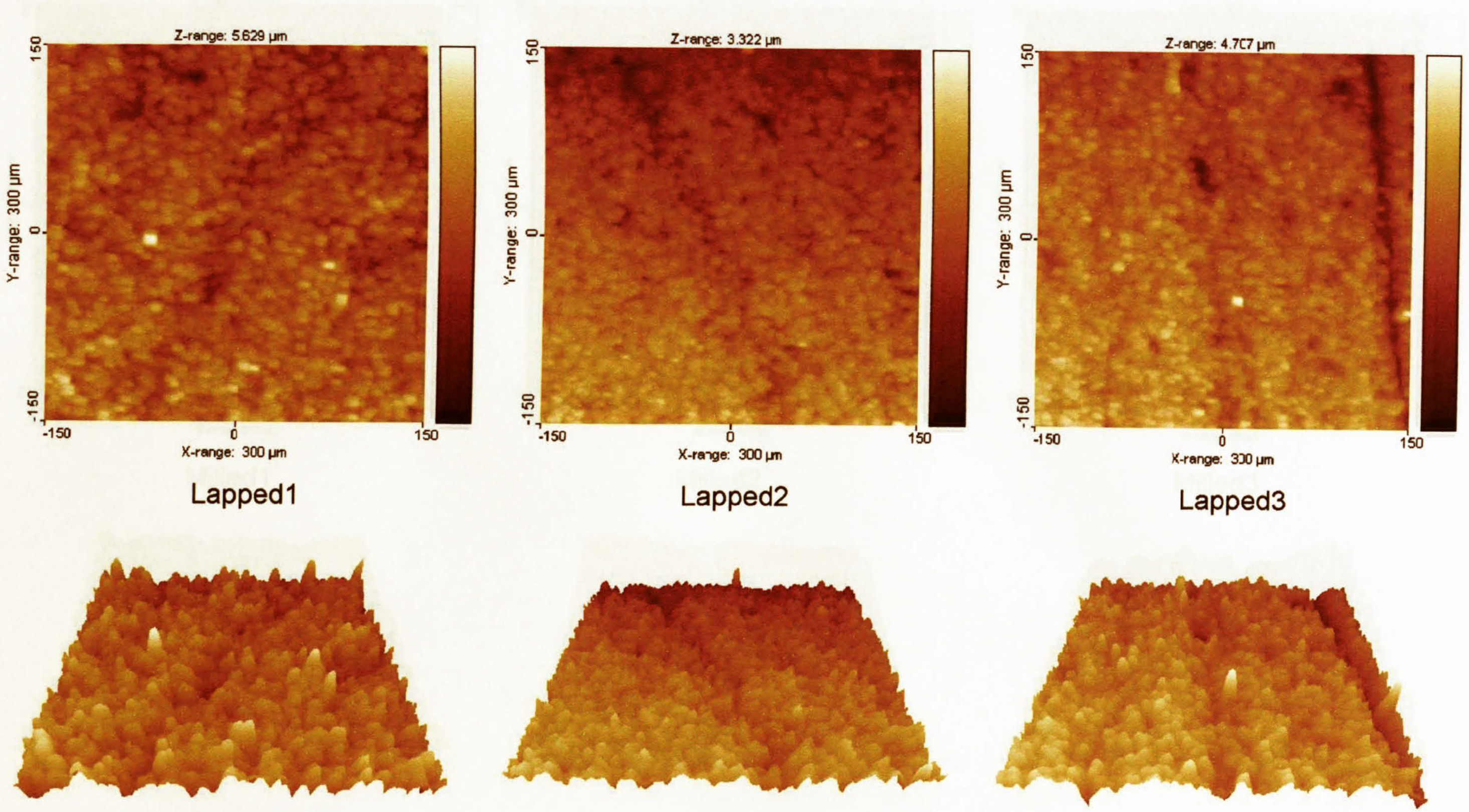

Figure 4.11: Lapped specimens measured by tip1

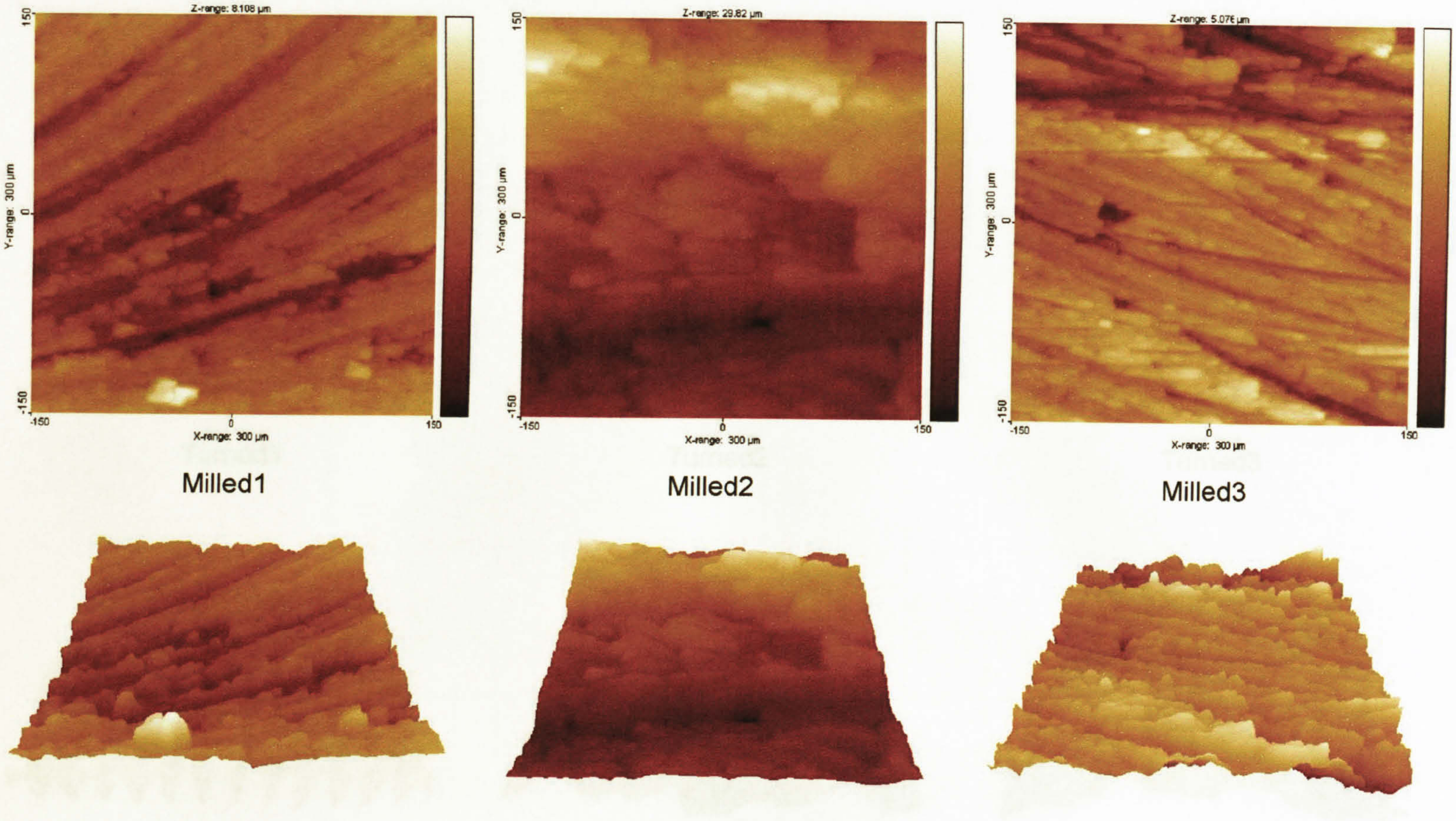

Figure 4.12: Milled specimens measured by tip1

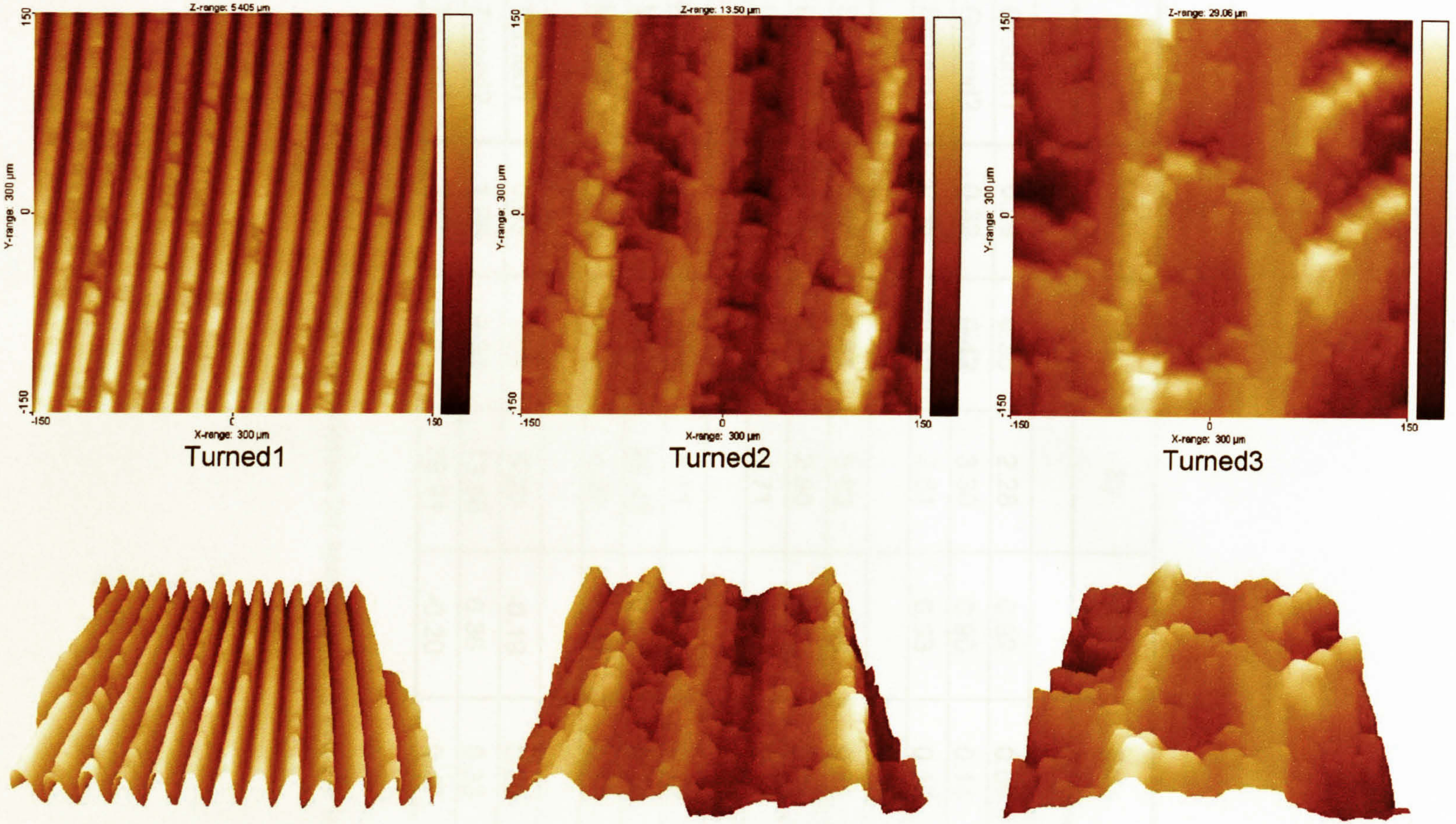

Figure 4.13: Turned specimens measured by tip1

	Sa	Sq	Sy	Ssk	Sdq	Sds
Ground1	0.29	0.36	2.28	0.02	0.06	13666
Ground2	0.32	0.42	3.30	0.90	0.14	11082
Ground3	0.35	0.45	3.61	0.33	0.15	11002
Lapped1	0.48	0.61	5.63	-0.01	0.23	10629
Lapped2	0.37	0.45	2.90	-0.13	0.12	16104
Lapped3	0.44	0.57	4.71	-0.66	0.17	13813
Milled1	0.74	0.93	8.11	-0.09	0.19	10310
Milled2	4.98	5.91	29.43	0.41	0.34	5648
Milled3	0.58	0.74	4.90	-0.52	0.19	8698
Turned1	0.93	1.09	5.27	-0.19	0.29	3197
Turned2	1.86	2.32	13.50	0.36	0.33	4915
Turned3	3.73	4.57	28.91	-0.20	0.47	3716

Table 4.2: Roughness parameters for specimens measured with tip1

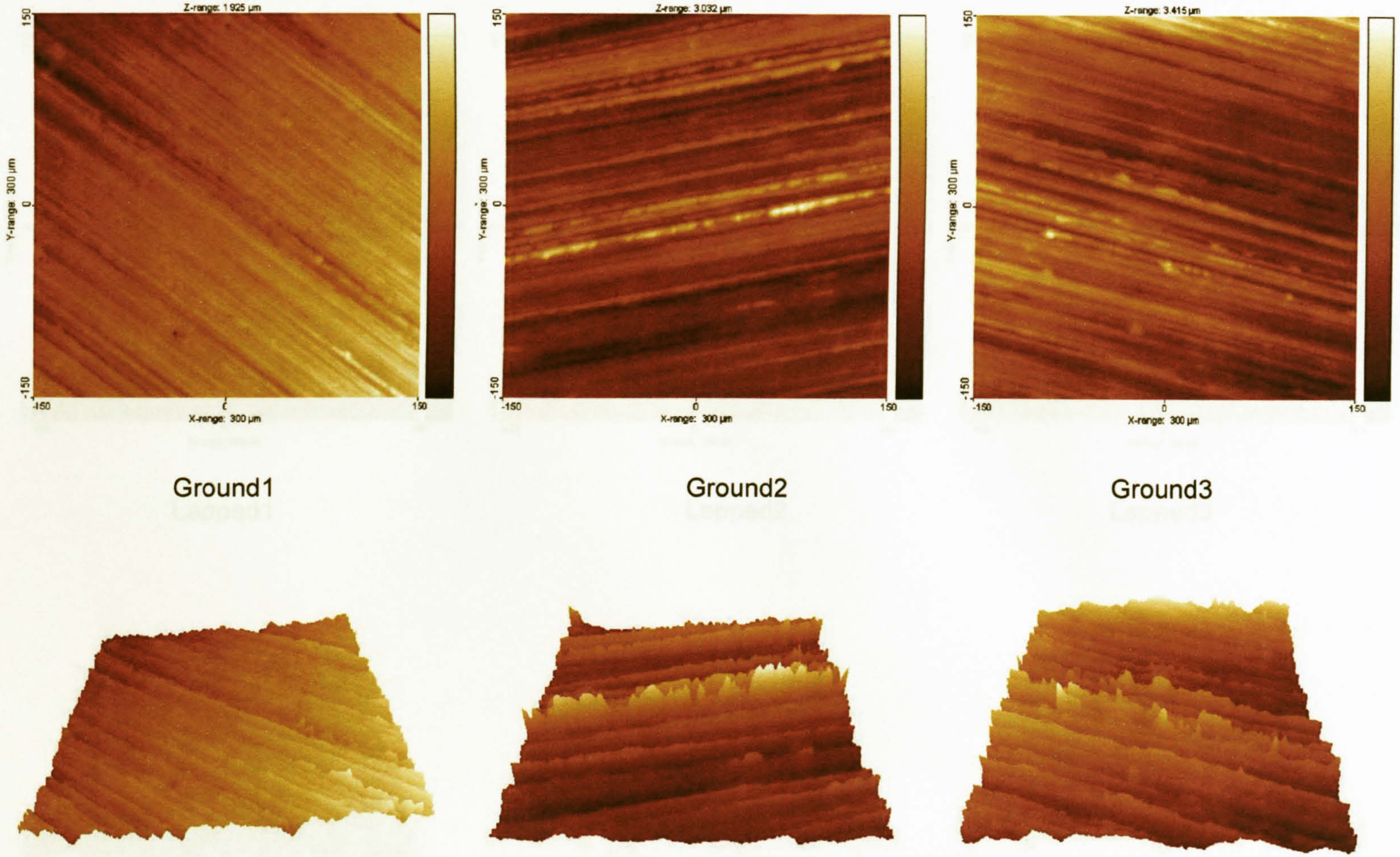

Figure 4.14: Ground specimens measured by tip2

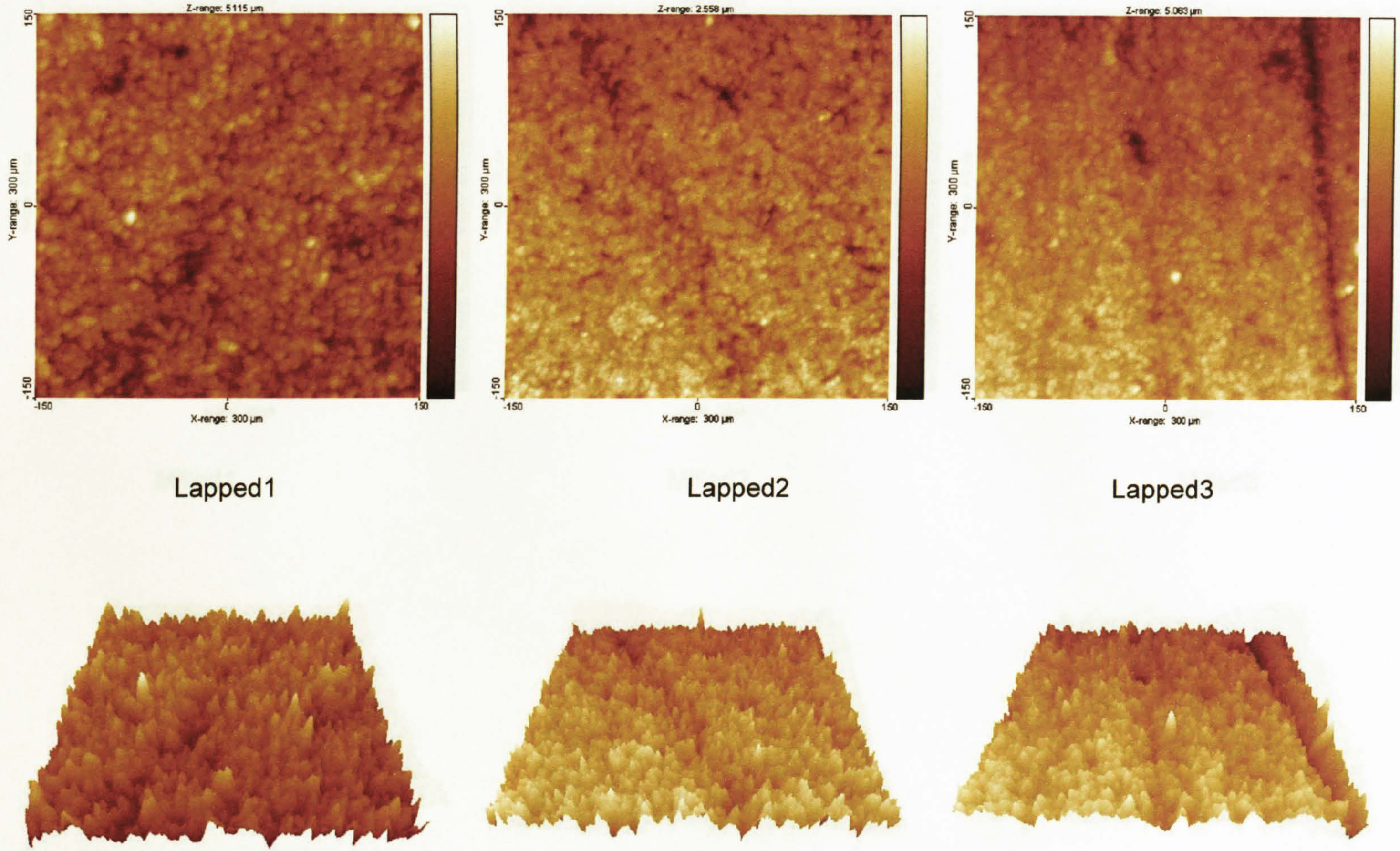

Figure 4.15: Lapped specimens measured by tip2

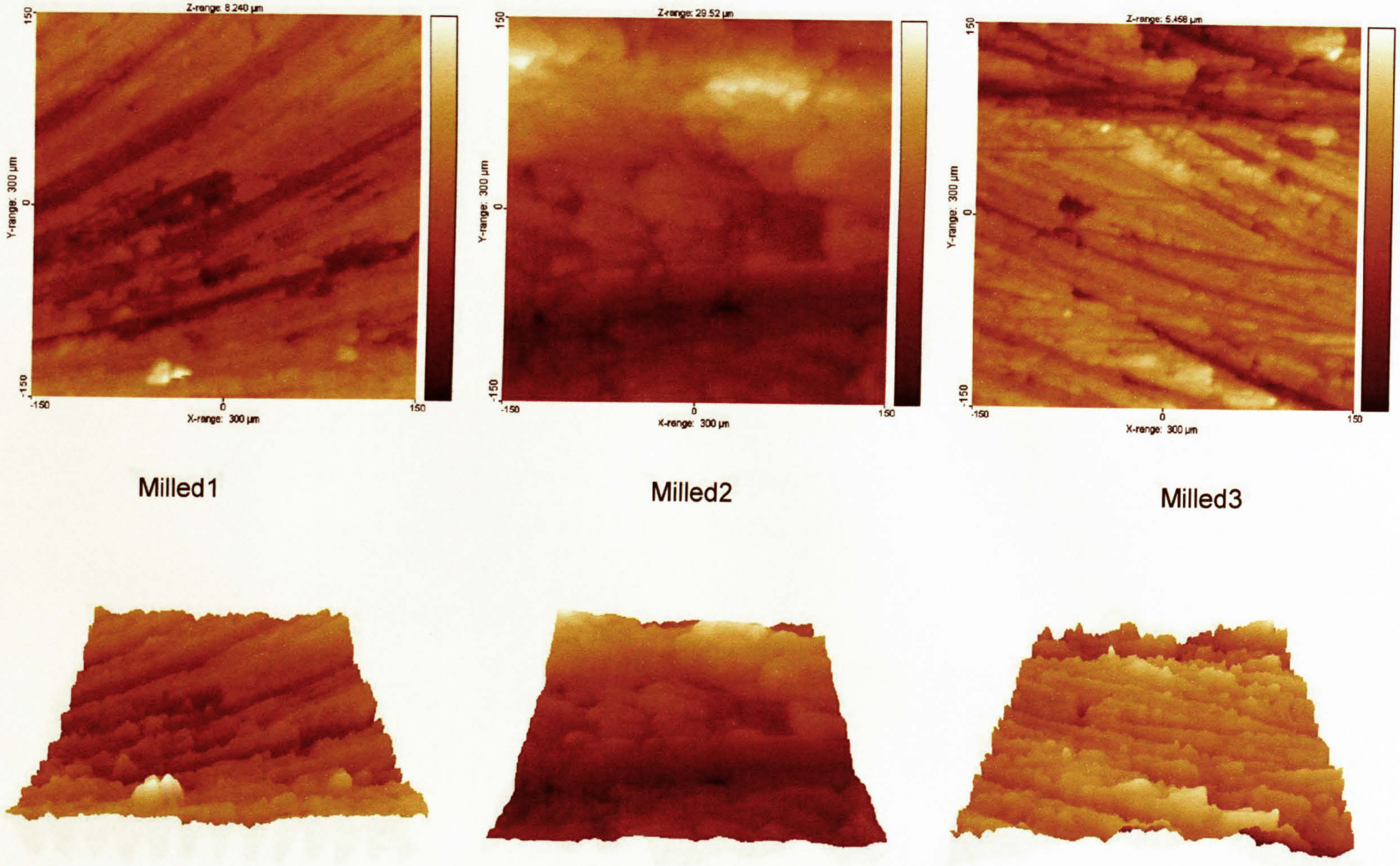

Figure 4.16: Milled specimens measured by tip2

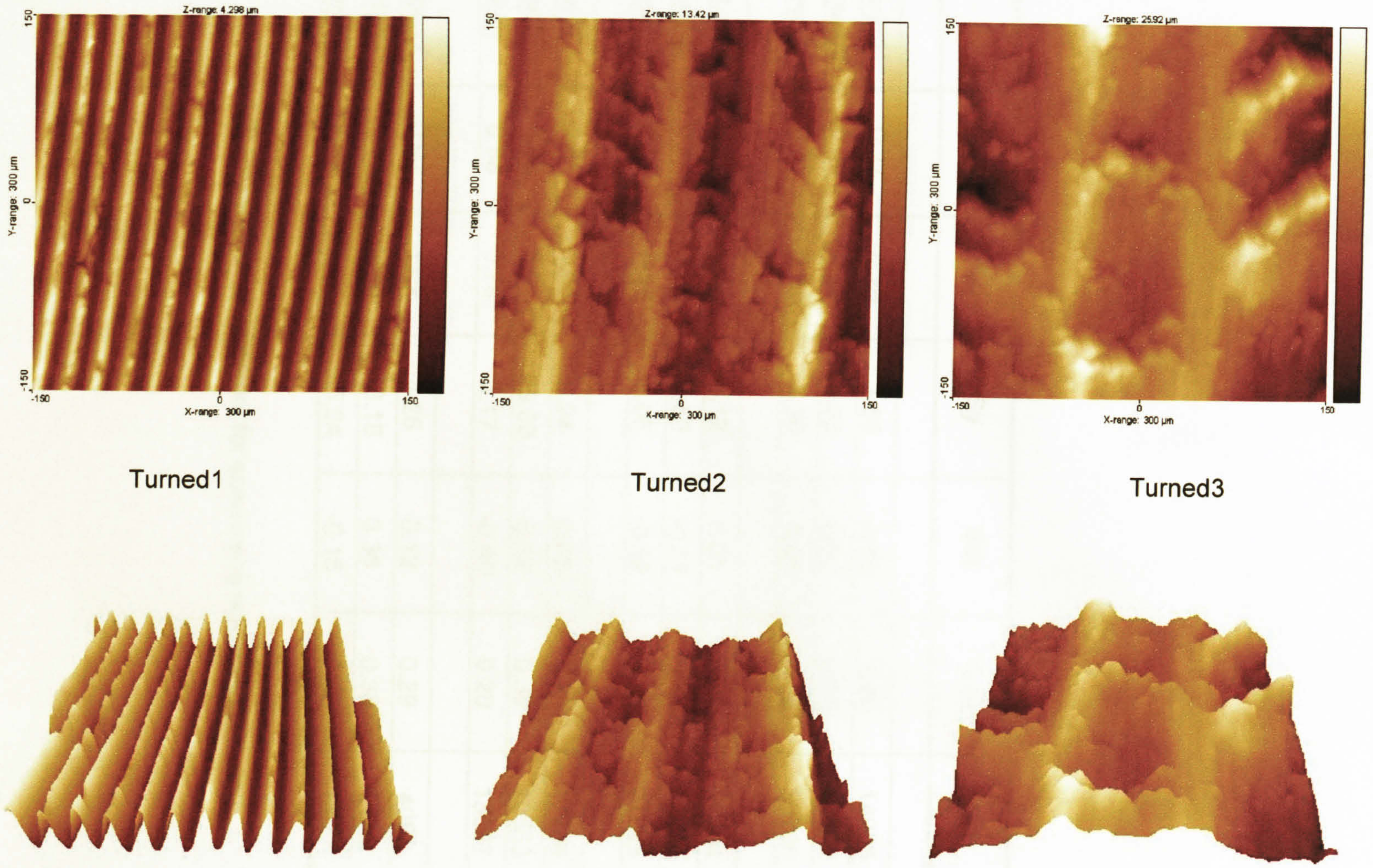

Figure 4.17: Turned specimens measured by tip2

	Sa	Sq	Sy	Ssk	Sdq	Sds
Ground1	0.21	0.26	1.85	-0.02	0.06	14985
Ground2	0.30	0.39	3.03	0.81	0.15	14172
Ground3	0.35	0.44	3.30	0.21	0.16	20766
Lapped1	0.42	0.53	5.12	0.01	0.24	15984
Lapped2	0.24	0.30	2.56	-0.31	0.13	24668
Lapped3	0.54	0.68	5.06	-0.42	0.19	21525
Milled1	0.81	1.01	8.24	0.05	0.21	17769
Milled2	4.98	5.91	29.08	0.39	0.36	10563
Milled3	0.58	0.74	5.17	-0.49	0.20	13067
Turned1	0.92	1.02	4.25	0.12	0.29	4089
Turned2	1.83	2.28	13.18	0.36	0.35	8764
Turned3	3.40	4.17	25.64	-0.16	0.43	5927

Table 4.3: Roughness parameters for specimens measured with tip2

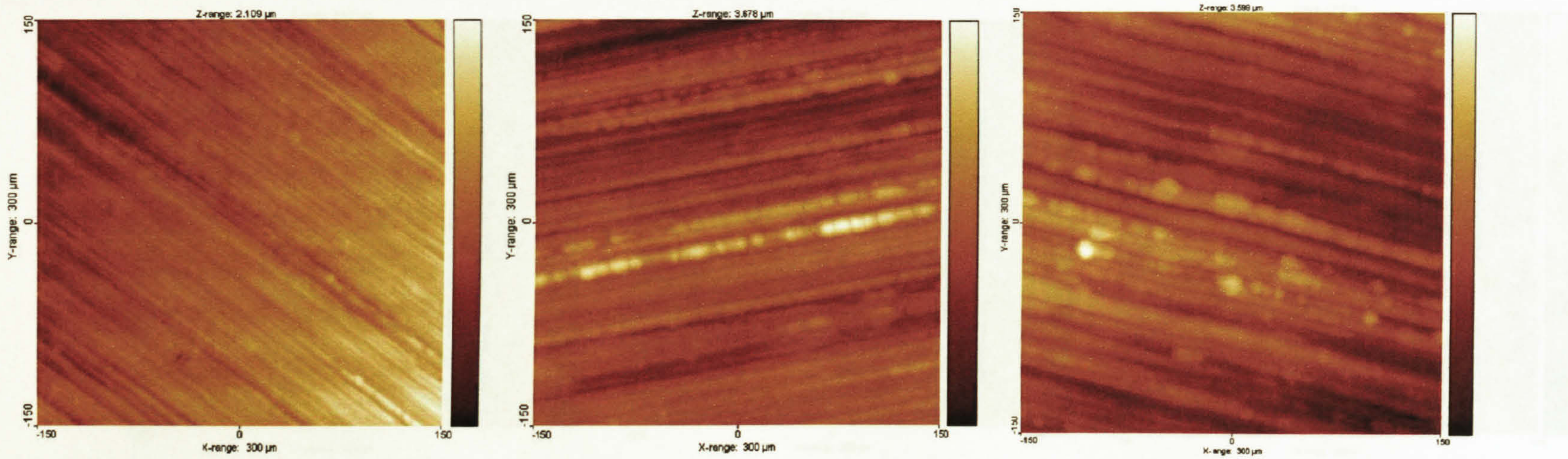

Ground1 Ground2 ground3

Figure 4.18: Ground specimens measured by tip3

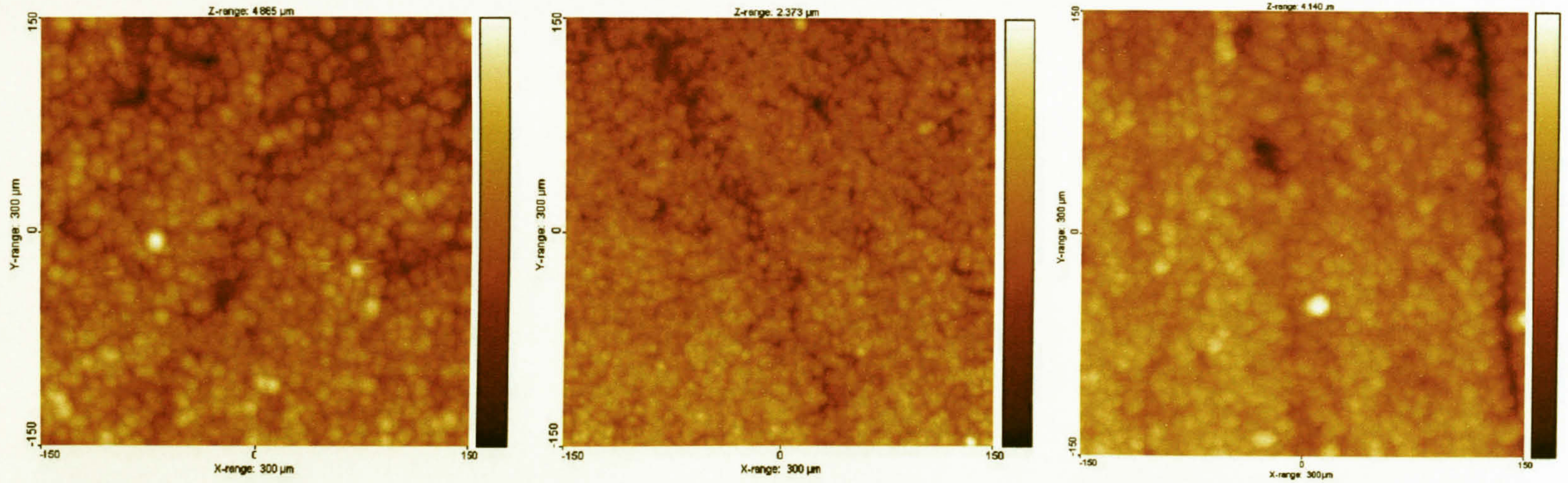

Lapped1 Lapped2 Lapped3

Figure 4.19: Lapped specimens measured by tip3

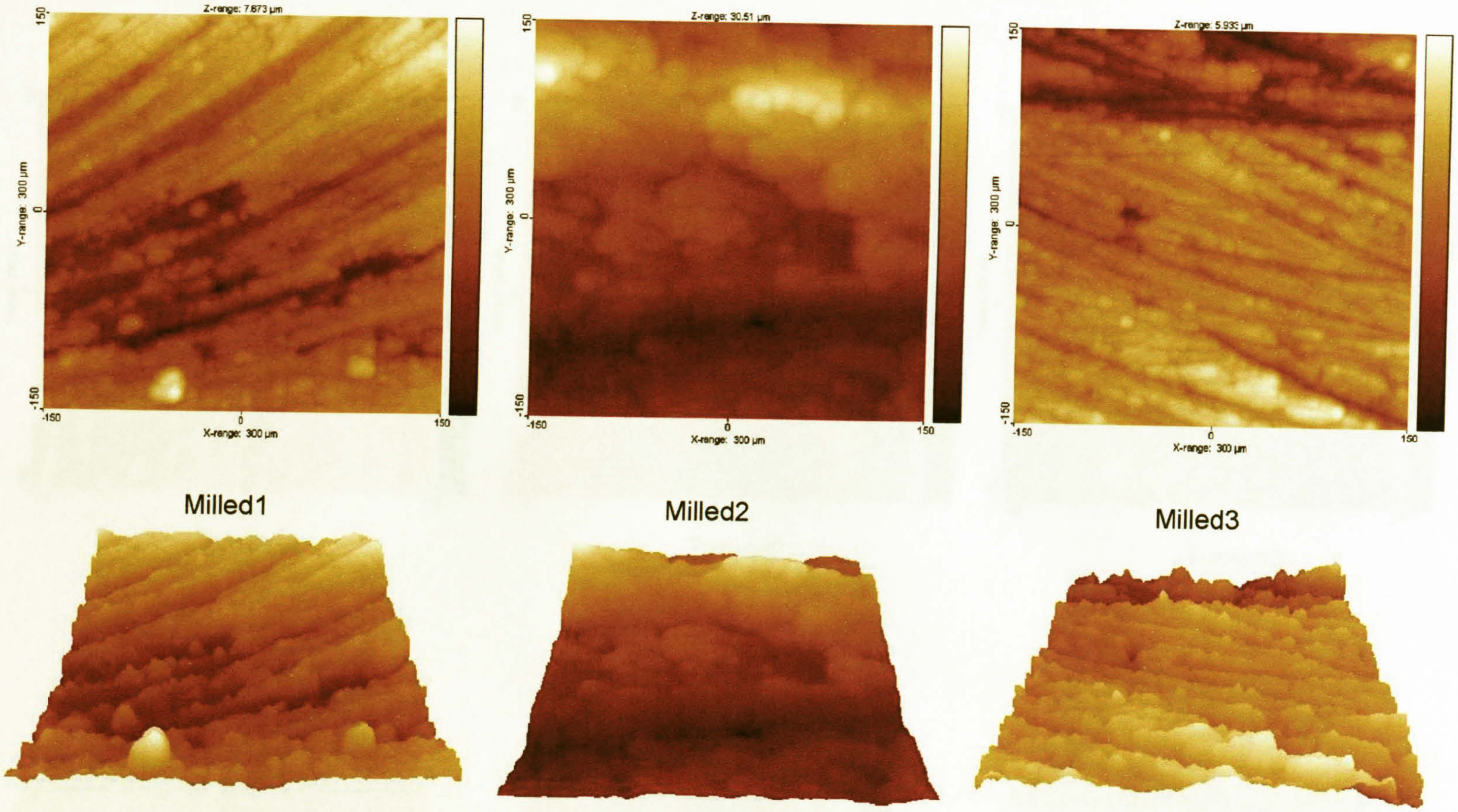

Figure 4.20: Milled specimens measured by tip3

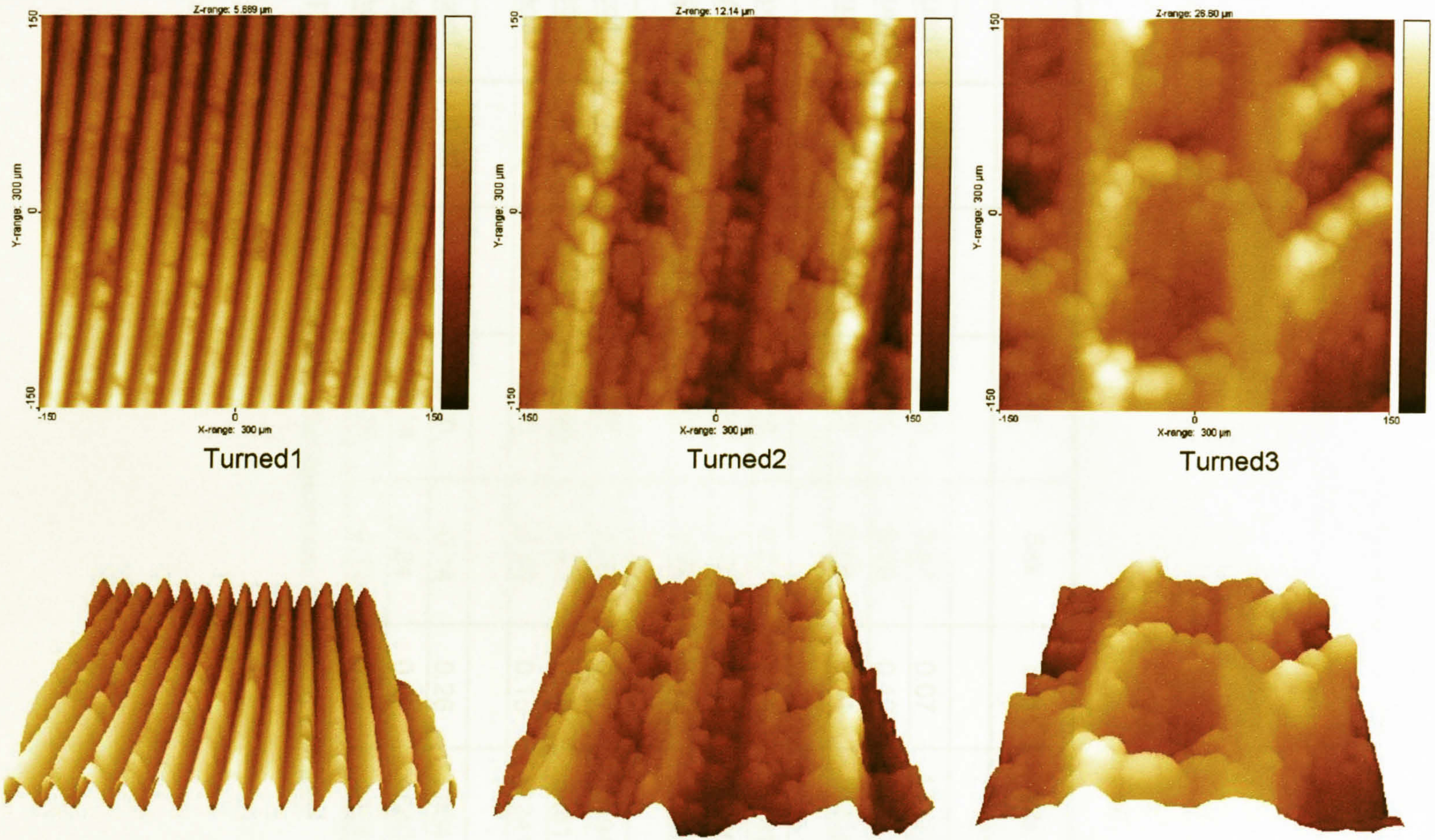

Figure 4.21: Turned specimens measured by tip3

	Sa	Sq	Sy	Ssk	Sdq	Sds
Ground1	0.24	0.29	2.03	0.07	0.07	17422
Ground2	0.31	0.42	3.60	0.70	0.12	13773
Ground3	0.38	0.46	3.31	0.48	0.11	15238
Lapped1	0.44	0.55	4.86	0.07	0.18	12787
Lapped2	0.19	0.24	1.99	-0.21	0.10	23030
Lapped3	0.35	0.46	4.13	-0.80	0.12	12547
Milled1	1.00	1.23	7.67	0.09	0.17	12494
Milled2	5.27	6.24	29.56	0.42	0.29	5461
Milled3	0.70	0.89	5.50	-0.65	0.15	12241
Turned1	0.92	1.13	5.60	-0.14	0.26	2904
Turned2	1.86	2.27	12.14	0.24	0.27	6540
Turned3	3.46	4.23	26.26	-0.12	0.42	3024

Table 4.4: Roughness parameters for specimens measured with tip3

4.6 Comparison of surfaces measured by different tips

It is obvious from the previous real measurements that the different tips do not show many effects on the 3D images of the surfaces (just very few effects may be noticed). But comparing the roughness parameters of each specimen when measured with different tips could show some effects with most of the specimens.

4.6.1 Comparing the roughness of the ground specimens:

Table 4.5 shows the roughness parameters of the ground specimens when measured with different tips. The stylus shape shows some effects on the roughness parameters of the ground specimens. The largest effect on the amplitude (Sa, Sq, Sy) occurs on the finest surface (Ground1, as initiation could suggest). The maximum deviation in Sa and Sq values is nearly 38% of their minimum values which looks potentially significant. The maximum deviation in Sy is 23% of its minimum value. The Skewness Ssk is generally +ve and sometimes quite high on Ground2. It varies as strong interaction of the surface and the stylus (i.e. not in the same way for all styli). The slope is also affected as the maximum deviation is 33% of its minimum value on surface ground3. Tip2 gives the minimum values the amplitude parameters with all surfaces. Tip2 gives the maximum values of the slope with the ground surfaces except Ground1. Tip1 gives the minimum values of the density of summits parameter Sds with all the ground specimens.

		Sa	Sq	Sy	Ssk	Sdq	Sds
Ground1	Tip1	0.29	0.36	2.28	0.02	0.06	13666
	Tip2	0.21	0.26	1.85	-0.02	0.06	14985
	Tip3	0.24	0.29	2.03	0.07	0.07	17422
Ground2	Tip1	0.32	0.42	3.30	0.90	0.14	11082
	Tip2	0.30	0.39	3.03	0.81	0.15	14172
	Tip3	0.31	0.42	3.60	0.70	0.12	13772
Ground3	Tip1	0.35	0.45	3.61	0.33	0.15	11002
	Tip2	0.35	0.44	3.30	0.21	0.16	20765
	Tip3	0.38	0.46	3.31	0.48	0.11	15237

Table 4.5: Roughness parameters for ground specimens measured with different tips

4.6.2 Comparing the roughness of the Lapped specimens:

Table 4.6 shows the roughness parameters of lapped specimens when measured with different tips. All roughness parameters of the lapped surfaces are affected by the stylus tip geometry. The worst variations in the amplitude parameters (Sa, Sq, Sy) occur on surface Lapped2. The maximum deviation in Sa is nearly 95% of its minimum value (nearly doubling the minimum value). The maximum deviation in Sq is 88% of its minimum value. The maximum deviation in Sy is 46% of its minimum value. The Skewness Ssk is generally -ve and sometimes quite high on Lapped3. The slope is highly affected as the maximum deviation is 58% of its minimum value on surface Lapped3. Tip3 mostly gives the minimum values of the amplitude parameters with all surfaces and also gives the minimum values of the slope with all lapped surfaces. Tip2 gives the maximum values of the slope with the lapped surfaces. Tip2 also gives the maximum density of summits Sds with all the lapped specimens.

		Sa	Sq	Sy	Ssk	Sdq	Sds
Lapped1	Tip1	0.48	0.61	5.63	-0.01	0.23	10629
	Tip2	0.42	0.53	5.12	0.01	0.24	15984
	Tip3	0.44	0.55	4.86	0.07	0.18	12787
Lapped2	Tip1	0.37	0.45	2.90	-0.13	0.12	16104
	Tip2	0.24	0.30	2.56	-0.31	0.13	24668
	Tip3	0.19	0.24	1.99	-0.21	0.10	23030
Lapped3	Tip1	0.44	0.57	4.71	-0.66	0.17	13813
	Tip2	0.54	0.68	5.06	-0.42	0.19	21525
	Tip3	0.35	0.46	4.13	-0.80	0.12	12547

Table 4.6: Roughness parameters for Lapped specimens measured with different tips

4.6.3 Comparing the roughness of the milled specimens:

Table 4.7 shows the roughness parameters of milled specimens when measured with different tips. All roughness parameters of the surfaces are affected by the stylus tip geometry but to less extent than the ground and the lapped surfaces. Tip3 gives the worst variations in most amplitude parameters (Sa, Sq, Sy). The maximum deviation in Sa is 36% of its minimum value. The maximum deviation in Sq is 32% of its minimum value. The maximum deviation in Sy is only 12% of its minimum value. The Skewness Ssk has shown significant effect of the tip shape on the surface Milled1 which is more than the other surfaces. The slope is affected as the maximum deviation is 33.5% of its minimum value on surface Milled1. Tip3 gives the minimum values of the slope with all the milled surfaces. Tip2 gives the maximum values of the slope and the density of summits with the milled surfaces.

		Sa	Sq	Sy	Ssk	Sdq	Sds
Milled1	Tip1	0.74	0.93	8.11	-0.09	0.19	10310
	Tip2	0.81	1.01	8.24	0.05	0.21	17769
	Tip3	1.00	1.23	7.67	0.09	0.17	12494
Milled2	Tip1	4.98	5.91	29.43	0.41	0.34	5648
	Tip2	4.98	5.91	29.08	0.39	0.36	10563
	Tip3	5.27	6.24	29.56	0.42	0.29	5461
Milled3	Tip1	0.58	0.74	4.90	-0.52	0.19	8698
	Tip2	0.58	0.74	5.17	-0.49	0.20	13067
	Tip3	0.70	0.89	5.50	-0.65	0.15	12241

Table 4.7: Roughness parameters for Milled specimens measured with different tips

4.6.4 Comparing the roughness of the turned specimens:

Table 4.8 shows the roughness parameters of turned specimens when measured with different tips. Most roughness parameters of the turned surfaces are affected by the stylus tip geometry but still to less extent than the ground and the lapped surfaces. Tip1 gives the worst variations in most amplitude parameters (Sa, Sq, Sy). The maximum deviation in Sa is 55% of its minimum value. The maximum deviation in Sq is only 11% of its minimum value. The maximum deviation in Sy is 32% of its minimum value. The Skewness Ssk has shown significant effect of the tip shape on the surface Turned1 which is more than the other surfaces. The slope is affected as the maximum deviation is 30% of its minimum value on surface Turned2. Tip3 gives the minimum values of the slope with all the turned surfaces. Tip2 gives the maximum values of the slope and the density of summits with the turned surfaces except Turned3.

		Sa	Sq	Sy	Ssk	Sdq	Sds
Turned1	Tip1	0.93	1.09	5.27	-0.19	0.29	3197
	Tip2	0.92	1.02	4.25	0.12	0.29	4089
	Tip3	0.92	1.13	5.60	-0.14	0.26	2904
Turned2	Tip1	1.86	2.32	13.50	0.36	0.33	4915
	Tip2	1.83	2.28	13.18	0.36	0.35	8764
	Tip3	1.86	2.27	12.14	0.24	0.27	6540
Turned3	Tip1	3.73	4.57	28.91	-0.20	0.47	3716
	Tip2	3.40	4.17	25.64	-0.16	0.43	5927
	Tip3	3.46	4.23	26.26	-0.12	0.42	3024

Table 4.8: Roughness parameters for Turned specimens measured with different tips

4.7 3D Simulation on real surfaces data with real tips data

The previous real results show that the stylus shape often has a significant effect on the roughness parameters of engineering surfaces under practical conditions. This effect could be as large as doubling the value of the roughness parameter. Real tests don't reveal much about the nature of the actual surface-stylus contact that causes this variation. Consequently, simulation has been run using the shapes and surfaces encountered in real tests. The information so generated on the distribution of contacts around the tip may help to explain what is going on. The pattern of roughness parameters variation in the simulation will help to confirm the extent to which the simulation reasonably represents real behavior. In each simulation, the input surface is that measured by the finest tip (tip2) and simulated 3D scans are performed with representations of all three experimental tips, including tip2. Note that running tip2 on a surface created by the same tip (tip2) is not a null operation as there is a cumulative effect.

The bold numbers in the following tables give the original values of the roughness parameters of the surface before scanning it with tips while the non-bold numbers give the values of the parameters when scanned in simulation with tips.

4.7.1 Scanning ground specimens

Table 4.9 shows the roughness parameters of different outputs when scanning the ground specimens with different tips. It is noticed that all the original parameters of the ground surfaces are affected by the tip shape. There is no much variation in the amplitude parameters of each surface with different tips. All tips show nearly the same effect on Rq and Ry of each surface. The maximum deviation in Ra is 20% on the surface Ground2 when scanned with Tip3. The slopes of all surfaces are less than their original values except Ground1 with Tip3 which remains unchanged. There is a significant variation of the slope of the surface Ground1 as Tip2 has reduced the slope by 50% from its original value. All tips give the same effect on the slope of the surface Ground2 as it is reduced by 40% of its original value. The skewness Ssk of the surface Ground2 hasn't been affected too much compared to the other surfaces. It is noticed that tip3 gives the maximum values of the Sds while tip1 gives the lowest values for all the ground surfaces.

The contacts distributions on the different tips when scanning the ground specimens are shown in figures 4.22. It is noticed that the contacts on the different tips with different ground surfaces do not occur on the whole tip. Most contacts are generally around one side/corner of Tip1 and Tip2 but there are more contacts distributed on tip2. None of the tips touches a surface at its centre point. Since different tips contact most of the measured surfaces at one side only, the size and shape of these tips have little effect on the roughness parameters. This is obviously because the tips are worn so that the effective size of the tip is smaller than the apparent one. That also could be a result of not levelling the specimens accurately before measuring it.

		Sa	Sq	Sy	Ssk	Sdq	Sds
		0.21	**0.26**	**1.85**	**-0.02**	**0.06**	**14985**
Ground1	Tip1	0.21	0.25	1.60	0.06	0.04	13600
	Tip2	0.20	0.25	1.60	0.11	0.03	14452
	Tip3	0.21	0.25	1.63	0.03	0.06	14492
		0.30	**0.39**	**3.03**	**0.81**	**0.15**	**14172**
Ground2	Tip1	0.34	0.44	2.87	0.79	0.09	8631
	Tip2	0.34	0.44	2.83	0.82	0.09	13187
	Tip3	0.36	0.45	2.78	0.75	0.09	17316
		0.35	**0.44**	**3.30**	**0.21**	**0.16**	**20766**
Ground3	Tip1	0.36	0.45	3.07	0.35	0.10	14798
	Tip2	0.36	0.45	2.88	0.36	0.09	17795
	Tip3	0.36	0.45	2.92	0.42	0.10	22817

Table 4.9: Roughness parameters for ground specimens scanned with different tips

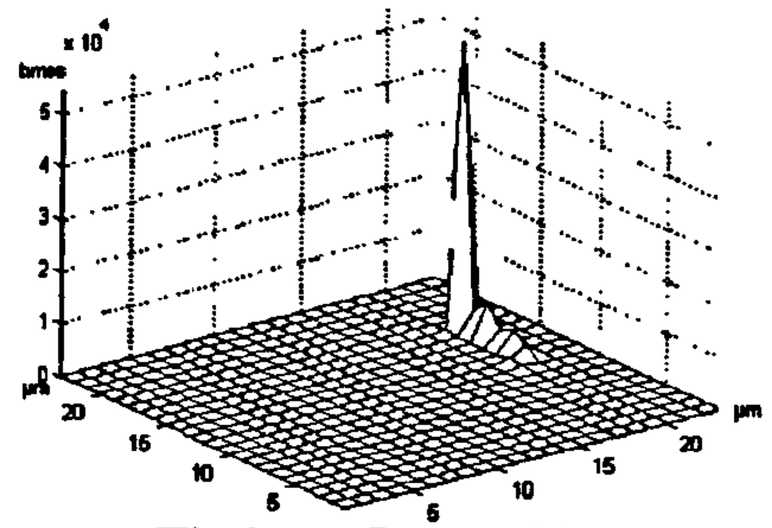

Tip1 on Ground1

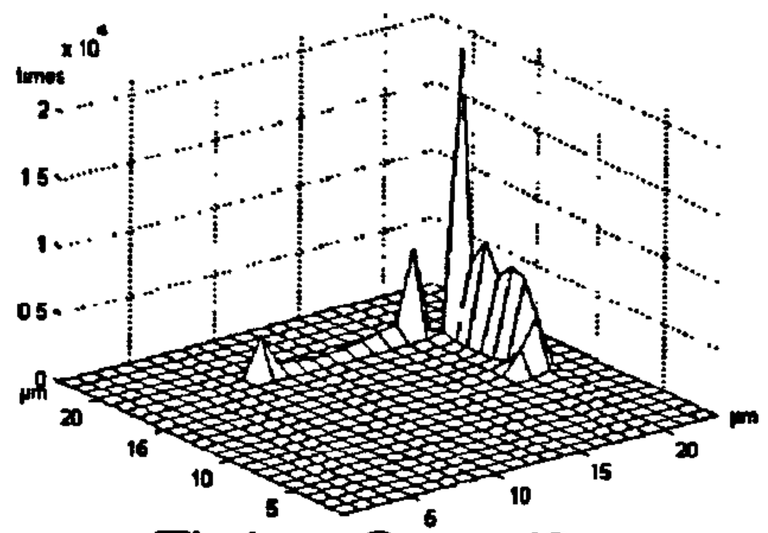

Tip1 on Ground2

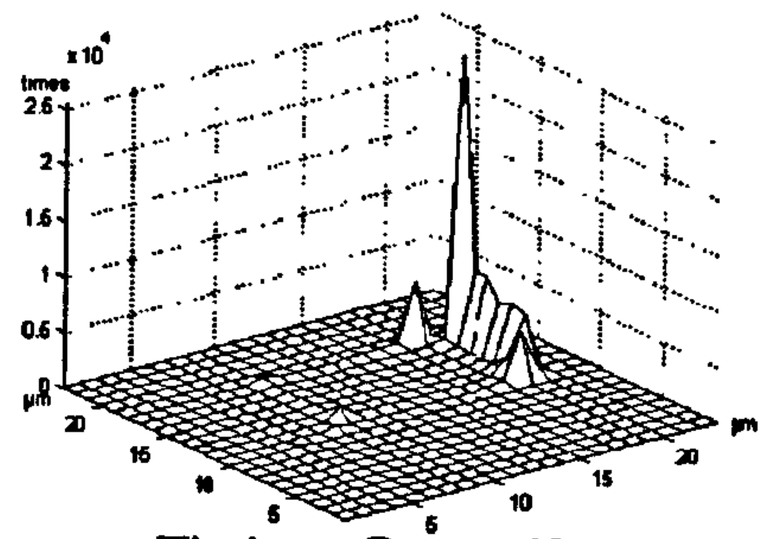

Tip1 on Ground3

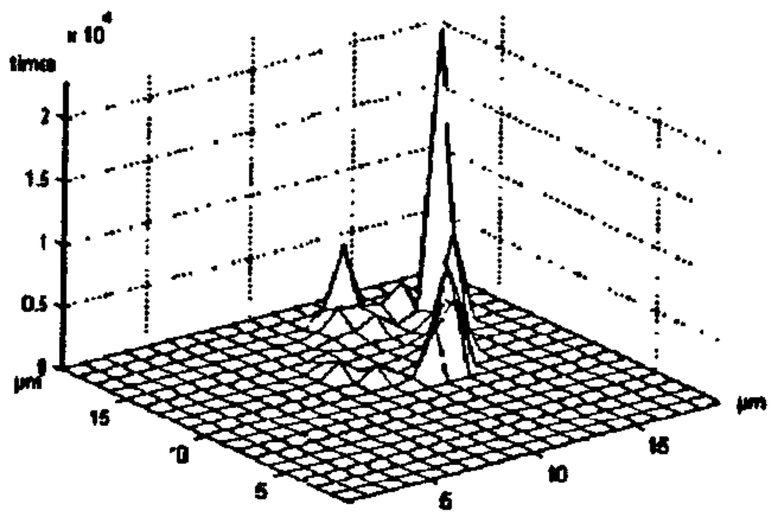

Tip2 on Ground1

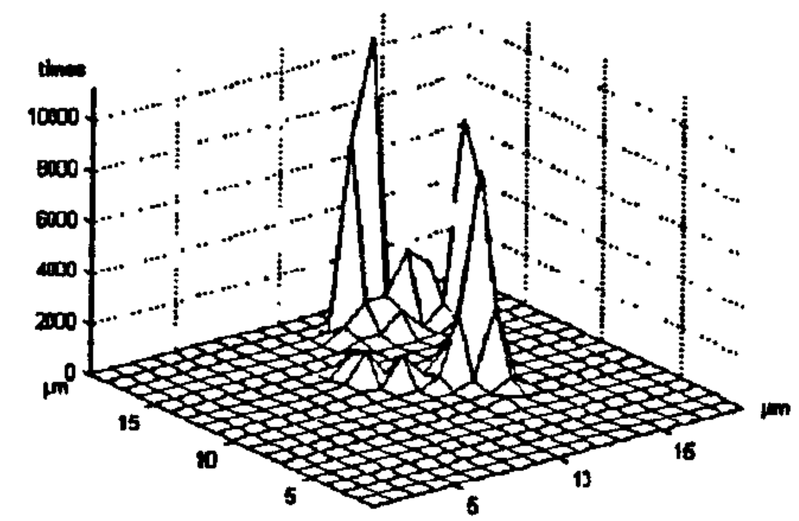

Tip2 on Ground2

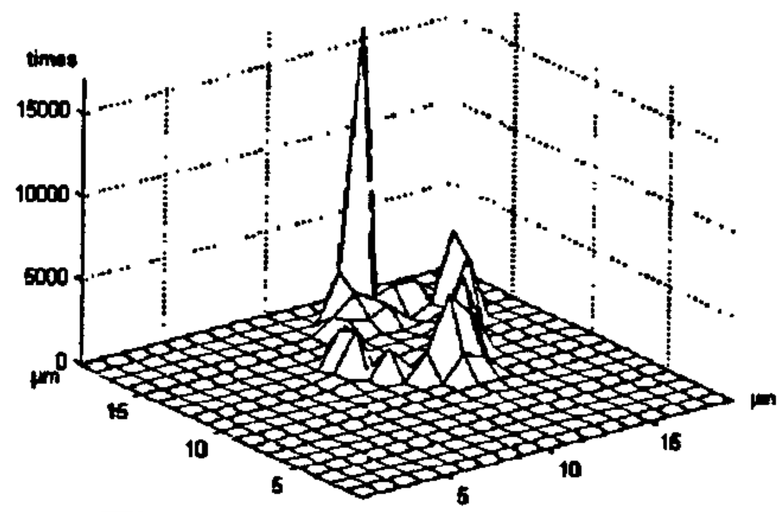

Tip2 on Ground3

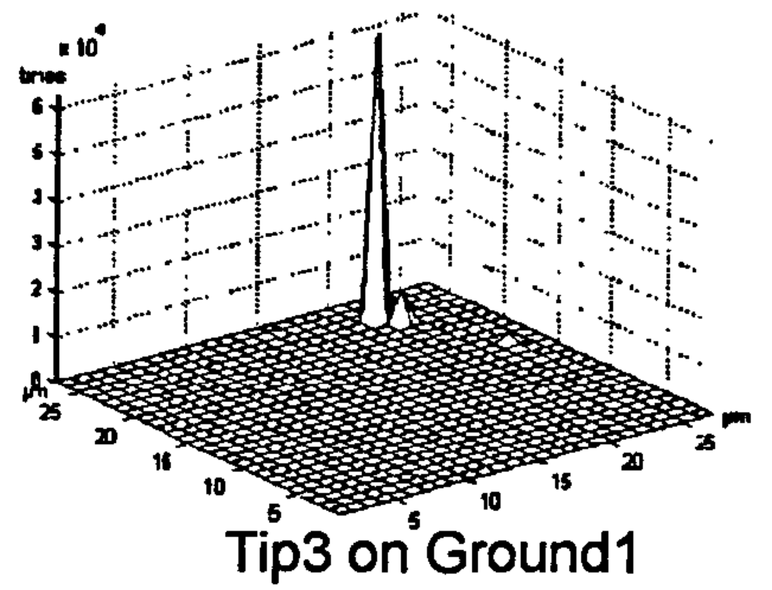

Tip3 on Ground1

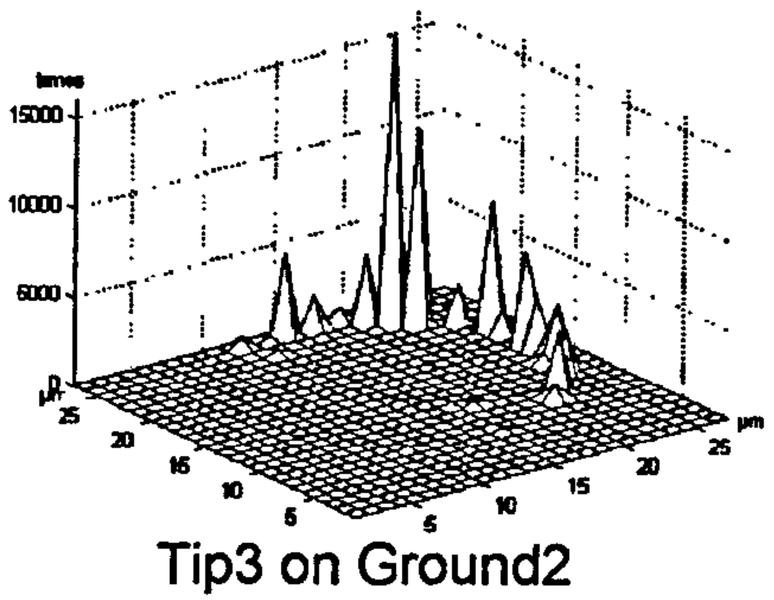

Tip3 on Ground2

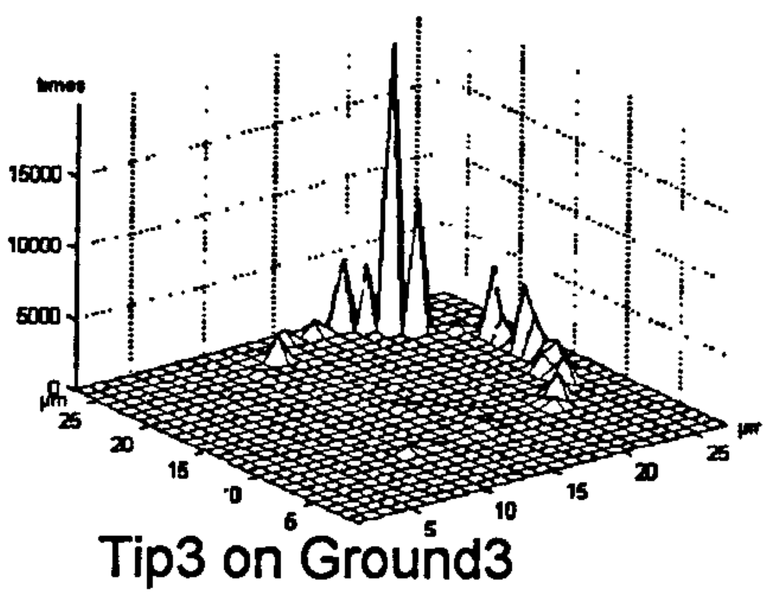

Tip3 on Ground3

Figure 4.22: Scanning ground specimens with different tips

4.7.2 Scanning Lapped specimens

Table 4.10 shows the roughness parameters of different outputs when scanning the lapped specimens with different tips. It is noticed that all the original parameters of the lapped surfaces are affected by the tip shape even more than the ground surfaces. Tip2 gives the minimum deviations of all the amplitude parameters of all surfaces. All tips have reduced the values of the amplitude parameters Ra, Rq and Ry as well as the slope. The maximum deviation in Ra and Rq is nearly 23% on the surface Lapped1 when scanned with Tip3. The maximum deviation in Ry is 32% on the surface Lapped3 when scanned with Tip3. The skewness of the first surface Lapped1 is mostly affected by the tip shape. The slopes of all surfaces are nearly 40% less than their original values. It is noticed that tip3 gives the maximum values of the Sds and tip1 gives the lowest values for all the lapped surfaces.

The contacts distributions on the different tips when scanning the lapped specimens are shown in figures 4.23. It is noticed that the contacts on the different tips with different lapped surfaces do not occur on the whole tip but only around the external profile of the tips. None of the tips touches a surface at its centre point and most contacts are generally around one side/corner of Tip1 and Tip3 but there are more contacts distributed on tip2. The contacts on the tips with lapped surfaces are more spread than the contacts with the ground surfaces and always relevant to the tip shape. For this reason, the deviations in the different roughness parameters here are more than the ground surfaces.

		Sa	Sq	Sy	Ssk	Sdq	Sds
		0.42	**0.53**	**5.12**	**0.01**	**0.24**	**15984**
Lapped1	Tip1	0.34	0.43	3.81	0.36	0.13	6913
	Tip2	0.35	0.45	3.95	0.23	0.14	15891
	Tip3	0.32	0.41	3.72	0.60	0.13	22231
		0.24	**0.30**	**2.56**	**-0.31**	**0.13**	**24668**
Lapped2	Tip1	0.21	0.25	1.81	-0.11	0.08	16024
	Tip2	0.21	0.25	1.89	-0.16	0.07	21658
	Tip3	0.21	0.25	1.75	-0.12	0.08	29743
		0.54	**0.68**	**5.06**	**-0.42**	**0.19**	**21525**
Lapped3	Tip1	0.50	0.60	4.03	-0.18	0.10	9271
	Tip2	0.51	0.62	4.23	-0.28	0.11	18222
	Tip3	0.49	0.59	3.72	-0.14	0.11	26826

Table 4.10: Roughness parameters for Lapped specimens scanned with different tips

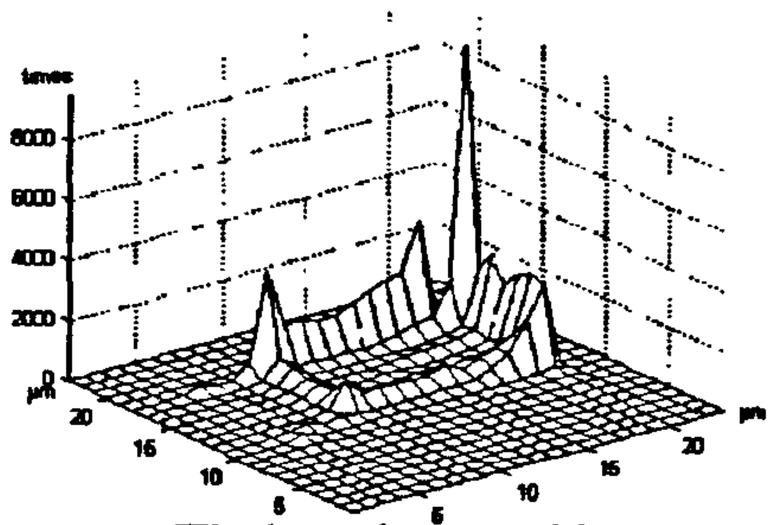

Tip1 on Lapped1

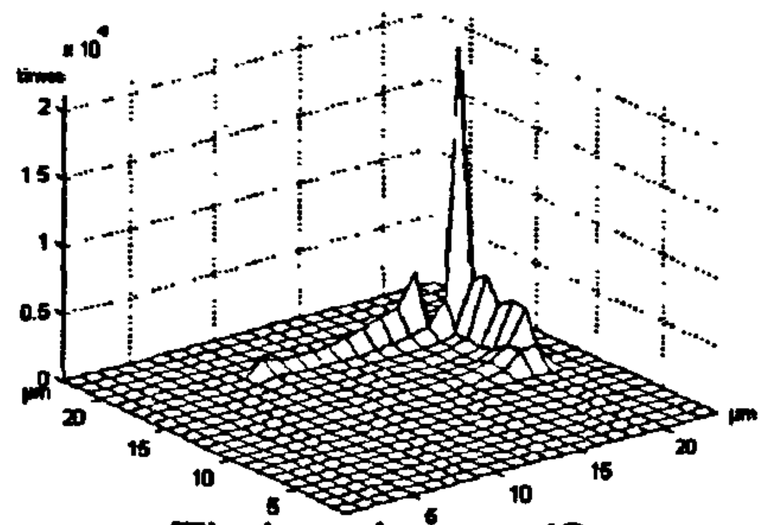

Tip1 on Lapped2

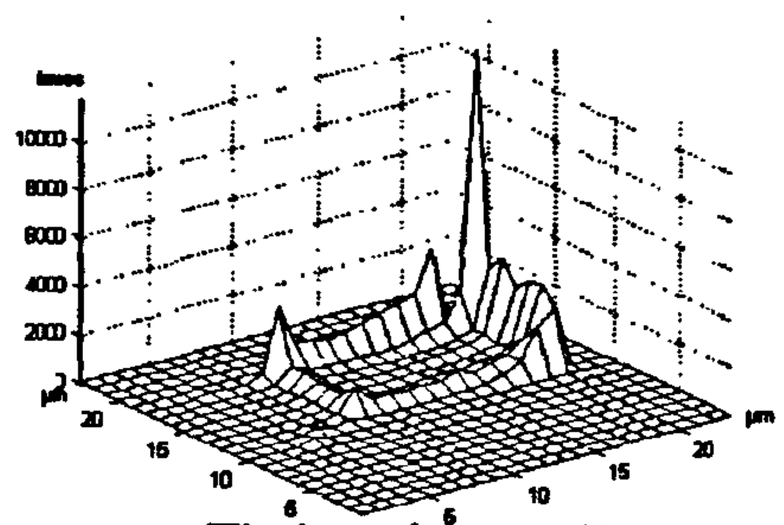

Tip1 on Lapped3

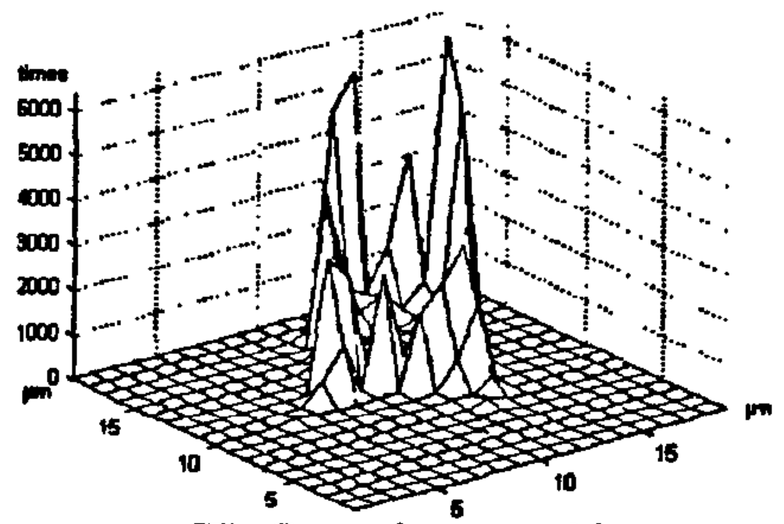

Tip2 on Lapped1

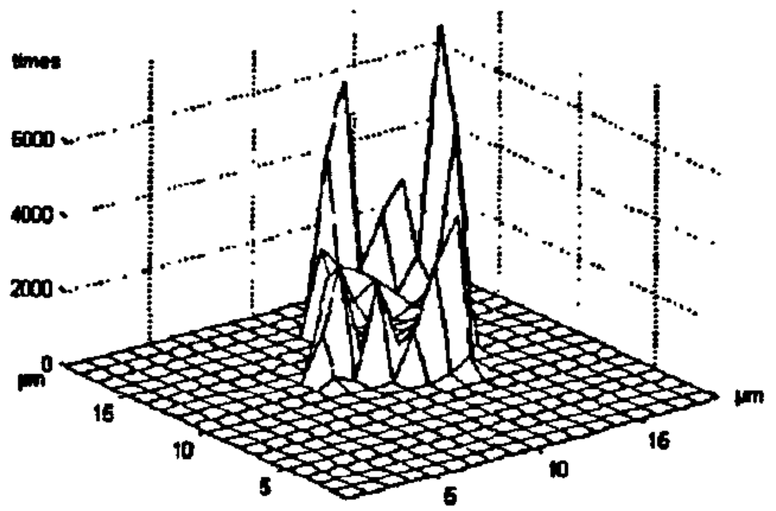

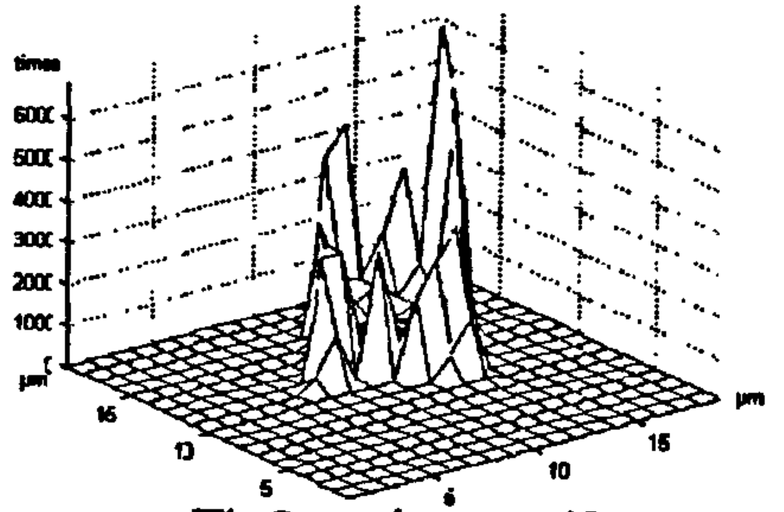

Tip2 on Lapped3

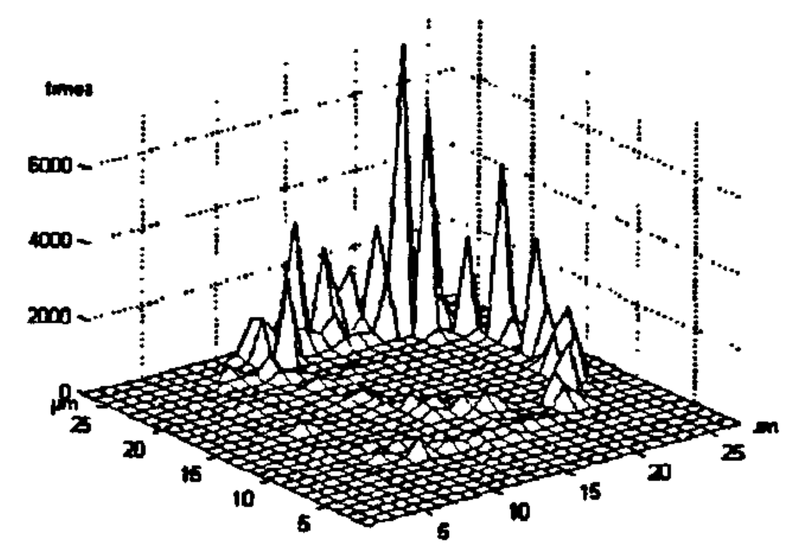

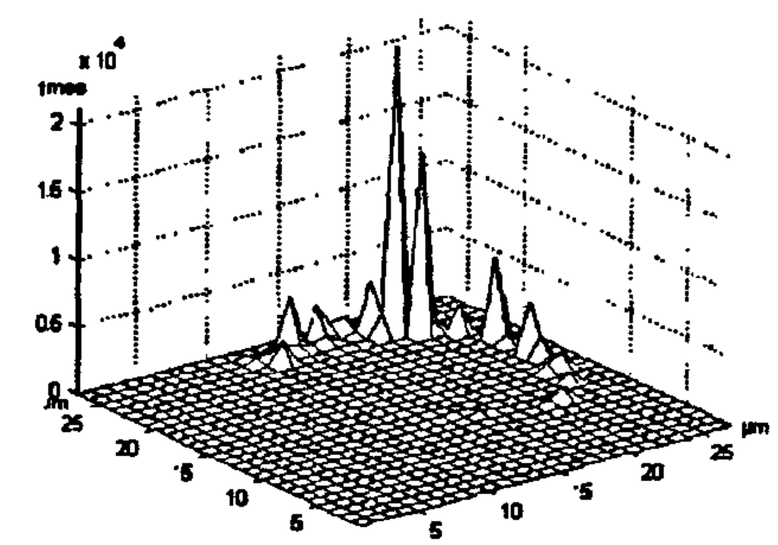

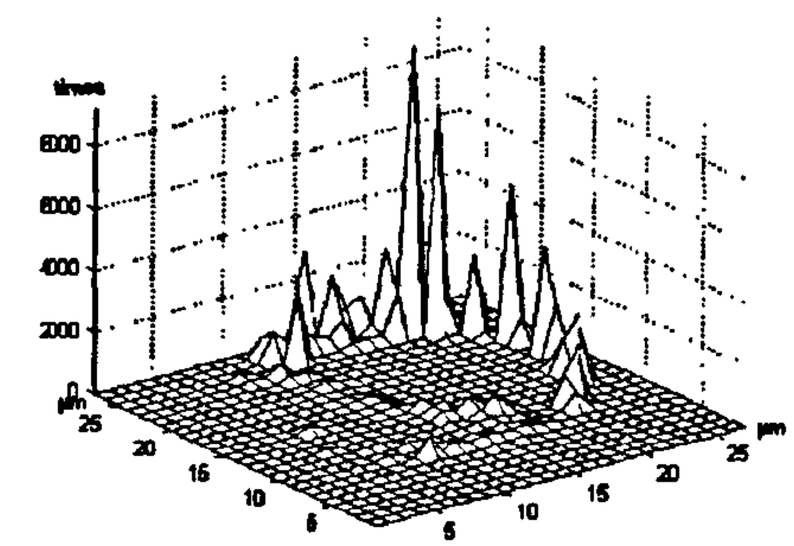

Figure 4.23: Scanning lapped specimens with different tips

4.7.3 Scanning Milled specimens

Table 4.11 shows the roughness parameters of different outputs when scanning the milled specimens with different tips. It is noticed that all the original parameters of the lapped surfaces are affected by the tip shape but less than the lapped surfaces. Tip2 also gives the minimum deviations of all the amplitude parameters of all surfaces. All tips have reduced the values of the amplitude parameters Ra, Rq and Ry of the surfaces Milled1 and Milled3. The surface Milled2 shoes the least effect of the tip shape. The maximum deviation in Ra and Rq is nearly 26% on the surface Milled3 when scanned with Tip3. The maximum deviation in Ry is 32% on the surface Milled1 when scanned with Tip3. The skewness of the first surface Milled1 is mostly affected by the tip shape. All the slopes of all surfaces have been reduced between 25-40% less than their original values. tip3 still gives the maximum values of the Sds while tip1 gives the lowest values for all the milled surfaces.

The contacts distributions on the different tips when scanning the milled specimens are shown in figures 4.24. It is noticed that the contacts on the different tips with different milled surfaces do not occur on the whole tip but only around the external profile of the tips. None of the tips touches a surface at its centre point and most contacts are generally around one side/corner of Tip1 and Tip3 but there are more contacts distributed on tip2. Tip1 shows nearly the same contacts distribution as with the lapped surfaces but with more contacts.

		Sa	Sq	Sy	Ssk	Sdq	Sds
		0.81	**1.01**	**8.24**	**0.05**	**0.21**	**17769**
Milled1	Tip1	0.71	0.88	6.74	0.40	0.13	8738
	Tip2	0.73	0.90	6.77	0.27	0.14	15051
	Tip3	0.68	0.84	6.31	0.62	0.11	20979
		4.98	**5.91**	**29.08**	**0.39**	**0.36**	**10563**
Milled2	Tip1	5.02	5.93	27.15	0.39	0.26	3277
	Tip2	5.01	5.92	27.69	0.37	0.27	8711
	Tip3	5.11	5.99	25.94	0.39	0.25	11988
		0.58	**0.74**	**5.17**	**-0.49**	**0.20**	**13067**
Milled3	Tip1	0.48	0.62	4.37	-0.46	0.11	7739
	Tip2	0.48	0.63	4.43	-0.50	0.12	12081
	Tip3	0.42	0.55	3.98	-0.36	0.10	16903

Table 4.11: Roughness parameters for Milled specimens scanned with different tips

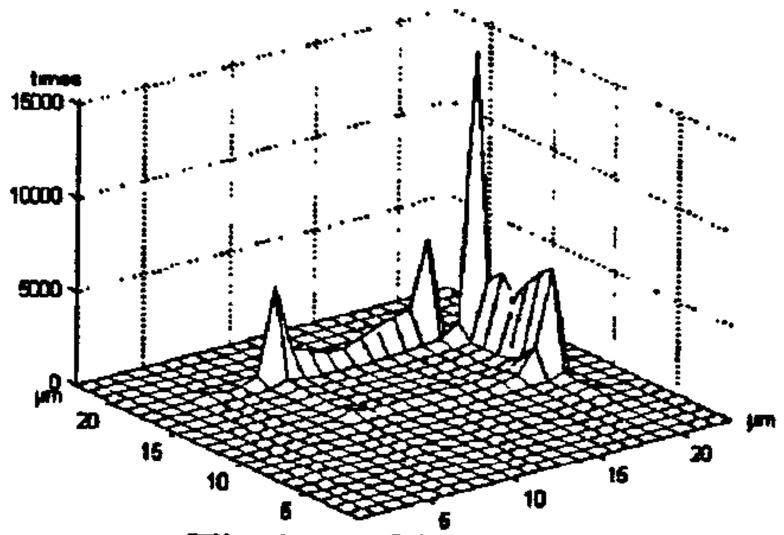

Tip1 on Milled 1

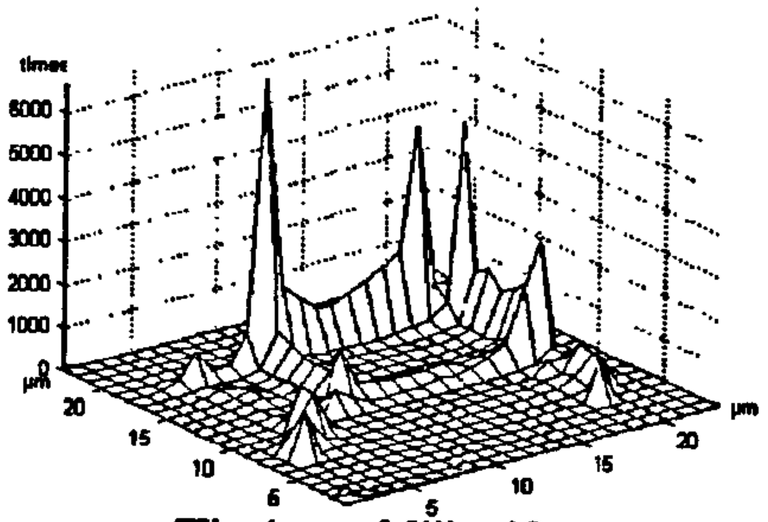

Tip1 on Milled2

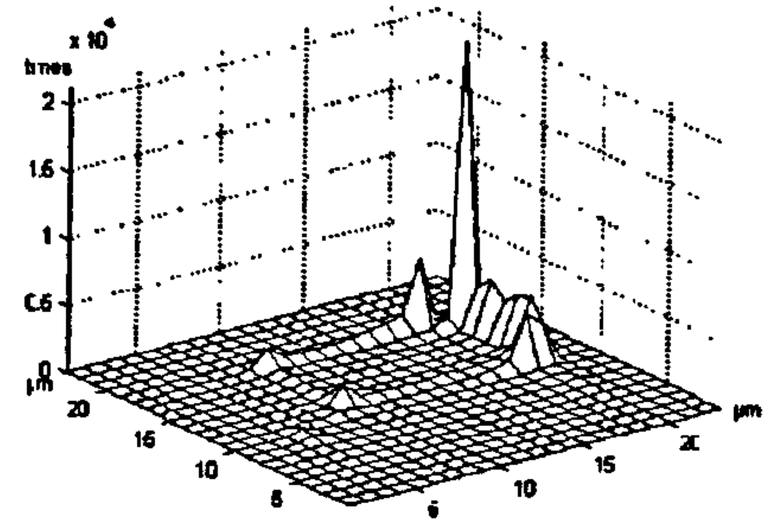

Tip1 on Milled3

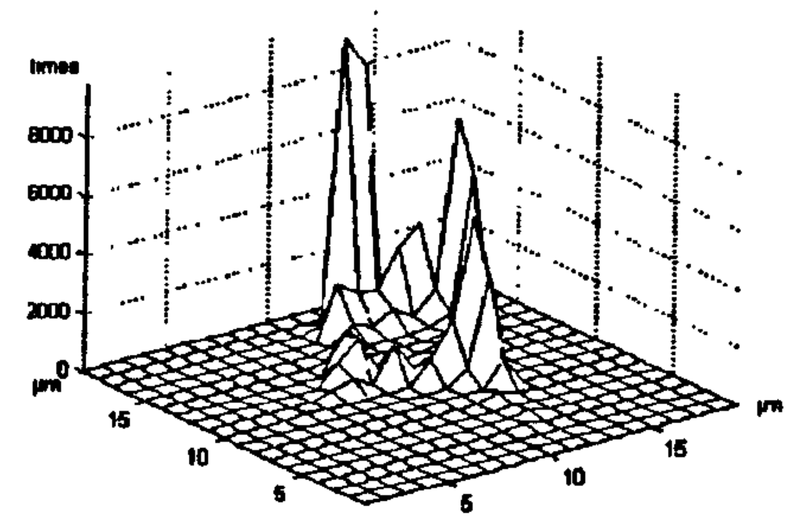

Tip2 on Milled1

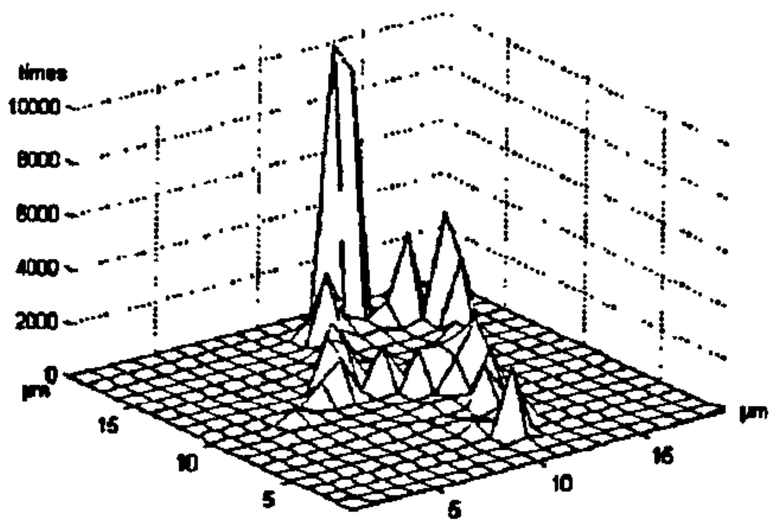

Tip2 on Milled2

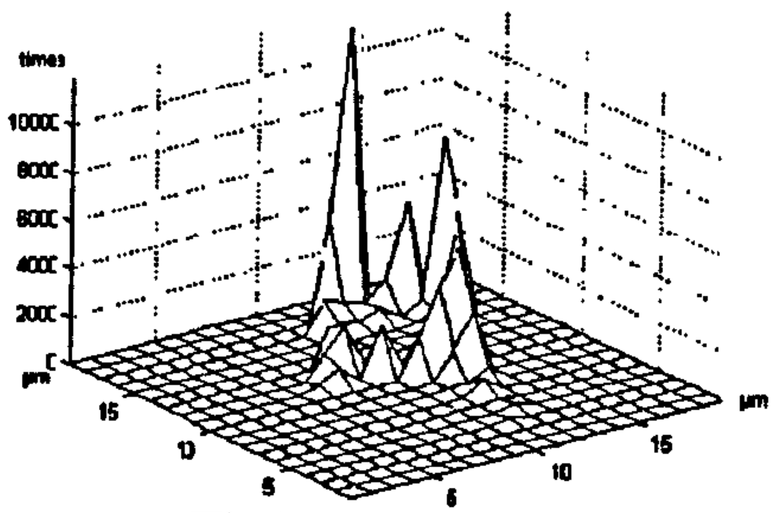

Tip2 on Milled3

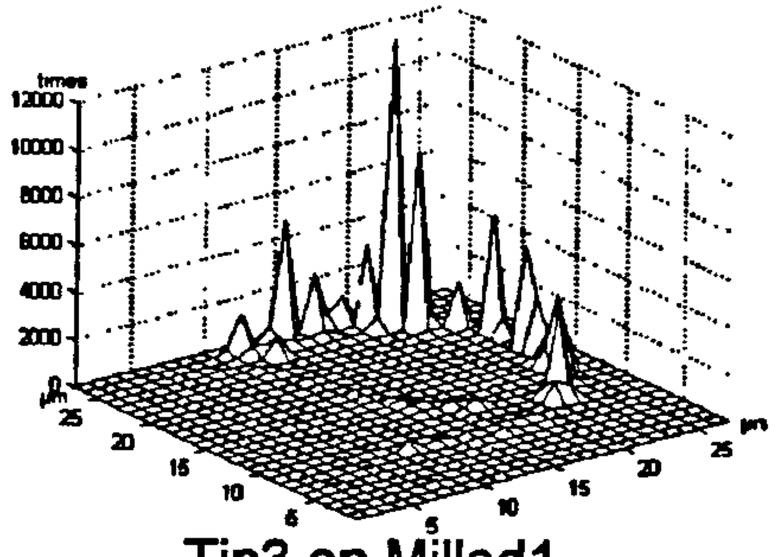

Tip3 on Milled1

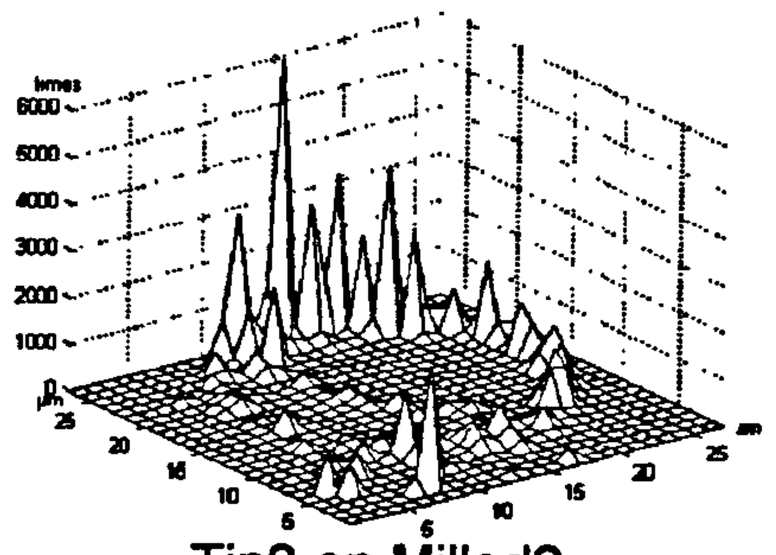

Tip3 on Milled2

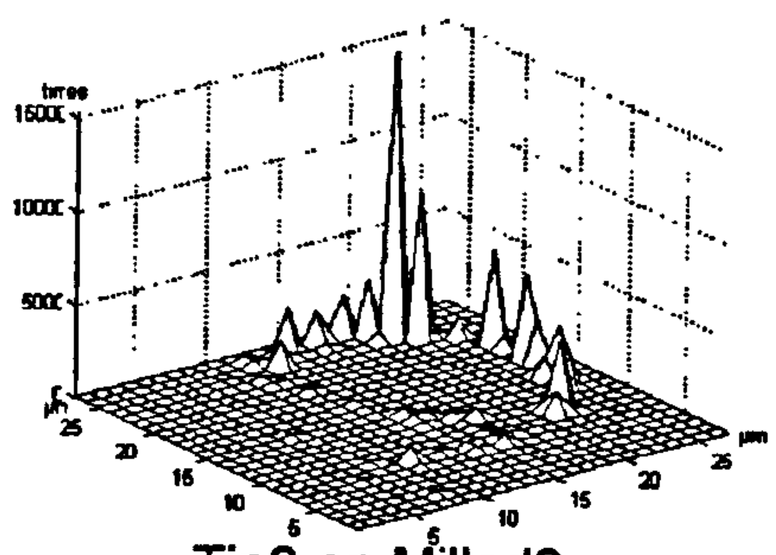

Tip3 on Milled3

Figure 4.24: Scanning milled specimens with different tips

4.7.4 Scanning Turned specimens

Table 4.12 shows the roughness parameters of different outputs when scanning the turned specimens with different tips. It is noticed that all the original parameters of the turned surfaces are affected by the tip shape but strongly with the surface Turned1. Tip2 gives the minimum deviations of all the amplitude parameters of all surfaces. All tips have nearly reduced the values of all the parameters including Ra, Rq, Ry, Ssk ad the slope. The maximum deviation in Ra and Rq is nearly 70% on the surface Turned1 when scanned with Tip3. The maximum deviation in Ry is 41% on the surface Turned3 when scanned with Tip3. The skewness of the first surface Turned1 is mostly affected by the tip shape. All the slopes of all surfaces have been reduced between 17-65% less than their original values. It is also noticed that tip3 gives the maximum values of the Sds while tip1 gives the lowest values for all the turned surfaces.

The contacts distributions on the different tips when scanning the turned specimens are shown in figures 4.25. It is noticed that none of the tips touches a surface at its centre point and most contacts are generally around one side/corner of Tip1 and Tip3 but the contacted are more distributed on tip2. It is also noticed that the tip area which contacts the turned surfaces are bigger than the area with the previous cases. This is logically as the turned surfaces have a regular pattern shape with larger wavelength so the tips can get through and touch the surface more than the other surfaces.

		Sa	Sq	Sy	Ssk	Sdq	Sds
		0.92	**1.02**	**4.25**	**0.12**	**0.29**	**4089**
Turned1	Tip1	0.32	0.40	2.71	-0.51	0.14	3530
	Tip2	0.59	0.70	3.23	-0.68	0.24	7579
	Tip3	0.25	0.31	2.48	-0.27	0.10	15025
		1.83	**2.28**	**13.18**	**0.36**	**0.35**	**8764**
Turned2	Tip1	1.85	2.21	11.53	0.25	0.23	3849
	Tip2	1.83	2.23	11.77	0.33	0.25	7859
	Tip3	1.82	2.17	10.82	0.21	0.21	10176
		3.40	**4.17**	**25.64**	**-0.16**	**0.43**	**5927**
Turned3	Tip1	3.24	3.95	23.15	-0.14	0.32	2291
	Tip2	3.27	3.98	23.25	-0.11	0.34	5847
	Tip3	3.18	3.88	21.74	-0.13	0.31	8618

Table 4.12: Roughness parameters for Turned specimens scanned with different tips

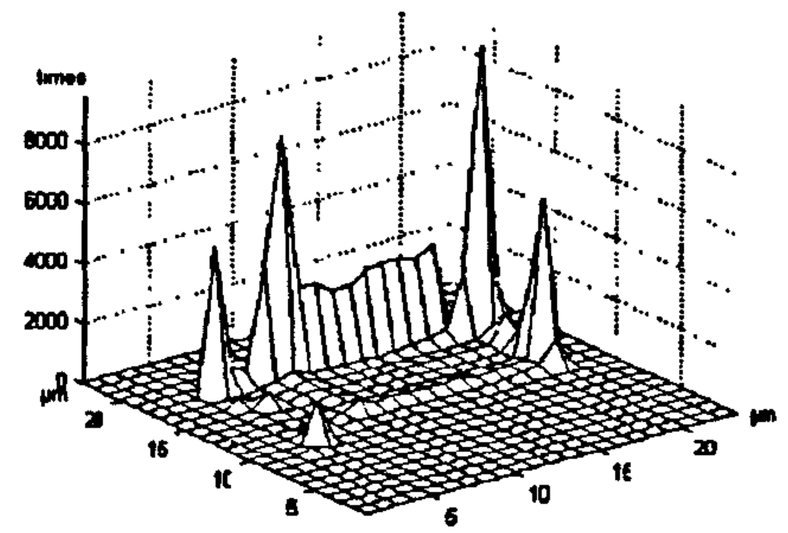

Tip1 on Turned1

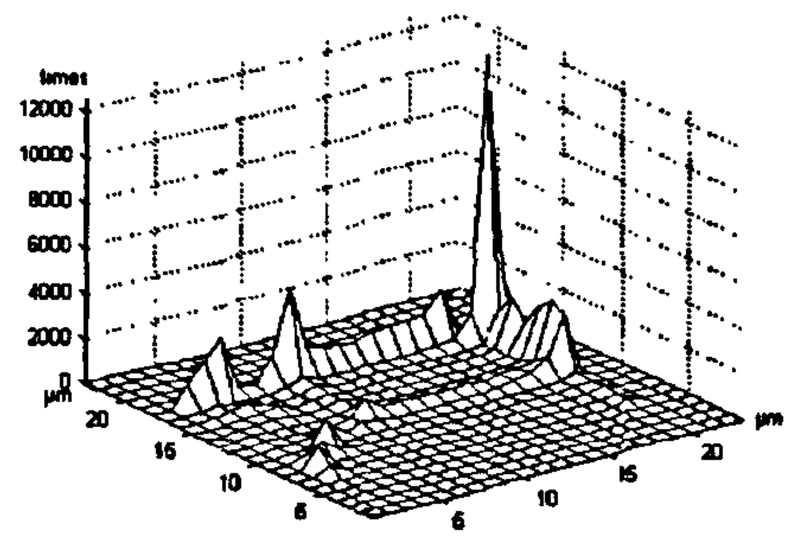

Tip1 on Turned2

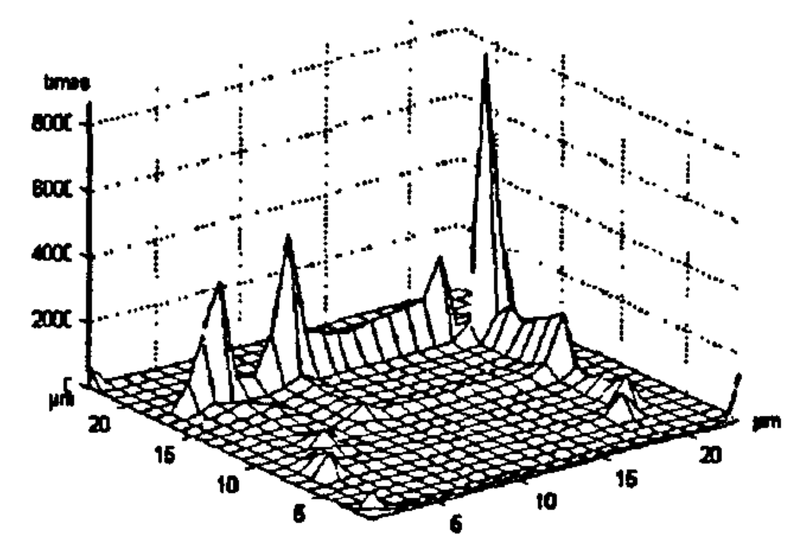

Tip1 on Turned3

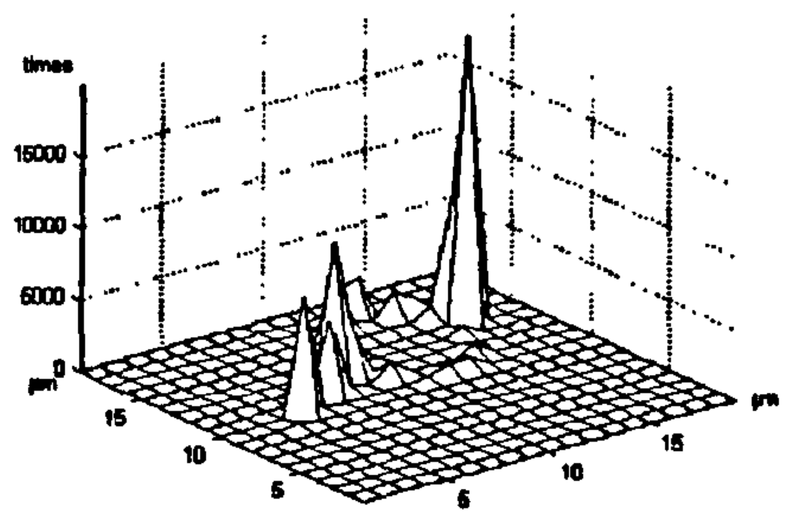

Tip2 on Turned1

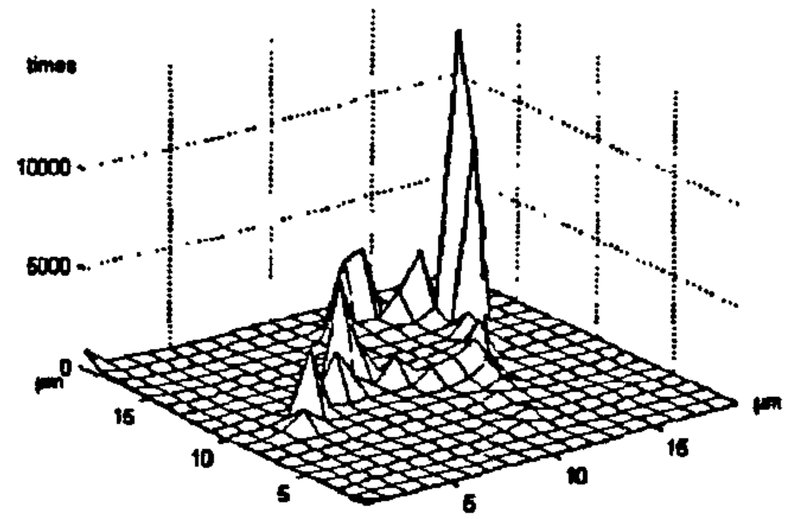

Tip2 on Turned2

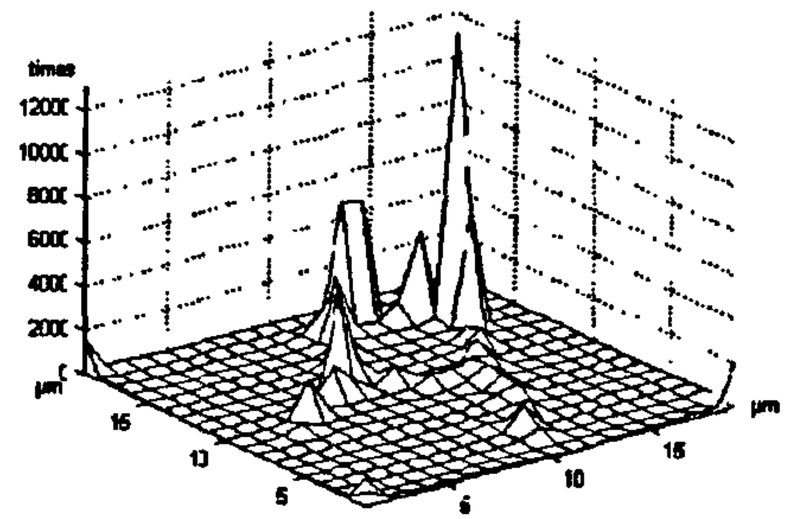

Tip2 on Turned3

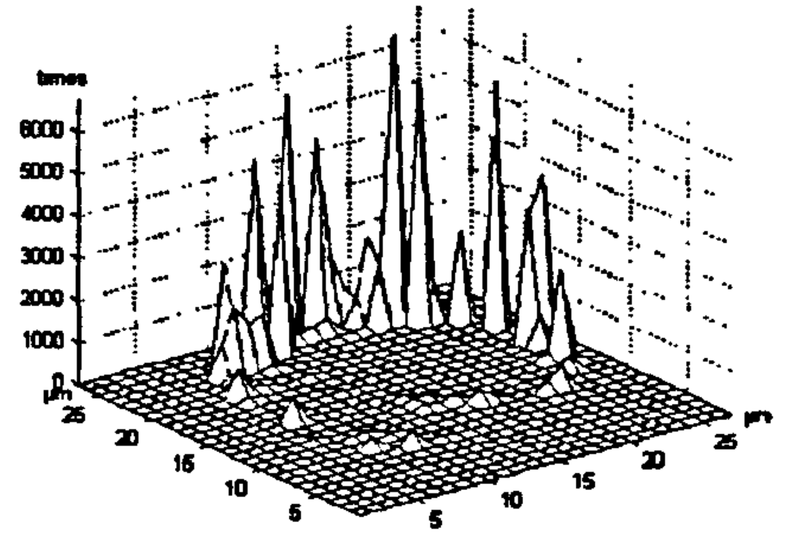

Tip3 on Turned1

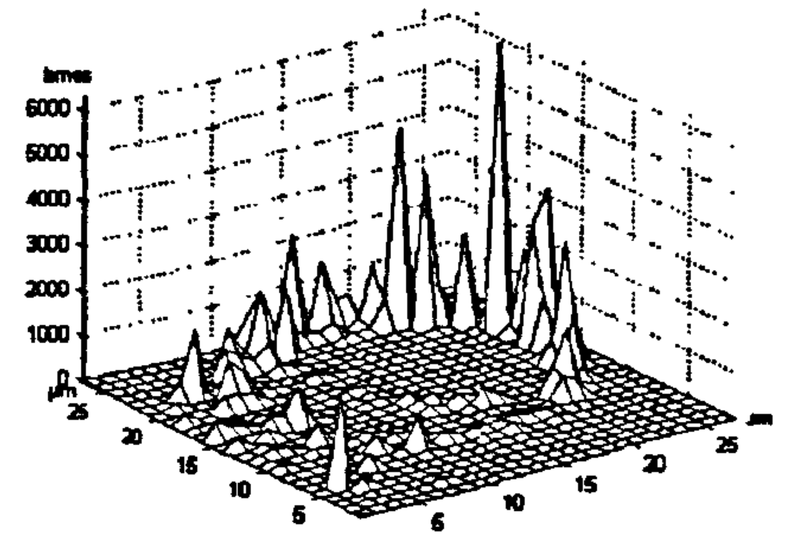

Tip3 on Turned2

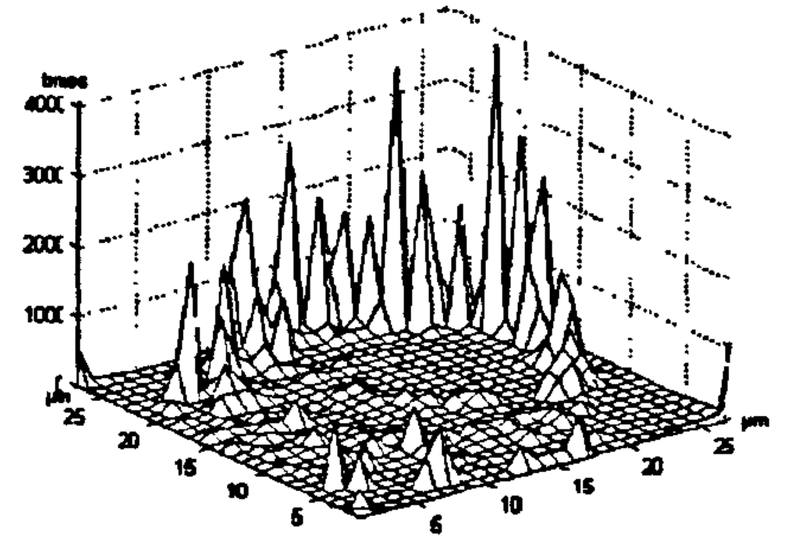

Tip3 on Turned3

Figure 4.25: Scanning turned specimens with different tips

5. Further Discussions & Conclusion

The work presented in this thesis falls naturally into several parts which have been covered in previous chapters, including discussion of thesis individual results. This brief chapter serves to bring the themes together, introducing some further observations, while not repeating more of earlier discussions than is needed to make the summary coherent.

5.1 General Summary

A computer simulation of the 3D geometric interaction of the stylus and surface has been done using arbitrary tip shapes on artificially generated surfaces with both regular and random patterns which were created by the computer. Most previous work broadly similar to this study, involved idealised styli although most were spherical shape. But, the major new feature of this simulation is that it collects data on the distribution of contacts on any stylus tip when scanning a surface in 3D.

Significant variation in roughness parameters values was demonstrated with changes in stylus size and shape when artificially generated surfaces were scanned by idealised tips. This variation could be 100% of the original value of the parameter. This is as expected for surfaces generated to test the further characteristics of the stylus.

The contacts distribution on each tip when scanning each surface has been determined. This has shown a wide range of contacts distributions depending on the tip shape and the surface.

Simulations with idealised truncated tips (as if worn) caused further changes to surface parameterization. Less predictably, and of some importance, the destination of contact points on the tips changes quite dramatically as 'wear' occurs.

Real surfaces measured optically by another measuring system, were treated by the simulation using the same set of tip shapes. Broadly, the same patterns of behaviour were observed as with the artificial ones, although variations were rather smaller, probably because of the restricted spectral content of the surfaces.

A bespoke measuring system has been built to measure the surface roughness in 3D of real surfaces by real styli with different tip shapes. A rig has been developed to allow exchanging the styli of the measuring system with the minimum effect on the overall accuracy of the system. Different specimens with different surface patterns have been measured by the system in 3D with the different available tips. Data representing the real surfaces have been analysed and shown also variations in the roughness values with different styli. The shape of each stylus tip has been determined using a technique based on the replica method. The indentation of the tip with its real orientation is created using the measuring system and a soft substrate (typically lead). The indentation has been measured by an atomic force microscope. The data representing the different tips have been stored and fed to the personal computer of the measuring system. In order to obtain reasonable lateral resolution in the associated simulations, the surfaces and styli were rather larger than average normally encountered in finish processes on metals, but still with the normal range for surface roughness instruments.

The computer simulation has been used to scan the data representing the real surfaces in 3D with the data representing the different real tips. This simulation has shown significant variations of the roughness values of the surfaces when scanned with different tips and has also given an estimate of the real contacts of the different styli with each surface. The distributions would be very different to the predicted in advance and could not be represented sensibly by any classical statistical distribution for the purpose, for example of uncertainty estimation.

The roughness values of the real surfaces when scanned (theoretically) by the real tips have been compared to the roughness values of the same surfaces when measured by the measuring system with different tips. This comparison has shown a good compliance of both the theoretical and the practical results.

5.2 The theoretical results

The initial verification of the computer simulation in this study was based on theoretical data which are not real in the surface roughness measurements. This is to demonstrate the idea and show the extreme cases of the effect of the stylus shape on the roughness of the measured surface. Tips have been used in their perfect shapes; spherical, pyramid and conical. Even the worn tips have been truncated uniformly producing a perfect worn shape where the top and bottom of the tip are totally flat and parallel. Also the tips have been used in their ideal orientations where the central line of the tip is absolutely vertical and the base of the tip is absolutely horizontal. The specimens have been used in their ideal orientations without any levelling error. All other sources of error including mechanical and electrical error have been neglected. Figure 5.1 shows the perfect orientation of the stylus and the measured surface.

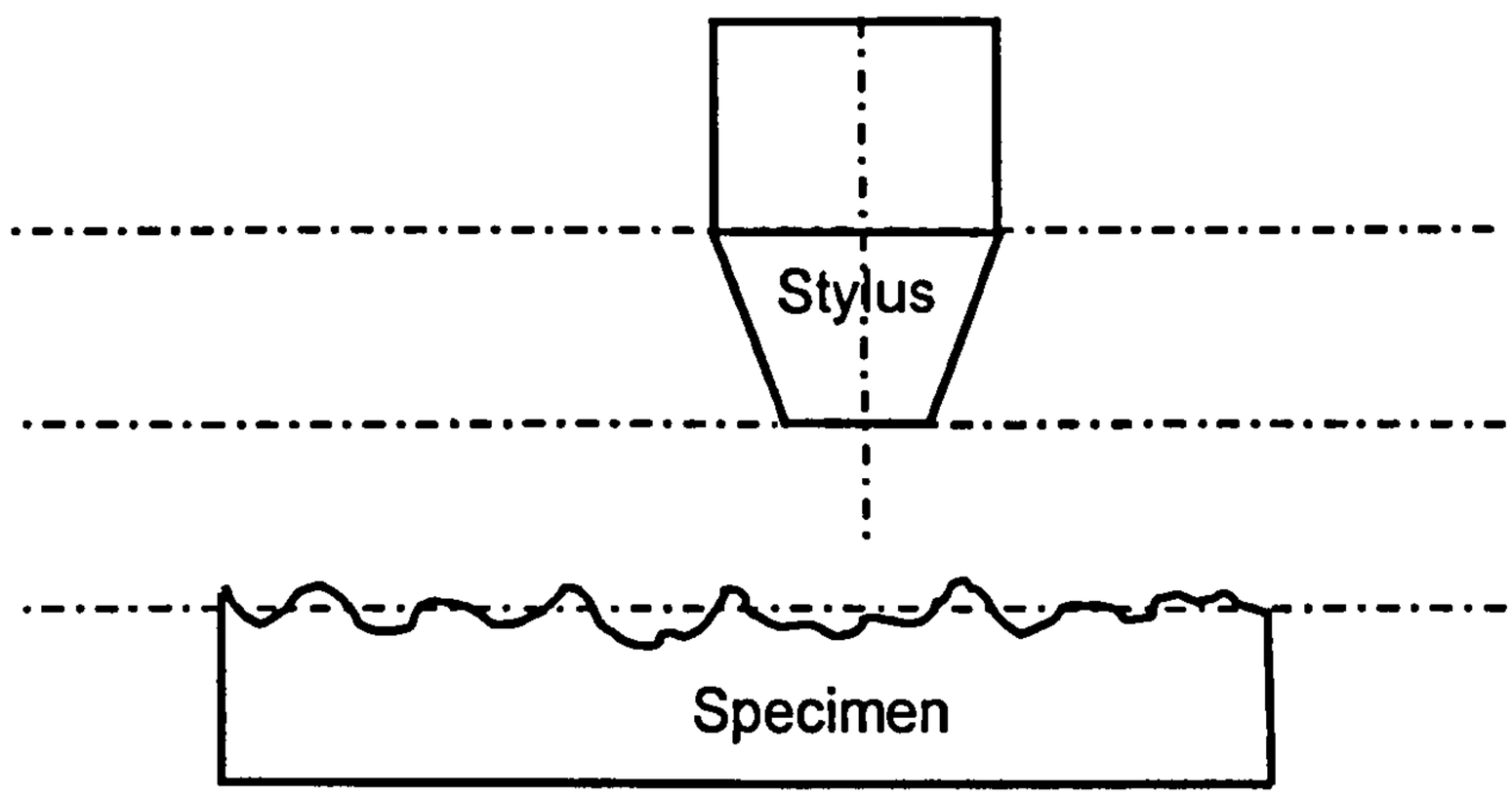

Figure 5.1: the perfect orientation of the stylus and the measured surface

The simulation on the theoretical surfaces has shown that the stylus geometry has an effect on all measured roughness parameters. Even with the perfect conical and pyramid tips where the contact with the scanned surface and the tip is always at one point; there is an effect. This effect may not be too much on some roughness parameters but it exists. On the other side, demonstrating the contacts distribution on the tip has shown a very good imagination of what could be happening on that small area of the stylus contacting the surface.

Scanning real surfaces theoretically by theoretical tips has pushed the simulation one step toward the real metrology. Surfaces produced by different machining processes (lapping, Grinding and Milling) have been scanned by the simulation program. The actual values of the roughness parameters of these of these surfaces have been previously determined by another surface roughness measuring system. The simulation has shown that the stylus shape and size have affected all the surface roughness parameters of all specimens.

Generally, from the simulation on the real and non-real surfaces, it has been noticed that the measured values of the roughness parameters Sa, Sq and Sy are always less than the actual values of the surface. It has been also noticed that the conical and pyramid tip shapes give closely similar results of the roughness parameters and the contacts distribution. This is simply because the two types of tips are very similar in shape and size at their ends.

It has been noticed that the contacts distribution on the tip doesn't only depend on the tip shape but also on the topography of the measured surface. Figure 5.2, shows a spherical tip scanning a sinusoidal surface. If the wavelength and the amplitude of the surface are slightly bigger than the tip as in figure 5.2a, the tip will not be able to fully penetrate the valleys and touch the surface and most contacts will

occur on the sides of the tip. The lowest point of the tip will only touch the surface at the highest points of the peaks. This is exactly the case of scanning the sinusoidal surface with a spherical tip in figure 2.8 in chapter 2. Where, the tip has the maximum contacts on its sides and the minimum contacts on its central point. If the wavelength of the surface is much bigger than the stylus tip and the amplitude is smaller as shown in figure 5.2b, the contacts on the central point of the tip will relatively increase and the contact area of the tip will decrease. This has been demonstrated by scanning a milled surface with a spherical tip in chapter 2, figure 2.27 where the maximum contacts occur on the central point of the tip. The last case where the stylus tip is bigger than the wavelength of the surface as shown in figure 5.2c, the contacts will mainly be concentrated on the central point of the tip and within a small area around it. This is the case of scanning any surface with random pattern for example scanning a lapped surface with a spherical tip in chapter 2, figure 2.31.

From the simulation of scanning real and non-real surface, it has also been noticed that the lapped surface has shown very similar shapes of contact distributions to the ones of the random surface on all tips (spherical, conical and pyramid). This is expected as both surfaces have random patterns. The ground and the milled surfaces have shown similar contacts distributions because both surfaces have regular surface patterns.

The other important notice is that if contacts distribution is typical of real instruments, there is considerable lateral uncertainty in where the repeated surface heights occur, perhaps approaching the nominal tip dimension. This cuts doubt on benefit of closely spaced samples of surface.

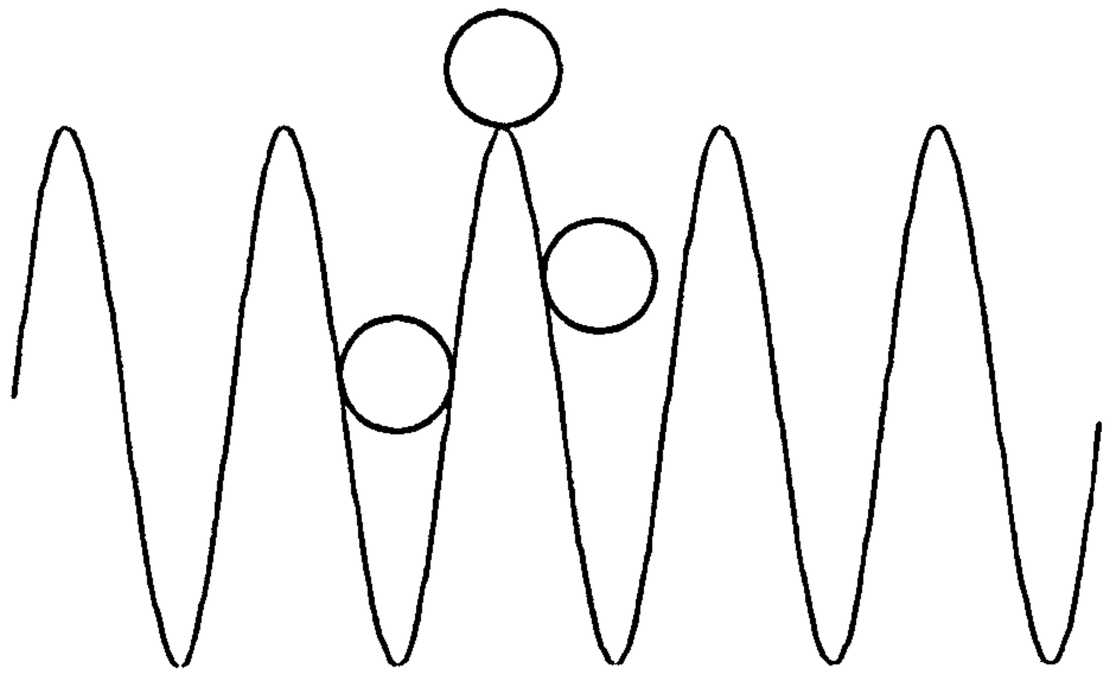

(a)

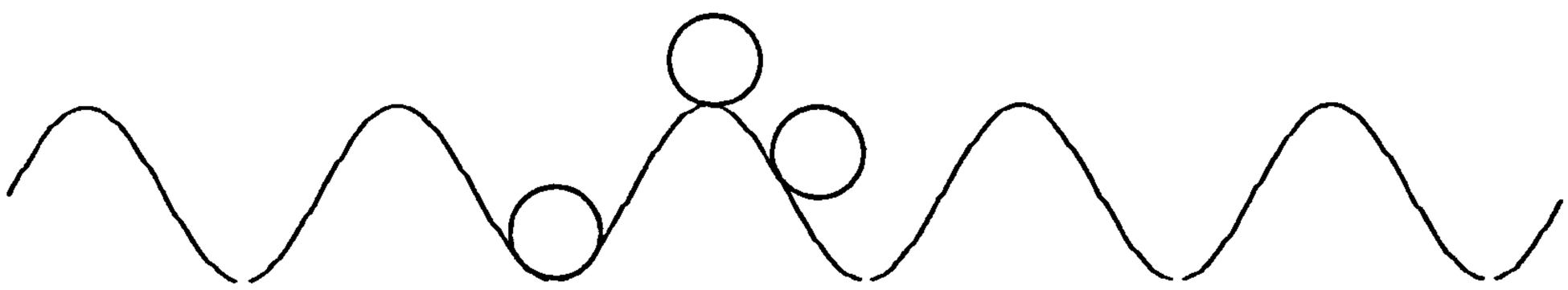

(b)

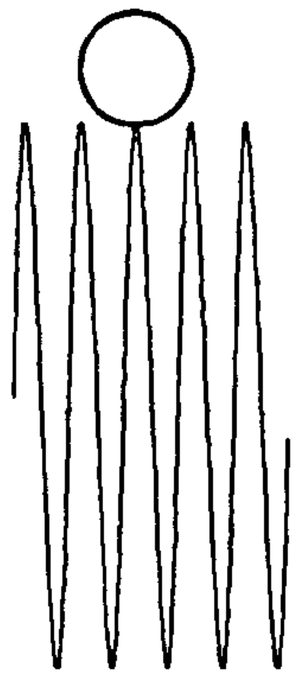

(c)

Figure 5.2: Scanning a sinusoidal surface by a spherical tip.

5.3 The practical results

A 3D surface roughness measuring system has been set-up to determine practically the effect of the stylus tip geometry on the measured roughness of a surface. The idea is to measure the surface roughness of a small area of a surface with different but known styli and compare the results of different styli and also to compare the practical results with theoretical ones. The main measuring problems such as temperature drift and relocating the specimens have been refined as explained in chapter 3. Different specimens have been measured by different styli in 3D. The surfaces of the specimens were machined by Grinding, Lapping, Milling and Turning. Due to the lack of the local resources, three styli tips only have been used in this study. The two original styli of the measuring device have been used and the third tip was made locally of a record-player tip. While many tests are needed to generate a definitive survey of tip behaviour, this is sufficient to demonstrate the value of the technique.

From the practical results, it has been noticed that the different styli have shown slightly different profiles on each specimen. This is a strong evidence that the tip geometry has an effect on the surface roughness and also verifies the reliability and repeatability of the measuring system. Also the different real tips have shown variations in the surface roughness parameters of the different specimens. There is no general trend of the changes with the different tips to predict which tip is better or worse than the others, simply because the tips used in this research have different shapes and sizes. Generally, a good tip is believed to be the finest one which reveals more details of the surface. In other words, it is the tip that can penetrate the surface more than the others i.e. giving maximum amplitude parameters. There should be a proper comparison of the results if the tips have the same shape with different sizes.

However, the lapped specimens have shown strong variations of the amplitude parameters with the different tips (up to 95%, 88% and 46% of the minimum values of the Ra, Rq and Ry measured for the same surface respectively. The behaviour of the skweness is very similar to its behaviour in the simulation on the artificial surfaces and tips. It strongly varies with different tips. The slope has also been affected by the stylus shape as it has been changed by nearly 60% of the minimum value of the same surface when measured with the three tips. This is not surprising as the lapped specimens used for the comparison have relatively high amplitudes and short wavelengths. This is very similar to case of figure 5.2c but with a random pattern.

Based on the tips shapes figures 4.4, 4.5 and 4.6, tip2 is believed to be the finest tip. But, comparing the roughness parameters obtained with the different tips in chapter 4, tip2 doesn't always give the maximum values of the amplitude parameters of all specimens. Sometimes tip1 or tip3 gives the maximum value of these parameters. But, tip2 still give the maximum Sds (density of summits) with nearly all specimens. This means it reveals details of the specimens more than the other tips. However, as an attempt to understand the previous results and how the tip interact with the surface, the 3D profiles of all the specimens when scanned with tip2 (pages 106 to 109) have been re-scanned theoretically by the three real styli measured in chapter 4 using the simulation process explained in chapter 2. The roughness parameters for all outputs have been determined and compared to the values shown in table 4.3. It has been noticed that the roughness parameters have slightly changed from the original values of each specimen showing but with a little difference among different values obtained with different tips with nearly all the surfaces. Except the density of summits Sds which has significantly changed with different tips on different surfaces. This means that the filtering effect of the tips is not the same on all surfaces

although the roughness parameters haven't changed too much. The reason for this could be the variation of the contact area of the tips with the different specimens.

As there is no certain way of detecting the real contacts distribution on a real tip when measuring a real surface, the contacts distributions on each tip with all surfaces have been produced by the simulation to predict the real contacts. From figures 4.22 to 4.25, it has been noticed that all contacts occur on the edges of the tips end with all surfaces. The contacts are mainly concentrated on one or two edges of tip1 and tip3 while the contacts on tip2 are more distributed on its four edges. This has given a good suggestion of the reason for not having very much variation in the practical results. As discussed earlier in this chapter, the tip has to be vertical and the specimen has to be horizontal. If either is inclined, the contacts distribution on the tip as well as the measured roughness parameters of that surface will significantly vary. Having, the stylus inclined as shown in figure 5.3 will reduce the contact area of the stylus and the scanned surface and will also affect the measured roughness parameters. The contacts will be mainly concentrated around the lowest edge of the stylus. Same effect will happen if the mean line of the specimen is not horizontal or if the tip end is tapered.

This is exactly what is happening to the predicted contacts distributions on the real tips as most contacts distributions are concentrated around one corner or one side of the tips. The tip shapes in figures 4.4 to 4.6 show that they are all having taper at the end with different degrees depending on the size of the tip and also tip3 has a non-uniform end. Also, the figures showing the measured surfaces in 3D in the previous chapter show that some surfaces are tapered or haven't been levelled before measuring them by system.

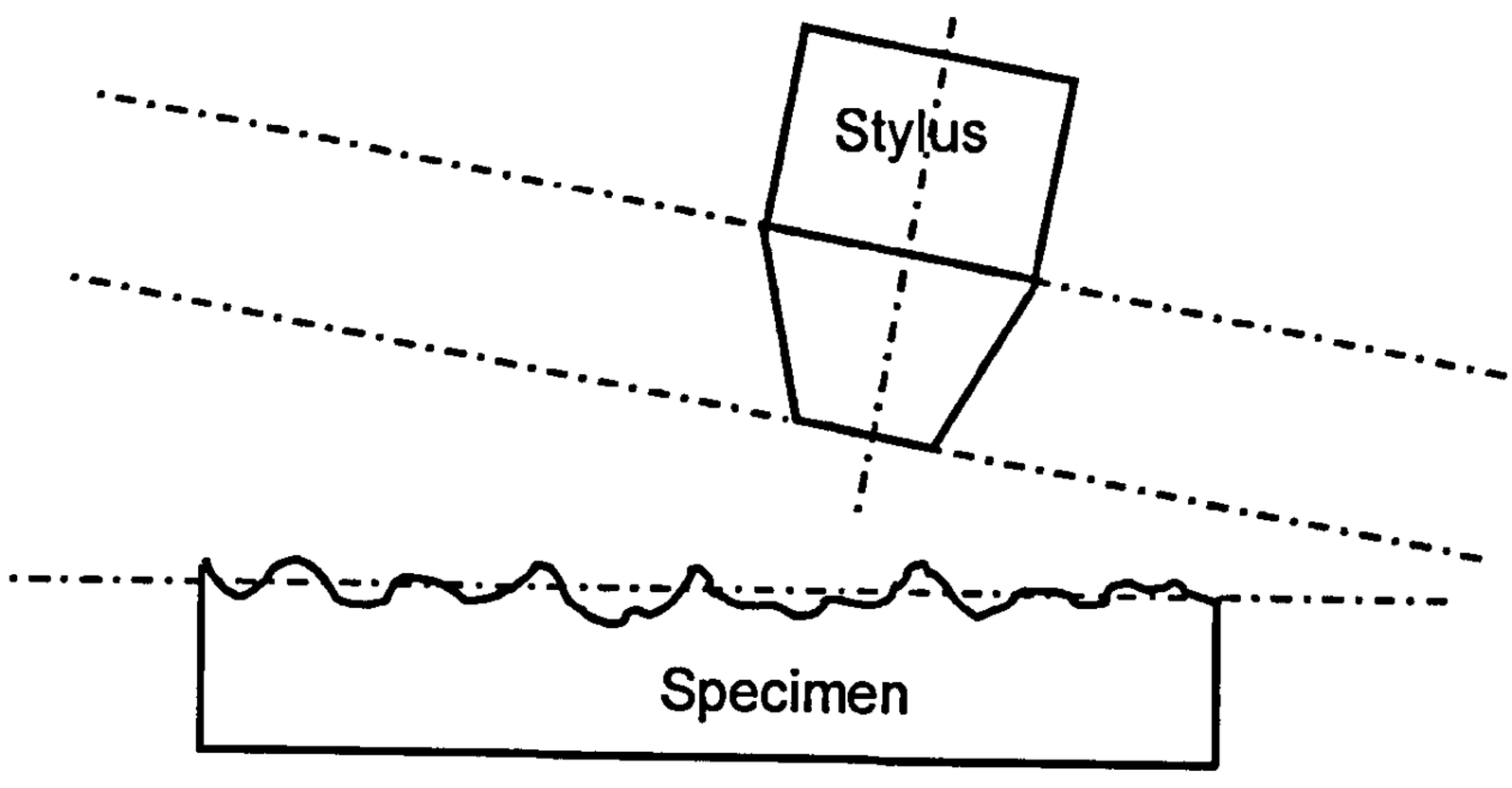

Figure 5.3: An inclined stylus to the measured surface

To fully understand this, the data obtained by scanning ground1 by tip2 has been virtually levelled using the feature available in SPIP program. Tip1 has also been levelled using the same feature. The levelled tip1 has been used to scan the levelled data of ground2 using the simulation program. Figure 5.4, shows the contacts distributions on tip2 before and after levelling the surface and tip data. Table 5.1, shows the roughness parameters before and after levelling surface ground1.

It is clear that the contact distributions on the tip has changed significantly by levelling the tip and the surface measured. More contacts are distributed on the edges of the tip. It is also clear that most roughness parameters have been changed as well.

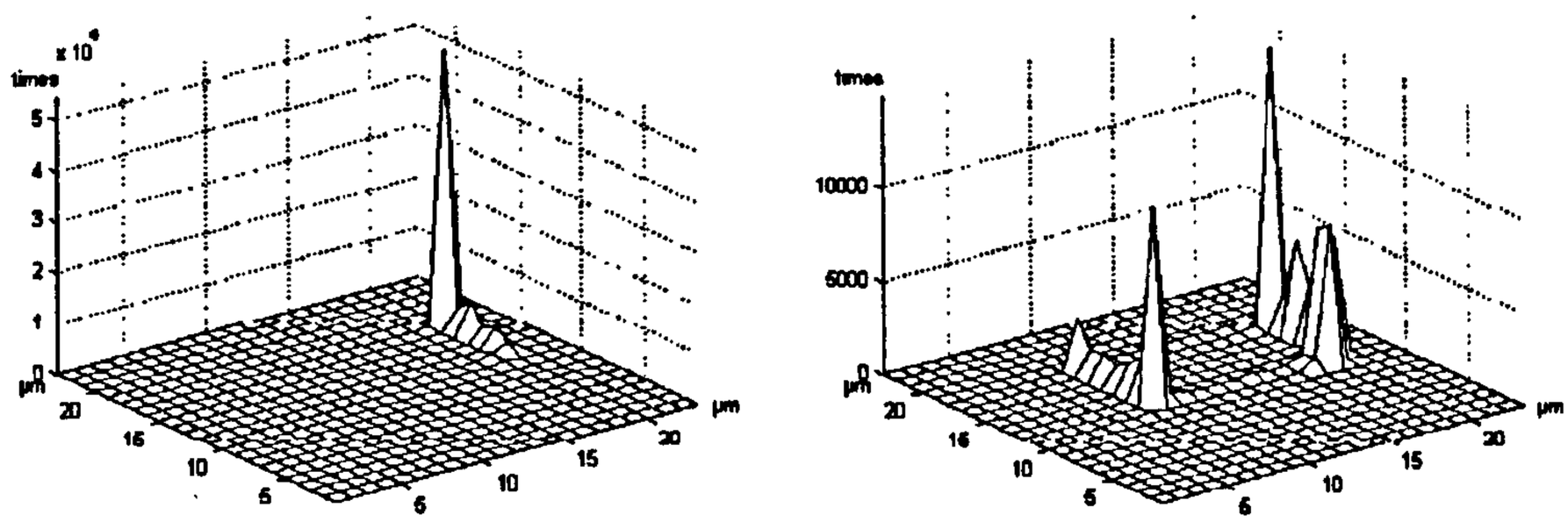

Before levelling After levelling

Figure5.4: The contact distributions on tip1 before and after levelling

	Sa	Sq	Sy	Ssk	Sdq	Sds
Before Levelling	0.21	0.25	1.60	0.06	0.04	13600
After Levelling	0.20	0.25	1.40	0.18	0.03	20232

Table 5.1: Roughness parameters of ground2 before and after levelling

Based on this discussion it has been found that, not only the tip geometry has an effect on the measured roughness of a surface but also the levelling of the tip and the measured surface. It means, if a surface is measured at a certain level, it will give different roughness parameters if it is measured at a different level.

5.4 Conclusions

The following points could be concluded from the work done during this thesis:

- A new simulation program has been developed and used to simulate the surface roughness measuring process by the stylus method. It can be used to scan any arbitrary surface with any arbitrary stylus tips shape.
- The simulation is not only used to measure the roughness of the surface but also to show the contacts distribution on the tip when scanning a surface, information not previously considered.
- The theoretical results of the simulation have confirmed that the stylus geometry can have a significant effect on most roughness parameters of the measured surface in 3D.
- The contacts distribution on the tip has shown that most contacts do not occur at the central point of the stylus in most cases, even with idealised shapes.
- A 3D surface roughness measuring system has been developed and verified. It can scan an area of the surface up to 50 mm x 50 mm with less than 1 µm sampling intervals.

- A rig has been developed to allow exchanging the stylus of the measuring system in order to measure an area of the surface with different tips. The rig has been verified and is showing good repeatability and reliability.

- A relocation technique has been developed and verified to allow scanning the same area of the surface by different styli. The relocation error hasn't exceeded 1 µm in both X and Y directions.

- A new technique has been used to measure the stylus tip geometry in 3D in the same orientations of the measuring process. The technique is based on the replica method and has shown very reliable results. The technique can be widely used for monitoring the stylus tip conditions.

- The same areas of surfaces of the different specimens, produced by different machining processes, have been measured with different styli by the measuring system. Different tips have given different results of each surface. However, the variation is smaller than might be expected from a study of pure simulation. This is a practical proof of the effect of the stylus geometry on the measured surface roughness.

- Applying the simulation on real tips and surfaces has given a better understanding of the interaction of the stylus and the measured surface. Especially, it emphasises the role of tip alignment as potentially dominated over tip wear.

- According to the simulation, simultaneous multiple contacts with the stylus occur more often than might have been expected. The number of the stylus contacts exceeds the number of surface points.

- The likelihood is higher than might be expected that the actual lateral position of contact is distant from the nominal tip centre by an amount approaching the nominal tip dimension. This has implications for high resolution measurements and for future standards that attempt to incorporate formal uncertainty statements.
- The evidence of the small numbers of tests undertaken here is that in practice stylus wear has less effect on feature resolution than would be expected intuitively. Misalignment and small scale structures tend to concentrate contacts in one region of a badly worn tip, reading its effective size.

5.5 Future Work

The work done in this thesis has demonstrated new techniques for studying geometrical interaction and has partially revealed some aspects of the stylus interaction with the surface in the real metrology. Considerations for continuing this work could be as follows:

- More simulation work can be done to study the effect of the worn tips on the roughness parameters of the surface when the tip wear is not parallel to the base of the tip or when the surface is inclined.
- More stylus tips with same shape and different sizes or conditions can be used to allow a proper comparison of the practical results of measuring a real surface with different tips.

- The measuring system could be upgraded by adding a precise computerised X-Y stage that can rotate in the horizontal plane by 90° or 180°. This will allow measuring the same area of the surface at different angles by the same tip to give a better ideal of the real interaction between the tip and the surface.

- The relocation technique can be widely used in the industry to study the effect of a treatment, cleaning or machining process on the surface roughness of a specimen.

- A large program of practical measurements and complementary simulation should be undertaken in order to provide guidance on a useful value for lateral uncertainty.

- Simple extension to existing simulation method would report data on which surface points actually made contact. Challenge to present the data in a useful way.

- Tip measurement technique can be developed to be offered to industry, perhaps using service-providing calibration laboratories to undertaken AFM measurements off-site on a routine basis.

6. REFERENCES

[1] ISO-4287-1997, Geometrical Product Specifications (GPS) . Surface Texture: Profile Method . Terms, Definitions, and Surface Texture Parameters, International Organization for Standardization (ISO), Geneva, Switzerland, (1997).

[2] Whitehouse, D.J., "Handbook of surface metrology", Institute of physics Publications, Bristol, 1994.

[3] Thomas, T.R., "Rough Surfaces", Imperial College Press, London, 1999.

[4] Mainsah, E., Greenwood, J.A., and Chetwynd, D.J., " Metrology and properties of engineering surfaces", Kluwer Academic Publishers, Boston, 2001.

[5] Whitehouse, D.J., "Surfaces and their measurement", Hermes Penton Science, London, 2002.

[6] Whitehouse, D.J., "Surface metrology", Measurement Science & Technology, Vol.8, No.9, pp.955-972, 1997.

[7] Song, J.F.; Vorburger, T.V., "Stylus profiling at high-resolution and low force", Applied Optics, Vol.30, No.1, pp.42-50, 1991.

[8] Beers, Winston A., "Computer assistance in surface topographic analysis", Proceedings of the New England Bioengineering Conference, pp 33-35, 1978.

[9] Chetwynd, D. G., "Digitization of surface profiles", Wear, Vol. 57, No. 1, pp 137-145, 1979.

[10] Sahwi, S.Z.; Mekawi, A.M., "Effect of noise on surface roughness measurements", Proceedings of the Joint 1996 IEEE Instrumentation and Measurement Technology Conference & IMEKO Technical Committee 7., Vol. 1, pp 232-235, 1996.

[11] Whitehouse, D.J.; Wang, W.L., "Dynamics and trackability of stylus systems", Proceedings of the Institution of Mechanical Engineers Part B-Journal of Engineering Manufacture, Vol.210, No.2, pp.159-165, 1996.

[12] Sayles R.S., Thomas, T.R., "Surface topography as a nonsatisfactory random process", Nature, Vol. 320, pp 431-434, 1978.

[13] Tsukada, Tadao; Sasajima, Kazuyuki, "Three-Dimensional measuring technique for surface asperities", Wear, Vol. 71, No. 1, pp 1-14, 1981.

[14] George, H.E.; Babus'Haq, R.F.; O'Callaghan, P.W.; Probert, S.D., "Stylus / computer system describing three-dimensional engineering surfaces", Computers in Industry, Vol. 13, No. 4, pp 295-304, 1990

[15] Jeng, Yeau-Ren; Lalonde, Giles A., "3-D surface topography measurement system and its applications", SAE Special Publications, No. 936, 922347, pp 175-182, 1992.

[16] Song; J.F., Vorburger; T.V., "Stylus flight in surface profiling", Journal of Manufacturing Science and Engineering-Transactions of the ASME, Vol.118, No.2, pp.188-198, 1996.

[17] Weingraber, H. Von, "Suitability of the envelope line as a reference standard for measuring roughness", Microtecnic, Vol. 11, 6-17, 1957.

[18] RadhaKrishnan, V., "Selection of an enveloping circle radius for E-system roughness measurement", International Journal of Machine tool Design & Research, Vol.2, 80-89, 1972.

[19] Radhakrishnan V, "Effect of stylus radius on the roughness values measured with tracing stylus instruments", Wear, Vol. 16, No. 5, pp 325-35, 1970.

[20] McCool, J. I. "Assessing the effect of stylus tip radius and flight on surface topography measurements", Journal of Tribology, Transactions of the ASME, Vol. 106, No. 2, pp 202-210, 1984.

[21] Church, E.L.; Takacs, P.Z., "Effects of the non-vanishing tip size in mechanical profile measurements", Proceedings of SPIE - The International Society for Optical Engineering, Vol. 1332, No. pt 2, pp 504-514, 1990.

[22] Odonnell, K.A., "Effects of finite stylus width in surface-contact profilometry", Applied Optics, Vol.32, No.25, pp.4922-4928, 1993.

[23] Liu, X.; Smith, S.T.; Chetwynd, D.G., "Frictional forces between a diamond stylus and specimens at low load", Wear, Vol. 157, No. 2, pp 279-294, 1992.

[24] Zahwi, S.; Mekawi, A.M., "Some effects of stylus force on scratching surfaces", International Journal of Machine Tools and Manufacture, Vol. 41, No. 13-14, pp 2011-2015, 2001.

[25] Kratz, Frank; Ringel, Gabriele; Toebben, Helmut; Schmitt, Dirk-Roger, "Comparison of a simulation model investigating the scanning of surfaces by mechanical profiling systems with current measurements", Proceedings of SPIE - The International Society for Optical Engineering, Vol. 2775, pp 263-268, 1996.

[26] Wu, J.J, "Spectral analysis for the effect of stylus tip curvature on measuring rough profiles", Wear, Vol.230, No.2, pp.194-200, 1999.

[27] Wu, Jiunn-Jong, "Spectral analysis for the effects of stylus tip curvature on measuring isotropic rough surfaces", Measurement Science and Technology, Vol. 13, No. 5, pp 720-730, 2002.

[28] Mendeleyev, Vladimir Ya. , "Dependence of measuring errors of rms roughness on stylus tip size for mechanical profilers", Applied Optics, Vol. 36, No. 34, pp 9005, 1997.

[29] Yang, Peizhong; Jiang, Shouwei, "The 3-D assessment of surface roughness and its implement with MATLAB", Proceedings of the Seventh International Conference on Industrial Engineering and Engineering Management, pp 47-52, 2000.

[30] Vorburger, T. V.; Teague, E. C.; Scire, F. E.; Rosberry, F. W., "Measurements of stylus radii", Wear, Vol. 57, No. 1, pp 39-49, 1979.

[31] Elewa, Ibrahim; Koura, Monir M., "Importance of checking the stylus radius in the measurement of surface roughness", Wear, Vol. 109, No. 1-4, pp 401-410, 1985.

[32] Radhakrishnan, V., "Analysis of surface profiles by computational methods", J. Instn. Engrs. (India) 51, Part ME6, 272-8, 1971.

[33] Dong WP, Sullivan PJ, Stout KJ. Comprehensive study of parameters for characterizing 3-D surface topography? III: Parameters for characterizing amplitude and some functional properties. Wear 1994;178:29–43.

[34] Dowidar, H. A. M.: M.Sc. Thesis, Ain Shams University, Egypt, (1996).

[35] Edmonds, M. J.; Jones, A. M.; O'Callaghan, P. W.; Probert, S. D. Source, "Three-Dimensional relocation profilometer stage", Wear, Vol. 43, No. 3, pp 329-340, 1977.

[36] Poon, Chin Y.; Bhushan, Bharat, "Comparison of surface roughness measurements by stylus profiler, AFM and non-contact optical profiler", Wear, Vol. 190, No. 1, pp 76-88, 1995.

[37] BS1134, "Assessment of surface roughness", Parts 1, British Standards Institution, London, 1988/1990.

[38] Sasajima, Kazuyuki (Meiji Univ); Naoi, Kazuya; Tsukada, Tadao , "Software-based relocation technique for surface asperity profiles and its application to calculate volume changes in running-in wear", Wear, Vol. 240, No. 1-2, pp 152-163, 2000.

[39] Condeco, J.; Christensen, L.H.; Rosen, B.-G., "Software relocation of 3D surface topography measurements", International Journal of Machine Tools and Manufacture, Vol. 41, No. 13-14, pp 2095-2101, 2001.

[40] Sherrington, I.; Smith, E.H., "Design and performance assessment of a Kelvin clamp for use in relocation analysis of surface topography", Precision Engineering, Vol. 15, No. 2, pp 77-85, 1993.

[41] Chetwynd D.G.; Liu X.; Smith S.T., "A controlled-force stylus displacement probe", Precision Engineering-Journal of the American Society for Precision Engineering, Vol.19, No.2-3, pp.105-111, 1996.

[42] Eckert, Jurgen D., "Replica techniques for the study of fracture surfaces and topography study in general", Practical Metallography, Vol. 33, No. 7, pp 369-372, 1996.

[43] Nilsson, L.; Ohlsson, R. , "Accuracy of replica materials when measuring engineering surfaces", International Journal of Machine Tools and Manufacture, Vol. 41, No. 13-14, pp 2139-2145, 2001.

[44] Vorburger, T.V.; Dixson, R.G.; Tsai, V.; Doi, T.; Song, J.F.; Renegar, T.B.; Fu, J., "Problems in surface metrology", International Journal of Machine Tools & Manufacture, Vol. 38, No. 5-6, pp 417-418, 1998.

Appendix A

The simulation program created by Matlab for scanning a small area of a surface with a stylus

```
clear all
clc
cla
clf

%********************************** Loading Data ************************************

load stylus.dat              % any set of data representing the surface
load surface.dat             % any set of data representing the stylus
z=surface;
s=stylus,

a=size(z);
n=a(1,1);                                  % number of traces
m=a(1,2);                                  % number of points in each trace

b=size(stylus);
r=b(1,1)/2;                                % radius of the tip
r=fix(r);

%************************* Calculations the locus and contacts ************************

l=0;                                % Setting all locus values to zeros
c=zeros(2*r+1);                     % Setting all contacts counts to zeros

for i=r+1:n-r,
    for j=r+1:m-r,
        xy=z(i-r:i+r, j-r:j+r);
        heights=s+xy;
```

```
maxi=max(max(heights));
l(i-r,j-r)=maxi;
for k=-r:r,
    for y=-r:r,
        nbar=k+r+1;
        mbar=y+r+1;
        if heights(nbar,mbar) == maxi
            c(nbar,mbar)=1+c(nbar,mbar);
        end
    end
  end
end
end
save contacts c -ascii
save locus l -ascii
```

Appendix B

Definition and Calculations of SurfaceRoughness Parameters

Procedures for calculation of surface roughness parameters as implemented in the SPIP program.

Symbol	Name	Unit
Amplitude parameters:		
S_a	Roughness Average	[µm]
S_q	Root Mean Square	[µm]
S_{sk}	Surface Skewness	[µm]
S_{ku}	Surface Kurtosis	[µm]
S_y	Peak-Peak	[µm]
Sz	Ten Point Height	[µm]
Hybrid Parameters:		
S_{sc}	Mean Summit Curvature	[1/µm]
S_{ti}	Texture Index	
S_{dq}	Root Mean Square Slope	[Rad]
S_{dr}	Surface Area Ratio	
Functional Parameters:		
S_{bi}	Surface Bearing Index	
S_{ci}	Core Oil Retention Index	
S_{vi}	Valley Oil Retention Index	
S_{pk}	Reduced Peak Height	[µm]
S_k	Core Roughness Depth	[µm]
S_{vk}	Reduced Valley Height	[µm]
Spatial Parameters:		
S_{ds}	Density of Summits	[1/mm2]
S_{td}	Texture Direction	[deg]
S_{tdi}	Texture Direction Index	
S_{rw}	Dominant Radial Wave Length	[µm]
S_{rwi}	Radial Wave Index	
S_{hw}	Mean Half Wavelength	[µm]

Most parameters are general and valid for any M x N rectangular image. However, for some parameters related to the Fourier transform it is assume that the image is quadrangular (M=N).

The parameters are divided into four groups as described in the following.

Amplitude parameters

The amplitude properties are described by six parameters, which give information about the statistical average properties, the shape of the height distribution histogram and about extreme properties.

The Roughness Average, S_a , is defined as:

$$S_a = \frac{1}{MN}\sum_{k=0}^{M-1}\sum_{l=0}^{N-1}|z(x_k, y_l)| \qquad \text{R 1}$$

The Root Mean Square S_q, is defined as:

$$S_q = \sqrt{\frac{1}{MN}\sum_{k=0}^{M-1}\sum_{l=0}^{N-1}(z(x_k, y_l))^2} \qquad \text{R 2}$$

The Peak-Peak Height, S_y, is defined as the height difference between the highest and lowest pixel in the image.

$$S_y = z_{\max} - z_{\min} \qquad \text{R 3}$$

The Ten Point Height, S_z , is defined as the average height of the five highest local maximums plus the average height of the five lowest local minimums:

$$S_z = \frac{\sum_{i=1}^{5} z_{pi} + \sum_{i=1}^{5} z_{vi}}{5} \qquad \text{R 4}$$

where z_{pi} and z_{vi} are the height of the ith highest local maximum and the ith lowest local minimum respectively. Only positive maximums and negative minimums are valid. When there are less than five valid maximums or five valid minimums, the parameter is not defined.

The Surface Skewness, S_{sk} , describes the asymmetry of the height distribution histogram, and is defined as:

$$S_{sk} = \frac{1}{MNS_q^3} \sum_{k=0}^{M-1} \sum_{l=0}^{N-1} z^3(x_k, y_l) \qquad \text{R 5}$$

If S_{sk}=0, a symmetric height distributions is indicated, for example, a Gaussian like. If $S_{sk} < 0$, it can be a bearing surface with holes and if $S_{sk} > 0$ it can be a flat surface with peaks. Values numerically greater than 1.0 may indicate extreme holes or peaks on the surface.

The Surface Kurtosis, S_{ku}, describes the peaked-ness of the surface topography, and is defined as:

$$S_{ku} = \frac{1}{MNS_q^4} \sum_{k=0}^{M-1} \sum_{l=0}^{N-1} z^4(x_k, y_l) \qquad \text{R 6}$$

For Gaussian height distributions S_{ku} approaches 3.0 when increasing the number of pixels. Smaller values indicate broader height distributions and visa versa for values greater than 3.0.

Hybrid parameters

There are three hybrid parameters. These parameters reflect slope gradients and their calculations are based on local z-slopes.

The Mean Summit Curvature, S_{sc}, is the average of the principal curvature of the local maximums on the surface, and is defined as:

$$S_{sc} = \frac{-1}{2n}\sum_{i=1}^{n}\left(\frac{\delta^2 z(x,y)}{\delta x^2}\right)+\left(\frac{\delta^2 z(x,y)}{\delta y^2}\right) \quad \text{for all local maximums} \qquad \text{R 7}$$

where δx and δy are the pixel separation distances.

The Root Mean Square Slope, S_{dq} , is the RMS-value of the surface slope within the sampling area, and is defined as:

$$S_{dq} = \sqrt{\frac{1}{(M-1)(N-1)}\sum_{k=0}^{M-1}\sum_{l=0}^{N-1}\left(\frac{z(x_k,y_l)-z(x_{k-1},y_l)}{\delta x}\right)^2+\left(\frac{z(x_k,y_l)-z(x_k,y_{l-1})}{\delta y}\right)^2} \qquad \text{R 8}$$

The Surfaces Area Ratio, S_{dr} , expresses the ratio between the surface area (taking the z height into account) and the area of the flat xy plane:

$$S_{dr} = \frac{\left(\sum_{k=0}^{M-2}\sum_{l=0}^{N-2} A_{kl}\right)-(M-1)(N-1)\,\delta x\,\delta y}{(M-1)(N-1)\,\delta x\,\delta y}\,100\% \qquad \text{R 9}$$

where

$$A_{kl} = \frac{1}{4}\sqrt{\delta y^2+(z(x_k,y_l)-z(x_k,y_{l+1}))^2}+\frac{1}{4}\sqrt{\delta y^2+(z(x_{k+1},y_l)-z(x_{k+1},y_{l+1}))^2}+\frac{1}{4}\sqrt{\delta x^2+(z(x_k,y_l)-z(x_{k+1},y_l))^2}+\frac{1}{4}\sqrt{\delta x^2+(z(x_k,y_{l+1})-z(x_{k+1},y_{l+1}))^2} \qquad \text{R 10}$$

For a totally flat surface, the surface area and the area of the xy plane are the same and S_{dr} = 0 %.

Functional parameters for characterizing bearing and fluid retention properties

The functional parameters for characterizing bearing and fluid retention properties are described by six parameters. All six parameters are defined from the surface bearing area ratio curve shown in the figures below.

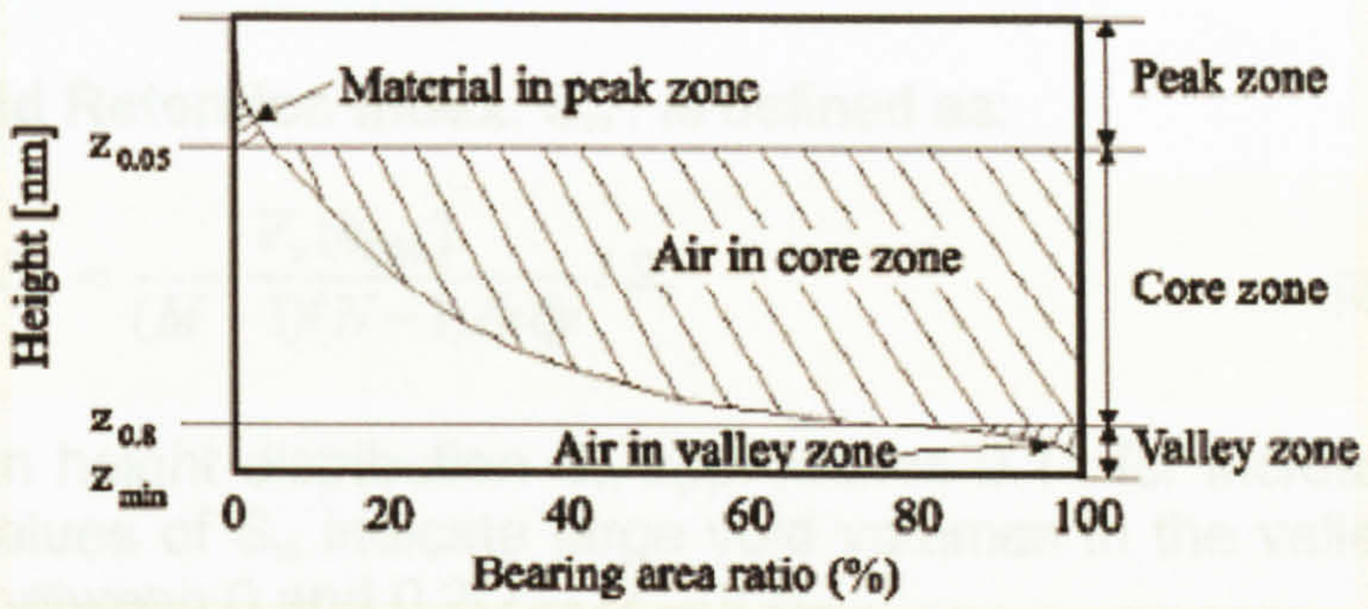

Figure 1: Bearing curve illustrating the calculation of Surface Bearing Index, Core Fluid Retention Index and Valley Fluid Retention Index

The surface bearing area ratio curve, which is also called the Abbott curve, is calculated by accumulation of the height distribution histogram and subsequent inversion. We divide both the histogram and the bearing curves into 1000 intervals except for images having less than 10000 pixels where the intervals equal 10% of the total pixels.

The hybrid parameters can be described graphically by the above figure. Horizontal lines are drawn through the bearing area ratio curve at the ratio values 5% and 80%. These lines are marked $Z_{0.05}$ and $Z_{0.8}$ and the three zones created are called the peak, the core and the valley zone. Three parameters are calculated based on this figure-

The Surface Bearing Index, S_{bi}, is defined as:

$$S_{bi} = \frac{S_q}{Z_{0.05}}, \qquad \text{R 11}$$

where $Z_{.05}$ is the distance from the top of the surface to the height at 5% bearing area. For a Gaussian height distribution S_{bi} approaches 0.608 for increasing number of pixels. Large S_{bi} indicates a good bearing property.

The Core Fluid Retention Index, S_{ci} , is defined as:

$$S_{ci} = \frac{V_v(h_{0.05}) - V_v(h_{0.08})}{(M-1)(N-1)\delta x \delta y} / S_q \qquad \text{R 12}$$

where $V_v(Z_x)$, is the void area over the bearing area ratio curve and under the horizontal line Z_x. For a Gaussian height distribution S_{ci} approaches 1.56 for increasing number of pixels. Large values of Sci indicate that the void volume in the core zone is large. For all surfaces S_{ci} is between 0 and 0.95 ($Z_{0.05}$ -$Z_{0.8}$) .

The Valley Fluid Retention Index, S_{vi} , is defined as:

$$S_{vi} = \frac{V_v(h_{0.08})}{(M-1)(N-1)\delta x \delta y} / S_q \qquad \text{R 13}$$

For a Gaussian height distribution S_{vi} approaches 0.11 for increasing number of pixels. Large values of S_{vi} indicate large void volumes in the valley zone. For all surfaces S_{vi} is between 0 and 0.2($Z_{0.8}$ -Z_{min})/ S_q .

Parameters associated with the two-dimensional DIN 4776 standard are also calculated based on the bearing area ratio curve. First, draw the least mean squares line fitted to the 40% segment of the curve that results in the lowest decline, see figure below. Extend this line so that it cuts the vertical axes for 0% and 100% and draw horizontal lines at the intersection points. Then draw a straight line that starts at the intersection point between the bearing area ratio curve and the upper horizontal line, and end on the 0% axis, so that the area of this triangle is the same as the area between the horizontal line and the bearing area ratio curve. Using the same principle, draw a line between the lower horizontal line and the 100% axis.

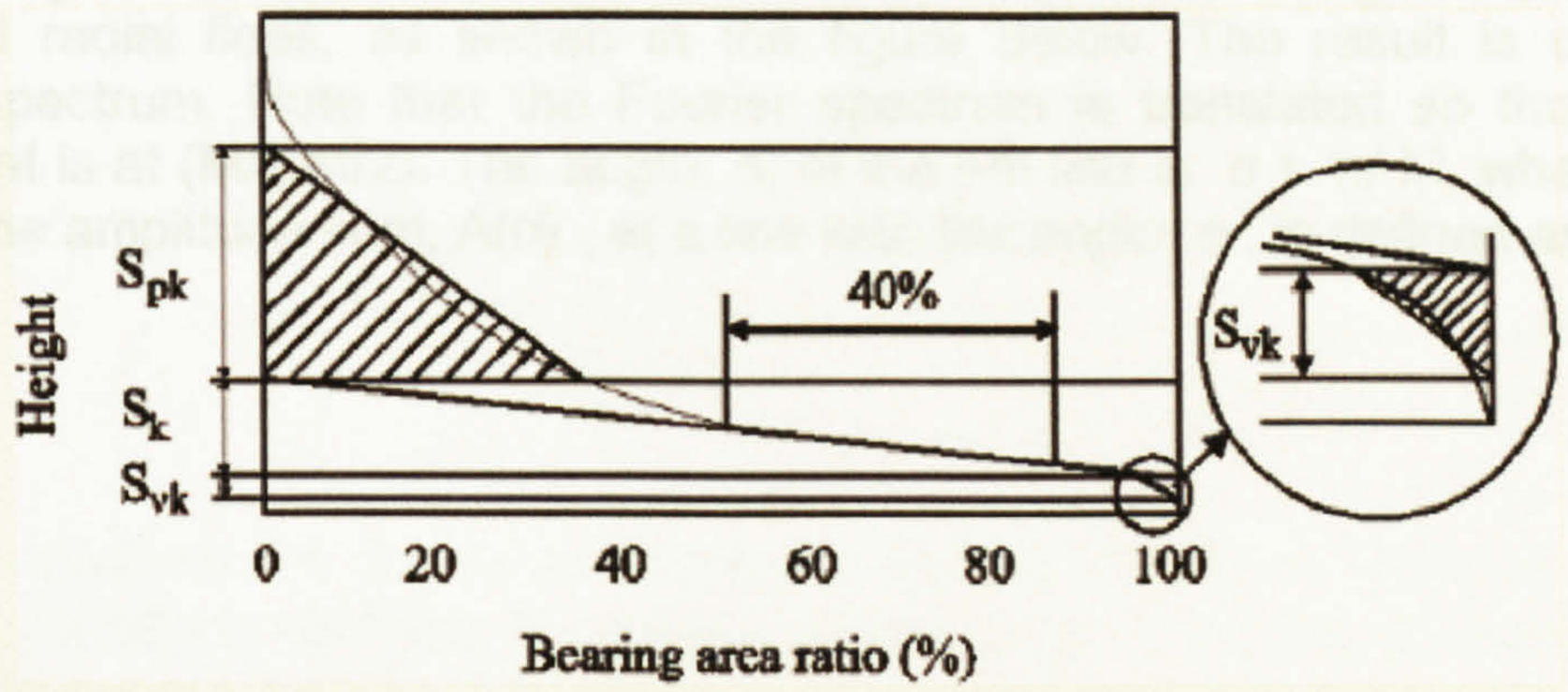

Figure 2: Bearing curve illustrating the calculation of Reduced Summit Height, Reduced Valley Height and Core Roughness Depth

The Reduced Summit Height, S_{pk} , is the height of the upper left triangle. The Core Roughness Depth, S_k, is the height difference between the intersection points of the found least mean square line, and the Reduced Valley Depth, S_{vk}, is the height of the triangle drawn at 100%.

Spatial parameters

The spatial properties are described by five parameters. These parameters are the density of summits, the texture direction, the dominating wavelength and two index parameters. The first parameter is calculated directly from the STM-image, while the remaining are based on the Fourier spectrum. For these parameters we require the images to be quadratic.

The Density of Summits, S_{ds} , is the number of local maximums per area:

$$S_{ds} = \frac{\text{Number of local maximums}}{(M-1)(N-1)\delta x \delta y} \qquad \text{R 14}$$

Because, the parameter is sensitive to noisy peaks it should be interpreted carefully.

The Texture Direction, S_{td}, is defined as the angle of the dominating texture in the STM-image. For images consisting of parallel ridges, the texture direction is parallel to the direction of the ridges. If the ridges are perpendicular to the X-scan direction $S_{td} = 0$. If the angle of the ridges is turned clockwise, the angle is positive and if the angle of the ridges is turned anti-clockwise, the angle becomes negative. This parameter is only meaningful if there is a dominating direction on the sample.

We calculate S_{td} from the Fourier spectrum. The relative amplitudes for the different angles are found by summation of the amplitudes along M equiangularly separated radial lines, as shown in the figure below. The result is called the angular spectrum. Note that the Fourier spectrum is translated so that the DC component is at (M/2,M/2). The angle, α, of the i-th line is $\alpha = \pi / M$, where i=0, 1, .., M-1. The amplitude sum, A(α) , at a line with the angle, α , is defined as:

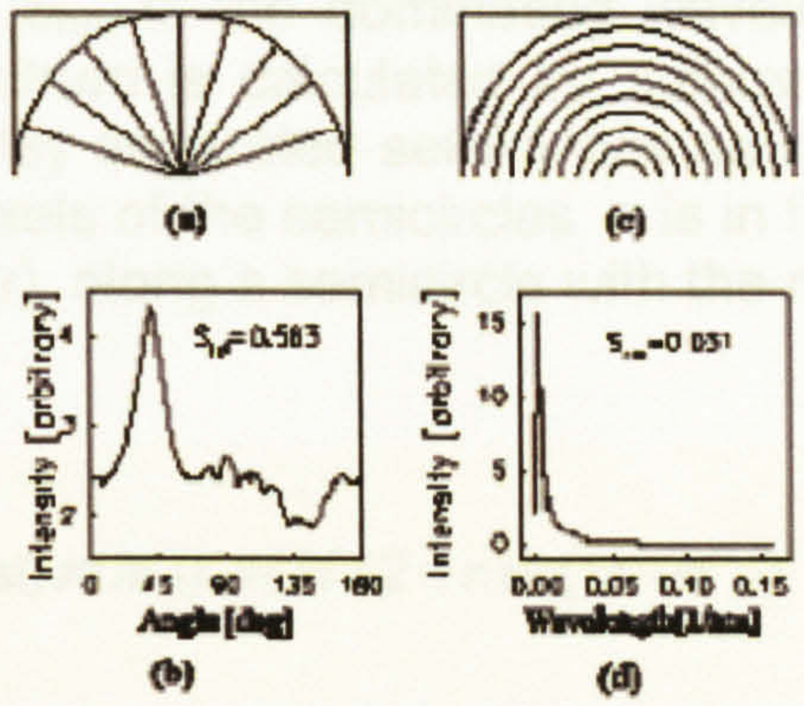

Figure 3: Fourier spectrum and the angular and radial spectrums (Modified from [6]). a) Equidistant lines used for calculation of the angular spectrum shown in b). c) Equidistant semicircles used for calculation of the radial spectrum.

$$A(\alpha) = \sum_{i=1}^{M/2-1} \left| F(u(M/2 + i\cos(\alpha)), v(M/2 + i\sin(\alpha))) \right| \qquad \text{R 15}$$

For non-integer values of $P = M / (2 + i\cos(\alpha))$ and $q = M / (2 + i\sin(\alpha))$, the value of $F(u(p),v(q))$ is found by linear interpolation between the values of $F(u(p),v(q))$ in the 2x2 neighboring pixels. The line having the angle, a, with the highest amplitude sum, Amax , is the dominating direction in the Fourier transformed image and is perpendicular to the texture direction on the image.

Note that due to 1/f noise often a dominating direction parallel to the x-axis is found.

The Texture Direction Index, S_{tdi} , is a measure of how dominant the dominating direction is, and is defined as the average amplitude sum divided by the amplitude sum of the dominating direction:

$$S_{tdi} = \frac{\sum_{i=0}^{M-1} A(i\pi / M)}{M A_{max}} \qquad \text{R 16}$$

With this definition the S_{tdi} value is always between 0 and 1. Surfaces with very dominant directions will have S_{tdi} values close to zero and if the amplitude sum of all direction are similar, S_{tdi} is close to 1.

The Radial Wavelength, S_{rw}, is the dominating wavelength found in the radial spectrum. The radial spectrum is calculated by summation of amplitude values around M/(2 -1) equidistantly separated semicircles as indicated in sub figure (b). The radius measured in pixels of the semicircles, r, is in the range r = 1, 2,.., M/(2 -1). The amplitude sum, β (r), along a semicircle with the radius, r , is

$$\beta(r) = \sum_{i=1}^{M-1} \left| F(u(M/2 + r\cos(i\pi/M)), v(M/2 + r\sin(i\pi/M))) \right| \quad \text{R 17}$$

Again the amplitude for non-integer values of

$p=M/2 + r\cos(i\,\pi/M)$ and $q=M/2 + r\sin(i\,\pi/M)$

is calculated by linear interpolation between the values of $F(u(p),v(q))$ in the 2x2 neighboring pixels.

The Dominating Radial Wavelength, S_{rw}, corresponds to the semicircle with radius, r_{max} , having the highest amplitude sum, β_{max}:

$$S_{rw} = \frac{\delta x(M-1)}{r_{max}} \quad \text{R 18}$$

The Radial Wave Index, S_{rwi} , is a measure of how dominant the dominating radial wavelength is, and is defined as the average amplitude sum divided by the amplitude sum of the dominating wavelength:

$$S_{rwi} = \frac{2}{M\,\beta_{max}} \sum_{i=1}^{M/2-1} \beta(i) \quad \text{R 19}$$

With this definition S_{rwi} is always between 0 and 1. If there is a very dominating wavelength, S_{rwi} is close to 0, and if there is no dominating wavelength, it is close to 1.

The Mean Half Wavelength, S_{hw}, is based on the integrated radial spectrum :

$$\beta_i(r) = \sum_{j=1}^{r} \beta(j) \qquad \text{R 20}$$

S_{hw} corresponds to the radius $r_{0.5}$ where :

$$\frac{\beta_i(r_{0.5})}{\beta_i(M/2-1)} = 0.5 \qquad \text{R 21}$$

Having found $r_{0.5}$, S_{hw} is calculated this way:

$$S_{hw} = \frac{\delta x(M-1)}{r_{0.5}} \qquad \text{R 22}$$